Effects of Chemical Treatments on Hemp Fibre Reinforced Polyester Composites

By

Mohammad Mazedul Kabir

Supervised by

Assoc Prof Hao Wang
Prof Alan Kin-tak Lau
Dr Francisco Cardona
Assoc Prof Thiru Aravinthan

A dissertation submitted for the award of

DOCTOR OF PHILOSOPHY

Centre of Excellence in Engineered Fibre Composites
Faculty of Engineering and Surveying
University of Southern Queensland
Toowoomba, Queensland, Australia.

September 2012

Abstract

Natural fibres have recently become an attractive alternative to synthetic fibres in the implementation in polymer composite structures. This is due to contemporary environmental concerns such as climate change which have caused engineers to consider renewable resources in composite structures. Inherent flaws within natural fibres in terms of their constituent contents (hemicellulose, cellulose and lignin) reduce the compatibility of these fibres with polymer matrices. Fibre surface modifications using chemical treatments have the potential to improve fibre-matrix compatibility.

In this study, the effects of chemical treatments on hemp fibres and the resulted polyester matrix composite are discussed. The fibres were treated with alkali (0-10% NaOH), acetyl and silane chemicals.

The structural composition and thermal decomposition of the fibres after treatments were investigated through chemical analysis, fibre morphology analysis, FTIR analysis, and TGA and DSC analyses. Fibre structure and morphology analysis showed that the amount of hemicellulose and lignin constituents decreased in the case of alkalised and acetylated fibres. Conversely, silane molecules formed couplings on fibre surfaces and there was no changes observed in terms of hemicellulose and lignin contents. Thermal analysis revealed that, due to the presence of hemicellulose constituents, the untreated fibres had lower thermal stability.

The tensile properties of treated hemp fibres were measured through DMA. Treated fibres exhibited lower strengths compared to the untreated fibres due to the removal of hemicellulose and lignin binder from their cellulose surfaces.

Long unidirectional fibre composites and sandwich structures were tested using tension, compression, shear, bending and impact tests. In both composite cases, 4% NaOH treatments reduced interface bonding strength and decreased composite properties compared to untreated samples. At higher concentrations (6-10% NaOH), composite properties increased as a result of greater interface bonding. The opposite results were achieved in the case of alkalised fibres that were further treated with acetyl and silane treatments. Failure analysis of tested composites was undertaken through OM and SEM. Micrographs showed results which were in agreement which the properties achieved.

Treated fibres were able to effectively improve the bonding properties of composites, even though the mechanical strength of these fibres could be decreased. Thus, the use of chemical treatments on fibres can be justified as overall composite mechanical properties increased when compared to untreated cases.

Certification of Dissertation

I certify that the ideas, experimental work, results, analysis and conclusions reported in this dissertation are entirely my own effort, except where otherwise acknowledged. I also certify that the work is original and has not been previously submitted for any award, except where otherwise acknowledged.

---------- / /

Signature of Candidate

Endorsed:

---------- / / ---------- / /

Signature of Supervisor/s Signature of Supervisor/s

---------- / / ---------- / /

Signature of Supervisor/s Signature of Supervisor/s

Acknowledgements

Applying oneself to pursue a PhD project is as challenging as rewarding. Throughout this process I have gained not only a greater insight into my topic but more importantly a greater understanding of how the efforts of many people and factors have come together to develop and present this work. I would like to convey my thanks and appreciation to those who have helped me reach the end of this chapter of work.

I would like to thank my Principle Supervisor, Associate Professor Hao Wang for his guidance and valuable suggestions, without which I would have been unable to complete this body of research. I would further like to convey my thanks to him for his supportive and kind nature as he continuously provided valuable advice and direction at times when it was most required. Many thanks go to Associate Supervisor, Professor Alan Kin-tak Lau for his continuing confidence in me throughout my studies. I am extremely appreciative of his constant support as he facilitated my learning through his rich academic and practical experience. His companionship and deep knowledge supported me greatly in this study. I am thankful and appreciative of the helpful advice given to me by Associate Supervisor, Dr. Francisco Cardona. Discussions with him helped me better understand specific topic areas such as thermal analysis of natural fibres. I am also thankful to Associate Supervisor, Associate Professor Thiru Aravinthan for his valuable suggestions and inspirations.

I greatly appreciate the helpful technical insights, suggestions and reflections I received as a result of discussions with Dr. Md. Mainul Islam and Mr. Ali Ashraf Khurshid. Special mention also goes to the quiet and humble Mr. Wayne Crowell for

his immense help through the many stages of my study, especially when it came to experimentation. I am very thankful for the technical and administrative support I received from Mr. Kim Larsen, Mr. Mohan Tadra, Mr. Martin Geach, Mr. Justin Xu, Miss Sandra Cochrane and Mr. Mubarok Hossain. I cannot thank all the postgraduate students at CEEFC enough for their suggestions, support and friendship as we all rallied together to further our research careers.

I greatly appreciate the academic, financial and technical support provided to me by the Faculty of Engineering and Surveying and the Centre of Excellence in Engineered Fibre Composites (CEEFC), which made this research possible. I am also thankful to Bangladesh Jute Research Institute (BJRI) for supporting my study.

Whilst I have thanked the many professionals involved in helping me complete my dissertation, I would like to express my sincere appreciation to my parents, brother, mother in-law, father in-law and brothers in-law for their unconditional and endless support. The most important “thank you” goes to my dear wife Sultana Jahan Kabir. Thank you for your endless patience, for comforting and encouraging me during the challenging periods of this phase of my life. Without your support I would not have been able to put a close to this chapter of my life.

All praise and thanks is to Almighty Allah who has blessed me with understanding and strength. His blessings towards me are innumerable as it is through Him that I have developed a sincere thirst for knowledge. To those whom I have failed to mention but have played a contributing part of this endeavour, thank you very much.

Associated Publications

Journals

Kabir, M.M., Wang, H., Lau, K.T., Cardona, F., Aravinthan, T. (2012). 'Mechanical properties of chemically-treated hemp fibre reinforced sandwich composites'. *Composites Part B: Engineering*, 43(2), 159-169.

Kabir, M.M., Wang, H., Lau, K.T., Cardona, F. (2012). 'Chemical Treatments on Plant-based Natural Fibre Reinforced Polymer Composites: An Overview'. *Composites Part B: Engineering*, 43B(7), 2883-2892.

Kabir, M.M., Wang, H., Lau, K.T., Cardona, F., Aravinthan, T. (2012). 'Effects of Surface Chemical Treatments on Hemp Fibre Structures'. *Applied Surface Science*, Accepted for publication.

Kabir, M.M., Wang, H., Lau, K.T., Cardona, F., Aravinthan, T. (2012). 'Tensile properties of chemically treated hemp fibres as reinforment for composites', *Journal of Natural Fibres*, Under review.

Refereed Conference Proceedings

Kabir, M.M., Wang, H., Lau, K.T., Cardona, F., Aravinthan, T. (2012). 'Compressive properties of chemically-treated unidirectional hemp fibre reinforced composites'. *Conference on Diversity in Composites*, *Composite Australia & CRC-ACS*, 15-16 March, Fairmont Resort Blue Mountains Leura, NSW, Australia, pp 1-14.

Wang, H., Kabir, M.M., Lau, K.T. (2012). 'The effect of fibre chemical treatments on hemp reinforced composites'. *ICCM18: The 18th International Conference on Composite Materials*, 21-26 August, Jeju International Convention Center, Jeju Island, South Korea.

Kabir, M.M., Wang, H., Lau, K.T., Cardona, F., Aravinthan, T. (2011). 'Effects of natural fibre surface on composite properties: A Review'. *eddBE2011 Procedings, Energy, Environment and Sustainability*, 27-29 April, Queensland University of Technology, Brisbane, pp 94-99.

Kabir, M.M., Wang, H., Cardona, F., Aravinthan, T. (2010). 'Effect of chemical treatment on the mechanical and thermal properties of hemp fibre reinforced thermoset sandwich composites'. *Incorporating sustainable practice in mechanics of structures and materials, 21st Australian Conference on the Mechanics of Structures and Materials*, 7-10 December, Melbourn, Australia, pp 439-444.

Kabir, M.M., Wang, H., Islam, M. (2010). 'Mechanical and thermal properties of untreated and chemically treated jute fibre reinforced composites'. *ICMIEE 2010: International Conference on Mechanical, Industrial and Energy Engineering*, 23-24 December, Khulna, Bangladesh.

Table of Contents

List of Figures

List of Tables

Chapter 1: Introduction

There has recently been a growing interest in the use of natural fibres as reinforcements in polymer composites. One of the main reasons for this is an increase in environmental consciousness. The introduction of natural fibres in composites can provide benefits to the environment as they are bio-degradable, cost effective and naturally available (Rout, et al. 2001). Conventionally used synthetic composite reinforcements are non-renewable resources and require substantial amounts of energy for production which releases excessive amounts of carbon dioxide.

Much research on natural fibres as reinforcements for thermoset and thermoplastic composites has been conducted over the last decade. Studies indicate that natural fibres display large variations in properties, as their structures are highly affected by contemporary environmental factors such as climate change. These factors result in natural fibres developing inconsistent cross-sectional areas and shapes along their lengths, which affect the ultimate loads that can be carried by them. Natural fibres can only stand up to certain temperature which complicates manufacturing processes. Another major drawback when using natural fibres is that their structure absorbs atmospheric moisture which makes the fibre hydrophilic in nature. Hydrophilic fibres are incompatible with hydrophobic polymers (thermoset and thermoplastics). Therefore natural fibres display poor fibre-matrix interfacial bonding which results in poor composite mechanical properties.

It is, therefore, necessary to modify the fibre to improve bonding with the matrix. Different treatments on fibres modify their structure and surfaces which lead to fibre thermal and mechanical property improvements, thereby improving fibre bonding with matrix and thus enhances composite properties.

Research objectives

The aim of this thesis was to achieve a greater understanding of the various parameters that contribute to natural fibre properties, and their reinforced composites. Hemp fibre reinforced polyester composites, in particular, were studied. The research objectives are summarised below:

- To gain an understanding of natural fibre reinforced polymer composites, and to gain an insight into work previously done by other researchers in this area.
- To investigate the influences of chemical treatments in terms of the following fibre parameters:
    - Constituent content change within structure and surface morphology through chemical analysis, microstructure analysis, FTIR analysis
    - Thermal properties through TGA and DSC analysis
    - Tensile properties of fibres
    - Interface bonding of hemp fibre reinforced polyester composites through the mechanical property (tension, compression, sheer, bending and impact testing) analysis of fibre composites.

Outline of thesis

This thesis is divided into 8 chapters.

Chapter 1 is an introduction and outlines the objectives of the study undertaken.

Chapter 2 entails a literature review which highlights fundamental knowledge and the current developments of the topic that is being investigated in this dissertation. This chapter begins by outlining the main constituents of both conventional synthetic fibre and natural fibre composites. The structure and properties of natural fibres are highlighted. Problems and inherent shortfalls associated with natural fibres that contribute to reduced composite properties are then listed. Fibre modification methods through various chemical treatments are discussed in order to improve fibre composite properties.

Chapter 3 covers the experimental process component of the dissertation. It describes in detail the equipment used, composite preparation and manufacturing methodology and the characterisation methods that were utilised. The chemical treatment processes that were applied to hemp fibres are extensively described and the manufacturing process used to prepare composites is outline. The testing procedures of fibre and their composites are presented.

Chapter 4 lists and explains the effects of chemical treatments on the fibre in terms of fibre constituents, structure, morphology and thermal properties.

Chapter 5 focuses on the effects of chemical treatments on fibre strengths.

Chapter 6 characterises the effects of treatments on fibre composite properties. Tension, compression, shear, flexure and impact properties of the composites are presented and discussed.

Chapter 7 discusses the effects of chemical treatments on sandwich structures through a mechanical properties analysis.

Chapter 8 concludes this body of research by presenting the conclusions drawn from the study. Recommendations for future work are offered.

Chapter 2: Literature Review

2.1 Introduction

Increasing environmental awareness throughout the world has greatly impacted materials engineering and design. Renewed interest in the utilisation of natural materials addresses ecological issues such as renewability, recyclability and environmental safety. Currently, synthetic fibres like glass, carbon and aramid are being widely used in polymer-based composites because of their high strength and stiffness properties (Rout, et al. 2001). However, these fibres have serious drawbacks in terms of their biodegradability, initial processing costs, recyclability, energy consumption, machine abrasion, health hazards, etc. (Bledzki & Gassan 1999). Most significantly, adverse environmental impact alters the attention from synthetic fibres to natural/renewable fibres. In recent years, the introduction of natural fibres (from annually renewable resources) as reinforcements in the polymer matrix is receiving great attention (Rout, et al. 2001).

Natural fibres like flax, hemp, jute, sisal etc. have been well recognised as good potential reinforcements for engineering fibre composites. The advantageous features of these fibres are that they are light in weight, have a high specific modulus, are non-toxic and are easily processed (Abdelmouleh, et al. 2007; Tserki, et al. 2005). These benchmarking properties open up the wide area of natural fibres to the composite sector and challenge the use of synthetic fibres. The successful use of these fibres is dependent on their well defined structural and mechanical properties. These properties are influenced by the locality in which they originate, climate conditions, age of the plants and the extraction methods that are used. These

parameters determine the characterisation factor for fibres (Bledzki & Gassan 1999; Tserki, et al. 2005).

However, natural fibres are not a problem-free alterative and they possess certain shortfalls in properties. Their structural constituents (cellulose, hemicellulose, lignin, pectin and waxy substances) allow moisture absorption from the environment which leads to poor bonding with the polymer matrix materials (Doan, Gao & Mader 2006). Therefore, certain chemical treatments on the surface of natural fibres are needed. These treatments are usually based on the use of reagent functional groups that are capable of reacting with the fibre structures thus changing their composition. The treatment is to reduce the tendency of moisture absorption of the fibres and facilitate greater compatibility with the polymer matrix (Abdelmouleh, et al. 2007). Many academics and industries focus on the improved compatibility of fibre and the polymer matrix.

2.2 Conventional fibre composites

Generally, a composite is a material mixture created by a synthetic/natural assembly of two or more physically and chemically distinct components. The first component is a selected reinforcing agent (discontinuous phase) whilst the second is a compatible matrix binder (continuous phase) (Bledzki & Gassan 1999). These two components are combined to achieve specific characteristics and properties. Different types of natural fibres, matrix and processing techniques are used for composite fabrication.

2.2.1 Fibre reinforcements

Fibres are strategically placed in the matrix with specific orientations to meet required strength and stiffness properties of the composites. The performance and load distribution of a fibre reinforced composite depends on its reinforcing fibre length, shape, orientation, content and composition in the matrix. The uniform load distribution from matrix to fibre enhances the composite properties under different loading conditions. The reinforcement orientation is capable of changing failure mechanisms and enhancing their composite properties as desired.

Long continuous unidirectional fibre, twisted fibre (yarn), woven fabrics and short discontinuous randomly oriented fibre are commonly used as reinforcement in composites. Long and unidirectional fibre with 0° orientation to the applied load, provides a continuous load transfer throughout the composite area. Optimum performance from longitudinal fibre reinforced composites can be obtained if the load is applied along its fibre direction. Conversely, fibre orientation perpendicular to the loading direction (90°) possesses very low transverse stress as fibre cannot act as a primary load carrying component. Cross play fabric, especially with 0° and 90° fibres orientation, shows good stress distribution in a longitudinal direction (0°) but the opposite results in a transverse direction (90°) (Ilomaki 2012).

The twisted fibre limits complete wet-out by the matrix, as fibre twisting prevents complete penetration of liquid matrix into the fibre bundle. During loading fibre may have less matrix support which reduces its composite mechanical properties.

Hybrid laminates combine different fibres and ply orientation within a matrix, aiming to produce a part that has high strength and stiffness properties (Esfandiari 2007). Similarly, a sandwich structure consisting of two stiff skins separated by a core material, aiming to produce a part that has high toughness values (Manalo, Aravinthan & Karunasena 2010). The load distribution of hybrid laminate and sandwich structures are complex as different material properties contribute to the load transfers mechanisms throughout the composite cross-sections.

Random fibre orientation in the matrix generates a discontinuous load transfer throughout its composites. Due to this, complex load distribution and non-uniform stress concentration take place in the matrix which may develop matrix cracking, debonding and failure of the composites. As a result, random fibre orientations in the matrix exhibit lower mechanical properties of the composites than the unidirectional fibre composites (Ilomaki 2012).

2.2.2 Polymer matrices

A matrix is a binding material that is used to hold the reinforcements (fibre). A polymer matrix provides support to the fibre, assists the fibre in carrying load, and usually has lower strength than the fibre. When load is applied to the composite assembly, the matrix distributes the loads evenly among the fibres (Joseph, et al. 2003; Khalil, et al. 2001; Pickering, et al. 2007). The matrix also protects the fibres from the environment and gives stability to the composite material.

Polymer matrix used in fibre composites are generally classified as thermosets and thermoplastics (Hayes & Gammon 2010). Thermosets have low viscosity which

provides good fibre wetting. Unsaturated polyester, vinyl esters and epoxy are the most commonly used as thermoset matrices. Catalyst is used to initiate the chemical reaction of these matrices and is transferred from a liquid to solid state. Thermosets undergo irreversible chemical cross-linking reactions upon heating and curing. Cured thermosets are infusible and insoluble materials. In addition, cured matrices have good mechanical properties, are easily processed and are resistant to environmental degradation. Thermosets have high glass transition and decomposition temperature, high ultimate strength and modulus (Hayes & Gammon 2010). However, cured matrices are brittle which results in poor resistance to crack propagation.

Conversely, thermoplastics do not undergo a chemical reaction on application of heat. Rather, they melt at an elevated temperature and pressure. Thermoplastics can be repeatedly reshaped by heating and hardened by cooling, as their viscosity changes under different temperatures. Polyethylene, polyamides (nylon), polyurethane, polyetheretherketone, and polyphenylene are commonly used as thermoplastic matrix (Ku, et al. 2011). These matrices do not require additional curing and thus necessitate less time to produce a part. There are a number of problems associated with incorporating fibres into thermoplastic matrices. Thermoplastics have high viscosity and thus high temperature and pressure must be employed for fibre wetting (Muzzy & Kays 1984). The reinforcing fibre may experience thermal damage with the high processing temperatures. When the material is dried, shrinkage of the fibres may take place resulting in dimensional instability, propagation of debonding, cracks and severe deterioration of mechanical properties. Table 2.1 outlines the differences in properties of thermoset and thermoplastic matrices (Joseph, PV, et al. 2003).

Table 2.1: Comparison of thermoset and thermoplastic matrices (Joseph, PV, et al. 2003)

	Advantages	Disadvantages
Thermoset	- Low viscosity - Good fibre wetting - Excellent thermal stability once polymerised - Chemically resistant	- Brittle - Non-recyclable via standard techniques - Not post-formable
Thermoplastic	- Recyclable - Easy to repair by welding and solvent bonding - Post formable - Tough	- Poor melt flow - Need to be heated above the melting point for processing purposes.

2.2.3 Fibre matrix interface

The interface is a boundary region where fibre and matrix phases come in contact with zero thickness (Khalil, et al. 2001). Matrices are connected to the fibre surface by chemical reaction, absorption and mechanical interlocking. Chemical reaction takes place between the fibre functional groups and the matrix monomers. The absorption occurs between the primary forces (forms ionic and covalent bonds) and the secondary forces (created by van der Waals forces, dipole interaction, dispersion interaction, hydrogen bonds and acid base interactions). Mechanical interlocking occurs when the liquid matrix is made to flow on the fibre surface. A strong interface is required for efficient load transfer from matrix to fibre to enhance the composites mechanical properties (Mohanty, Misra & Drzal 2005). Interface bonding strength can be evaluated through different mechanical property analyses of the composites such as tension, compression, shear, bending and impact tests.

2.2.4 Composite fabrication techniques

In principle, processing techniques of natural fibres composite are similar to those utilised in processing of synthetic fibres composite. Depending on the length, orientation and type of the fibre; randomly oriented (short), unidirectional (raw and carded) and woven fabrics are used as reinforcements in thermoset and thermoplastic matrices (Beckermann 2007).

For thermoset composites, the basic fabrication method is known as hand layup (Mohanty, Misra & Drzal 2005). This is a manual mixing procedure between the fibre and matrix. In this process, the uniformity of the composite in terms of thickness, fibre-to-matrix ratio and void content throughout the sample, depend on the workmanship. Conversely, in vacuum assisted resin transfer moulding (VARTM), resin is pulled inside the mould under vacuum pressure and mixed with the fibres. Under this condition, the resin impregnation quality in a composite is much better than that fabricated by the hand layup technique and the void content can be kept as minimal. Another method known as pultrusion, is used for both thermosets and thermoplastics. The composite profile is produced by pulling the reinforcement through a heated die which is then mixed with the matrix.

For the thermoplastic matrix, compression moulding (reinforcement is mixed with the matrix and pressed with a heated plate) and injection mouldings (fibre-resin is added as granulate to the machine and melted into fluid mass, then injected under high pressure into the form) are used for composite fabrication (Adekunle, Akesson & Skrifvars 2010). These processes involve high temperature (over 200°C) and pressure (5 MPa) for complete mixing between the fibre and matrix.

2.2.5 Composite properties

Composites are macroscopically inhomogeneous as the reinforcing fibres and matrix have different material properties. To characterise the composites as a combined material, require further property analysis to ensure that the component satisfies product requirements and material limitations.

Composites have different mechanical properties under different loading conditions. Under the tensile loading, the matrix plays a minor role, whilst fibre can sustain higher tensile load parallel to the fibre direction. In the case of compression loading, the matrix prevents the fibres from buckling. Generally, unidirectional fibre composites are stronger in tension but weaker in compression (Fleck & Liu 2001; Jelf & Fleck 1992). The combination of tension and compression produces friction due to the fibre sliding from the surrounding matrix and exhibiting shear properties. During bending, the composite undergoes tension, compression and shear deformation. The frictional resistance and ultimate composite failure reflects the energy absorption capacity of the material which can be measured through impact property analysis.

Composite property can also be investigated through micro-structural analysis. Micro-structure analysis is a valuable tool for materials investigation, failure analysis and quality analysis. The most widespread micro-structural analysis of fibre composites is done by using an optical microscope (OM) and scanning electron microscope (SEM). The use of a reflected-light (OM) and infrared beam (SEM) provides insight through detailed analysis of the fibre surface, fibre microstructure,

fibre orientation into the matrix, degree of fibre matrix interface bonding, void content, failure mechanisms, etc. (Ilomaki 2012).

2.3 Natural fibres

Plant based natural fibres are lignocellulosic in nature and are composed of cellulose, hemicellulose, lignin, pectin and waxy substances. The structural constituents of fibres are presented in Table 2.2 (Fakirov & Bhattacharyya 2007; Mohanty, Misra & Hinrichsen 2000). The contents (weight %) of structural constituents are varied in accordance to different natural fibre. The cellulose content ranges from 60-80%, lignin content ranges from 1-15% and hemicellulose content ranges from 5-20%. The other constituents are extractives (pectin, wax) which are usually less than 10% of the total weight of the dry fibre.

Table 2.2: Structural constituents of natural fibres (Fakirov & Bhattacharyya 2007; Mohanty, Misra & Hinrichsen 2000)

Name of the Fibres	Cellulose (wt%)	Lignin (wt%)	Hemicellulose (wt%)	Pectin (wt%)	Wax (wt%)	Micro-fibril/spiral angle (^{0})	Moisture Content (wt%)
Bast Fibres							
Jute	61-71.5	12-13	13.6-20.4	0.2	0.5	8.0	12.6
Flax	71	2.2	18.6-20.6	2.3	1.7	10.0	10.0
Hemp	70.2-74.4	3.7-5.7	17.9-22.4	0.9	0.8	6.2	10.8
Ramie	68.6-76.2	0.6-0.7	13.1-16.7	1.9	0.3	7.5	8.0
Leaf Fibres							
Sisal	67-78	8.0-11.0	10.0-14.2	10.0	2.0	20.0	11.0
PALF	70-82	5-12	-	-	-	14.0	11.8
Seed Fibres							
Cotton	82.7	0.7-1.6	5.7	-	0.6	-	33-34

Figure 2.1 shows schematically the structural composition of a natural fibre in which the fibre stem consists of fibre bundles (Kasuga, et al. 2001). Each fibre bundle

contains individual technical fibres and technical fibres consist of elementary fibres. The elementary fibre consists of microfibrils. Microfibrils are the basic unit of cellulose. Cellulose is glued together by hemicellulose and lignin constituents.

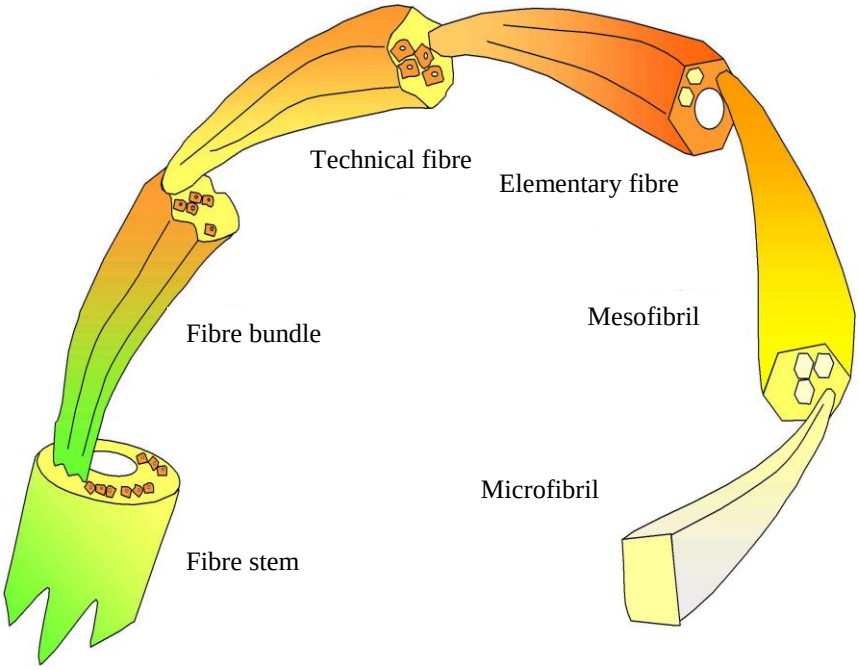

Figure 2.1: Composition of natural fibre (Kasuga, et al. 2001)

The elementary fibre structure consists of multi cell walls. Figure 2.2 shows a schematic structure of a elementary fibre cell wall and Figure 2.3 presents the model of the structural organisation of the three major structural constituents (cellulose, hemicellulose and lignin) (Madsen 2004). In accordance with a specific type of fibre, each fibre cell wall is made up of two distinct parts, namely the primary cell wall and the secondary cell wall, which again, is made up of three layers (S_1, S_2 and S_3). These layers contain varying amounts of cellulose, hemicellulose and lignin constituents. The fibre structure develops in the primary cell wall and is deposited during its growth (John & Anandjiwala 2008). The cellulose content increases

steadily from primary to secondary walls, while the hemicellulose amounts are similar in both walls. However, lignin content decreases from primary to secondary walls. Cellulose content is highest at the secondary cell wall and is composed with crystalline and amorphous cellulose microfibrils which are bonded together by amorphous hemicellulose and lignin. The secondary cell wall makes up the fibre diameter and determines its mechanical properties.

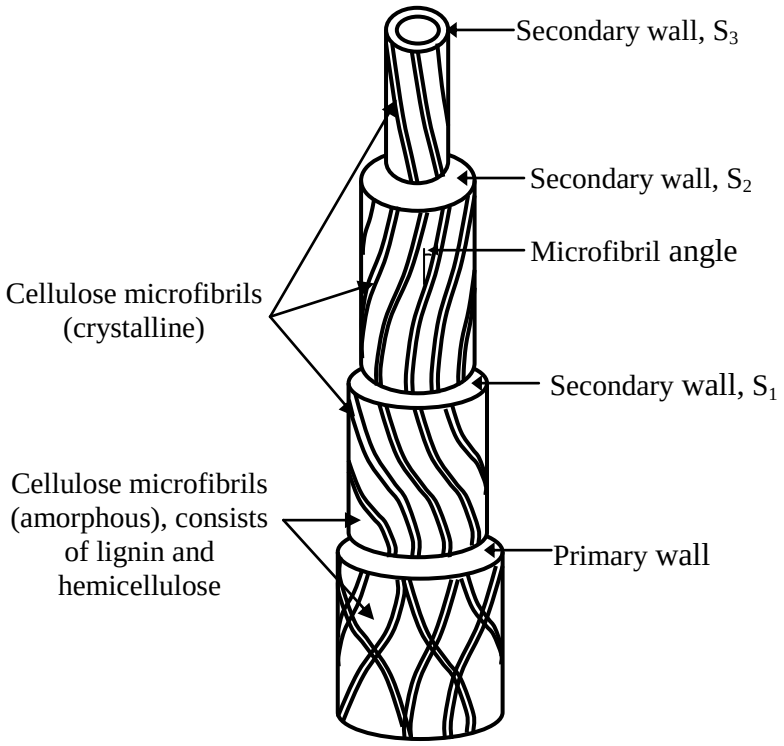

Figure 2.2: Structure of elementary fibre (Madsen 2004)

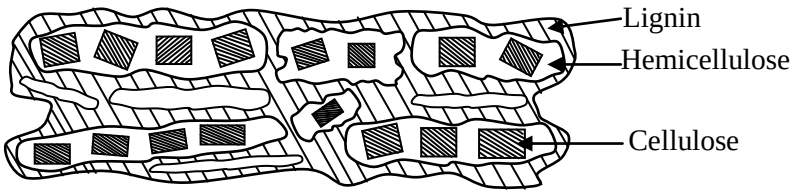

Figure 2.3: Structural organisation of the three major constituents in the fibre cell wall (Madsen 2004)

Cellulose is considered the major framework component of the fibre structure. It provides strength, stiffness and structural stability of the fibre. The chemical structure of cellulose (Figure 2.4a (Bledzki & Gassan 1999)) consists of three hydroxyl groups (-OH). Two of these form hydrogen bonds within the cellulose macromolecules (intramolecular) whilst the rest of the group forms a hydrogen bond with other cellulose molecules (intermolecular) (Mwaikambo & Ansell 2002).

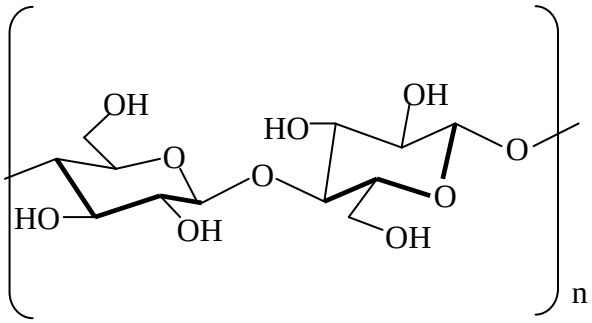

(a)

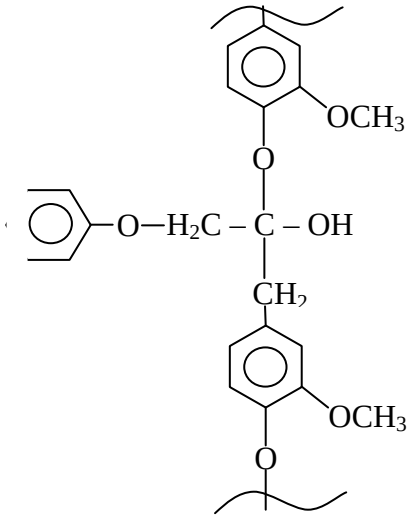

(c)

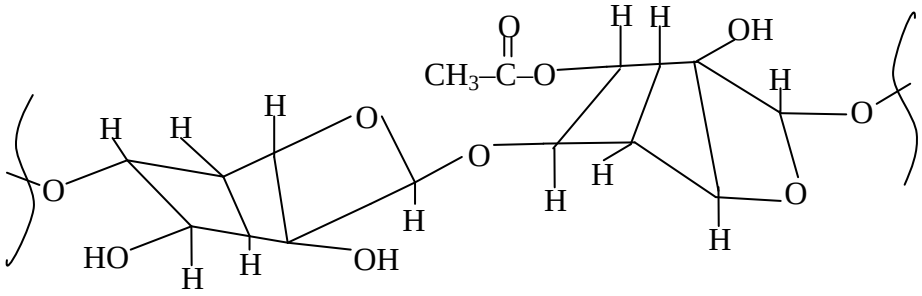

(b)

Figure 2.4: Chemical structure of (a) cellulose (b) hemicellulose and (c) lignin (Bledzki & Gassan 1999, Saheb & Jog 1999)

Hemicellulose occurs mainly in the primary cell wall and has branched polymers (Figure 2.4b) structures. Hemicellulose is completely amorphous and has a lower molecular weight than cellulose (Mwaikambo & Ansell 2002). Hemicellulose molecules are hydrogen bonded with cellulose microfibrils and they form cementing materials for the fibre structure.

Lignin is amorphous and has an aromatic structure (Figure 2.4c) (Saheb & Jog 1999). Lignin is coupled with the cellulose-hemicellulose network and provides an adhesive quality to hold the microfibrils together as a fibre unit, as well as joining the adjacent fibres together to form a fibre bundle. This adhesive quality provides the strength and stiffness properties of the fibre. There are also small amounts of other organic (extractives) and inorganic (ash) components present in the fibre structure. These organic extractives are responsible for colour, odour and decay resistance, whilst the inorganic constituents enhance the abrasive nature of the fibre.

Generally, fibres with a higher cellulose content and a lower microfibrillar angle (the angle between the fibre axis and cellulose microfibrilis) have better strengths (Fakirov & Bhattacharyya 2007; Mwaikambo & Ansell 1999). Mechanical properties of natural fibre over synthetic fibre are presented in Table 2.3 (Dhakal, Zhang & Richardson 2007; Fakirov & Bhattacharyya 2007; Mohanty, Misra & Hinrichsen 2000). Although natural fibres have relatively lower strengths compared to the synthetic fibres, the specific modulus and elongation at break signifies the potentiality of these fibres to replace synthetic fibres in engineering polymer composites.

Table 2.3: Comparative properties of natural fibres with conventional manmade fibres (Dhakal, Zhang & Richardson 2007; Fakirov & Bhattacharyya 2007; Mohanty, Misra & Hinrichsen 2000)

Name of fibres	Density (g/cm^3)	Tensile strength (MPa)	Young`s modulus (GPa)	Specific strength ($GPa/g/cm^3$)	Specific modulus ($GPa/g/cm^3$)	Elongation at break (%)
Jute	1.3-1.4	393-773	13-26.5	0.3-0.5	10-18.3	1.16-1.5
Flax	1.50	345-1100	27.6	0.2-0.7	18.4	2.7-3.2
Hemp	1.14	690	30-60	0.6	26.3-52.6	1.6
Ramie	1.50	400-938	61.4-128	0.3-0.6	40.9-85.3	1.2-3.8
Sisal	1.45	468-640	9.4-22.0	0.3-0.4	6.4-15.2	3-7
PALF	1.52	413-1627	34.5-82.51	0.3-1.1	22.7-54.3	1.6
Cotton	1.5-1.6	287-800	5.5-12.6	0.2-0.5	3.7-7.8	7.0-8.0
E-glass	2.5	2000-3500	70	0.8-1.4	28	2.5
S-glass	2.5	4570	86	1.8	34.4	2.8
Aramid	1.4	3000-3150	63-67	2.1-2.2	45-47.8	3.3-3.7

2.4 Issues in natural fibre composites

The properties of natural fibre reinforced polymer composites are generally governed by the fibre properties and the quality of fibre matrix interface bonding. The inconsistent fibre structure, hydrophilicity of fibre, poor fibre compatibility into the matrix and low thermal resistance of fibre are the main causes of the reduction of the composites' thermal and mechanical properties.

2.4.1 Hydrophilicity of fibre

Natural fibre consists of cellulose microfibrils which are covered by hemicellulose and lignin constituents. The cellulose structure of the fibres is distinguished through crystalline and amorphous regions, whereas hemicellulose and lignin are completely amorphous (Figure 2.2). In cellulose crystalline region, large numbers of strongly linked hydroxyl groups are present. These hydroxyl groups are inaccessible and so other chemicals have difficulty penetrating the crystalline region (Figure 2.5) (Walker 2006). However, in the amorphous region, the hydroxyl groups are loosely

linked with the fibre structure and are relatively free to react with other chemicals. Due to this freedom, hydroxyl groups present in the amorphous region can easily combine with water molecules from the atmosphere. The hydroxyl groups present in the amorphous hemicellulose and lignin initially give the access of water molecules to penetrate the fibre surface. Water molecules then combine with the hydroxyl groups that are present in cellulose (in the amorphous region) and stay in the fibre structure. This makes the fibre hydrophilic and polar in character.

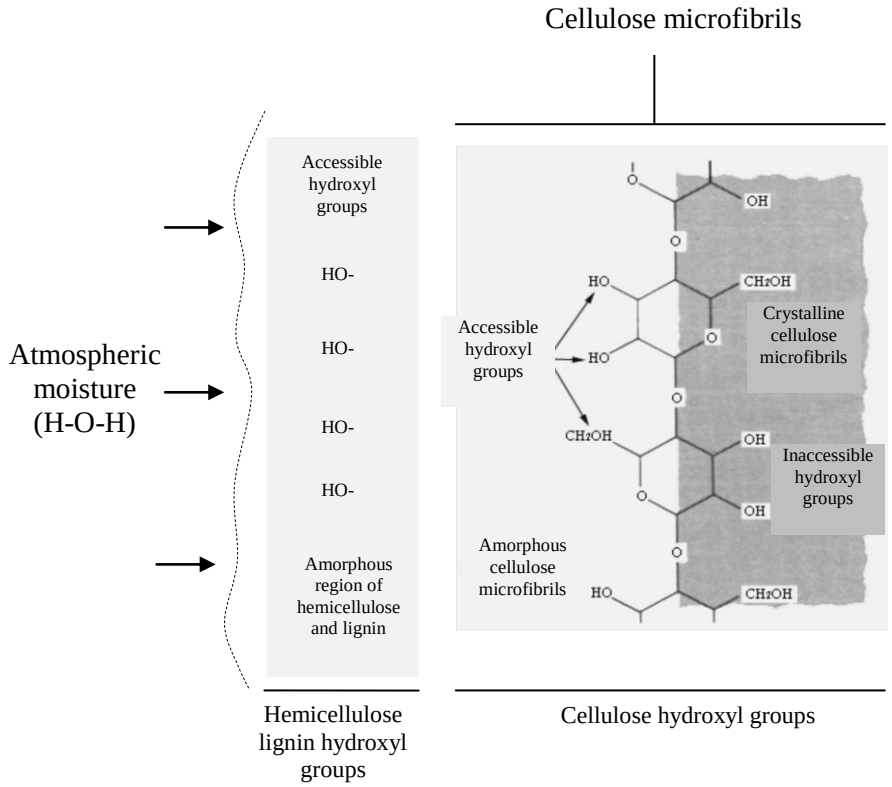

Figure 2.5: Schematic presentation of the orientation of fibre constituents that absorb moisture (Walker 2006)

The hydrophilic fibres are incompatible with most hydrophobic thermoset and thermoplastic matrices. As a result, incomplete fibre wetting into the matrix takes place and weak bonding exists at their interfaces. In addition, the hydrophilic fibre causes fibre swelling within the matrix. Fibre swelling generates extra stresses on the

surrounding matrix. Weak interface bonding and the induced swelling stress results in propagation of debonding, cracks and severe deterioration of composites' mechanical properties (Zakaria & Poh 2002). In order to develop composites with good properties, it is necessary to improve the interface bonding strength between the fibre and matrix. Therefore, the removal of moisture from fibres is an essential step for the preparation of composites. The moisture absorption of fibres can be reduced by eliminating the hydroxyl groups in amorphous region from the fibre structure through different chemical treatments (Wang, et al. 2007). Chemical reagents contain functional groups that are capable of forming chemical bonds with the hydroxyl groups of the fibre, thus providing good compatibility with the matrix. Interfacial compatibility improves the stress transfer at the interface and leads to the improvement of mechanical properties of the produced composites.

2.4.2 Inconsistence fibre properties

The physical dimensions of natural fibre are not uniform throughout its length. The elementary fibre that comes from different parts of a plant has various lengths and widths. Several elementary fibres associate with one another to form fibre structures, which also have diverse lengths and widths. This variable fibre dimension affects the fibre aspect ratio (length/diameter) which is a critical parameter for composite properties. The critical fibre aspect ratio is defined as the minimum ratio in which the maximum fibre stress can be achieved for a given load (Joseph, et al. 2003). The critical fibre length determines greater load transfer from the fibre to matrix through the interface.

2.4.3 Poor fibre compatibility into the matrix

The incorporation of natural fibres into a matrix is often associated with poor fibre compatibility as their cellulose surface is covered by the hemicellulose and lignin constituents. Hemicellulose and lignin act as a weak boundary layer between the cellulose (elementary fibre) and the matrix. Due to the presence of weak boundary layer at the fibre matrix interface, the stress distribution capacity throughout the composite area is reduced. To obtain a satisfactory performance of the composite, it is necessary to remove the weak boundary layers from the elementary fibres. A weak boundary layer can be removed by dissolving hemicellulose and lignin coverings through different chemical treatments of the fibre.

2.4.4 Fibre degradation at high temperature

Natural fibre generally starts degrading at about 240°C. Structural constituents of the fibre (cellulose, hemicellulose, lignin etc) are sensitive to different ranges of temperature. It was reported that, hemicellulose starts degrading at a temperature around 200°C and cellulosic constituents degraded at higher temperatures (Joseph, et al. 2003). Fibre degradations result in the exclusion of some high temperature manufacturing processes (Hayes & Gammon 2010). Thermal stability of the fibre can be enhanced by removing certain proportions of hemicellulose and lignin constituents through different chemical treatments. The degradation of natural fibres is an important issue in the development of composites in both manufacturing (curing, extrusion or injection moulding) and materials in service (Sgriccia, Hawley & Misra 2008; Taj, Munawar & Khan 2007).

2.5 Surface treatment of natural fibres

Natural fibre reinforced thermoset and thermoplastic matrices have inherently poor mechanical properties due to weak interface bonding between the fibres and matrix. To enhance interfacial bonding, modifications of fibre can be made by using different chemical treatments on the reinforcing fibre. Chemical treatments allow cellulose surface to react with the matrix (Dash, et al. 2000). Due to this, strong fibre-matrix interface bonding can be achieved which ultimately results in greater mechanical properties of the composites.

Several research activities have been conducted to improve fibre adhesion properties with the matrix through chemical treatments. The following are reviews of different chemical treatments on the fibre, and their effects on composite properties.

2.5.1 Alkaline treatment

The treatment on natural fibres by sodium hydroxide (NaOH) is being widely used to modify fibre structure. Natural fibre absorbs moisture due to the presence of hydroxyl groups in the amorphous region of cellulose, hemicellulose and lignin constituents. During alkali treatment, alkalised groups (NaO-H) react with these hydroxyl groups (-OH) of the fibre and produce water molecules (H-OH) which are consequently removed from the fibre structure. Then the remaining alkalised groups (Na-O-) react with the fibre cell wall and produce Fibre-cell-O-Na groups (John & Anandjiwala 2008). The chemical reaction of the fibre-cell and NaOH is presented in Equation 2.1. These chemical activities reduce the moisture related hydroxyl groups (hydrophilic) and thus improve the fibres' hydrophobicity. Treatment also takes out a certain portion of hemicellulose, lignin, pectin, wax and oil coverings (weak

boundary layer) from the cellulose surface (Li, Tabil & Panigrahi 2007; Mwaikambo, Tucker & Clark 2007; Ray, et al. 2001). As a result, cellulose microfibrils are exposed to the fibre surface. Consequently, treatment changes the orientation of the highly packed crystalline cellulose order, forming an amorphous region (Beckermann & Pickering 2008). This amorphous region of cellulose can easily mix with matrix materials and form strong interface bonding which results in greater load transfer capacity of the composites.

$$\text{Fibre-cell-OH} + \text{NaOH} \longrightarrow \text{Fibre cell-O}^{-}\text{Na}^{+} + \text{H}_2\text{O} \qquad (2.1)$$

Alkaline treatment also separates the elementary fibres from their fibre bundles by removing the covering materials. Thus increasing the effective surface area of fibre for matrix adhesion, and improving the fibre dispersion within the composite. Treated fibre surfaces become rougher, which can further improve fibre-matrix adhesion by providing additional fibre sites for mechanical interlocking (Joseph, et al. 2003). Mechanical and thermal behaviours of the composite are improved significantly by this treatment. However, too high of alkali concentration can cause an excess removal of covering materials from the cellulose surface, which results in weakening or damage to the fibre structure (Li, Tabil & Panigrahi 2007; Wang, et al. 2007).

Table 2.4 summaries the recent results of alkali treatments on natural fibres and their effects on the mechanical and thermal properties of the composites. From Table 2.4 it can be observed that a wide range of different treatment concentrations (NaOH), time and temperature were used on different plant based natural fibres. The treatment effects were presented in terms of thermal and mechanical properties of their

composites. It is important to select a treatment condition for a particular natural fibre (such as hemp fibre) to analyse the treatment effects on the fibre structure (cellulose, hemicellulose and lignin) and the morphological changes. These changes need to be systematically explored through the thermal property analysis of the fibre, compatibility with the matrix and their composites' mechanical property analysis.

Table 2.4: Recent works on alkali treated fibre composites

Fibre matrix composites	Applied treatment methods	Results on mechanical and thermal properties	References
Flax-Epoxy	NaOH treatment	30% increase in tensile strength and modulus.	(Li, Tabil & Panigrahi 2007)
Sisal-Polyester	Various concentrations of NaOH treatment at room temperature	4% alkali treatment reported maximum tensile strength.	(Li, Tabil & Panigrahi 2007)
Hemp-Euphorbia	0.16% NaOH for 48 hours	Tensile strength was increased by 30% and doubled the shear strengths.	(Mwaikambo, Tucker & Clark 2007)
Jute-Vinylester	5% NaOH for various times	4 hour alkali treated composite accounted for 20% and 19% increase in flexural strength and interlaminar shear strength.	(Ray, et al. 2001)
Sisal-Polycaprolactone	10% NaOH for various times	Increase in elastic modulus with the increase in reaction time.	(Vallo, et al. 2004)
Hemp fibre	8% NaOH treatment	Thermal stability was increased by 4%.	(Ouajai & Shanks 2005)
Coir-Polyester	5% NaOH treatment for 72 hours	Flexural and impact strength was increased by 40% with respect to the untreated fibre composites.	(Prasad, Pavithran & Rohatgi 1983)

2.5.2 Acetyl treatment

Acetyl treatment is known as the esterification method to modify the natural fibre structure. The acetyl group (CH_3CO-) reacts with the hydroxyl groups (-OH) that

present in the amorphous region of the fibre and remove the existing moisture, thus reducing the hydrophilic nature of the fibre (Bledzki, et al. 2008). Moreover, treatment provides rough fibre surface topography that gives better mechanical interlocking with the matrix (Li, Tabil & Panigrahi 2007; Tserki, et al. 2005). Treatment also improves the fibres dispersion in to the matrix and thus enhances dimensional stability of the composite. Acetylation process with and without acid catalyst on fibre are given in Equations 2.2 and 2.3 (Mwaikambo & Ansell 1999).

Acetylation with acid catalyst

$$\text{Fibre-OH} + CH_3COOH \xrightarrow[\text{Conc. } H_2SO_4]{(CH_3CO)_2O} \text{Fibre} - O - \overset{\overset{O}{\|}}{C} - CH_3 + H_2O \qquad (2.2)$$

Acetylation without acid catalyst

$$\text{Fibre-OH} + CH_3 - \overset{\overset{O}{\|}}{C} - O - \overset{\overset{O}{\|}}{C} - CH_3 \longrightarrow \text{Fibre} - O - \overset{\overset{O}{\|}}{C} - CH_3 + CH_3C\text{ - OH} \qquad (2.3)$$

Fibres are acetylated with and without an acid catalyst to graft the acetyl groups onto the cellulose surface. In general, acetic acid does not react sufficiently with the fibres. As a result, it is necessary to use a catalyst to speed up the acetylation process. Acetic anhydrides, pyridine, sulphuric acid, potassium and sodium acetate etc. are commonly used catalysts for acetylation process. However, strong acid catalysts cause hydrolysis of cellulose which in results the damaging of the fibre structure. For this, selection of catalyst is an important factor for the acetyl treatment. The acetylation process is also influenced by the reaction time. Longer reaction time allows acetic anhydride (catalyst) to access fibre constituents. The reagent then reacts with hemicellulose and lignin constituents and removes them from the fibre,

resulting in the opening of cellulose surface to allow reaction with the matrix molecules.

Mwaikambo & Ansell (1999) used acetic acid and acetic anhydride (catalyst) to treat hemp, flax, jute and kapok fibres. Rowell & Young (1997) investigated acetic anhydride treatment on different types of natural fibres to analyse the effects of equilibrium moisture content. They reported improved moisture resistance properties of the treated fibres. This was due to the removal of hemicellulose and lignin constituents from the treated fibre. Mishra, et al. (2003) used an acetic anhydride treatment (with glacial acetic acid and sulphuric acid) on an alkali pre-treated (5% and 10% NaOH solution for an hour at 30°C) sisal fibre and reported, improved fibre matrix adhesion of the final composites. Bledzki, et al. (2008) studied different concentrations of acetyl treatment on flax fibre and reported 50% higher thermal properties. Moreover, 18% acetylated flax fibre polypropylene composites showed 25% higher tensile and flexural properties as compared to the untreated fibre composites.

2.5.3 Silane treatment

Silane is a multifunctional molecule which is used as a coupling agent to modify fibre surfaces. Silane molecules form a chemical link between the fibre surface and the matrix through a siloxane bridge. Silane undergoes several stages of hydrolysis, condensation and bond formation during the treatment process of the fibre. Silane forms silanol in the presence of fibre moisture (hydrolysis, see Equation 2.4 (Sreekala, et al. 2000)). During the condensation process, one end of silanol reacts with the cellulose hydroxyl group (Si-O-Cellulose, see Equation 2.5 (Sreekala, et al.

2000)) and the other end reacts (bond formation) with the matrix (Si-Matrix) functional group. This co-reactivity provides molecular continuity across the interface of the composite. It also provides the hydrocarbon chain that restrains the fibre swelling into the matrix (George, Sreekala & Thomas 2001; Wang, et al. 2007). As a result, fibre matrix adhesion improves and stabilises the composite properties (Li, Tabil & Panigrahi 2007). Natural fibres exhibit surface micro-pores and silane couplings act as surface coatings to penetrate the pores. In this case, silane coating is used as a mechanical interlocking material for the fibre surface.

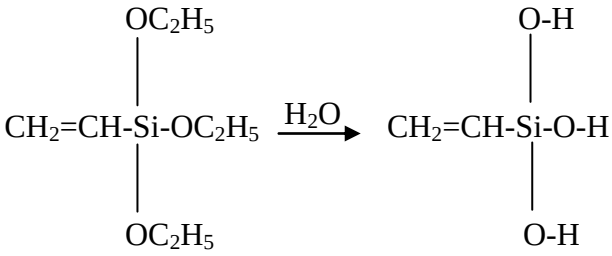

(2.4)

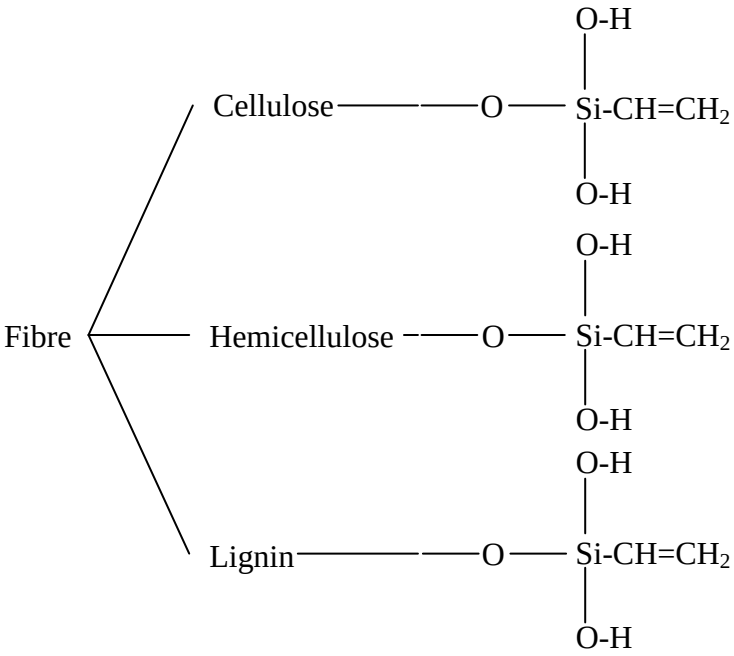

(2.5)

During the silane treatment, hydroxyl groups on the fibre surface are covered by silane molecules. Due to this, hydroxyl groups that presents in hemicellulose and lignin constituents cannot absorb the atmospheric moisture. As a result, moisture absorption capacity of the treated fibres is reduced.

Seki (2009) investigated the effect of alkali (5% NaOH for 2 hours) and silane (1% oligomeric siloxane with 96% alcohol solution for an hour) treatments on flexural properties of jute-epoxy and jute-polyester composites. For jute-epoxy composites, silane over alkali treatments showed about 12% and 7% higher strength and modulus properties compared to the alkali treatment alone. Similar treatments reported around 20% and 8% improvement for jute-polyester composites. Sever, et al. (2010) applied different concentrations (0.1%, 0.3% and 0.5%) of silane (γ-Methacryloxy-propyl-trimethoxy-silane) treatments on jute fabrics polyester composites. Tensile, flexural and interlaminar shear properties were investigated and compared with the untreated samples. The results for the 0.3% silane treated sample showed around 40%, 30% and 55% improvement in tensile, flexural and interlaminar shear strength respectively. Silane treated fibre composites provided better tensile strengths than the alkali treated fibre composites (Valadez-Gonzalez, et al. 1999).

2.5.4 Benzoyl treatment

Benzoyl treatment uses benzoyl chloride to decrease the hydrophilic nature of the fibre and improves interfacial adhesion, thereby increasing the strength of the composite. Treatment also enhances the thermal stability of the fibre (Li, Tabil & Panigrahi 2007; Manikandan, Thomas & Groeninckx 2001).

During benzoyl treatment alkali pre-treatment is used. At this stage, extractable materials such as lignin, waxes and oil covering materials are removed from the fibre and more hydroxyl groups (-OH) attached with cellulose are exposed on the fibre surface. Then the fibres are treated with benzoyl chloride. OH groups of the fibre are further replaced by the benzoyl group and it attaches to the cellulose backbone. This results in a more hydrophobic nature of the fibre and improves adhesion with the matrix. The reaction between the cellulosic –OH group of fibre and benzoyl chloride is given in Equations 2.6 and 2.7 (Joseph, et al. 2003).

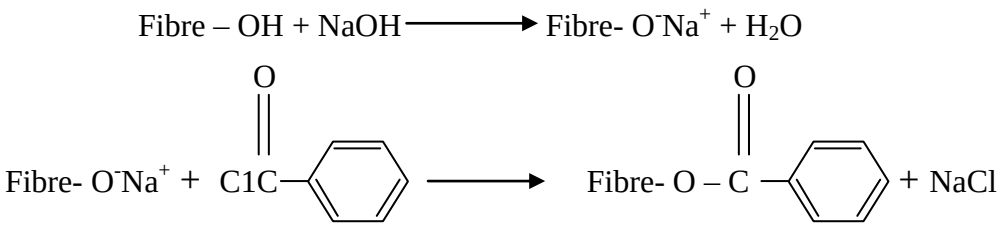

Joseph, Thomas & Pavithran (1996) applied benzoyl chloride treatment on alkali pre-treated sisal fibre and reported higher thermal stability compared to the untreated fibre composites. Similar treatment was carried out on flax fibre reinforced in low density polyethylene composites by Wang, et al. (2007). The reported result was a 6% and 33% higher tensile strength and moisture resistance properties respectively.

2.5.5 Peroxide treatment

Interface properties of fibre and matrix can be improved by peroxide treatment. The peroxide-induced grafting of polyethylene adheres to the fibre surface. Additionally, peroxide initiates free radicals that react with the cellulose surface of the fibre as well as with the matrix. As a result, good fibre matrix adhesion along the interface occurs. This treatment also reduces the moisture absorption capacity of the fibre and

improves thermal stability (Kalaprasad, et al. 2004; Wang, et al. 2007). The reaction between the cellulosic –OH group of the fibre and the peroxide is given in Equations 2.8 and 2.9 (Sreekala, et al. 2000).

$$RO—OR \longrightarrow 2RO \quad (2.8)$$

$$RO + Cellulose – H \longrightarrow R – OH + Cellulose \quad (2.9)$$

R= peroxide functional group

Sapieha, Allard & Zang (1990) reported pre-treatment of fibre by benzoyl (or dicumyl) peroxide and showed higher mechanical properties of the composites. The mechanism of peroxide treatment involves alkali pre-treatment on the fibre then coated with benzoyl peroxide or dicumyl peroxide (around 6% concentration) in acetone solution for 30 minutes. Complete decomposition of peroxide can be achieved by heating the solution at a higher temperature (Kalaprasad, et al. 2004; Li, Tabil & Panigrahi 2007). Joseph, Thomas & Pavithran (1996) investigated optimum concentration of benzoyl peroxide (6%) and dicumyl peroxide (4%) treatments on short sisal fibre-reinforced polyethylene composites and reported improved tensile strengths.

2.5.6 Maleated coupling agents

Maleated coupling agents provide efficient interaction between the fibre surface and matrix. During grafting, maleic anhydride reacts with the hydroxyl groups in the amorphous region of fibre and removes them from the fibre. Treatment also produces a brush like long chain polymer coating on the fibre surface and reduces the hydrophilic tendency. Additionally, maleated coupler forms a carbon-carbon bond to

the polymer chain with the matrix (George, Sreekala & Thomas 2001a). This covalent bonding between the fibre surface and matrix provide balanced properties to make a bridge interface (fibre-matrix) for efficient interlocking (Keener, Stuart & Brown 2004). The reaction mechanism of maleic anhydride, polypropylene (MAPP) and the fibre are presented in Equations 2.10 and 2.11.

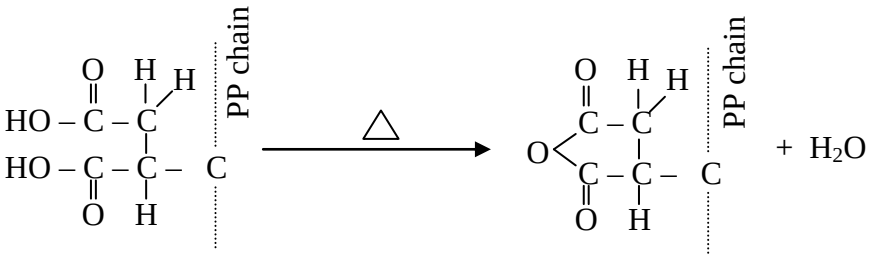

(2.10)

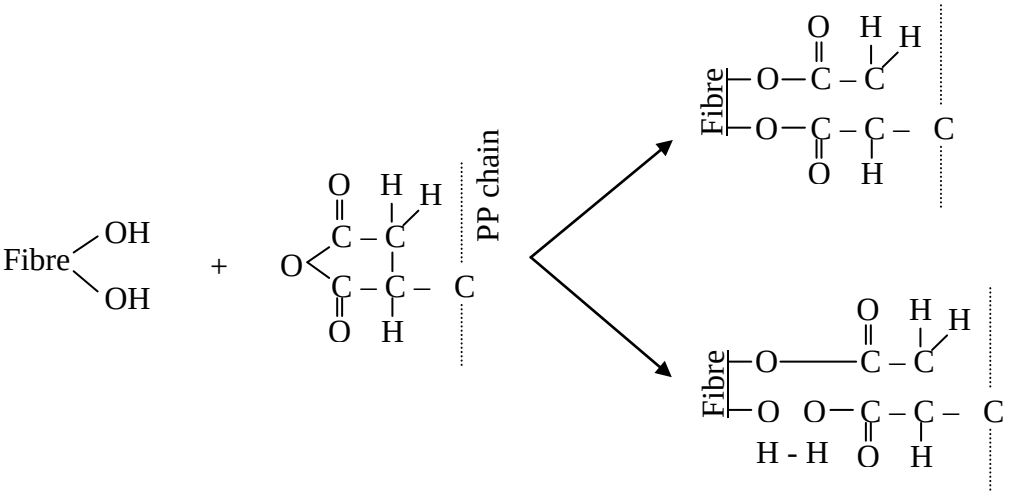

(2.11)

MAPP copolymer is activated at a temperature of 170°C and then the esterification of the cellulose fibres is carried out. This treatment results in better wettability of the fibre and enhanced interfacial adhesion (Keener, Stuart & Brown 2004; Li, Tabil & Panigrahi 2007). Mohanty, et al. (2004) used jute fibre (30% fibre loading, 6 mm on fibre length) treated with a 0.5% MAPP concentration in toluene for 5 minutes and reinforced in a polypropylene (PP) matrix. The composite showed around 72% higher flexural strengths compared to the untreated fibre composites. Water

absorption tendency by the treated fibre composite was also reduced. Similar studies were performed by Mohanty, et al. (2004) who reported that 1% MAPP treated sisal fibre-PP composite exhibited around 50%, 30% and 58% higher tensile, flexural and impact strengths respectively.

2.5.7 Sodium chlorite treatment

Sodium chlorite ($NaClO_2$) is used for the bleaching of fibres in acid solution. $NaClO_2$ is acidified and liberates choleric acid ($HClO_2$), which undergoes an oxidation reaction and forms chlorine dioxide (ClO_2). ClO_2 reacts with lignin constituents and removes them from the fibre. It also reacts with the hydroxyl groups that presents in the hemicellulose (Chattopadhyay & Sarkar 1945). These combined effects remove moisture from the fibre and enhance the hydrophobic fibre nature. After delignification, fibres become more flexible and have lower stiffness properties (Li, Tabil & Panigrahi 2007).

Li, Panigrahi & Tabil (2009) studied the effects of sodium chlorite (sodium chlorite: water = 1: 25 (by weight), at 70°C for 24 hours) treatment on alkali pre-treated (5% NaOH for an hour) sisal fibre and found a higher tensile strength and a lower moisture absorption rate. Similar results were reported by Misra, et al. (2002) on sisal fibre reinforced polyester composites.

2.5.8 Isocyanate treatment

Isocyanate works as a coupling agent for fibre surface modification. The functional group of isocyanate (-N=C=O) reacts with the hydroxyl groups attached in cellulose and lignin constituents of the fibres and, therefore, a urethane linkage is formed. This

chemical linkage provides strong covalent bonds between the fibre and matrix. Isocyanate also reacts with the moisture present on the fibre surface and forms urea which can further react with the hydroxyl groups of the cellulose (George, Sreekala & Thomas 2001). This secondary reaction results in higher moisture resistance properties of the fibre and provides better bonding with the matrix to enhance composite properties (Kalia, Kaith & Kaur 2009). The reaction between the fibre and isocyanate coupling agent is shown in Equation 2.12, where R could be different chemical groups.

$$\text{Fibre} - \text{OH} + \text{R} - \text{N} = \text{C} = \text{O} \longrightarrow \text{Fibre} - \text{O} - \overset{\overset{\text{O}}{\|}}{\underset{|}{\text{C}}} - \overset{\overset{\text{H}}{|}}{\text{N}} - \text{R} \qquad (2.12)$$

George & Verpoest (1999) used isocyanate with dimethyl formamide (DMF) solvent to treat flax fibre. The DMF solvent has a higher boiling point and better solubility with isocyanates and the fibre. Due to this, thermal stability of the fibre was increased. Compared to the untreated fibre composite, the resultant treated (flax-epoxy) fibre composite showed 13% and 18% higher tensile strength and modulus properties respectively.

2.5.9 Stearic acid treatment

Stearic acid ($CH_3(CH_2)_{16}COOH$) in ethyl alcohol solution is used to modify fibre surfaces. The carboxyl group of stearic acid reacts with the hydrophilic hydroxyl groups of the fibre and improves the fibre's water resistance properties. Treatment also removes pectin, wax and oil covering materials from the fibre surface which results more cellulose microfibrils to expose on fibre surface (Paul, et al. 2010). Cellulose microfibrils dispersion into the matrix facilitates better bonding at the

interface and provides improved properties of the composites. The reaction between fibre and stearic acid is presented in Equation 2.13.

$$\text{Fibre-OH} + CH_3(CH_2)_{16}COOH \longrightarrow CH_3(CH_2)_{16}COO\text{-O-Fibre} + H_2O \qquad (2.13)$$

Kalaprasad, et al. (2004) used stearic acid treatment on sisal fibre in ethyl alcohol solution and showed higher tensile strength and modulus properties. Torres & Cubillas (2005) used 3% stearic acid to treat sisal fibre reinforced in polyethylene composites and reported 23% higher shear strength compared to the untreated samples.

2.5.10 Permanganate treatment

Permanganate treatment on natural fibres is conducted by potassium permanganate ($KMnO_4$) in acetone solution. This treatment forms highly reactive permanganate ions (Mn^{3+}) which react with the cellulose (hydroxyl groups) and form cellulose-manganate and initiates graft copolymerization. This treatment enhances chemical interlocking at the interface and provides better fibre adhesion with the matrix (Rahman, Mallik & Khan 2007). Treatment also reacts with the OH groups in lignin and removes them from the fibre, thus the hydrophilic nature of the fibre is reduced. Higher concentrations of $KMnO_4$ (more than 1%) cause excess delignification from the fibre structure and degrade its strengths (Li, Tabil & Panigrahi 2007; Paul, et al. 2010). The reaction between the fibre–OH group and potassium permanganate is given in Equation 2.14.

$$\text{Fibre - OH} + KMnO_4 \longrightarrow \text{Fibre} - O - H - O - \overset{\overset{O}{\|}}{\underset{\underset{O}{\|}}{Mn}} - OK^+ \qquad (2.14)$$

Paul, et al. (2010) reported that, during oxidation reaction, $KMnO_4$ etches the fibre surface and makes it physically rougher to improve mechanical interlocking with the matrix. Flexural strength and modulus properties were increased by 5% and 10% for the treated banana fibre reinforced in polypropylene composites. Li, et al. (2004) applied 0.2% $KMnO_4$ solution (in 2% acetone) on alkali pre-treated (2% NaOH for an hour) flax fibre and reported treated fibre-LLDPE and HDPE composites had higher tensile strengths compared to the untreated samples.

2.5.11 Triazine treatment

Triazine treatment is used for the surface modification of the natural fibres. A triazine ($C_3H_3N_3$) derivative has multifunctional groups (e.g. $C_3H_3N_3Cl_3$) in its structure. The reactive chlorines esterify the hydroxyl groups of the fibre and provide linkage between the cellulose surface and the matrix. Treatment also provides better moisture resistance properties of the fibre (Kalia, Kaith & Kaur 2009; Li, Tabil & Panigrahi 2007; Mengeloglu & Karakus 2008). Due to this, strong adhesion at the interface takes place and thus improves composite properties (Bledzki & Gassan 1999). The possible reaction between triazine derivative and fibre-OH groups are given in Equations 2.15 and 2.16.

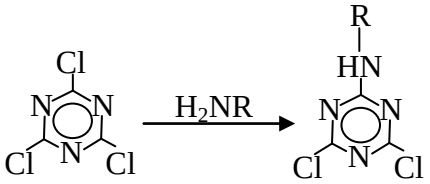

(2.15)

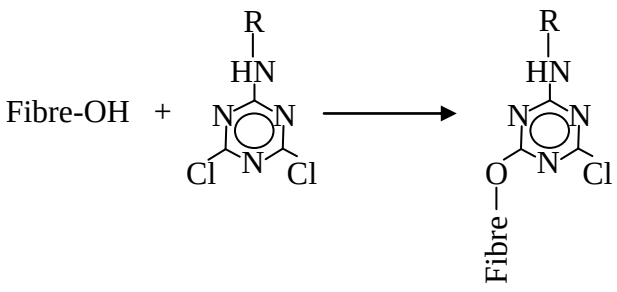

(2.16)

Zadorecki & Flodin (1985) used trichloro-s-triazine based different coupling agents to treat cellulose fibres and was reinforced in polyester matrix. Improved fibre matrix adhesion and higher moisture resistance properties were reported for the treated fibre composites.

2.5.12 Fatty acid derivate (oleoyl chloride) treatment

Fatty acid derivative is used as a coupling agent to modify the fibre surface while improving wettability and interfacial adhesion characteristics. Oleoyl chloride is a fatty acid derivate which reacts with the fibre hydroxyl groups (esterification) and grafts to the cellulose backbone. Treatment also makes the fibre hydrophobic in nature which improves the wetting and adhesion of fibre with the matrix. Modification on jute fibre with dichloromethane and pyridine solvent under a dry nitrogen atmosphere resulted in more hydrophobic characteristics and increased composite properties (Corrales, et al. 2007).

2.5.13 Fungal treatment

Fungal treatment has been recently considered as a promising alternative for natural fibres' surface modification. This biological treatment is environmentally friendly and efficient. During treatment, fungi are used to remove wax and oil covering materials from the fibre surface through the action of specific enzymes. White rot fungi produces extracellular oxidases enzymes that react with lignin constituents (lignin peroxidase). The enzyme also increases hemicellulose solubility and thus reduces the hydrophilic tendency of the fibre. Fungi also produces hyphane that creates fine holes on the fibre surface and provides a rough surface for better interlocking with the matrix (Jafari, et al. 2007; Pickering, et al. 2007).

The treatment process involves sterilisation of the fibres in an autoclave for 15 minutes with 120°C. Afterwards, fungi are added proportionally with the fibre and incubated for 2 weeks at 27°C. Fibres are then sterilised, washed and oven dried. Pickering, et al. (2007) studied fungal treatment on hemp fibre and reported a 22% higher composite strengths than the untreated sample.

2.6 Summary

The use of natural fibres as reinforcement in polymer composites is attracting much interest due to its potential mechanical properties, processing advantages and environmental benefits. However, the hydrophilic nature of the fibres lowers the compatibility with the matrix which results in poor mechanical properties of the composites. Chemical treatment is an essential processing parameter to reduce the hydrophilic nature of the fibres and thus improving adhesion with the matrix. Pre-treatments of fibre change its structure and surface morphology. Hydrophilic hydroxyl groups are removed from the fibre by the action of different chemicals. Significant improvements in the mechanical properties of the composites are reported by using different chemical treatment processes on the reinforcing fibre.

In this study hemp fibre is selected as reinforcement due to its potential mechanical properties compared to the other natural fibres. Widely used alkaline, acetyl and silane treatments are chosen to modify the fibre structure. Most commercially available polyester (thermoset) matrix is utilised to prepare composites. The effect of treatments on the fibre surface and structure are investigated through thermal and mechanical property analysis. The interface bonding strength between the treated fibres and the polyester matrix are examined through mechanical property analysis of their composites.

Chapter 3: Materials and Experimental Methods

3.1 Introduction

Natural fibres are potential alternative material resources that have the ability to replace synthetic fibres in engineering fibre composites. The successful utilisation of natural fibres as reinforcement requires pre-processing to achieve the desired thermal and mechanical properties of composites. A good understanding of fibre and composite behaviour and their failure mechanisms is necessary before this material can be implemented in engineering applications. In this chapter, material preparation and experimental details are presented with respect to fibre characterisation, thermal analysis and mechanical property analysis of composites.

The experimental methods described in this chapter are: (1) the chemical treatments on hemp fibre, which change the fibre structure and morphology, which in turn affects the fibres' thermal and mechanical properties; (2) experimental methods to analyse the fibre properties; (3) manufacturing processes that combine the chemically treated fibres with polyester matrix to produce composites; (4) mechanical testing on hemp-polyester composites to analyse the fibre treatment affects on composite properties under different loading conditions.

3.2 Materials

3.2.1 Hemp fibre

Hemp fibres (*Cannabis sativa L*) of various sizes and orientations (Figure 3.1) were used for composite preparation. Long fibres (approximately 1 m in length) and woven fabrics (combining 0° and 90° fibre orientation) were obtained from Eco Fibre Industries, Australia. Long fibres were cutted into 5-10 mm in length to produce short fibres. Long fibres were used to produce unidirectional fibre composites. Short, randomly orientated fibres were used to prepare sandwich cores and woven fabrics (380 g/m^2) were used for sandwich skins.

(a) (b) (c)

Figure 3.1: Hemp fibre (a) long (b) short and (c) woven fabric

Fibre surface treatments

Alkaline, acetyl and silane treatments on hemp fibres (long fibre, short fibre and woven fabrics) were performed. Figure 3.2 shows the treatment outline on the hemp fibres.

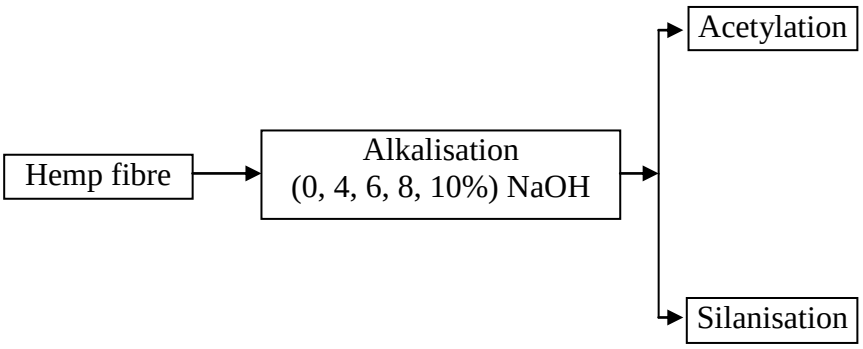

Figure 3.2: Stages of chemical treatments on fibre

The alkali treatments used different concentrations of NaOH solution. The solution was prepared by adding 0%, 4%, 6%, 8%, and 10% NaOH (by weight) in a water ethanol mixture (water: ethanol = 80: 20). It was then stirred at room temperature for an hour. Hemp fibres were soaked with different concentrations of NaOH solutions for 3 hours at room temperature. The fibres were then washed several times with distilled water to allow absorbed alkali to leach from the fibre. The washed fibres were dried at room temperature for 8 hours, and then oven dried at 100°C for another 6 hours. The dried fibres were stored in a sealed plastic bag to avoid atmospheric moisture contamination prior to chemical analysis, thermal analysis and composite processing.

For acetyl treatments, alkali pre-treated hemp fibres were soaked in acetic acid (glacial) and subsequently treated with acetic anhydride at room temperature for 3 hours. Following this treatment, the fibres were washed in distilled water several times to remove residual acetic anhydride and then dried in the manner described above.

For silane treatments, oligomeric siloxane (3% by weight) was dissolved in a methyl alcohol solution (alcohol: water = 60: 40). The solution was stirred at room temperature for an hour. Alkali pre-treated fibres were then immersed in the solution for 3 hours at room temperature. The fibres were then dried in a similar manner to the other treatments described above.

Determination of fibre constituents

The cellulose, hemicellulose and lignin contents in chemically treated hemp fibres were determined. Figure 3.3 shows the cellulose, hemicellulose and lignin constituents extracted from the hemp fibre.

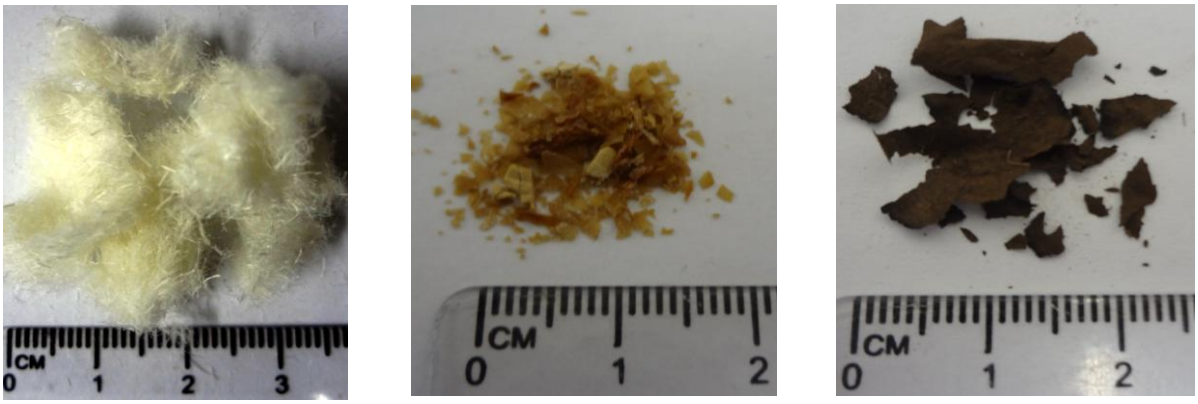

(a) (b) (c)

Figure 3.3: Hemp fibre constituents (a) cellulose (b) hemicellulose and (c) lignin

Cellulose

Treated fibres were crushed into powder and oven dried at 100°C for 2 hours. The dried hemp powder (4 g) was placed in an Erlenmeyer flask and 50 ml of distilled water was added. The flask was then placed in a thermostat water bath and the solution was heated at 80°C with constant stirring. Sodium chlorite and acetic acid were added repeatedly to the solution mixture four times in one hour intervals. After

that, the flask was placed in an ice bath and cooled down below 10°C. The residue from the solution mixture was collected by filtration and washed with distilled water and rectified spirit. The collected residue was oven dried at 105°C for 8 hours before being weighed.

The dried residue was placed in a beaker and mixed with potassium hydroxide (24% KOH). The mixture was kept at room temperature for 8 hours. The residue was then collected through filtration and the filtered residue was kept for hemicellulose estimation. The residue (cellulose) was washed with water and rectified spirit, oven dried at 105^0C for 8 hours, cooled down in a desiccators and weighed. The drying and weighing was repeated until a constant weight was achieved. The percentage of cellulose was calculated by measuring weight differences.

Hemicellulose

The filtration from the cellulose was collected in a beaker. A solution of rectified spirit containing 10% acetic acid was prepared and added to the beaker and stirred constantly. During stirring, a gel-like precipitate formed, and was collected and washed several times with rectified spirit, and then oven dried at 100^0C for 8 hours. The constant weight was recorded and the hemicellulose percentage was calculated.

Lignin

Hemp powder (0.4 g) was mixed with sulphuric acid (72% concentration) and the mixture was kept in an ice bath for 12 hours where it was stirred frequently. The mixture was then diluted to an acid strength of 4% and refluxed for six hours. Following cooling, the mixture was filtered, transferred to the crucible and washed

repeatedly with hot water until free from acid. The residue was dried at 105^0C for 15 hours, cooled in desiccators, and weighed. The drying and weighing was repeated until a constant weight was achieved. The lignin weight percentage was calculated by measuring the weight difference.

3.2.2 Polyester matrix

Unsaturated polyester was used as a thermoset matrix to prepare composites. A chemical formula of the polyester matrix is presented in Figure 3.4. Generally, unsaturated polyester matrix (($C_8H_6O_2$, $C_8H_{16}O_4$, $C_5H_{12}O_2$, $C_4H_2O_3$)$_n$) is formed through a reaction of a dibasic acid (acid has two hydrogen ions) and a glycol (glycol containing two hydroxyl groups). The resulting polymeric liquid is blended in a monomer (a molecule that may bind chemically to other molecules to form a polymer) in the presence of styrene (an organic compound, chemical formula $C_6H_5CH=CH_2$). Styrene contains carbon carbon double bonds (C=C) which act as cross-linking sites (Li, et al. 2000). Cross-linking begins in the presence of a catalyst. Catalysts such as methyl ethyl ketone peroxide (MEKP, chemical formula $C_8H_{18}O_6$) reacts with styrene (C=C) and polymerisation of polyester matrix begins at room temperature (Han & Lem 1984). The resulting material is a solid polyester matrix.

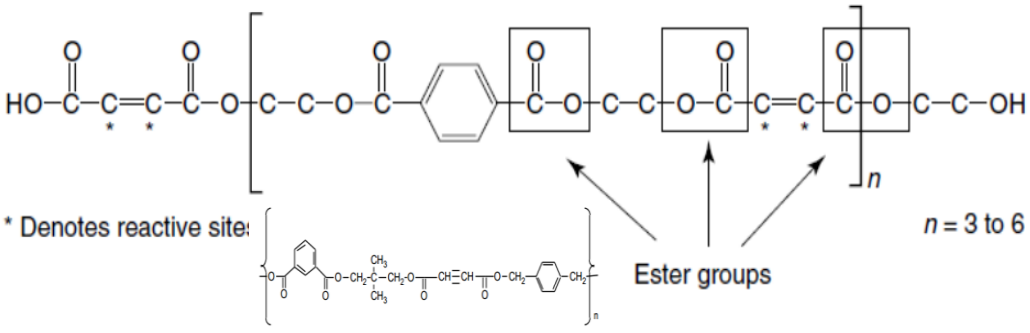

Figure 3.4: Chemical formula of polyester matrix

A clear casting of the polyester matrix was prepared by pouring liquid polyester mixed with 1.5 wt% of MEKP into glass moulds. The 4 mm thick casting was then allowed to gel and cure at room temperature overnight. The solid casting was then oven dried at 80°C for 4 hours to post cure. The casting was then cut into shapes required for mechanical testing.

3.3 Composite manufacturing processes

Hemp fibre polyester composites were prepared by utilising Vacuum Assisted Resin Transfer Moulding (VARTM) and hand layup processes. Generally, VARTM is a safer manufacturing process compared to hand layup techniques (Cicala & Lo Faro 2012). In VARTM, fibre and matrix are mixed in a mould covered by a flexible plastic vacuum bag. Mould covering prevents the exposure of volatile organic matter to humans during sample preparation. Vacuum pressure, used in the VARTM process, removes air voids from individual fibre spacing's and facilitates thorough fibre mixing with the matrix. Proper sealing of the vacuum bag on to the mould ensures void-free composite fabrication. However, in hand layup processes, the fibre-matrix mixing occurs in an open mould which involves manual material handling under an exposed resin fume environment.

3.3.1 VARTM process

The VARTM process was used to prepare long unidirectional fibre composites. Figure 3.5 presents a schematic diagram of the VARTM process for composite preparation.

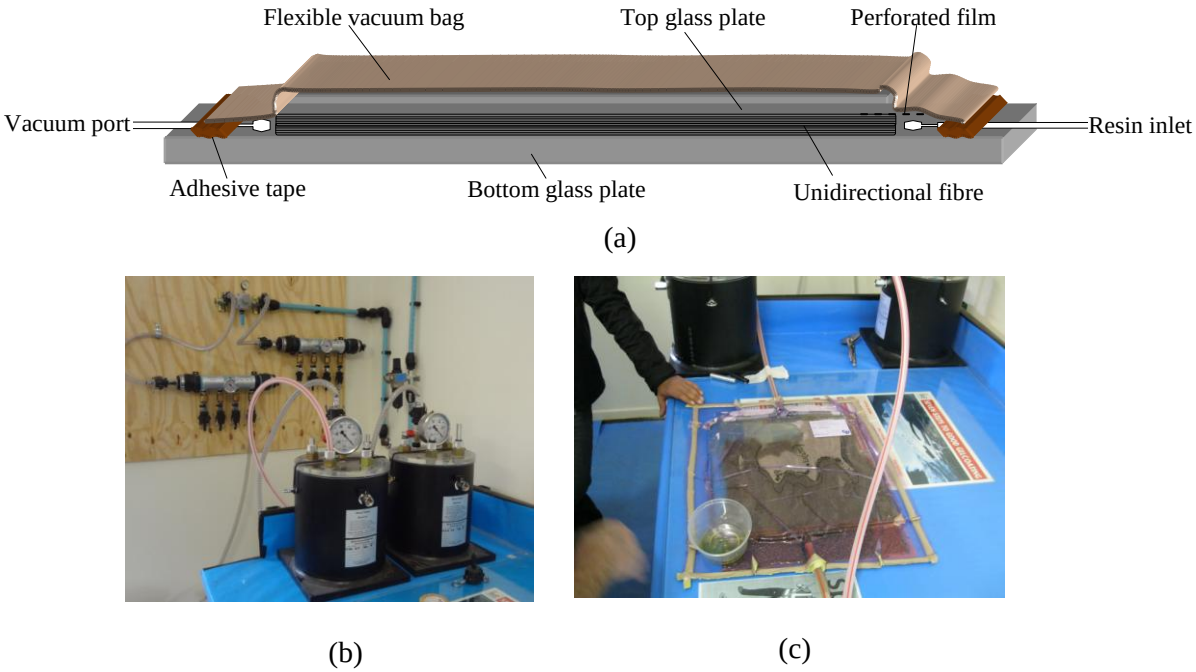

Figure 3.5: VARTM process for unidirectional fibre composites (a) schematic diagram (b) vacuum suction chamber (c) sample preparation

During composite processing, two rectangular flat glass plates (1000×1000 mm^2) were used as a mould. The glass moulds were utilised to maintain a consistent thickness throughout the samples, with smooth surface finishes being achieved in the final composites. Initially, the glass moulds were waxed several times with a mould releasing agent (Meguiars Universal Mould Release Wax, item number 88). Unidirectional fibres (100 g) were placed (600×600 mm^2) between the glass moulds. The fibre weight remained constant for all treatment cases to produced composite samples. A distribution media layer was placed on the top of the fibres to allow effective flow of the matrix across the fibres. The mould (glass-fibre) assembly was then covered with a vacuum bag and sealed with adhesive tape. Two ports were created in the mold; a matrix inlet port and a vacuum port. The complete mould assembly was then depressurised via the vacuum port. All air voids present in the assembly were removed by vacuum pressure (92 kPa). At this stage, the matrix inlet port was opened to allow the liquid polyester (mixed with the 1.5 wt% MEKP

catalyst) to enter into the depressurised mould. The polyester matrix spread quickly into the mould and mixed with the fibres. Once the fibres were fully impregnated with the matrix, the matrix inlet port was closed while the vacuum port was left open for an hour. The infused composite was then cured under vacuum pressure at room temperature for 24 hours. The laminate was released from the mould and kept in an oven at 80°C for 4 hours to post-cure. The cured panel (600×600 mm^2) was trimmed and sectioned for mechanical testing. The weight fractions of fibres were 55% of the produced composites.

3.3.2 Hand layup process

A hand layup process was used to prepare the sandwich composites. The manufacturing process of the sandwich structures is presented in Figure 3.6.

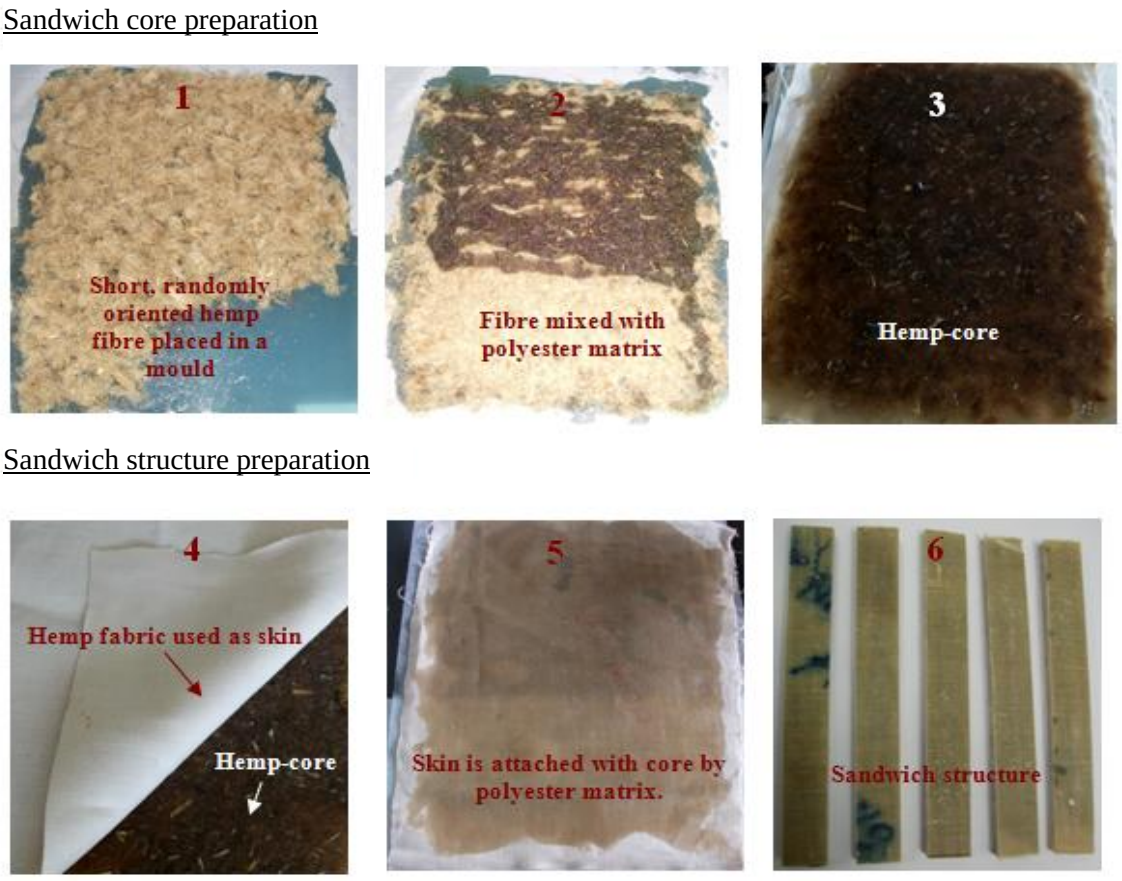

Figure 3.6: Sandwich structure fabrication steps (hand layup)

The processing of sandwich structures involved two stages of sample preparations. First, the sandwich cores were prepared. During the core manufacturing process, a flat carbon steel sheet was used as a mould. The mould was waxed several times with a mould releasing agent. Hemp fibres (chopped into 5–10 mm lengths) were laid over the mould and the polyester matrix (with 1.5% MEKP) was spread over the fibre carefully to ensure maximum fibre matrix wetting. A roller brush was used in the fibre-matrix mixing process. Extreme care was taken to achieve a uniform matrix distribution throughout the fibre cross-sections in the sample. The fibre content was 20% of the weight of the produced samples. The samples were kept at room temperature overnight then post cured at 80°C for 4 hours. The cured composite sample was used as a hemp core (thickness = 3.5 mm) for the sandwich composites.

In the second stage, sandwich skins were prepared by using hemp woven fabrics. Woven fabrics were placed on the waxed mould and wet with the polyester matrix. The hemp cores were then placed between the wetted fabrics. A roller brush was used to remove excess matrix from the samples. The whole assembly was covered with another flat mould to achieve uniform surface finishing on both sides of the sandwich structure. The samples were kept at room temperature overnight followed by post curing at 80°C for 4 hours. One layer of woven fabric was used to prepare sandwich skin (thickness 0.75 mm/layer). The overall thickness of the prepared sandwich structure was 5 mm.

3.4 Structure and microstructure analysis

3.4.1 Fourier Transform InfraRed (FTIR) spectroscopy analysis

FTIR spectroscopy is an effective analytical tool for used in identifying functional groups present in fibre structures. In FTIR, InfraRed radiation passes though the sample. The bonds present within the functional groups absorb the radiation energy and vibrate with different frequencies (strong/weak), depending on the strength of the bonds. The energy absorption produce peaks corresponding to vibration frequencies and a molecular fingerprint of the samples are generated. The sample fingerprint presents an IR transmission (absorbance) versus frequency curve to explain the molecular structure of the fibre. Each molecule has a unique combination of bonds that produce peaks at specific frequencies. The size and shape of the peaks indicate the amount of materials present in the fibre (Smith 2009; Stuart 2005). Figure 3.7 shows a typical FTIR spectrum for hemp fibres. The peak appears at certain frequencies from which the existence of fibre constituents can be identified.

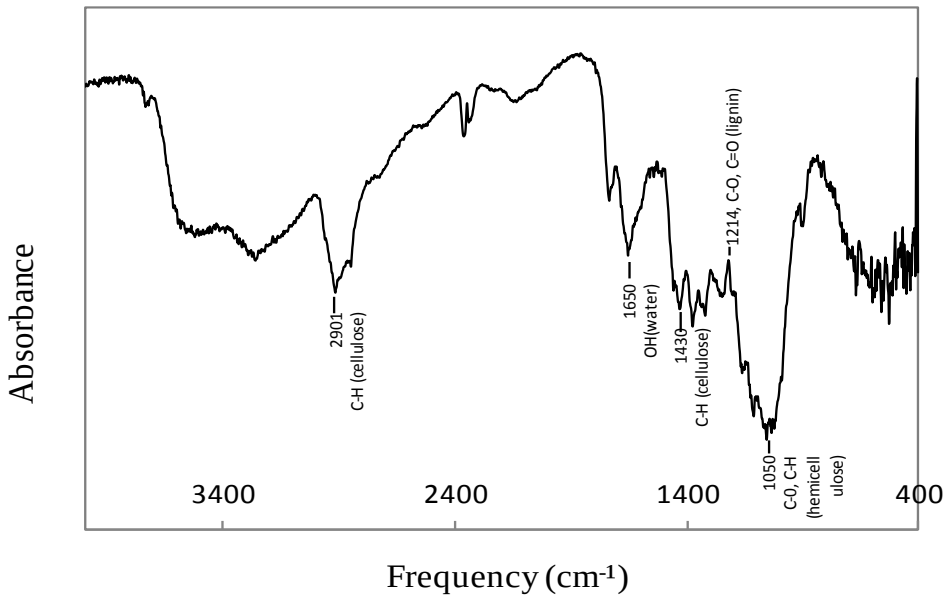

Figure 3.7: Typical FTIR spectrum of hemp fibre

An FTIR analysis on the fibre constituents of treated and untreated fibre samples were carried out using a Thermo Nicolet FTIR spectrometer Model Nexus. About

3mg of fibres was crushed into small particles and mixed with KBr (potassium bromide) and pressed into a disc. The FTIR spectra were recorded at wave numbers from 400 to 4000 cm^{-1} with 4 cm^{-1} resolution. An average of 64 scans was recorded for each spectrum. A background spectrum of KBr (without sample) was measured to determine a relative scale for absorption intensity. The background spectrum was compared to the spectrum with sample in KBr to determine a resultant spectrum which had no instrumental character. Thus, the presented spectrum is produced only from the fibre sample.

3.4.2 Optical microscopy analysis

Optical microscopy (OM) was used in measuring fibre dimensions and composite failure surfaces. The Olympus BX41 with a CC12 soft imaging system was used to collect images. Figure 3.8a presents a typical OM image of a fibre surface along its length from which fibre widths can be measured. Figure 3.8b presents a typical fibre cross-section from which fibre diameters can be measured. Figure 3.8c shows a failure surface of a composite sample where matrix cracking and fibre failures can easily be identified to analyse composite failure modes.

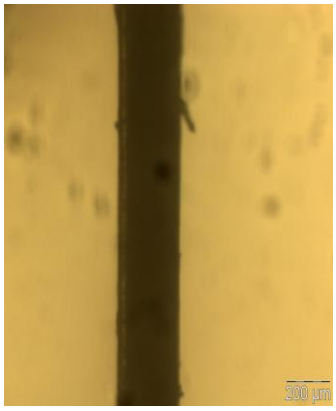

(a)

(b)

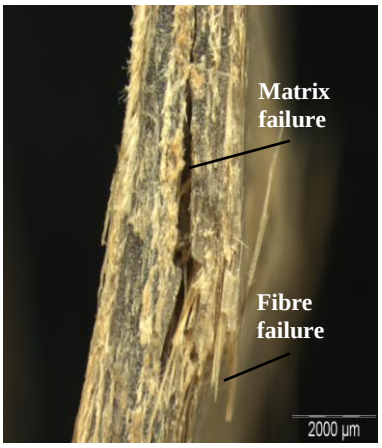

(c)

Figure 3.8: Typical OM images of (a) sing fibre surface (b) cross-sectional area of the fibre (c) composites failure surface

3.4.3 Scanning Electron Microscopy (SEM) analysis

Fibre surface morphology and the extent of fibre matrix interface bonding was analysed through SEM. Figure 3.9 shows SEM micrographs of a single fibre surface and the embedded fibre in a matrix.

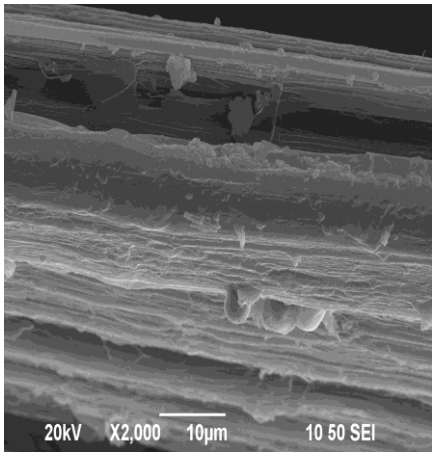

(a)

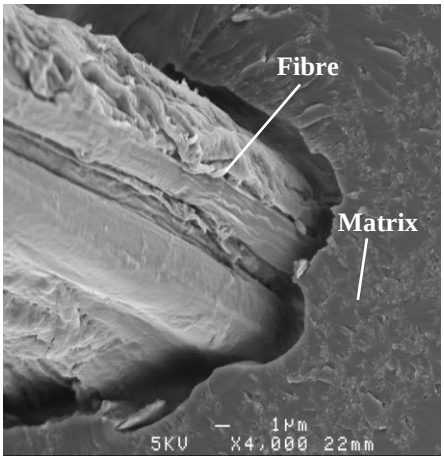

(b)

Figure 3.9: SEM images of (a) fibre surface (b) fibre embedded in a matrix

SEM produces electrons which were spread over the sample. The electronic ray reacts with the sample, generating several types of signals. The intensity of the signals varies according to the sample size. The signals were collected by a detector and their output synchronised in a picture form.

SEM Model JSM-6400F (JEOL, Japan) was used to investigate fibre surface conditions (20 kV) of different chemically-treated fibres and their bonding with the matrix (5 kV). Samples were placed on aluminium discs using double-sided electrically conductive adhesive tape. A conductive layer of carbon was spread on the samples' surfaces to prevent electronic charge formation. The samples were then placed in a vacuum chamber and coated with 20-30 angstroms of aluminium. A high voltage was applied on the coated samples and output images were collected for analysis.

3.5 Thermal property analysis

3.5.1 Thermogravimetric Analysis (TGA)

TGA was used to determine the thermal stability of the fibre. Fibre constituents have different thermal reactivities and decompose at different temperatures. TGA analysis on treated fibres was carried out by a thermal gravimetric analyser (TGA-Model No. Q500). Between 6 mg to 10 mg of fibres was taken for analysis. Fibre samples were heated between the temperature range of 10°C to 500°C at a rate of 10°C/min. Experiments were carried out in a helium medium (60 ml/min) and the weight was recorded as a function of increasing temperature. A differential thermogravimetric analysis (DTGA) curve was collected from the TGA analysis. The heating conditions were constant for all treated fibre samples.

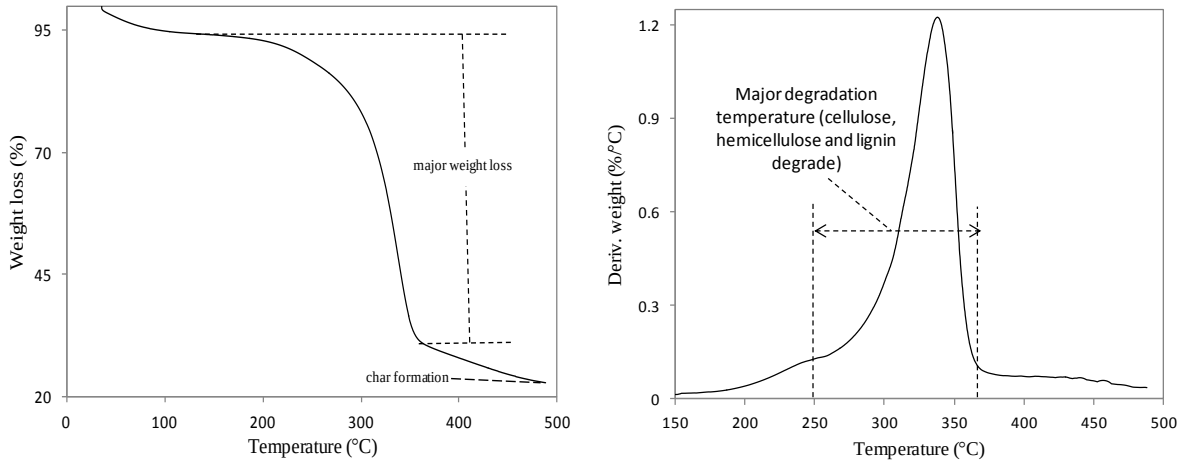

(a) (b)

Figure 3.10: Typical (a) TGA and (b) DTGA curve of hemp fibre

Figure 3.10 presents a typical TGA thermograph for hemp fibres. From the curve, different stages of weight loss of the fibre can be identified during the heating process. The weight loss stages were used to analyse the thermal decomposition process of the fibre.

3.5.2 Differential Scanning Calorimetry (DSC)

DSC analysis is used to determine the thermal energy released or absorbed via chemical reactions of the fibre constituents during heating. A series of exothermic and endothermic reactions take place during sample decomposition at different temperatures (Menczel, et al. 2009). The magnitude and location of the exothermic and endothermic peaks indicate the thermal phase transformation of the fibre. In the case of an endothermic event, heat is absorbed by the sample, whereas heat is released in an exothermic event. Endothermic reactions provide information on sample melting, phase transitions, evaporation, dehydration and pyrolysis.

Exothermic reactions provide information on crystallisation, oxidation, combustion, decomposition and chemical reactions (Ball, McIntosh & Brindley 2004).

DSC analysis on treated fibres was performed by using a thermal analyser (DSC Instrument, Model No. Q100). Sample preparation and heating rate were applied in the same manner as seen in TGA. The experiment was conducted in a nitrogen environment purged at 20 ml/min. Nitrogen was used for efficient heat transfer and removal of volatiles from the sample.

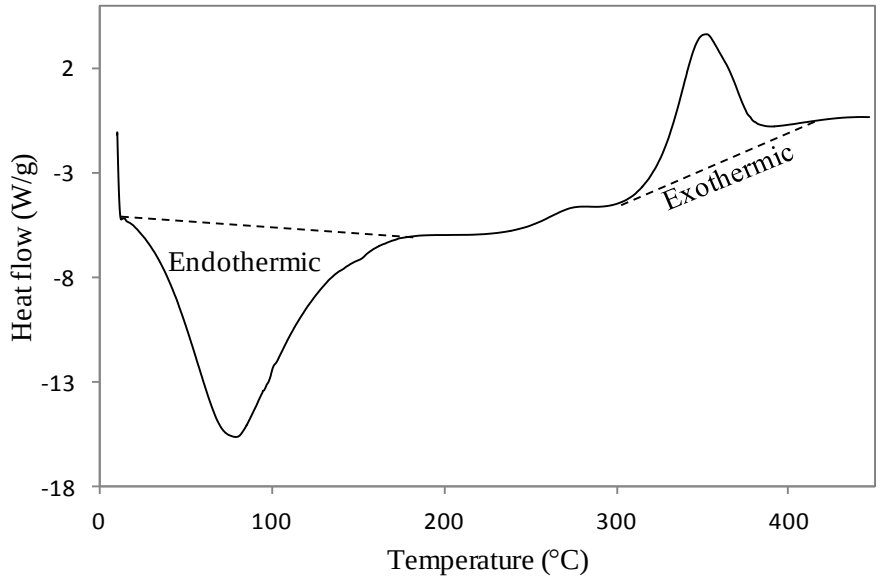

Figure 3.11: Typical DSC curve of hemp fibre

Figure 3.11 shows a typical DSC curve for hemp fibres. Several endothermic and exothermic peaks at different temperatures can be identified from the curve. These were used to analyse the thermal stability of fibres.

3.6 Mechanical property testing

3.6.1 Tensile test

Tensile tests were carried out on single hemp fibres, polyester matrix and unidirectional fibre composites. A dynamic mechanical analyser (DMA), Model Q800 was used for single fibre testing. A 100 kN INSTRON Universal testing machine (MTS) was used for matrix and composite testing.

Single fibre tensile test

Single hemp fibre tensile testing was performed under a controlled ambient temperature of 30°C. DMA was operated in a stress-strain tension mode and the ramp force rate was 0.5 N/min. All test fibres were wrapped around mandrels with adhesive (3M super 77 multipurpose spray) and cured at room temperature for 24 hours. The wrapped fibres were then gripped in the DMA film/fibre grip from two sides with a 10 mm gauge length maintained between them. Fibres were stretched at a constant strain rate until failure. Figure 3.12 shows a mandrel wrapped specimen gripped in DMA. Ten specimens of each sample were tested.

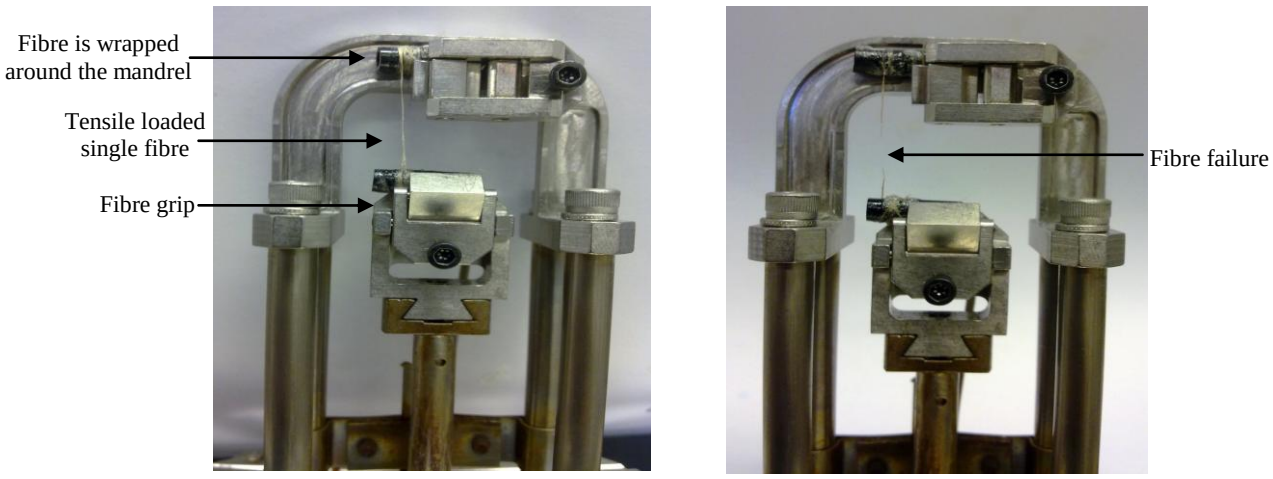

Figure 3.12: Mandrel wrapped fibre sample mounted in DMA

The tensile strength was determined by dividing the applied load by the average cross-section diameter (methods of measurement are described in Chapter 5) of the fibres. Strain was measured by the change in fibre length. A typical tensile stress–strain curve of a single fibre is given in Figure 3.13. The modulus of elasticity was calculated from the linear portion of the curve.

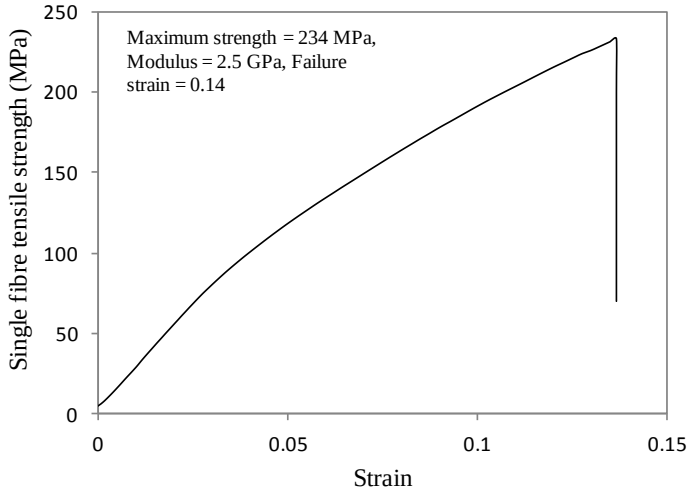

Figure 3.13: Typical stress-strain curve of a single hemp fibre

Matrix and composite tensile test

The polyester matrix specimens were prepared in a dog-bone shape. At the gage region the specimen width was 10 mm and thickness was 4 mm (Figure 3.14a). For the composite sample, rectangular flat specimens were used. The ends of the specimens were carefully attached with the tabs using epoxy glue (Epiglue - 2 Part Epoxy Glue) cured at room temperature for 24 hours (Figure 3.14b). The tabs were used to prevent specimen slippage and premature fracture at the gripping area. The test set-up and instrumentation is presented in Figure 3.14c.

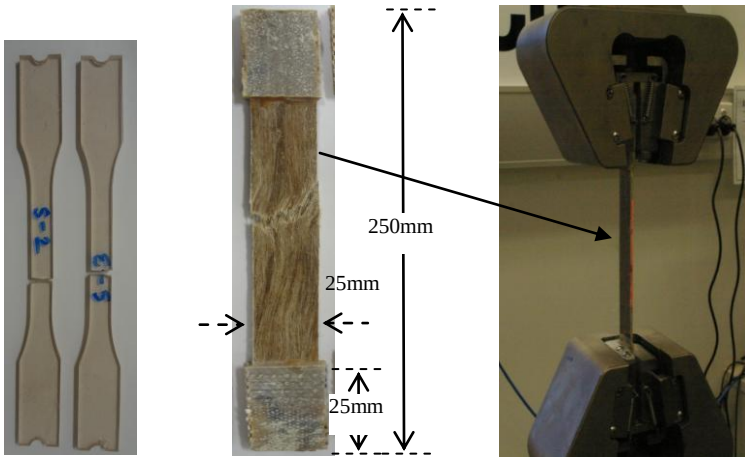

(a) (b) (c)

Figure 3.14: Tensile specimens (a) matrix (b) composite (c) test setup

Tensile testing of the polyester matrix and long and unidirectional fibre reinforced composites were performed following the ISO 527 test standard. A load was applied to the specimen (parallel to the fibre direction) at a rate of 2 mm/min, and strain in the specimen during loading was monitored using a laser extensometer. Six specimens were tested for each sample. Figure 3.15 is a sample of the stress-strain curve from the tensile test from which specimen's maximum strength, modulus and failure strain can be obtained.

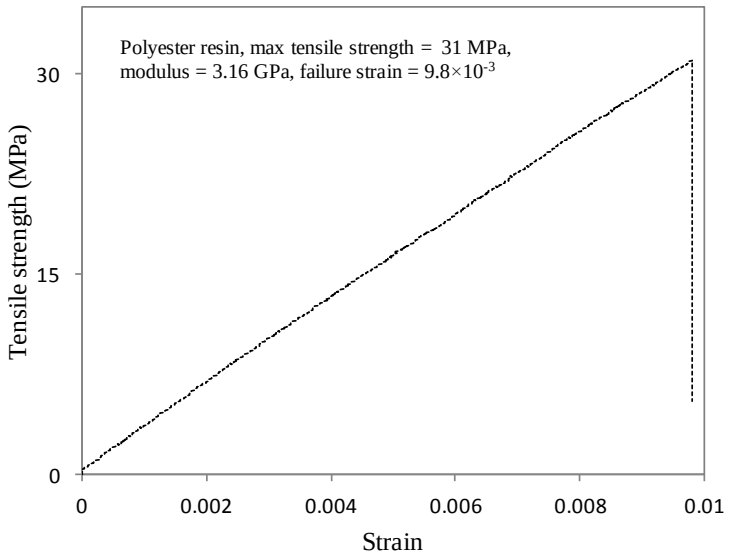

Figure 3.15: Typical tensile stress-strain curve of polyester matrix

3.6.2 Compression test

Compression testing was carried out on the polyester matrix, unidirectional fibre composites and sandwich structures using a 100 kN MTS machine with a loading rate of 1 mm/min. Eight specimens were tested for each sample.

Figure 3.16 shows the test set-up for the matrix and sandwich structures. The test was conducted by following ISO 604B with a specimen size of 10 mm in length and width for the matrix, and 10 mm length and 5 mm width for the sandwich structures.

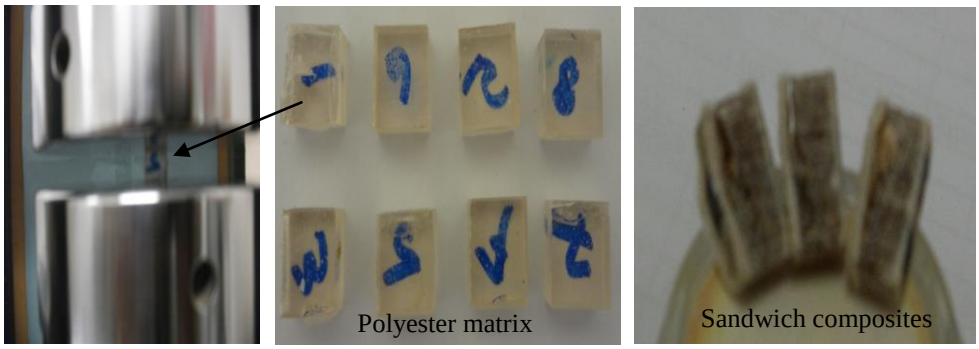

Figure 3.16: Compression test setup of matrix and composites

For unidirectional fibre composites, the test was carried out following ISO 14126. Figure 3.17 shows the test set-up and instrumentation for compression testing. The specimens were cut along the longitudinal fibre direction (L×W = 140 mm ×12 mm) and were clamped in a Wyoming Modified Celanese Compression test fixture. The load was applied in parallel to the fibre direction and the resulting deformation was recorded until failure. After each test, the specimen was carefully removed from the test fixture and the failure mode was observed and recorded.

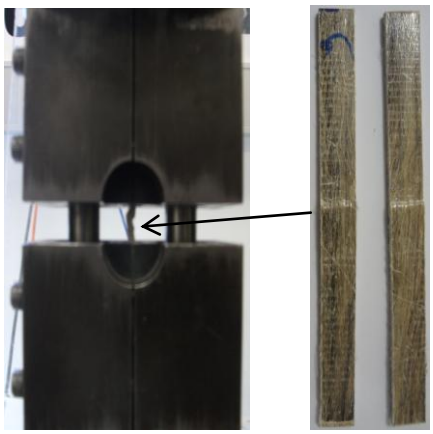

Figure 3.17: Compressive test setup of unidirectional fibre composites

Figure 3.18 shows a sample stress-strain curve from the compression test. The sample deformed elastically, followed by plastic deformation. After they reached maximum strength, the materials failed either by fibre buckling, matrix cracking or fibre-matrix debonding. In the case of the sandwich structures, the failure could be due to either core crushing, skin delamination or shear crimping, or any combination of these.

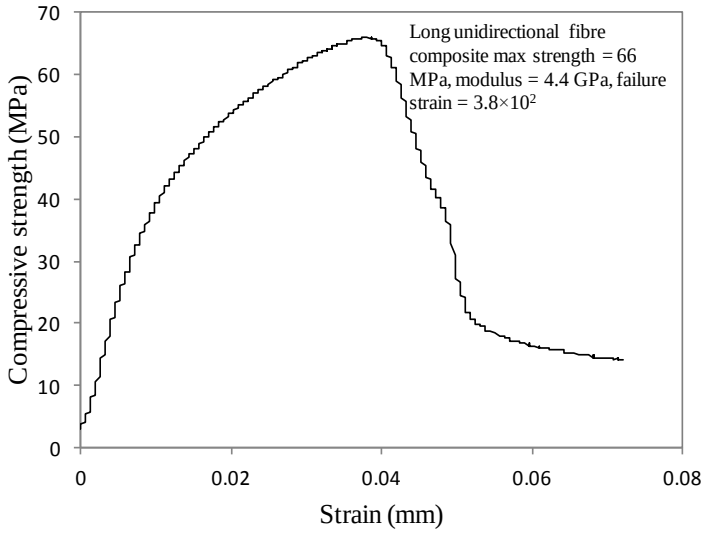

Figure 3.18: Typical compressive stress-strain curve of the unidirectional fibre composite

3.6.3 Shear test

Shear testing of the unidirectional fibre composite was conducted following the ASTM D 5379. The specimen was loaded in a modified Iosipescu shear test fixture and placed in a 10kN MTS machine. Six specimens were tested for each sample.

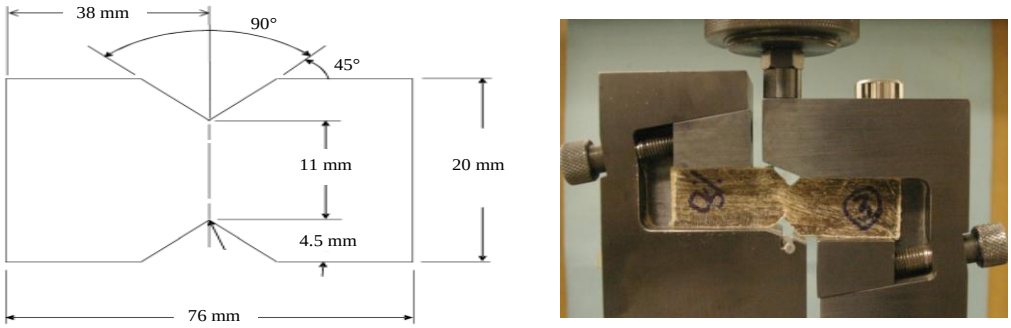

Figure 3.19: V-notch shear test setup of the unidirectional fibre composite

Load was applied perpendicular to the fibre direction at a constant rate of 2 mm/min. The shear strength was determined by dividing the applied load by the area of the cross section between the notches. Figure 3.19 shows the v-notch shear test setup of unidirectional fibre composite.

3.6.4 Flexural test

Three point bending test

Flexural testing of the polyester matrix (following ISO 178), and unidirectional fibre composites and sandwich structures (following ISO 14125) were conducted using a 10 kN MTS testing machine at a loading rate of 2 mm/min. The specimens were simply supported and tested under 3-point loading with the span set at approximately 16 times the thickness of the specimen. Six specimens were tested for each sample. The load was applied at mid-span of the specimens, perpendicular to the fibre

direction. To determine the strength and elastic properties in bending the load and mid-span deflection were recorded up to failure. The failure mode was also observed after each test. Figure 3.20 shows the test setup for flexural testing. Before each test, the loading pin was set to almost touch at the top surface of the specimen. The load and specimen deflection were recorded up to failure to determine the strength and elastic properties of the sandwich composites.

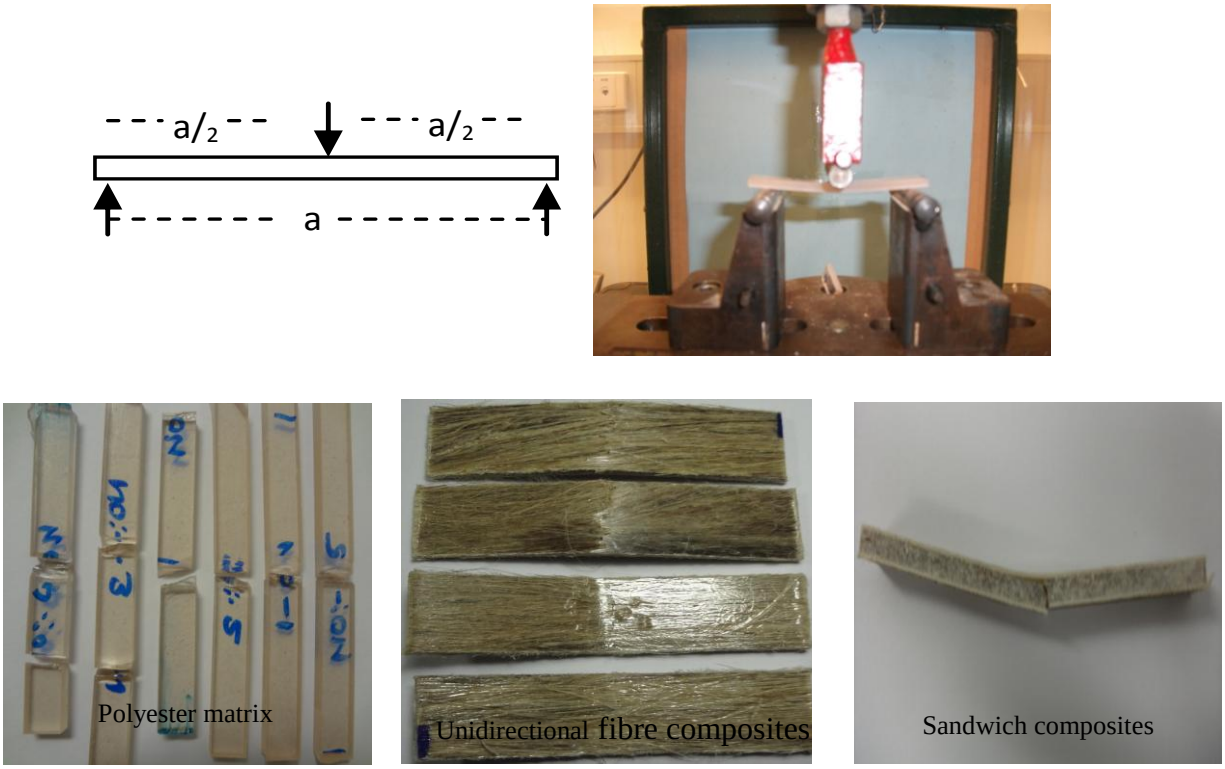

Figure 3.20: Flexural (three point bending) test setup

A sample of flexural stress-strain curves of the matrix and fibre composite are shown in Figure 3.21. Based on the curve, the maximum flexural strength, modulus and failure strain of the polyester matrix and fibre composites were determined.

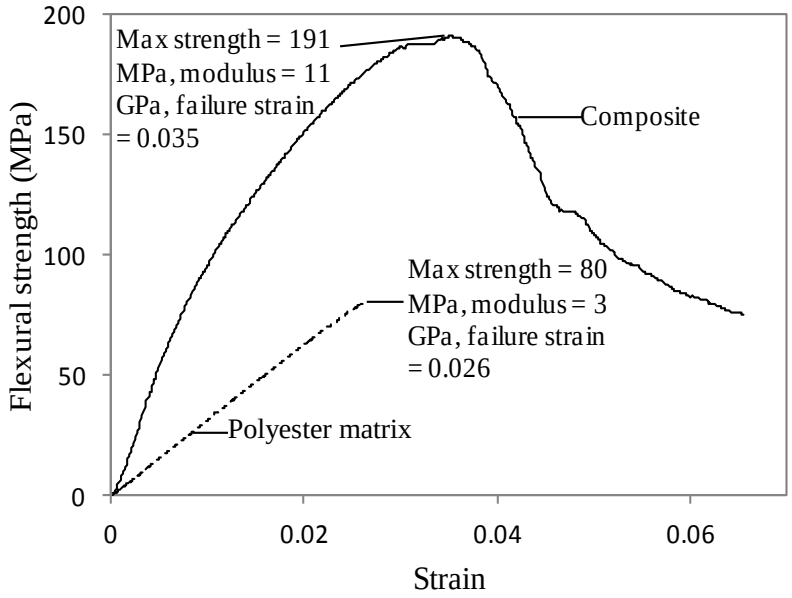

Figure 3.21: Typical flexural stress-strain curves of the polyester matrix and unidirectional fibre composite

Four point bending test

Sandwich structures were tested under four point bending following ISO 14125 with the same 10 kN MTS machine at the same cross-head speed of 2 mm/min. Figure 3.22 shows the test setup of sandwich structure shear test. Six specimens were tested for each sample.

Figure 3.22: Four-point bending (shear) test setup of sandwich structure

3.6.5 Impact test

The impact behaviour of the polyester matrix and unidirectional fibre composite was tested through Charpy (without notches) impact testing by using an Instron Dynatup impact tester. The experiment was conducted by following ASTM D 256. During testing, the specimen (L×W = 160 mm × 20 mm) rested freely and an impactor (projectile) was stuck at the centre of the specimen. The experimental setup and instrumentation used is presented in Figure 3.23. Six specimens were tested for each sample. The load was applied perpendicular to the fibre direction. The potential impact energy was the product of impactor mass (6.05 kg), nominal drop height and acceleration due to gravity.

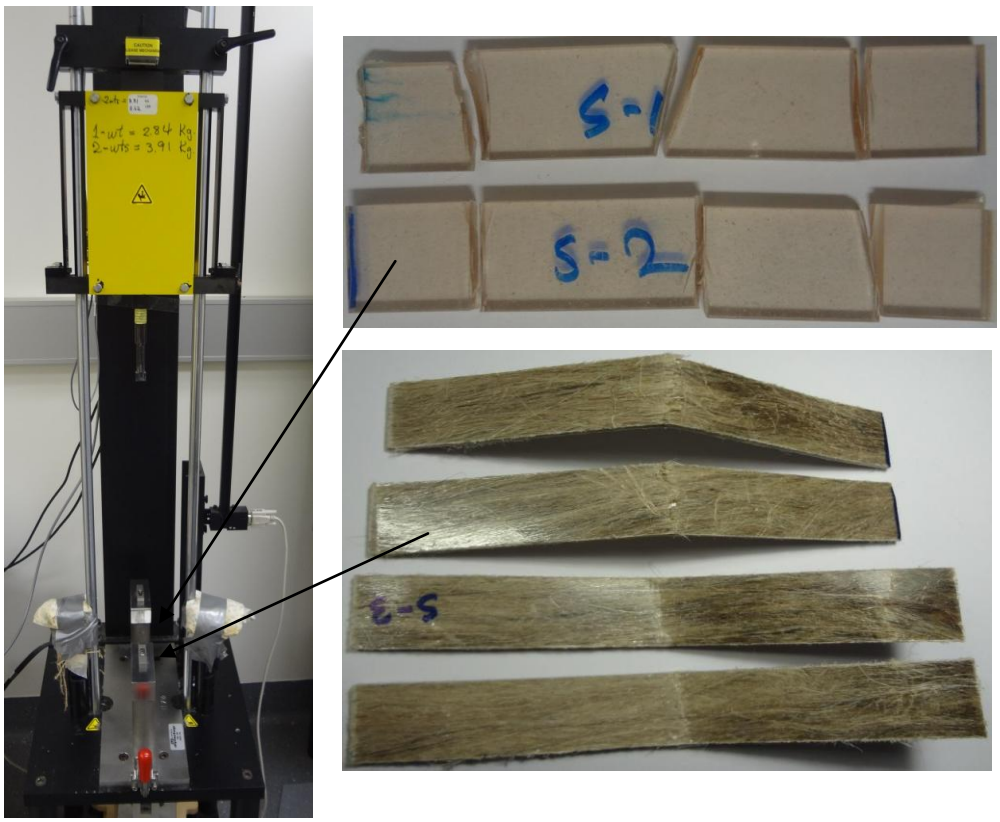

Figure 3.23: Charpy impact test setup

A sample of the impact test curve is presented in Figure 3.24. From the curve, the impact force, maximum impact energy, absorbed energy and rebounded energy of the specimen can be measured.

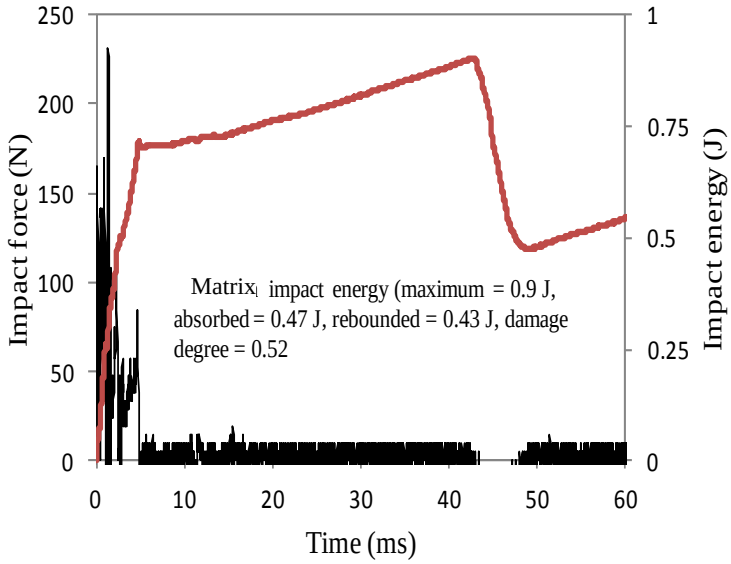

Figure 3.24: A sample of impact test curve

Chapter 4: Effects of Chemical Treatments on Hemp Fibre Structure

4.1 Introduction

The structure of hemp fibres consist of three main constituents, i.e. cellulose, hemicellulose and lignin. These components of the fibres contribute to determining the thermal and mechanical properties of the fibres. Fibre constituents are sensitive to the actions of different chemical reagents, treatment times and temperatures.

In this study, alkali treatments on hemp fibres with different (0%, 4%, 6, 8% and 10%) NaOH concentrations were carried out. Alkalised fibres were further treated with acetyl and silane chemicals. Fibre treatment methods were outlined in Chapter 3 (Section 3.2.1). The celluloses, hemicellulose and lignin constituents were separated from the treated fibres (Chapter 3, Section 3.2.1). SEM, FTIR, TGA and DSC analysis of these constituents was performed separately to develop a basic understanding of the individual fibre constituent behaviours. These constituent behaviours were used to systematically analyse treatment effects on fibre thermal properties.

4.2 Result and discussion

4.2.1 Chemical analysis

The content of fibre constituents of different treated fibres are presented in Table 4.1.

Table 4.1: Amount of fibre constituents (weight %) presents in the treated fibres

Fibre treatments	Alkalisation			Alkalisation + Acetylation			Alkalisation + Silanisation	
%NaOH	Cell*	Hemicell*	Lignin	Cell*	Hemicell*	Lignin	Cell*	Hemicell*
0	77.20	5.40	6.67	81.29	4.96	10.26	83.36	5.69
4	78.91	4.93	4.66	82.47	5.66	4.70	90.70	6.07
6	81.46	4.51	5.02	85.80	5.10	4.80	88.25	6.51
8	83.73	7.76	3.55	88.14	7.57	3.48	84.50	9.41
10	88.35	4.67	3.46	92.58	3.85	2.65	89.69	5.57

*Cell: cellulose; *Hemicell: hemicellulose

From Table 4.1 it can be observed that the hemicellulose and lignin contents were decreased with higher concentrations of (4-10%) NaOH treatment compared to the untreated fibres (0% NaOH). Removal of hemicellulose and lignin increased the relative amount of cellulose contents on the treated fibres. These results indicate that, NaOH treatments dissolved a portion of hemicellulose and lignin constituents from the fibres.

Acetyl treatments on the untreated fibres reduced the hemicellulose contents but increased the lignin contents. This indicates that hemicellulose initially reacted with the acetyl groups, then the acetylated hemicellulose were deposited on the lignin constituents. The effect of the treatments can, therefore, be expressed as a weight percentage gained by the formation of acetyl linkages with the lignin. Therefore, acetyl treatment on alkali pre-treated fibres showed that the amount of cellulose contents were increased with higher concentrations of (4-10%) NaOH pre-treatment. This was due to the extraction of more lignin in two consecutive treatment processes as compared to the NaOH treated samples.

In the case of silane treatments, the amount of cellulose and hemicellulose was increased compared to the untreated fibres. This may be due to the fact that silane

molecules formed couplings with the fibre constituents and were deposited on the fibre surfaces which in turn contributed to the weight percentage gains of the fibres. Similar results were also found for alkali pre-treated silanised fibre samples.

From the above discussion it can be stated that, alkali treatments have higher reactivity in removing hemicellulose and lignin constituents from the fibre when compared to the acetyl treatments, whereas silane treatments provide couplings with the fibre constituents.

4.2.2 Fibre morphology analysis

Figure 4.1 shows SEM micrographs of untreated hemp fibres and its constituents i.e. cellulose, hemicellulose and lignin. Images show that the cellulose microfibril surface (Figure 4.1b) was the cleanest when compared with original fibre (Figure 4.1a). Hemicellulose (Figure 4.1c) and lignin (Figure 4.1d) were black in colour and gummy in appearance. This indicated that hemp fibre structure consists of cellulose microfibrils where the microfibril surfaces were covered with hemicellulose and lignin constituents. From these micrographs it can be seen that the cellulosic fibre surface (cellulose microfibrils) was covered by non-cellulosic constituents (hemicellulose and lignin).

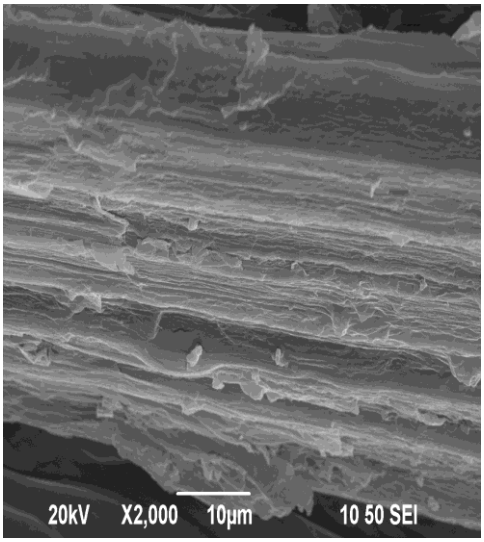

(a)

(b)

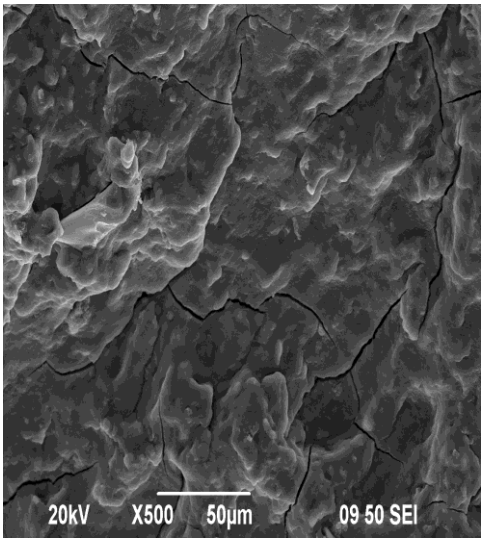

(c)

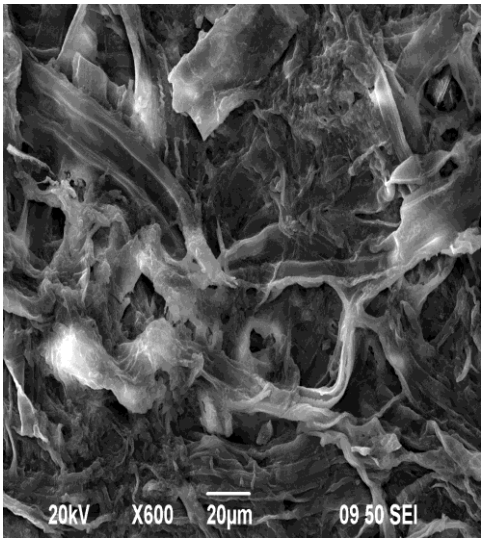

(d)

Figure 4.1: SEM micrograph of hemp (a) untreated fibre (b) cellulose microfibril (c) hemicellulose (d) lignin

(a)

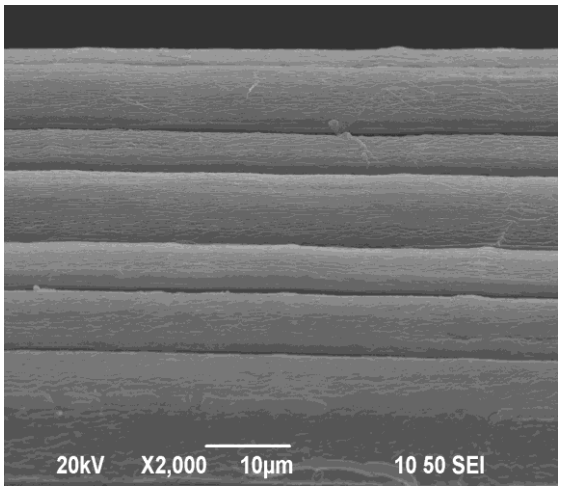

(b)

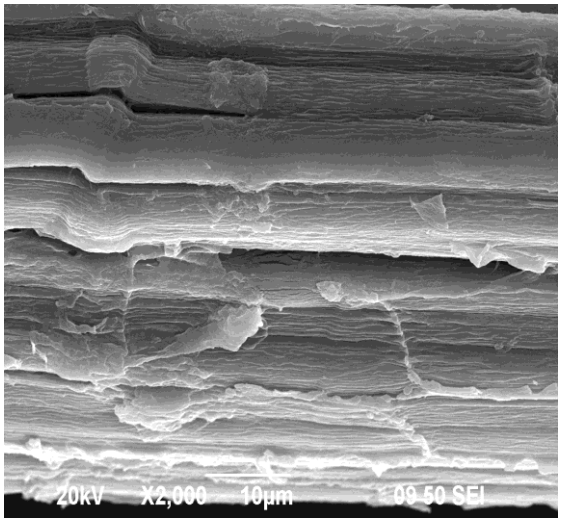

(c)

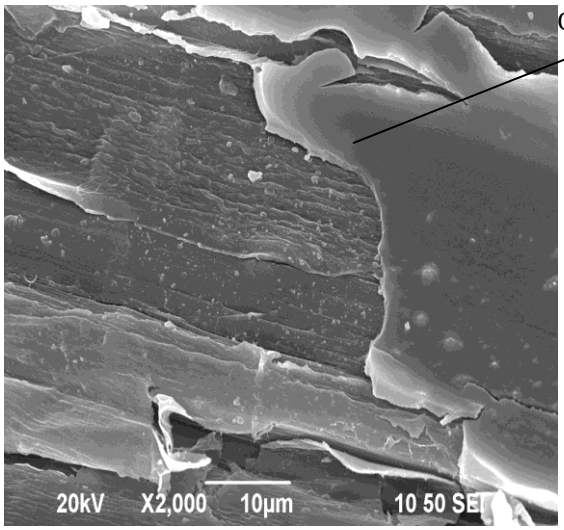

Figure 4.2: SEM micrograph of (a) alkalised (b) acetylated (c) silanised fibre surface

Figure 4.2a shows alkalised fibre surfaces which appeared as bundles of continuous cellulose microfibrils (elementary fibre). These microfibrils were well aligned along the fibre direction. Several patterns of partitions formed among these microfibril bundles which could not be seen in the original untreated fibres (Figure 4.1a). This observation clearly indicated that NaOH treatments could remove the hemicellulose and lignin coverings from the cellulose surfaces. This observation is also supported by the results in Table 4.1.

Acetylated fibre surfaces (Figure 4.2b) also exhibited the partitioning of cellulose microfibrils and cleaner surfaces in relation to the untreated fibres (Figure 4.1a). This was a result of a removal of the coverings from the cellulose microfibrils.

Silanised fibre samples (Figure 4.2c) exhibited the formation of coatings on fibre surfaces. The coatings also filled the spaces between the cellulose microfibrils and thus the fibre surfaces were seen to be smooth.

4.2.3 FTIR analysis

The chemical structures of the cellulose, hemicellulose and lignin constituents extracted from hemp fibres were analysed through FTIR. The functional groups present in these constituents and their related IR spectra (wave number) were analysed and are listed in Table 4.2. These constituents' spectra were used to investigate the shifts in functional groups that occurred as a result of chemical treatments. By investigating these shifts, it is possible to determine the effectiveness of chemical treatments on the fibres. The IR spectra of the constituents and treated fibres are shown in Figure 4.3.

Table 4.2: Infrared transmittance peaks (frequency number, cm^{-1}) of fibre constituents

Assigned functional groups	Frequency number	References
Cellulose structure		
The C-H bending of amorphous and crystalline cellulose	900, 1430	(Lojewska, et al. 2005)
The C-OH in plane stretching of cellulose	1373	(Yang, et al. 2007)
Hemicellulose structure		
The C-O and C-C stretching band of xylanes and C-O-C stretching of the glycosidic linkage in hemicellulose	1050	(Wang, et al. 2010)
The C-H bending and C-O stretching frequencies of hemicellulose	1348, 1412, 1465	(Peng, et al. 2009)
-OH bending mode principally related to the presence of water in hemicellulose	1650	
Acetyl and uronic ester groups attached to hemicellulose	1740	(Liu, et al. 2011)
Lignin Structure		
Aromatic C-H in plane deformation and C-O stretching of lignin	1024	(Sun, et al. 2005)
Aromatic ring breathing with C-O and C=O stretching of lignin	1214	(Yang, et al. 2007)
Conjugated carbonyl groups of hydroxycinnamic acids	1713	(Sun, et al. 2005)
C-H stretching in aromatic methoxyl group and methylene group	2920	

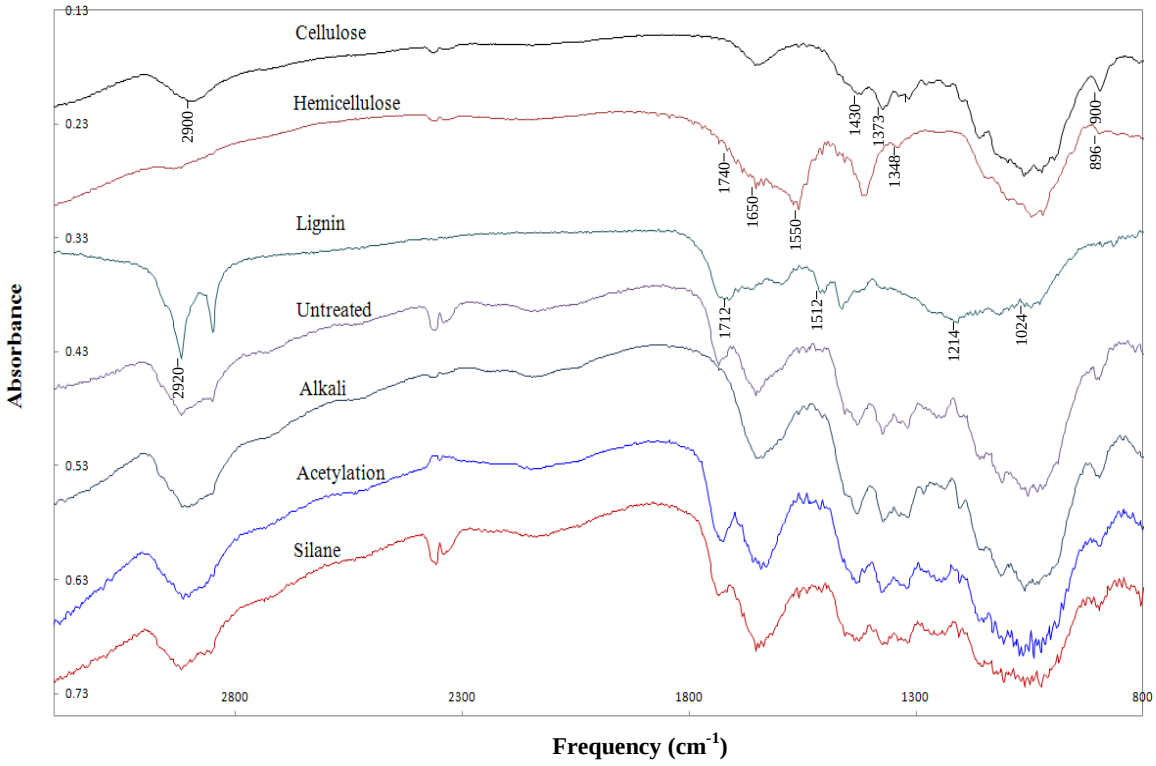

Figure 4.3: FTIR spectra of fibre constituents and treated fibres

Generally, cellulose structures consist of carbonyl, carboxyl and aldehyde groups. Hemicellulose structures consist of a number of different polysaccharides, where extensive hydrogen bonding is present between individual polysaccharides (Bjerre, Schmidt & Riso 1997). These polysaccharides contain xylanes, xylose, arabinose, glucose, galactose, mannose and ketone groups. Xylanes are linked together by glycosidic bonds and are attached to a number of arabino and glucuronic acid residues (Peng, et al. 2009). Lignin is a highly branched aliphatic and phenolic structure which contains aromatic syringyl, guaiacyl, hydroxycinnamic, methoxyl and methylene groups. It is tightly linked to polysaccharides in the cell wall by ether linkages of the alcoholic hydroxyl groups or ester linkages of the cinnamic acid unit

in the alcoholic hydroxyl groups. Majority of lignin in the cell wall is directly linked to arabinos side chains of xylane by ether bonds (Peng, et al. 2009).

Cellulose related functional groups

From Figure 4.3 the characteristic peaks at 900 cm^{-1} and 1430 cm^{-1} were designated as the C-H bending of amorphous and crystalline cellulose. Moreover, the peak at 1373 cm^{-1} was due to the C-OH stretching of the hydrogen bond intensity of crystalline cellulose. These peaks remained unchanged for alkalised, acetylated and silanised fibres. This suggests that the treatments did not affect the cellulose structure of the fibre.

Hemicellulose related functional groups

The peak at 1050 cm^{-1} was the due to the presence of xylane and the glycosidic linkages of hemicellulose. This peak was shifted to a higher side at 1062 cm^{-1} and 1063 cm^{-1} for alkalised and acetylated fibre indicating the removal of hemicellulose after treatment.

The small peak at 1348 cm^{-1} was due to the C-H bending and C-O stretching of hemicellulose. This peak was shifted to a higher number of 1354 cm^{-1} for alkali treatment. This indicates that the hemicellulose degradation occurred due to alkalisation. However, untreated and silanised fibres showed similar peaks at 1348 cm^{-1} indicating that no reaction had taken place in the hemicellulose from the silane treatment.

The peak at 1650 cm^{-1} was due to the presence of bonded water in hemicellulose. For acetylated fibres, this peak shifted to a lower number of 1623 cm^{-1} compared to the untreated fibres (1650 cm^{-1}). This indicates the removal of bonded water from the hemicellulose as a result of the acetyl treatments.

The characteristics' peak at 1740 cm^{-1} was due to substantial acetyl and uronic ester groups becoming attached to the hemicellulose. This peak was not present in the alkalised fibres. The removal of hemicellulose from the fibre surfaces caused this peak to disappear.

Lignin related functional groups

The characteristics peak at 1024 cm^{-1} was assigned to the aromatic C-H in plane deformation and C-O stretching in primary alchohols (guaiscyl) of lignin. For alkali and acetyl treatments these peaks increased by 12 cm^{-1} and 8 cm^{-1} respectively. This indicated that lignin was removed from the treated fibres. However, for silane treated fibres, a similar peak as the untreated fibres appeared at this region. This indicates that there was no reaction between lignin and silane chemicals.

The peak at 1214 cm^{-1} was due to the aromatic ring breathing with C-O and C=O stretching in condensed guaiacyl units of lignin. This band was shifted to a lower number at 1210 cm^{-1}, 1208 cm^{-1} and 1205 cm^{-1} for alkali, acetyl and silane treatments respectively, indicating that treatments caused the degradation of a portion of lignin.

The peak at 1713 cm^{-1} originated from conjugated carbonyl stretching due to the presence of hydroxycinnamic acids associated with the alcoholic polysaccharides of lignin. For alkali treated fibres, this peak disappeared due to the removal of lignin.

Untreated fibres showed a C-H stretching peak at 2918 cm^{-1}. Lignin also showed a strong peak at 2920 cm^{-1}. This indicates that C-H stretching of lignin aromatic hydrocarbon, methoxyl and methylene groups of lignin had taken place. In the case of alkalised and acetylated fibres, these peaks shifted to 2910 cm^{-1} and 2916 cm^{-1} compared to the untreated fibres. This indicated that the alkalisation and acetylation removed lignin constituents. However, the silane had no reactivity with the lignin constituents as it had a similar peak to the untreated fibre.

From the above analysis it can be concluded that, alkali and acetyl treatments had a degree of reactivity in removing hemicellulose and lignin constituents from the fibre. However, silane treatments did not show any reactivity on the fibre constituents as there were no changes of FTIR spectra as compared to the untreated fibres.

4.2.4 TGA analysis

Thermo gravimetric analysis (TGA) was used to measure the weight loss of fibres as a function of rising temperature. The weight loss in fibres occurs due to the decomposition of cellulose, hemicellulose and lignin constituents during heating. Higher decomposition temperatures give greater thermal stability (Kim & Eom 2001; Manikandan, Thomas & Groeninckx 2001). In this study, TGA analysis was first carried out on cellulose, hemicellulose and lignin constituents and then compared

with untreated fibres. TGA analysis was also carried out on the treated fibres to determine the effect of treatment on fibre.

The fibre degradation process was divided into four stages: moisture evaporation, hemicellulose degradation, cellulose degradation and lignin decomposition. Moisture presents in the fibre in two forms: free water and linked water. Free water attached on the fibre surface and evaporates at lower temperature (25-150°C). The linked water form chemical bonds with the hydroxyl groups presented in hemicellulose and lignin, and evaporate at higher temperatures (Randriamanantena, et al. 2009). After the removal of free water, between the temperature ranges of 150-500°C, the degradation process begins in the cellulose, hemicellulose, lignin constituents and the associated linked water (Kim & Eom 2001).

TGA analysis of cellulose, hemicellulose and lignin constituents

The decomposition behaviour of fibre constituents and untreated fibre are presented in Figure 4.4.

Cellulose

From Figure 4.4a it can be observed that the cellulose decomposition process (weight loss) was very mild until around 250°C. Then a sharp and large weight loss occurred at about 350°C. At these temperature ranges (250-350°C) the cellulose was entirely decomposed due to the breaking down of its molecular structures. The degradation temperature of cellulose was higher than the hemicellulose (25-290°C) and lignin (150-420°C). This was due to the fact that most of the cellulose structure was crystalline, which is strong and resistant to hydrolysis. The crystalline structure

contained strong intramolecular and intermolecular hydrogen bonding which required higher energies to be broken down (Placet 2009; Tajeddin, et al. 2009; Thakur & Singha 2010). Derivative of TGA curves (Figure 4.4b) show the degradation of cellulose is at about 320°C.

(a)

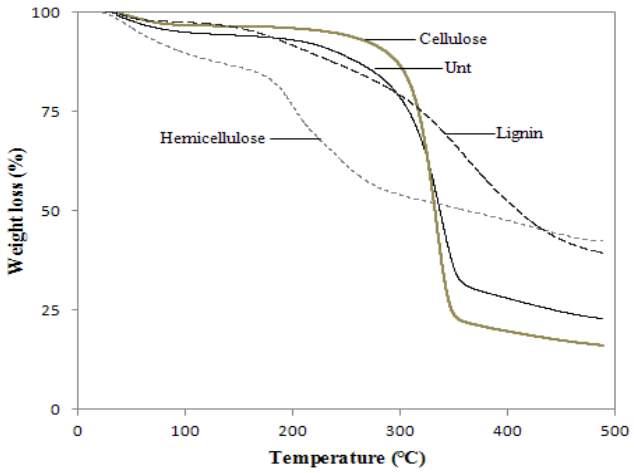

(b)

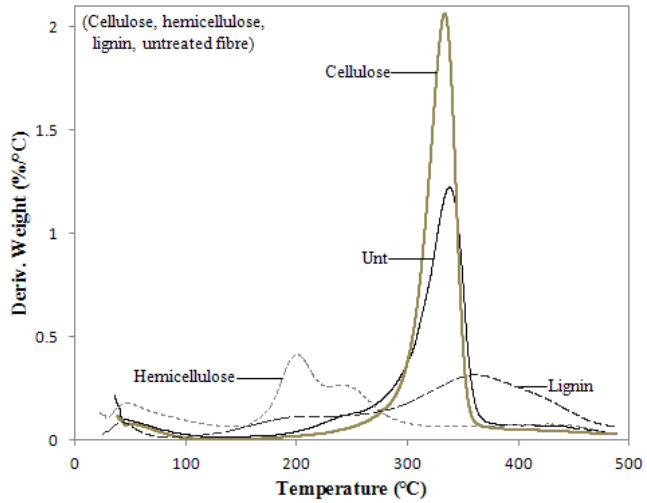

Figure 4.4: (a) TGA (b) DTGA curves of fibre constituents and untreated fibre

Hemicellulose

The decomposition of hemicellulose began at lower temperatures compared to cellulose and lignin. The thermograph of hemicellulose presented three stages of

decomposition (from 25 to 180°C, from 180 to 280°C and from 280 to 500°C). The first stage indicated the removal of moisture absorbed by hemicellulose. In the second stage, the majority of the hemicellulose decomposed with rapid weight losses. At this stage, xylane decomposed and constituent water evaporated. At the last stage, hemicellulose decomposed leaving only a char residue. Derivative of TGA curves (Figure 4.4b) show the degradation of hemicellulose is at about 200°C.

Lignin

The thermal decomposition of lignin took place over a broader temperature range (150-450°C) than the cellulose and hemicellulose. During heating, lignin formed aromatic hydrocarbons, hydroxyphenolics, guaiacyl and syringyl compounds (Brebu & Vasile 2010). All of these components contained –OH groups which became unstable at higher temperatures. These unstable groups underwent further reactions amongst themselves which resulted in structural rearrangements due to radical-radical interactions. Accordingly, the lignin consists of guaiacyl and syringyl which act as intermediate degradation products. The guaiacyl is formed at lower temperatures, while syringyl is formed at higher temperatures (Brebu & Vasile 2010). As a result, a secondary decomposition reaction of guaiacyl and syringyl also contributed to the lignin degradation processes. These molecular activities increased the degradation steps of lignin under prolonged temperatures with a smaller amount of weight losses. Derivative of TGA curves (Figure 4.4b) show the lignin decomposition had a wide and flat peak, featuring a gently sloping baseline over a wide range of temperatures.

From the above analysis it was observed that the amount of moisture evaporation of hemicellulose was much higher than the cellulose and lignin. Due to this, the hydrophilic nature of the fibre was predominantly caused by the presence of hemicellulose. The major fibre decomposition was caused in the second stage where large weight losses were recorded. This was primarily caused by the decomposition of hemicellulose and partly by the lignin degradation. The decomposition temperature of cellulose was much higher than hemicellulose and lignin.

TGA analysis of treated fibres

Alkalised fibres

Figure 4.5a shows the TGA thermographs of alkalised fibre samples. The alkalised (4-10% NaOH) fibres showed higher decomposition temperatures compared to the untreated fibres (0% NaOH). For the main fibre decomposition region (250-350°C), the alkalised fibres had less weight loss than the untreated fibres. These results indicate that alkali treatments removed portions of hemicellulose and lignin constituents from the fibre. Due to this, the decomposition process mainly occurred on the cellulose which in turn increased the overall degradation temperature of the treated fibres.

(a)

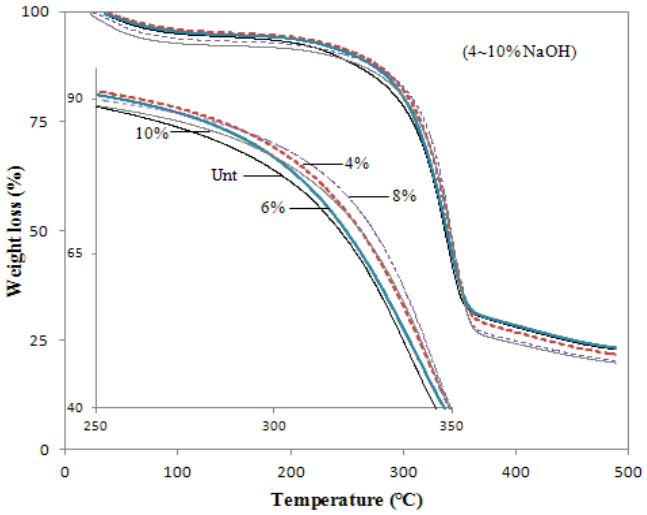

(b)

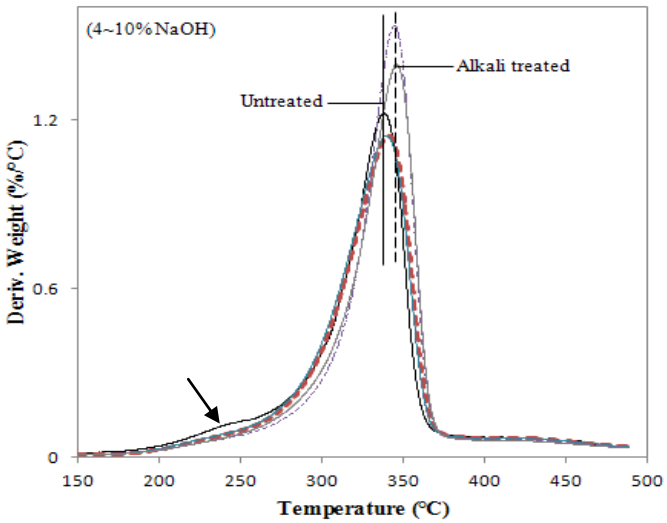

Figure 4.5: (a) TGA and (b) DTGA curves of alkalised fibres

DTGA (Figure 4.5b) curves also showed a lower temperature peak at around 240°C for untreated fibres which corresponded with the decomposition of hemicellulose. For the treated fibres, this peak was not visible, indicating the removal of hemicellulose from the fibre. In addition, a large peak at a temperature around 320°C was due to cellulose and lignin decomposition. At this stage, all the treated fibres showed higher decomposition temperatures compared to the untreated fibres. This again proved that hemicellulose and lignin were removed from the treated fibres.

Acetylated fibres

The effects of acetyl treatments on the alkalised fibres are presented in Figure 4.6. Similar to alkalised fibres, acetylated fibres also showed higher thermal stability when compared to the untreated fibres at the temperature range of 250-350°C. In addition, the DTGA curves also exhibited higher temperature peaks for the alkali pre-treated acetylated fibres. These results also indicated the portion of hemicellulose and lignin constituents were removed from the treated fibres.

(a)

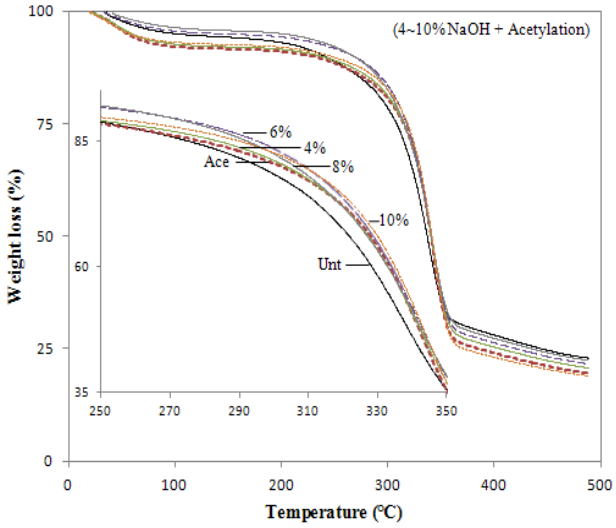

(b)

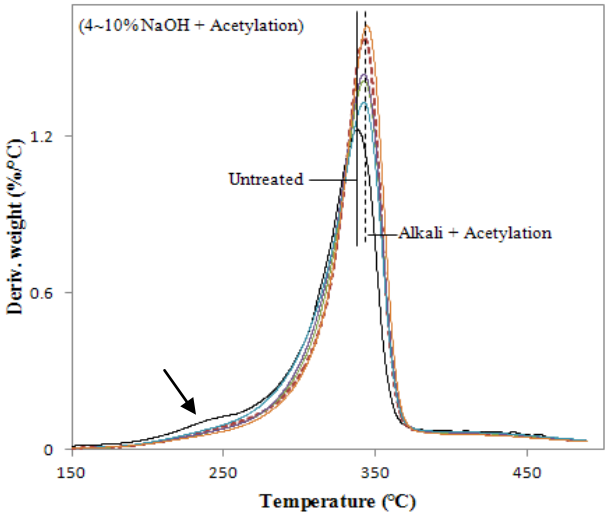

Figure 4.6: (a) TGA and (b) DTGA curves of acetylated fibres

Silanised fibres

The effects of silane treatments on the alkalised fibres are presented in Figure 4.7. From Figure 4.7b it can be observed that silane treatments on the 0% NaOH treated fibres exhibited a hemicellulose peak at around 240°C, similar to the original untreated fibres. This indicated that silane treatments were not capable of removing hemicellulose from the fibre. Instead, silane molecules formed couplings with the hemicellulose and lignin constituents of the fibre. These chemical couplings acted as a covering layer on the fibre surface (Figure 4.2c). This silane covering protected the fibre from thermal decomposition at higher temperatures. These actions prevented the breakdown of the fibre's molecular structure thus enhancing the overall thermal stability of the silane treated fibres at higher temperatures (250-350°C) compared to the untreated fibres. Therefore, hemicellulose peaks for alkali pre-treated silanised fibres were not observed, indicating that the initial NaOH pre-treatment removed the hemicellulose from the fibre. The further silane coverings on the pre-treated fibres enhanced the thermal resistance at 250-350°C thus increasing the decomposition temperatures.

(a)

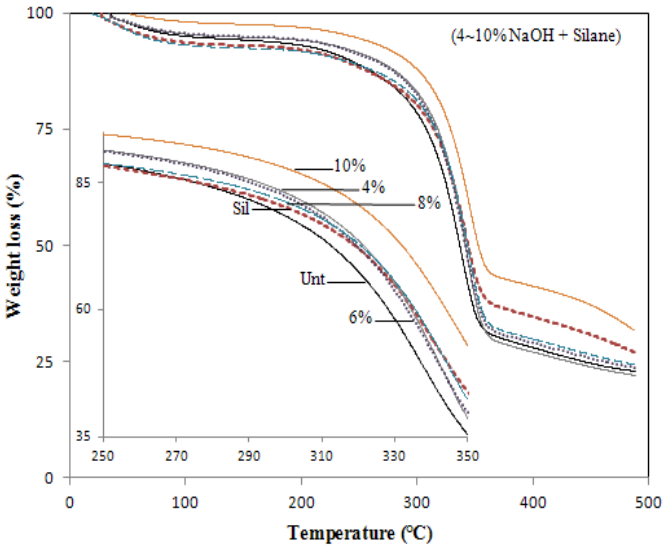

(b)

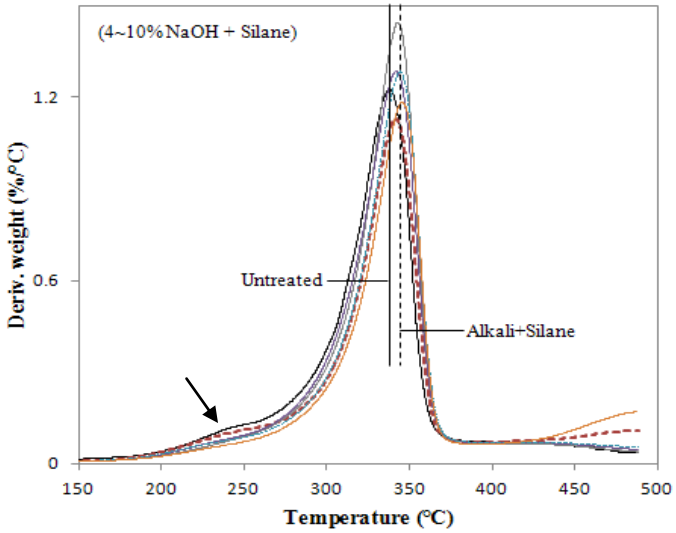

Figure 4.7: (a) TGA and (b) DTGA curves of silanised fibres

From the above analysis it can be stated that, alkali and acetyl treatments removed a portion of hemicellulose and lignin constituents from the fibre thus exhibiting a higher thermal stability at a temperature range of 250-350°C. However, silane molecules formed couplings with hemicellulose and lignin which prevented thermal decomposition of fibre constituents thus improving the fibres' thermal stability.

4.2.5 DSC analysis

DSC analysis allowed for the detection of phase transformation during the heating of fibre. Cellulose, hemicellulose and lignin constituents showed separate peaks of decomposition which appeared through the sequence of endothermic and exothermic peaks of phase transformation at defined temperatures (Reh, Kraepelin & Lamprecht 1986). Ball, McIntosh & Brindley (2004) reported that the endothermal reactions occurred due to the volatilisation (gases) of the molecules, whereas exothermal reactions occurred due to the formation of charring (solid residue). In this study, DSC analysis was first carried out on the cellulose, hemicellulose and lignin

constituents and then compared with untreated fibres. DSC analysis was also carried out on the treated fibres to determine the effect of treatment on fibre.

DSC analysis of cellulose, hemicellulose and lignin constituents

The decomposition behaviour of fibre constituents and untreated fibre are presented in Figure 4.8.

Cellulose

The DSC curve of cellulose exhibited an endothermic event at the temperature range of 10-150°C. Heat absorbed in this endothermic region was due to the evaporation of water (volatilisation) in the intercellular region of the fibre. Generally, free water was removed easier than the linked water (attached to the cellulose). Linked water requires higher temperatures (about 100°C) to be removed (MonteiroI, et al. 2010). In the temperature range of 315-360°C one broad endothermic event occurred and a small exothermic event took place at around 360°C. In the endothermic event, depolymerisation of cellulose had taken place with the formation of volatiles. The depolymerisation process also generated cellulose char residue via exothermic reactions. This behaviour was supported from the reported information that the cellulose structure did not completely decompose until the temperature had reached 340°C (Kim & Eom 2001).

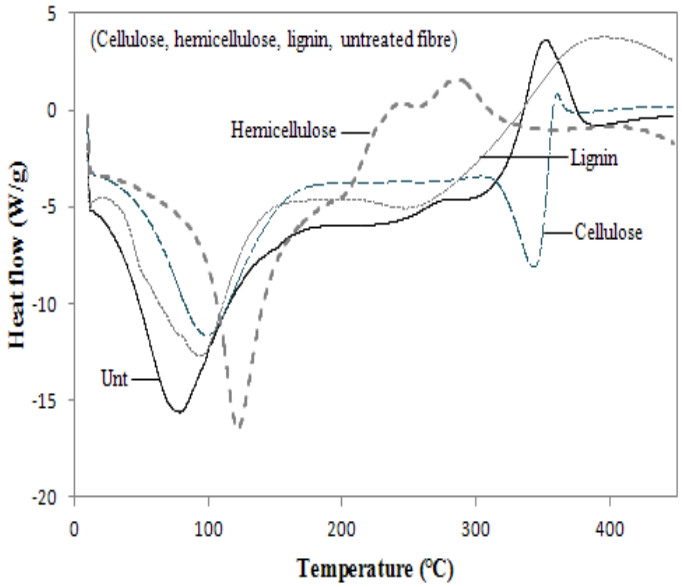

Figure 4.8: DSC curves of fibre constituents and untreated fibre

Hemicellulose

The DSC curve of hemicellulose showed an endothermic peak at the temperature range of 10-200°C followed by an exothermic event at 200-320°C. During the exothermic events, the amorphous structure of hemicellulose decomposed and formed char residues.

Lignin

The Lignin curve showed a broad exothermic peak at the temperature range of 250-450°C. Lignin possesses aromatic rings with many branches in which a large number of chemical links exist. As a result, degradation of lignin occurs over a broad range of temperatures.

From the above fibre constituents' behaviour it can be observed that, hemicellulose has a higher endothermic peak (around 120°C) compared the cellulose (around 100°C), lignin (around 95°C) and the untreated fibres (around 80°C). From this, it

can be stated that hemicellulose absorbs more water compared to the other constituents of the fibre. This may be due to the fact that the structure of hemicellulose consists of rich amorphous branches of hydroxyl groups that link with water molecules from the atmosphere.

Exothermal peaks of cellulose (around 360°C), hemicellulose (200-320°C) and lignin (250-450°C) indicate that hemicellulose and lignin generate higher solid residues (char) compared to cellulose. These results were also supported by the TGA curves (Figure 4.4a) in which the weight of solid residue (400-500°C) was higher for hemicellulose and lignin compared to the cellulose. Based on this, it can be stated that hemicellulose begins to degrade earlier than lignin and cellulose. Cellulose possesses higher thermal stability and lignin decomposes over broad temperature ranges. These decomposition mechanisms of fibre constituents were used to analyse the behaviour of treated fibres.

DSC analysis of treated fibres

Alkalised fibres

Figure 4.9 shows DSC curves of alkalised fibres. Alkalised fibres (6-10% NaOH) showed a higher endothermic peak (around 100°C) for water evaporation compared to the untreated fibres (around 80°C). This result indicates that the treatment removed hemicellulose from the fibre. However, the endothermic peak of 4% NaOH treated fibre took place at the same temperature (around 80°C) as untreated fibres. This indicates that 4% NaOH concentration was not strong enough to remove hemicellulose from the fibre.

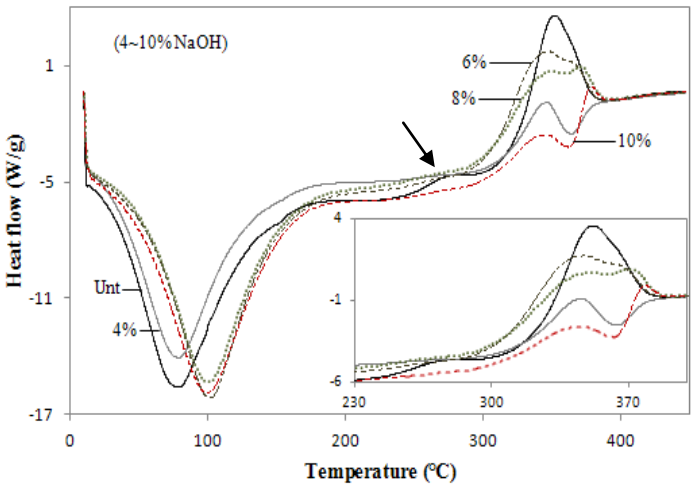

Figure 4.9: DSC curves of alkalised fibres

A small exothermic peak (arrow mark) appeared at the temperature range of 250-290°C for untreated fibres. This peak was mainly due to the decomposition of hemicellulose and a portion of lignin degradation. This exothermic peak disappeared from the alkali treated fibres indicating that greater amount of hemicellulose and lignin were removed from the fibre.

Untreated fibres showed one strong exothermic peak at 300-400°C, whereas treated fibre showed exothermic (390-380°C) and endothermic peaks (around 360°C) in this region. The initial exothermic peak on treated fibres indicated complete decomposition of the hemicellulose and the later endothermic peak indicated decomposition of the cellulose. This exothermic peak differences between the untreated and treated fibres gave further evidence of hemicellulose removes from the fibre during alkali treatments.

Acetylated fibres

Figure 4.10 shows the effect of acetyl treatments on the alkalised fibres. The acetylated fibres had higher endothermic peaks (90-110°C) compared to the untreated fibres (80°C). Similar to alkalised fibres, acetylated fibres also exhibited small exothermic and endothermic peaks at the temperature range of 310-380°C. These results indicate that acetyl treatments also remove hemicellulose and a portion of lignin constituents from the fibre.

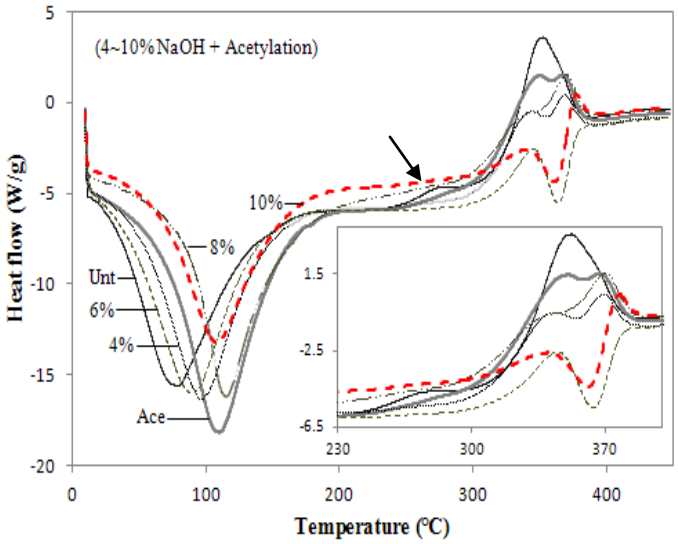

Figure 4.10: DSC curves of acetylated fibres

Silanised fibres

Figure 4.11 shows the effect of silane treatments on the alkalised fibres. Silane treatments on the untreated fibre exhibited a higher endothermic peak temperature (around 110°C) compared to the untreated fibre. This was due to the fact that silane molecules formed couplings with the hemicellulose and lignin constituents of the fibre. The water molecules held by the hemicellulose were covered by the silane coupling layers. As a result, removal of water molecules from the silane treated

fibres required higher temperatures. Therefore, silane treated fibres had similar a DSC profile to untreated fibre at the temperature range of 230-450°C indicating the presence of hemicellulose on the silanised fibres. All of these results indicate that, hemicellulose and lignin remained on the silane treated fibres.

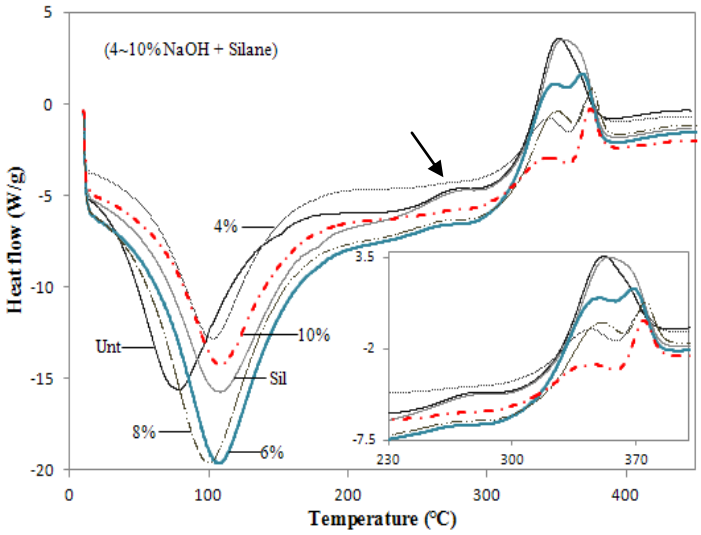

Figure 4.11: DSC curves of silanised fibres

From the above analysis, it is confirmed that alkali and acetyl treatments on the fibres remove hemicellulose and lignin constituents, whereas silane formed couplings with these constituents and provided a covering on fibres protecting them from thermal degradations.

4.3 Summary

Chemical treatments change fibre structures by reacting with its constituents. Alkalisation and acetylation reduce the content of hemicellulose and lignin from the fibre. These treatments also expose cellulose microfibrils on their fibre surface. Whereas, silane treatments forms coverings on the fibre surfaces and fills the spaces among the microfibrils.

FTIR analysis shows that alkali and acetyl treatments remove hemicellulose and lignin constituents from the fibre surface whereas silane has no reactivity with these constituents.

Thermal analysis (TGA and DSC analysis) of fibre revealed that hemicellulose is the most reactive constituent and decomposes early. Cellulose is more thermally stable and lignin decomposes under a wide temperature range. Treated fibres show higher thermal stability compared to the untreated fibres.

Chapter 5: Chemical Treatments on Fibre Strength

5.1 Introduction

Among the three main structural constituents of hemp fibre, cellulose was the primary load carrying component while hemicellulose and lignin acts as a binder to hold the cellulose. Chemical treatments reacted with hemicellulose and lignin constituents, and as a result reconfigured their proportions within the fibres. These changes play a role in affecting fibre strengths. In this chapter, the effects of chemical treatments on single fibre strength are discussed.

In single fibre tensile tests, accurate fibre diameter measurement is a particular challenge. Unlike synthetic fibres, natural fibres have irregular shapes and textures along their lengths. Single fibres consist of a bundle of elementary fibres. Cross-sectional geometries of fibre bundles are generally not circular and diameters are not uniform along their lengths. Also, there are inherent natural and artificial defects within these fibres (Hu, et al. 2010). These factors contribute to the presence of variations within natural fibres.

Accurate measurements of cross-sectional areas are essential for measuring the tensile properties of single fibres. Different microscopic measurements have been used to determine fibre diameter. Eichhorn & Young (2004) used SEM to measure hemp fibre diameters with an assumption that the fibres had a circular cross section. Devi, Bhagawan & Thomas (1997) used a stereo microscope to obtain pineapple

fibre diameters based on the same assumption. Considering circular cross-sections of fibres may lead to an underestimation in the calculation of fibre tensile properties.

During tensile tests, particular attention must be given to the manner in which the fibres are mounted in the apparatus to avoid the introduction of stress concentrations at various locations on the grip. Also, load cells need to be sensitive enough to detect small forces and to make precise measurements of fibre elongation. Slippage in the gripping assembly can result in error of elongation values and lead to underestimated fibre modulus. Fan (2010) used paper frames, in which hemp fibres were glued and mounted to the testing machine. The paper was cut to open in the middle to free the fibre to perform the test. This method was efficient in handling and transferring the fibres to the testing machine without fibre damage. Similar fibre preparation was also performed by Feih, Thraner & Lilholt (2005) on glass fibres. A number of studies have also reported on strain measurements by means of non-contacting video extensometer (Adusumalli, et al. 2006).

In this study, the tensile properties of single hemp fibres were measured by taking into account, the variations in fibre diameters. Alkali, acetyl and silane treatments' effects on the fibres with respect to tensile properties are discussed. The relationship between tensile properties of the treated fibres and the variation of their diameters were also studied.

5. 2 Results and discussion

5.2.1 Influences of fibre diameter on tensile properties

Fibre diameters are also subject to variances due to the loss of hemicellulose and lignin coverings as a result of chemical treatments. Two methods were used to determine the diameter of the treated fibres.

The first method used the averaged fibre widths at different locations along the fibre's length. For this, fibres were placed horizontally under the microscope (Chapter 3, Section 3.4.2) and attached with glue tag to avoid movement. At least 20 locations were measured and average values were reported. The second method measured the diameters around the breakage of the tested fibres. For this case, it was important to obtain a flat and clear cross-section at the fracture end. Tested fibres were perpendicularly attached with glue tag and the equivalent diameters were obtained through image analysis. The fracture end of the tested fibres was strained and had relatively smaller cross sections. Therefore fibre ends were cut close to unstrained points.

Figure 5.1a presents typical OM images of a single fibre which features an irregular shape and size along the fibre length. Figure 5.1b shows that the cross section of the fibre is not circular.

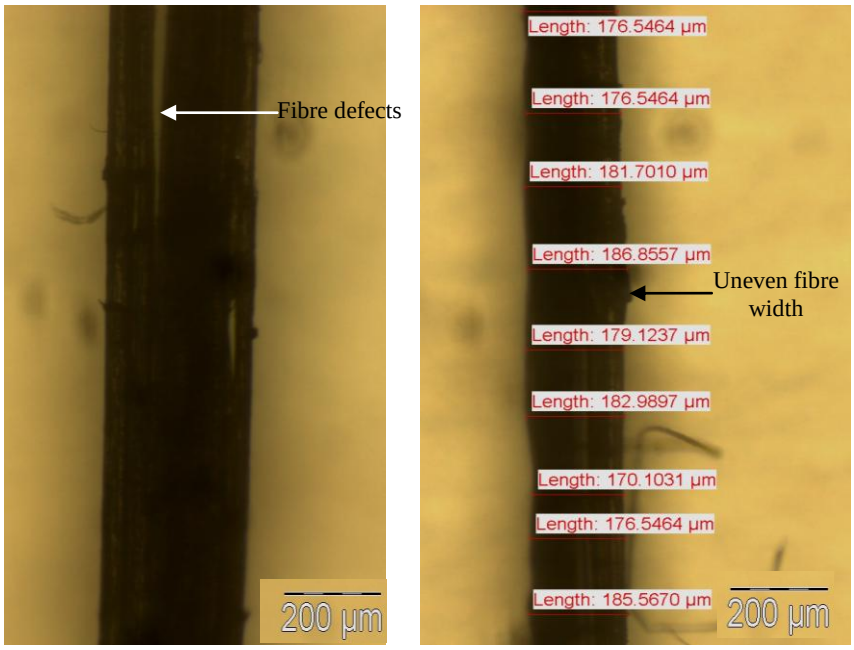

(a)

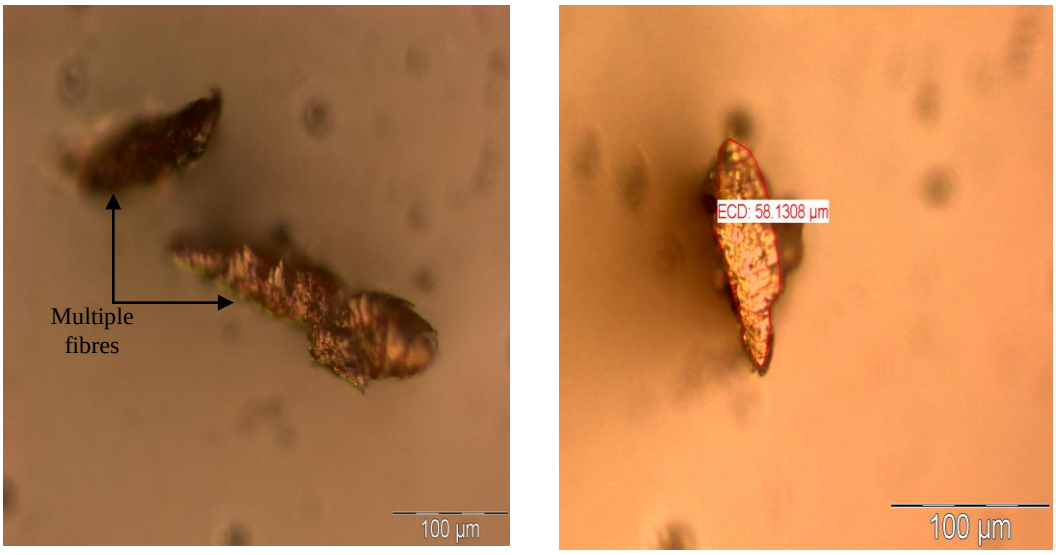

(b)

Figure 5.1: OM images of (a) fibre surface (b) cross-sectional area of fibre fractured surface

Table 5.1 summarises the differences in the measurements of the diameters of fibres achieved when using both methods of calculation. The results indicate that there is a great difference between measuring widths along the fibre and fibre cross sections at the fracture point. Cross-sectional measurement at fracture points were less when compared to widths along the fibre length. This variance in the results was due to the fact that the measurement of the widths along the fibre did not take into account the location of the fracture point. As a result, fracture point diameters were chosen in calculating single fibre tensile strengths.

Table 5.1: Comparison of two diameter (mm) measurement methods of treated fibres

Type of fibre	Width along the fibre length			Cross-section of fibre fracture end		
%NaOH	Alkalised	Acetylated	Silanised	Alkalised	Acetylated	Silanised
0	0.226 ±0.083	0.243 ±0.092	0.273 ±0.080	0.127 ±0.032	0.112 ±0.018	0.162 ±0.019
4	0.262 ±0.0435	0.180 ±0.040	0.301 ±0.081	0.149 ±0.031	0.127 ±0.030	0.135 ±0.041
6	0.169 ±0.041	0.168 ±0.029	0.404 ±0.178	0.119 ±0.028	0.121 ±0.041	0.182 ±0.045
8	0.223 ±0.072	0.184 ±0.087	0.323 ±0.123	0.150 ±0.048	0.085 ±0.030	0.145 ±0.025
10	0.178 ±0.059	0.277 ±0.011	0.289 ±0.092	0.110 ±0.027	0.177 ±0.039	0.138 ±0.040

Figure 5.2 presents strength variations as a function of fibre diameters of alkalised and acetylated fibres. In both treatment cases, a downward trend of fibre tensile strength was observed when the fibre diameter increased. These results highlight the fact that lower strengths would be obtained if the widths along the fibres were used instead of the cross-section measurements at the fracture point.

(a)

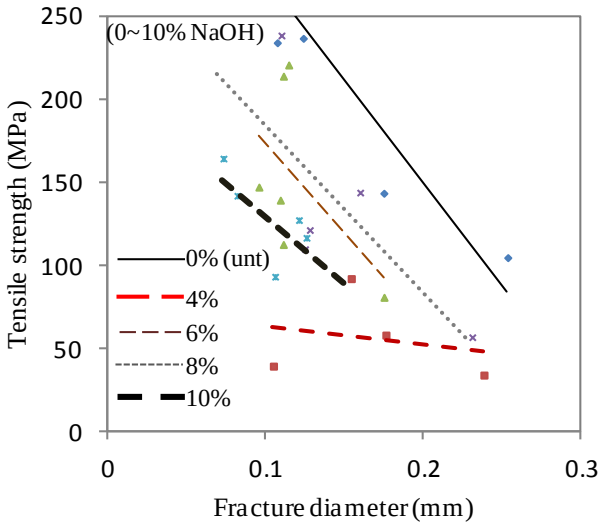

(b)

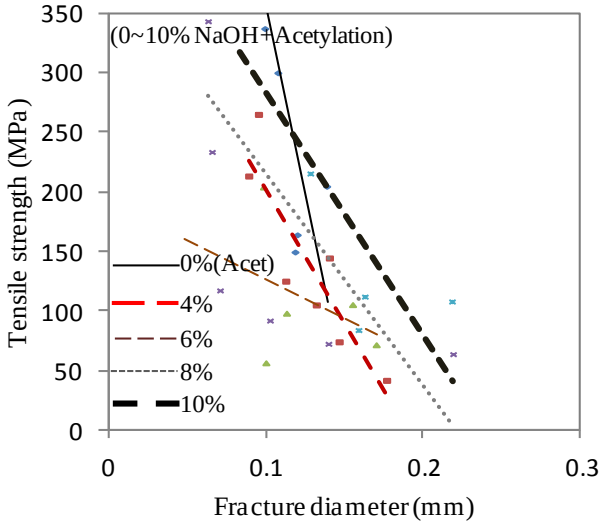

Figure 5.2: Tensile strength as a function of fibre diameter (cross-section) (a) alkalised (b) acetylated fibre

5.2.2 Influences of chemical treatments on tensile properties

The single fibre tensile test method is outlined in Chapter 3 (Section 3.6.1). The strength, modulus and failure strain was calculated from the diameter closest to the specimen failure and average values are shown in Table 5.2.

Table 5.2: Tensile properties of single fibre (considering fibre cross-section as diameter)

Fibre type	Alkalised			Alkalised + Acetylated			Alkalised + Silanised		
%NaOH	Stress (MPa)	Modulus (GPa)	Failure strain (%)	Stress (MPa)	Modulus (GPa)	Failure strain (%)	Stress (MPa)	Modulus (GPa)	Failure strain (%)
0	235.42 ±75.90	2.54 ±0.04	0.140 ±0.022	232.27 ±83.39	2.56 ±1.16	0.131 ±0.024	158.47 ±45.60	0.99 ±0.19	0.153 ±0.036
4	104.18 ±17.68	1.51 ±0.47	0.073 ±0.005	188.24 ±64.31	1.44 ±0.50	0.072 ±0.017	179.86 ±50.28	1.08 ±0.15	0.156 ±0.027
6	166.28 ±47.92	2.72 ±1.04	0.076 ±0.025	114.86 ±52.13	1.10 ±0.16	0.103 ±0.041	78.53 ±23.47	0.56 ±0.15	0.143 ±0.040
8	152.92 ±58.40	1.31 ±0.77	0.090 ±0.053	148.78 ±75.43	1.68 ±0.07	0.046 ±0.014	97.76 ±15.00	0.72 ±0.23	0.154 ±0.033
10	171.83 ±64.35	2.42 ±0.64	0.102 ±0.045	134.17 ±55.44	1.66 ±0.35	0.089 ±0.063	160.01 ±75.79	1.32 ±0.47	0.103 ±0.011

To explain the effects of treatments on fibres, background information regarding fibre structures and reaction mechanisms are outlined.

Natural fibres consist of cellulose microfibrils which are enveloped and interconnected by hemicellulose and lignin. Cellulose microfibril appears as crystalline and amorphous structures. In amorphous region, the microfibrils are less compacted and more irregularly oriented compare to the crystalline region. The hydroxyl groups present in the amorphous region are relatively free to react with other chemicals compared to the crystalline regions (Beckermann & Pickering 2008). Hemicellulose and lignin are always in amorphous structures where hydroxyl groups are also present. The orientation of cellulose, hemicellulose, lignin and their hydroxyl groups are outlined in Figure 5.3.

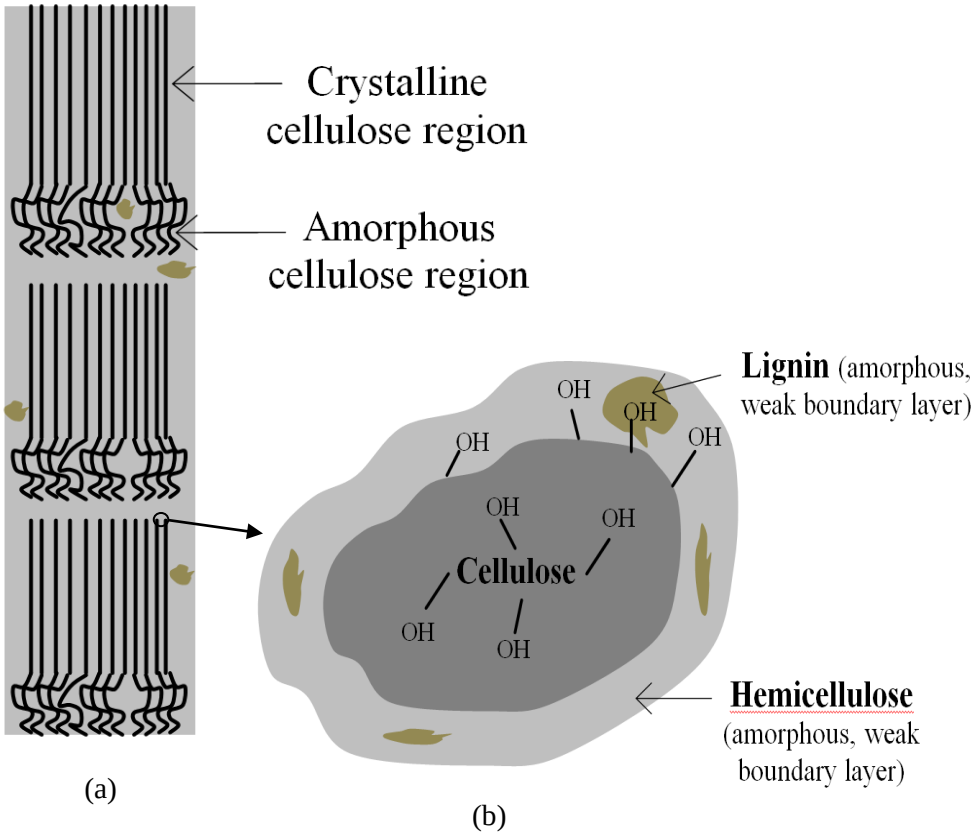

Figure 5.3: Schematic diagram of fibre (a) structure (a) cross-section

When fibres are loaded in tension, cellulose microfibrils are stretched and stress concentrations develop at their joints. These stress concentrations at the joints initiate microcracks and trigger ultimate fibre failure. Also, the load transfer in tension causes cellulose to undergo shearing between individual microfibrils (Fan 2010). The extent of this shearing is reflected in the fibre tensile properties. As a result, it is clear that hemicellulose and lignin constituents also play an important role in fibre structural stability in tensile loading cases. The effects on fibres as a result of alkalisation, acetylation and silanisation are discussed below.

Alkalisation on fibres

Figure 5.4 shows a typical stress-strain curve of alkalised fibres and Table 5.2 summarises their results. From Figure 5.5 it can be seen that the average tensile strength and failure strain of the treated fibres was lower than the untreated fibres. During tensile loading of the untreated fibres, cellulose underwent irreversible slippage between individual microfibrils. The presence of hemicellulose and lignin between the cellulose microfibrils held the microfibrils in position and resisted slippage to an extent. Hence, untreated fibres had greater resistance against tensile loading and exhibited higher properties compared to the NaOH treated fibres. In the case of NaOH treatments, hemicellulose and lignin were removed from the fibre resulting in easy deformations of cellulose microfibrils during tensile loading. Due to this, treated fibres exhibited lower tensile properties compared to untreated fibres.

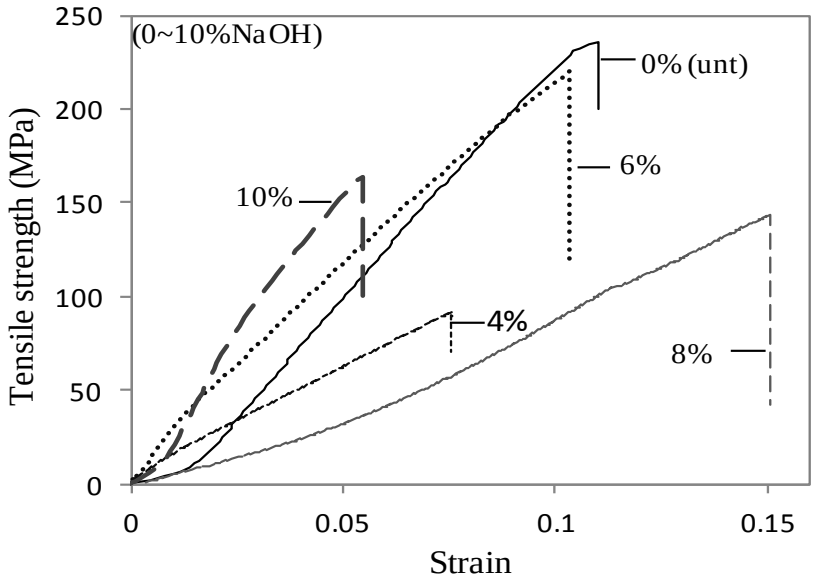

Figure 5.4: Typical stress-strain curves of alkalised fibres

(a)

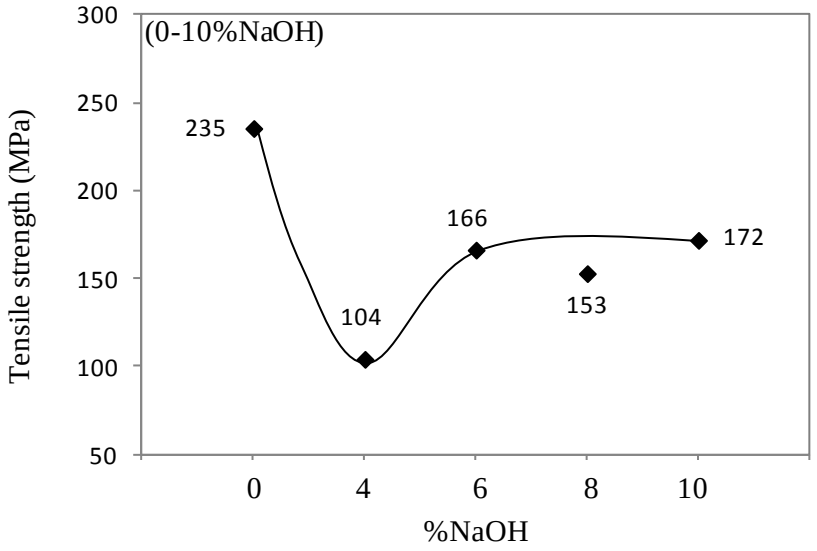

(b)

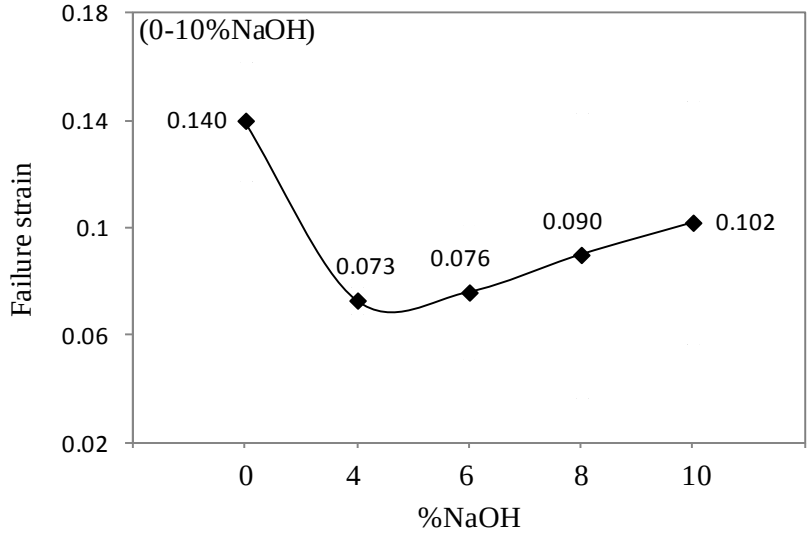

Figure 5.5: Tensile properties of alkalised fibre (a) strength (b) failure strain

From Figure 5.5a it can be observed that 4% NaOH treatments exhibited the lowest tensile properties. These samples exhibited about half the strength and failure strain of untreated fibres. At higher (6-10%) NaOH concentrations the strengths were increased and stabilised at around 165 ~ 170 MPa and failure strains at about 0.07 ~ 0.1 (Figure 5.5b).

These results indicated that the initial 4% NaOH concentrations were not strong enough to remove the covering layers (provided by hemicellulose and lignin constituents) from the cellulose microfibrils effectively. Rather, treatments split the hemicellulose and lignin coverings on the cellulose surfaces. Hemicellulose and lignin remained in the fibre structure at random orientations. These random orientations facilitated fibre hydroxyl groups in becoming free to react with atmospheric moisture. This caused the formation of a slippery layer which reduced the frictional resistance between microfibrils during tensile deformation of the fibre. Due to this, individual microfibrils deformed easily during loading and thus exhibited lower tensile properties compared to the untreated fibres.

Higher NaOH concentrations (6-10%) effectively removed hemicellulose and lignin coverings from fibre surfaces. Hydroxyl groups were also removed from the hemicellulose and lignin region within the fibre. The lack of these hydroxyl groups prevented the formation of the slippery materials layer among the microfibrils. Due to this, higher strengths and failure strains of the treated fibres were observed when compared to the 4% NaOH treated fibres.

Acetylation on alkali pre-treated fibres

Figure 5.6 shows the typical stress-strain curves of acetylated fibres and Table 5.2 summarises their results. The changes in strength of the acetylated fibres are shown in Figure 5.7. In Figure 5.7 it can be observed that an acetyl treatment on untreated fibres (0% NaOH) has not changed fibre strength (approximately 235 MPa). Acetylation on the 4% NaOH pre-treated fibre increased strength from about 105 to 190 MPa. However, acetylation on 8% and 10% NaOH pre-treated fibres diminished the fibre strengths.

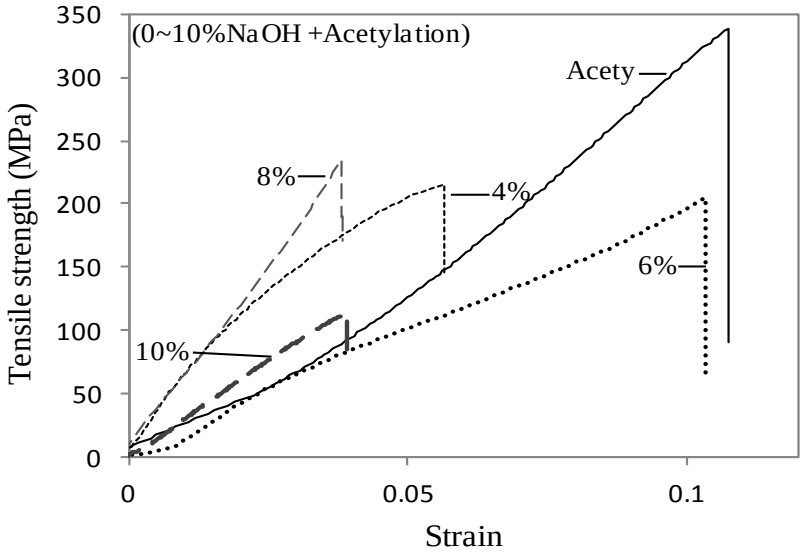

Figure 5.6: Typical stress-strain curves of acetylated fibres

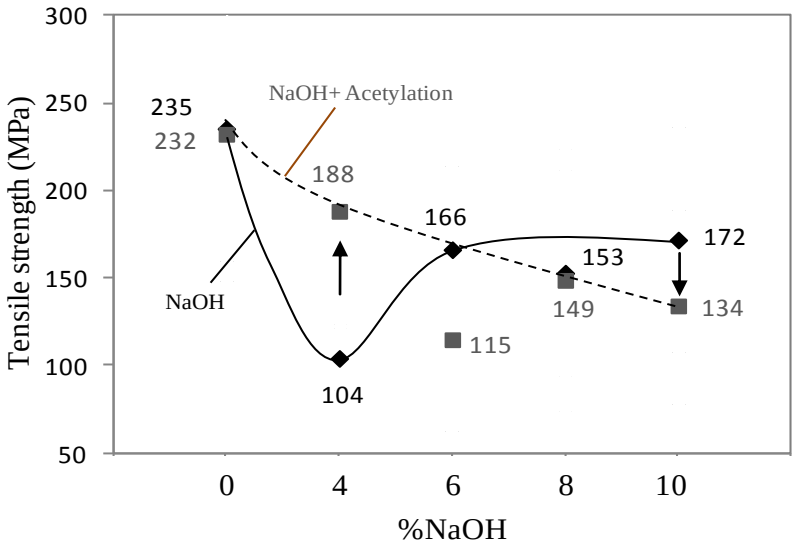

Figure 5.7: Tensile strength of alkali pre-treated acetylated fibres

During acetyl treatments, hydroxyl groups present in hemicellulose were esterified by the acetyl groups and consequently moved out from the fibre. Treatments also took out certain portions of covering layers of hemicellulose and lignin from the cellulose microfibrils. Thus, moisture absorption by the treated fibres reduced and enhanced frictional resistance among the microfibrils during tensile deformations.

As discussed previously, 4% NaOH treatments initially exposed free hydroxyl groups that present in hemicellulose and lignin in the fibre structure, which in turn absorb atmospheric moisture. Further acetyl treatments esterified the hydroxyl groups which existed on the pre-treated fibres. Due to this, the fibre became hydrophobic and eliminated the moisture related slippery materials among the cellulose microfibrils. During tensile loading, fibres experienced higher frictional resistances against irreversible microfibrils slippage and thus exhibited higher strength compared to the 4% NaOH treated fibres.

At higher pre-treatment concentrations (8% and 10% NaOH), the hemicellulose and lignin coverings and their hydroxyl groups were removed from the fibre. Further acetylation created more losses of covering materials from the cellulose microfibrils. The extensive removal of these covering materials led to easy fibre deformation in tensile loading. Thus, two consecutive treatment processes reduced the fibre strengths as compared to the (6-10%) NaOH treated fibres.

Silanisation on alkali pre-treated fibres

Figure 5.8 shows the typical stress-strain curves of silanised fibres and Table 5.2 summarises their results. The changes in strength and failure strain of the silanised fibres are shown in Figure 5.9. From Figure 5.9a it can be observed that silane treatments on untreated fibres reduced strength from around 235 MPa to 160 MPa. As the untreated fibre surface was covered by hemicellulose and lignin, silane molecules could not get access to cellulose microfibrils. Due to this, silane formed couplings with hemicellulose and lignin coverings instead of cellulose microfibrils. Generally, cellulose microfibrils can respond to bear high stresses while hemicellulose and lignin can withstand low stresses (Park, et al. 2006). Thus, the silane coupling effects with the hemicellulose and lignin constituents reduced the tensile properties of the fibre.

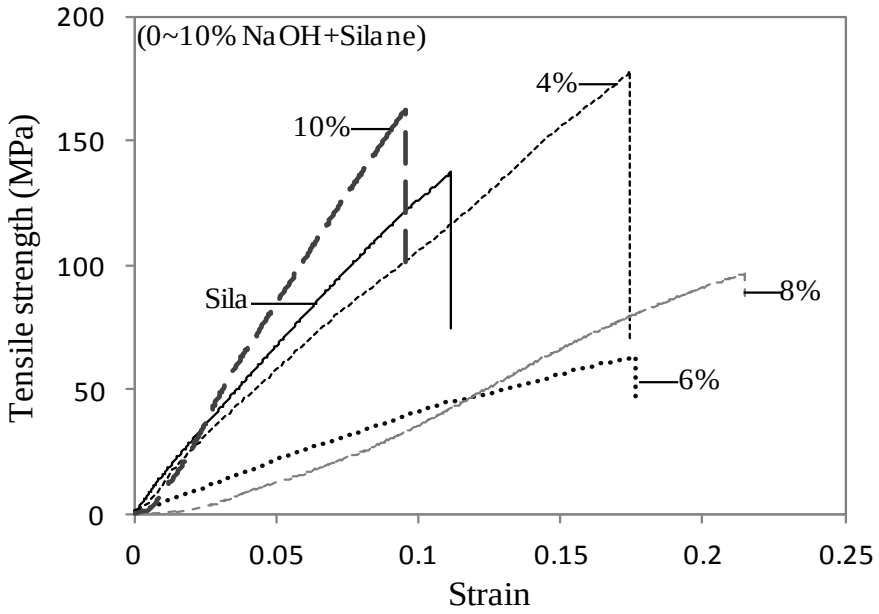

Figure 5.8: Typical stress-strain curves of silanised fibres

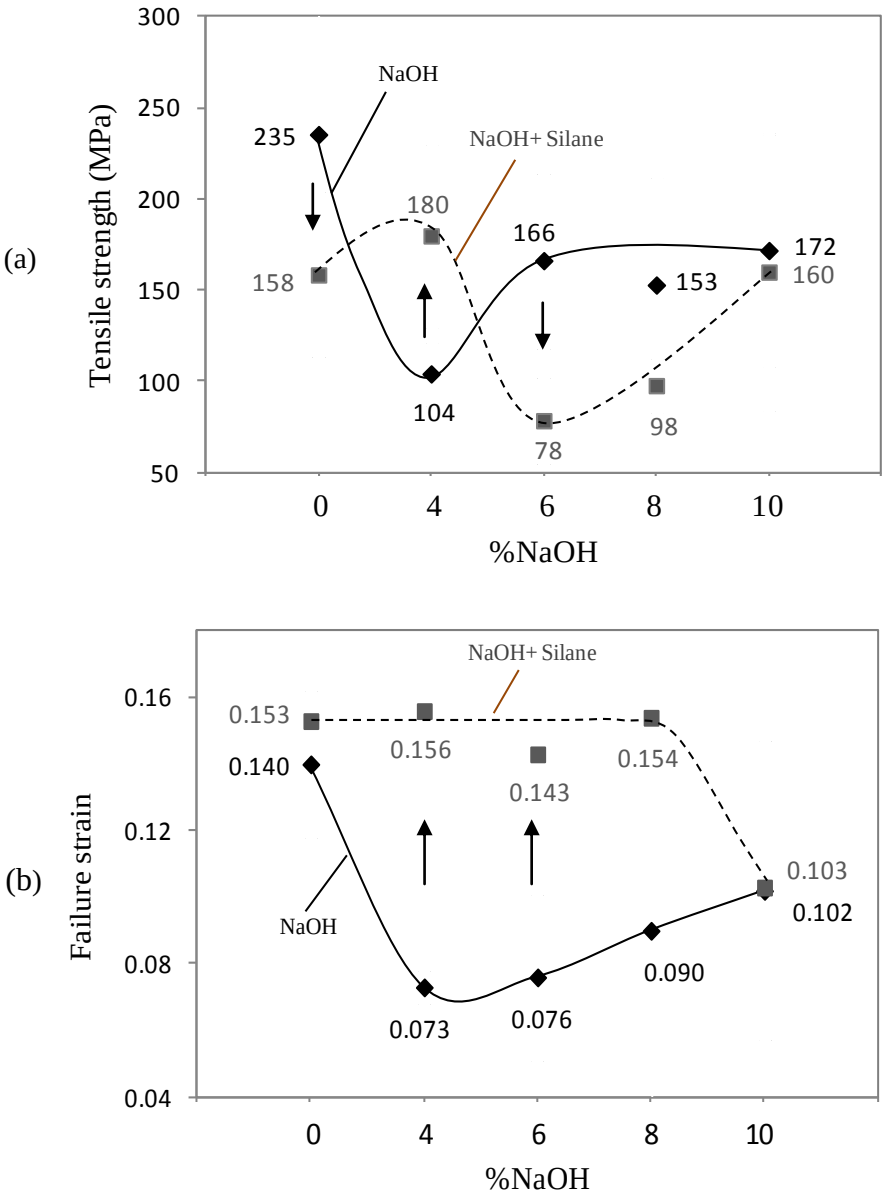

Figure 5.9: Tensile properties of alkali pre-treated silanised fibres (a) strength (b) failure strain

Silane treatments on the 4% NaOH pre-treated fibres increased the fibre strength from around 105 to 180 MPa. As the initial 4% NaOH pre-treatments provided atmospheric moisture to enter into the fibre, the follow-up silane treatments formed couplings with the cellulose microfibrils. These couplings provided support to the microfibrils against tensile deformation and thus the fibre exhibited higher strength than the 4% NaOH treated samples. These results again proved that the initial 4%

NaOH treatment was not strong enough to remove hydroxyl groups in hemicellulose and lignin effectively, and allowed the atmospheric moisture to remain in the fibre structure.

Silane treatments significantly reduced the strength of 6% NaOH pre-treated fibres from 166 to 78 MPa. Strengths also reduced at higher (8% and 10%) NaOH pre-treatment concentrations. This may be due to the fact that at higher pre-treatment concentrations (6-10% NaOH), hemicellulose lignin hydroxyl groups were removed effectively from the fibre and there were no available hydroxyl groups to make further couplings with silane molecules. The weak silane couplings led the cellulose microfibrils to deform under lower tensile loads, thus treated fibres exhibit lower tensile properties compared to the 6-10% NaOH treated fibres.

From Figure 5.9b, silane treatments on the (4-10% NaOH) alkali pre-treated fibres exhibited higher failure strains than the NaOH treated fibres. NaOH pre-treatments created more weakness among cellulose microfibrils and led to easy deformations of fibres during tensile loadings. Conversely, silane couplings tended to hold the microfibrils in the original position which in turn resulted in high fibre deformation. Silane couplings also developed a layer of chemicals on the surface on the microfibrils. The chemical layer provides shear resistance between the microfibrils and the couplings. The shear resistance also contributes to the longer microfibril deformations thus enhancing fibre failure strain.

It can be noted from Figure 5.9 that silane treatments on 10% NaOH pre-treated fibres increased fibre strength but lowered the failure strain when compared to the

6% and 8% NaOH pre-treated fibres. This may be due to the fact that 10% NaOH pre-treatment concentrations were strong enough to remove the hemicellulose-lignin covering layers in such a manner that greater amounts of cellulose microfibrils were exposed on the fibre surfaces. Consequently, the treatment reduced the crystalline cellulose structure to a more amorphous cellulose structure. As a result, greater amounts of hydroxyl groups were exposed. These amorphous cellulose hydroxyl groups may have absorbed atmospheric moisture which in turn facilitated silane molecules to form strong couplings with cellulose microfibrils. The strong coupling effect supported the microfibrils during tensile deformations and thus enhanced fibre strength. However, the extensive removal of hemicellulose and lignin caused a lack of interlocking adhesives of cellulose microfibrils and thus the individual microfibril deformations became easier. During tensile loading, strong silane couplings tended to hold the cellulose microfibrils in the original position but weak interlocking adhesion allowed the microfibrils to fail at lower elongations. Thus the treated fibres exhibited lower failure strain.

5.3 Summary

Hemp fibres have an irregular shapes, non-uniform transverse dimensions and defects along their lengths. To obtain accurate tensile properties, the cross-sectional area at the fibre failure point was used as fibre diameter instead of considering fibre width along their lengths.

The tensile strength of the chemically treated fibres decreased compared to untreated fibres. As hemicellulose and lignin coverings were removed from the treated fibres, cellulose microfibrils received less support against tensile loading.

Among all the NaOH pre-treatment conditions, alkalisation reduced the fibre strength, 4% NaOH had the lowest. Additional acetylation could recover some of the strength loss. Silane treatment increased the failure strain of the fibre.

Chapter 6: Chemical Treatments on Unidirectional Hemp Fibre Composites

6.1 Introduction

For composite preparation, it is desirable to have fibre surfaces which can facilitate strong bonding with the matrix. Composite properties depend greatly on the quality of interface bonding to overcome the intrinsic weaknesses of the structure. Weak bonding limits the efficiency of the composite's load bearing performance and leads to under-utilisation of material properties. Chemical treatments on the fibre can improve interface bonding with the matrix which ultimately enhances the overall load bearing capacity of the composites.

In this chapter, the effect of chemical treatments on hemp fibres, and the associated quality of interface bonding, will be illustrated through a composite mechanical property analysis. In this analysis alkali (0%, 4%, 6%, 8% and 10% NaOH), acetyl and silane treatments on hemp fibres were used. Long unidirectional hemp fibre composites were prepared by VARTM. Interface bonding was examined through tension, compression, shear, bending and impact testing. A possible sequence of failure initiation and propagation is explained through the analysis of stress-strain relationships and microscopic observations. The failure surfaces of the tested samples were examined through the Optical Microscopy (OM).

6.2 Result and discussion

In order to ascertain tension, compression, shear, bending and impact properties of the composites, experimentation was conducted in accordance with standards set out in Chapter 3 (Section 3.6). At least 6 specimens for each treatment case were tested and average values are reported.

6.2.1 Tensile properties of composites

The deformation characteristics of composites in tension are governed by the strength of reinforcing fibres and the interface bonding behaviour between fibres and the matrix (Van & Beukers 1999). During tensile testing, initial loading causes elastic stress transfer from matrix to fibres through the bonded interface. Progressive loading causes the matrix to yield and begin to plastically deform while the fibres deforms elastically. At this stage, interface debonding take place between the fibres and matrix (Fischer 2004).

Interface debonding initiate matrix cracking which then propagates along the interfaces of the neighbouring fibres. Interface debonding and matrix cracking separates the fibres from the matrix, which causes a discontinuation of stress transfer across the composite (Gonzalez & Lorca 2007). At the crack location, fibres are used to carry the applied stress to bridge the matrix cracking. Subsequent composite deformation increases the crack opening which adds further strain to the bridging fibres (Delaet, Lataillade & Wolff 1994). The fibre bridging stress reaches its critical level and result in fibre fractures follows by the fracture of the composite.

The ability of fibres to carry loads depends on the quality of interface bonding. During tensile testing, two types of interface failure are prevalent. First, interfacial debonding initiates fibre sliding within their surrounding matrix. Fibre sliding produces frictional stress transfers at the interface (Cho, Chen & Daniel 2007; Kitsutaka & Takahashi 2001). Second, matrix cracking reduces support to fibres which results in fibres being pulled-out from the matrix. A combination of interface debonding and matrix cracking reduce the strength and stiffness of the composites. Strong interfaces increase frictional resistance against tensile loading. From this it can be stated that, in order to enhance tensile properties of composites, interface bonding strength need to be increased.

Chemical treatments on fibres are used to improve fibre surfaces promoting strong interface bonding between fibres and matrix. In this section, the effect of alkali, acetyl and silane treatments on composite properties were analysed through tensile testing.

The tensile behaviour of untreated and treated fibre composites was analysed through stress-strain curves. Figure 6.1 shows a typical tensile stress-strain curve of a fibre composite. The curve path displays an elastic region where a rapid increase in stress is observed up to 30 MPa with increasing strain of 0.0015, followed by a plastic region. In the plastic region, the stress reaches up to 140 MPa and strain of 0.145. During plastic deformation debonding, interface cracking and matrix cracking develops which leads to final failure of the entire composite.

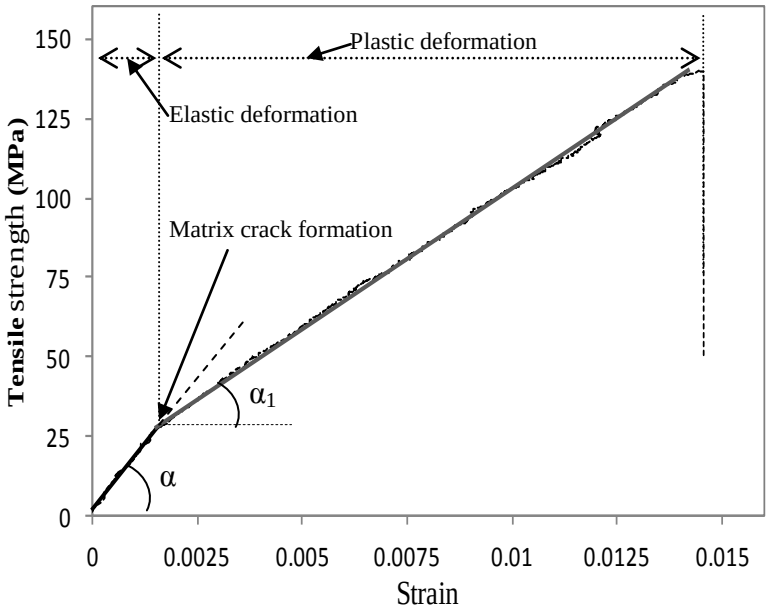

Figure 6.1: Typical tensile stress-strain curve of fibre composite

Fibre alkalisation on composites

Figure 6.2 shows the typical stress–strain curves of composites with different concentrations of NaOH treatments, and Table 6.1 summarises their results. The changes in strength and failure strain of the treated composites are shown in Figure 6.3.

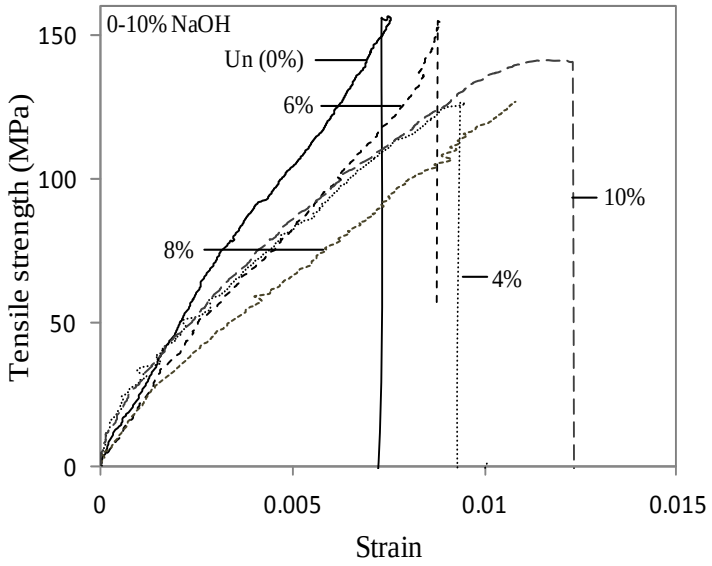

Figure 6.2: Typical tensile stress-strain curves of alkalised fibre composites

Table 6.1: Tensile properties of composites with different fibre treatments

Fibre treatments	Alkalisation				Alkalisation + Acetylation				Alkalisation + Silanisation			
	Strength (MPa)	Stages of modulus (GPa)		Strain at break (%)	Strength (MPa)	Stages of modulus (GPa)		Strain at break (%)	Strength (MPa)	Stages of modulus (GPa)		Strain at break (%)
%NaOH		α	α_1			α	α_1			α	α_1	
0	159.63 ±18.37	25.46 ±1.19	20.01 ±1.52	0.76 ±0.07	171.57 ±23.70	34.25 ±4.17	20.71 ±2.97	0.85 ±0.13	119.59 ±5.40	17.77 ±0.55	11.32 ±0.88	0.89 ±0.14
4	129.74 ±14.36	14.20 ±4.66	10.73 ±2.56	1.16 ±0.18	137.40 ±15.37	18.36 ±2.86	12.14 ±1.58	0.96 ±0.17	162.61 ±7.18	20.44 ±1.40	13.01 ±0.59	1.13 ±0.12
6	155.46 ±15.11	23.57 ±10.12	15.54 ±3.14	1.07 ±0.32	138.48 ±7.49	21.15 ±3.42	10.91 ±3.05	1.22 ±0.16	127.68 ±8.15	16.78 ±2.36	8.54 ±1.02	1.30 ±0.17
8	135.89 ±5.57	19.54 ±1.93	10.13 ±2.33	1.12 ±0.63	122.96 ±22.91	17.46 ±2.26	9.82 ±2.35	1.04 ±0.11	138.30 ±16.33	19.03 ±3.83	8.93 ±1.80	1.32 ±0.13
10	133.70 ±7.05	15.15 ±1.58	10.58 ±0.98	1.14 ±0.12	123.69 ±4.773	17.09 ±1.03	11.25 ±1.20	1.16 ±0.24	149.34 ±16.85	26.80 ±3.05	10.87 ±2.24	1.15 ±0.11

(a)

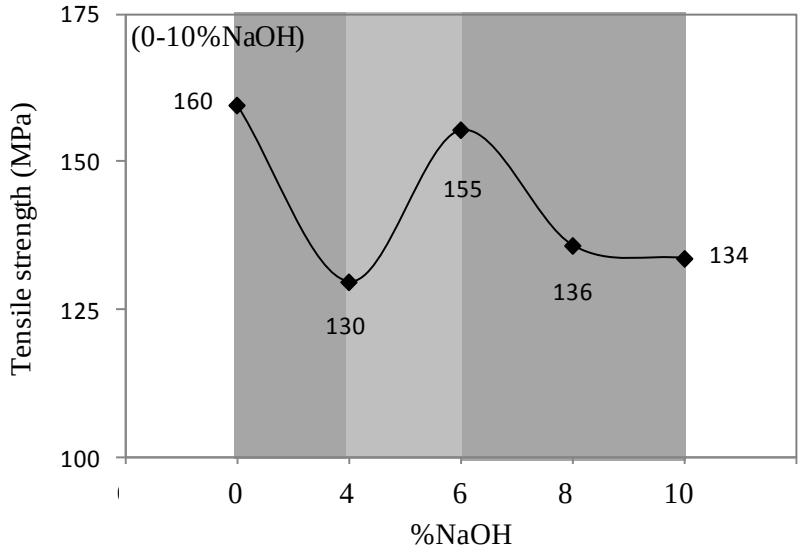

(b)

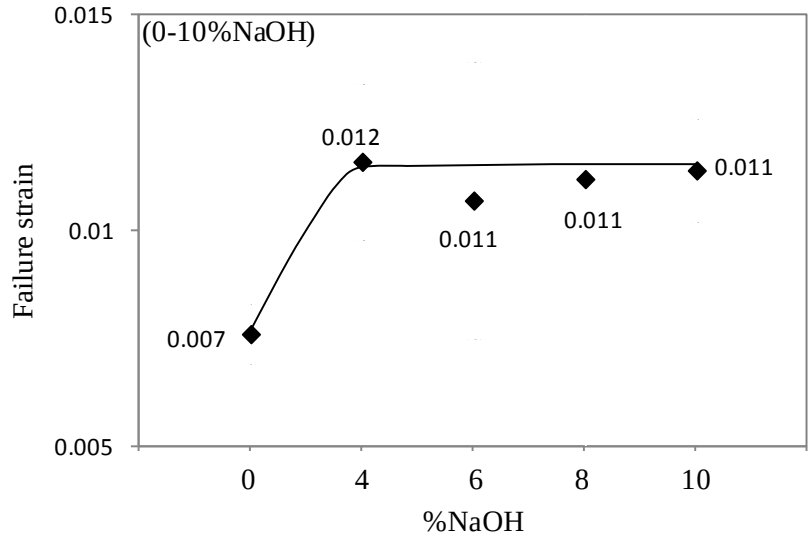

Figure 6.3: Tensile properties of alkalised fibre composites (a) strength (b) failure strain

From Figure 6.3, it can be observed that alkali treated fibre composites (4-10% NaOH) exhibited lower strengths but higher failure strains compared to the untreated (0% NaOH) samples. In the original untreated fibre composites, cellulose microfibrils were enveloped and joined together by hemicellulose and lignin constituents. Cellulose microfibrils were also joined together through hydrogen bonding (OH). The hemicellulose and lignin provided adhesion to hold the cellulose microfibrils in position. These orientations of fibre constituents gave structural

stability to the fibre against tensile loading. During alkali treatments, NaOH removed the hemicellulose and lignin constituents and their associated OH groups from the fibre. Consequently, cellulose microfibrils began to lose their structural strength. At higher concentrations of NaOH, more losses of hemicelluloses and lignin occurred, and this weakened fibres (Beckermann & Pickering 2008; Goda, et al. 2006). As a result, composite strengths gradually decreased (Figure 6.3a).

From Figure 6.3a it can be observed that 0-10% NaOH treated composites exhibit three stages of strength variations:

(i) at 4%, strength decreases

(ii) at 6%, strength increases

(iii) at 8-10%, strength decreases.

The strength decrease at 4% NaOH was a result of concentrations was insufficient to cause effective removal of the hemicellulose and lignin binders from the cellulose surfaces. Instead, treatments facilitated hydroxyl groups' absorption of atmospheric moisture. The presence of moisture in the fibre led to poor bonding with the matrix. The weak interface bonding reduced the composites' load carrying capacity and thus the composites failed at lower strength.

Whilst treatments reduced individual fibre strengths, the removal of hemicellulose and lignin from the fibre surfaces provided more accessible cellulose surfaces for matrix adhesion. Due to this, strong interface bonding between the fibres and matrix was made possible. Strong interfaces tended to hold the microfibrils in position but the weakness in strength of individual fibres eventually allowed gradual microfibril

deformation during tensile loading. As a result, treated composites showed higher failure strain compared to the untreated samples (Figure 6.3b).

At 6% NaOH concentrations, treatments effectively removed the hemicellulose, lignin and their associated hydroxyl groups from fibre surface. This facilitated strong fibre-matrix interface bonding and thus the composites exhibited higher strength.

At 8-10% NaOH concentrations, treatments sufficiently removed hemicellulose and lignin constituents from the fibre and so cellulose microfibrills became weaker in strength. When such fibres were used in reinforcing composites, plastic deformation took place at lower tensile loads which in turn caused the ultimate failure of composites.

Fibre acetylation on composites

Figure 6.4 shows the typical stress-strain curves of NaOH pre-treated acetylated fibre composites, and Table 6.1 summarises their results. The changes in strength and modulus of the acetylated composites are presented in Figure 6.5. From Figure 6.5, it can be observed that acetyl treatments on original hemp fibres (0% NaOH) increase composite strength from 160 MPa to 172 MPa and modulus from 14 GPa to 18 GPa.

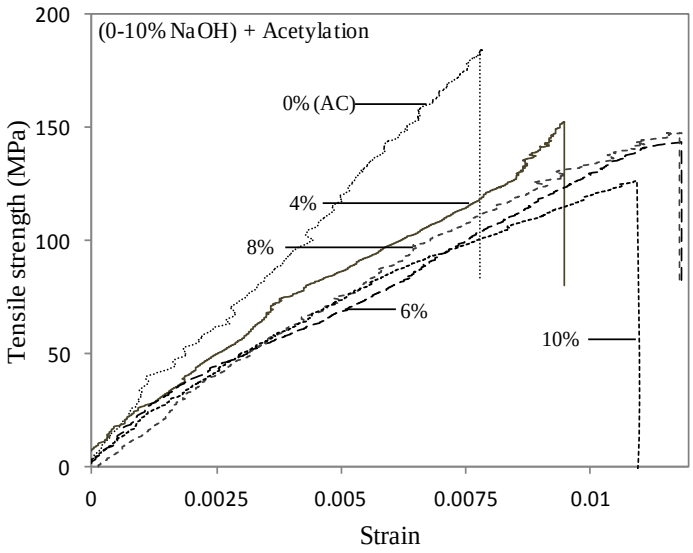

Figure 6.4: Typical tensile stress-strain curves of acetylated fibre composites

(a)

(b)

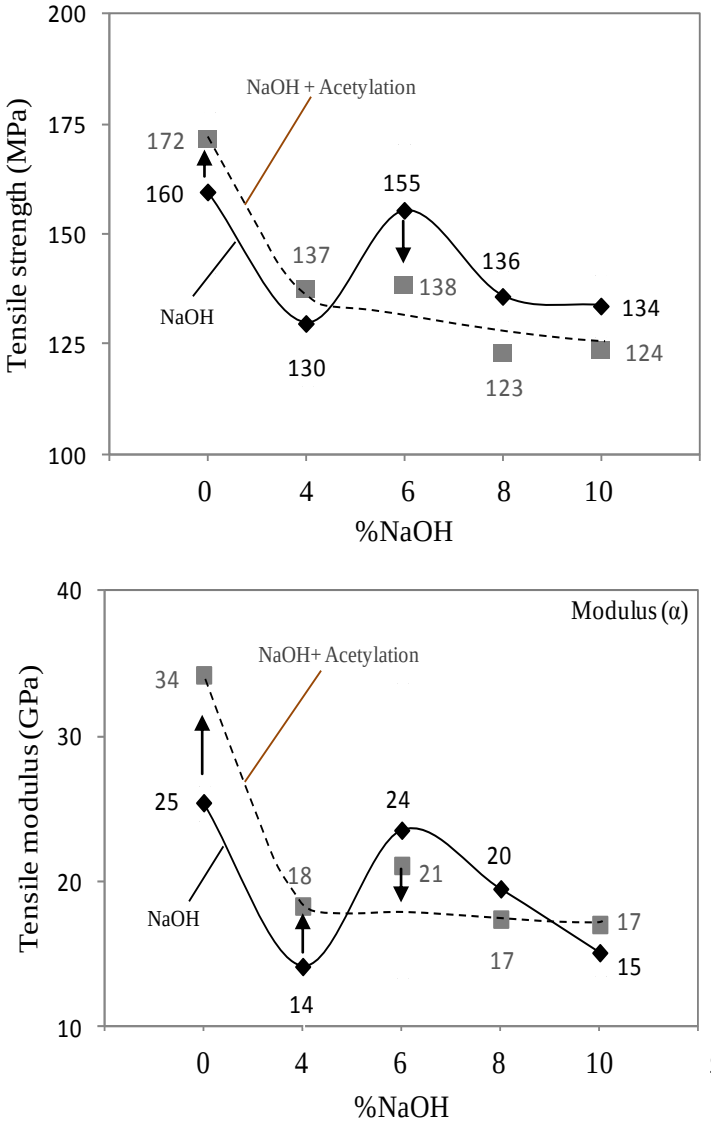

Figure 6.5: Tensile properties of alkali pre-treated acetylated fibre composites (a) strength (b) modulus (α)

During acetylation, fibres underwent two stages of chemical reactions. First, hemicellulose and lignin coverings from fibre surfaces were removed by the acetyl groups. Second, hydroxyl groups of the fibre were esterified by acetyl groups and eliminated from the fibres. This provided the hydrophobic fibre surfaces more accessibility to cellulose microfibrils for matrix adhesion. As a result, strong interface bonding between the fibres and matrix took place in the composites. Strong interfaces provided higher frictional resistance against tensile loading increasing overall composite properties.

Acetyl treatments on 4% NaOH pre-treated composites also exhibited higher strength and modulus compared to the 4% NaOH treated samples. Fibres with initial 4% NaOH treatments exposed hydroxyl groups on the fibre surfaces. Further acetylation esterified existing hydroxyl groups within the pre-treated fibres. Treatments also exposed cellulose microfibrils by removing further amounts of fibre surface coverings. Consequently, strong interface bonding was achieved and composites exhibited higher tensile properties.

For the higher concentrations of (6-10%) NaOH pre-treated fibres, large amounts of covering materials and their hydroxyl groups had already been removed by alkali treatments. Additional acetyl treatment caused further removal of coverings from the fibres and this had the effect of weakening fibre structures. Also, a lack of hydroxyl groups caused ineffective esterification with the fibres. These factors caused an inadequacy in interface bonding strengths of the composites. As a result, acetylation on 6-10% NaOH pre-treated samples exhibited lower strengths and moduli compared to NaOH treated samples.

Fibre silanisation on composites

Figure 6.6 shows typical stress-strain curves of NaOH pre-treated silanised fibre composites, and Table 6.1 summarises their results. The changes in strength and failure strain of the silanised composites are presented in Figure 6.7. From Figure 6.7a, it can be observed that silanisation on untreated fibres (0% NaOH) significantly reduced their associated composite strength from 160 MPa to 120 MPa. During silane treatments, silanol molecules formed in the presence of moisture. One end of the silanol molecule reacted with fibre hydroxyl groups and formed bonds with the fibres while the other end of the silonol molecule reacted with the matrix. These chemical couplings (linkages) between fibres and the matrix provided strong interface bonding in the composites. As untreated surfaces were covered with hemicellulose and lignin, the silane molecules could not achieve access to react with hydroxyl groups attached to the cellulose surfaces within the fibres. At this stage, silane molecules set an additional layer of coverings on the fibre surfaces, concealing the possible reaction sites of the fibres that would otherwise be able to react with the matrix. As a result, poor bonding between the fibres and matrix occurred, and composites exhibited lower strength.

During composite deformation, silane couplings (layers) between the fibres and matrix produced shear deformation at the interface. Interface shear enhanced the composite`s tensile deformation process thus increasing their failure strain compared to the untreated samples (Figure 6.7b).

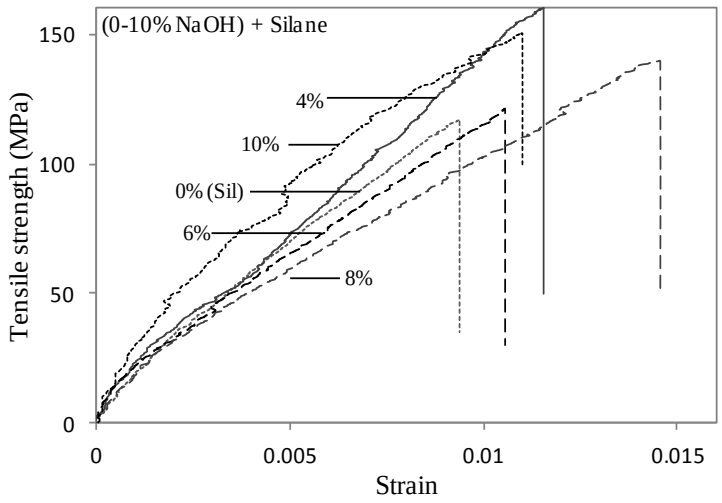

Figure 6.6: Typical tensile stress-strain curves of silanised fibre composites

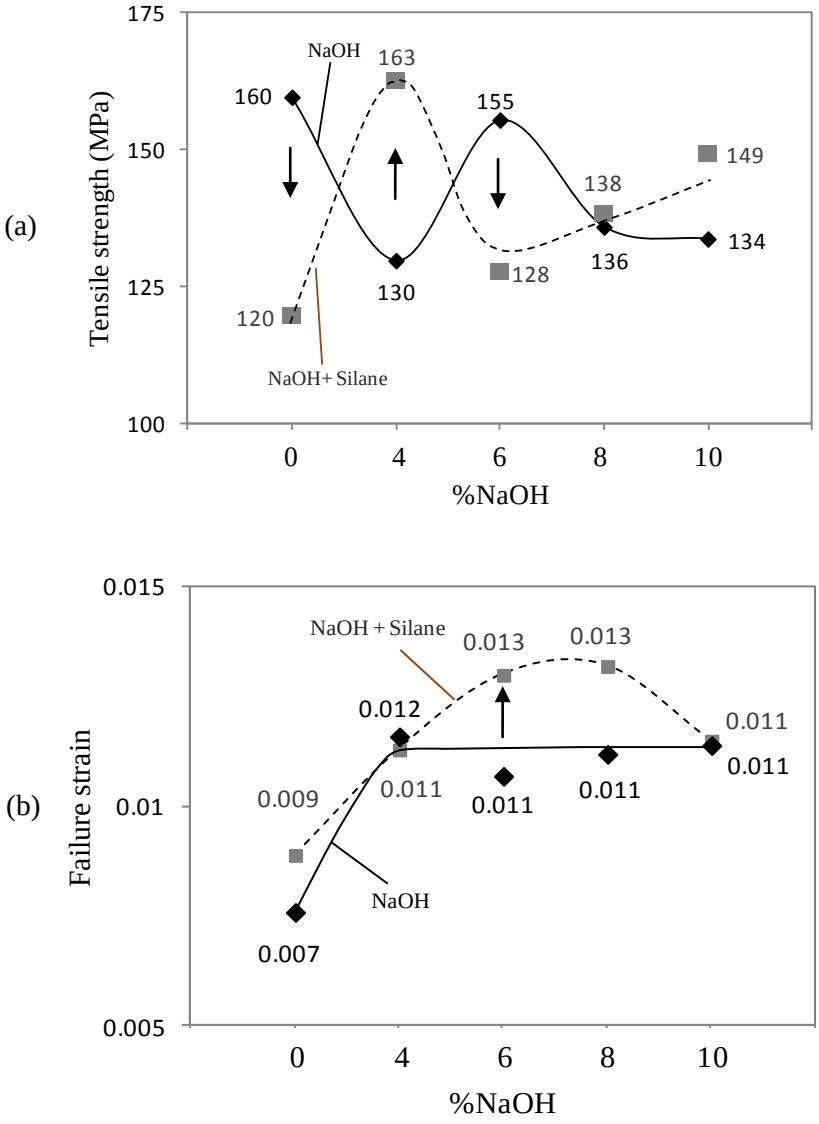

Figure 6.7: Tensile properties of alkali pre-treated silanised fibre composites (a) strength (b) failure strain

Silane treatments on 4% NaOH pre-treated composites exhibited higher strength (130 MPa to 163 MPa) compared to the 4% NaOH treated samples. Fibres with initial 4% NaOH treatments exposed hydroxyl groups on the fibre surface. Further silanisation sufficiently formed silanol molecules by reacting with the existing hydroxyl groups within the pre-treated fibres. The silanol molecules then formed strong couplings between the fibre surfaces and the matrix. As a result, better bonding at the interface was achieved facilitating higher resistance against tensile loading thus improving composite strength.

Silane treatments on 6% NaOH pre-treated composites exhibited lower strength (155 MPa to 128 MPa) compared to the 6% NaOH treated samples. This result indicates that 6% NaOH pre-treatments removed hemicellulose and lignin constituents and their associated hydroxyl groups from the fibres. Further silane treatments could not facilitate sufficient hydroxyl groups to form silanol molecules within the fibres. The lack of silanol formation reduced the coupling efficiency between the fibres and matrix. As a result, weak interface bonding took place and this ultimately reduced composite strength.

Silane treatments on (8-10%) NaOH pre-treated composites exhibited higher strengths compared to the (8-10%) NaOH treated samples. As discussed previously (in Chapter 5), higher NaOH concentrations enabled the rupturing of the crystallinity of cellulose structures which exposed hydroxyl groups to react with other molecules. Further silane treatments sufficiently enabled hydroxyl groups within the pre-treated fibre to form silanols and thus produced strong couplings between the fibre surfaces

and the matrix. Strong interfaces enhanced the load transfer capacity of the composites which caused the composites to exhibit higher tensile properties.

From the above analyses, it can be stated that alkali treatments removed hemicellulose and lignin binders from cellulose surfaces which ultimately lowered composite strength compared to the untreated samples. However, treatments exposed cellulose surfaces to react with matrix materials which enhanced their interface bonding. As a consequence, treated fibre composites exhibited higher failure strains.

Acetylation caused the replacement of hydroxyl groups present within the fibre with acetyl groups thus improving bonding at the interface. As a result, treated composites exhibited higher tensile properties compared to untreated samples. However, alkali pre-treated acetylated samples exhibited lower tensile properties. In two consecutive treatment processes, fibres lost large amounts of binding materials (hemicellulose and lignin) which decreased their structural strength and thus their ability to carry tensile load.

Silane treatments on the untreated fibres did not facilitate the formation of strong couplings between fibre surfaces and the matrix due to the presence of hemicellulose and lignin coverings. As a result, weak interface bonding took place which decreased the composite load carrying capacity. However, NaOH pre-treatments removed fibre coverings which exposed hydroxyl groups to form silane couplings between fibres and matrix. This enhanced interface bonding strength and allowed composites to exhibit higher tensile properties.

6.2.2 Compressive properties of composites

For unidirectional composites, fibres are the primary load-carrying component, whiles the matrix provides support to the fibres as a result of strong interface bonding. Under incremental compression loading, fibres begin to buckle at weak interface locations within the matrix (Ranganathan & Mantena 2003). Buckled fibres generate strains on neighbouring fibres and cause them to bend (Fleck, Jelf & Curtis 1995; Jelf & Fleck 1992). This leads to instability along the fibre-matrix interface and generates disproportionately high stresses on the matrix (Gonzalez & Lorca 2007). As a result, the matrix shifts from pre-buckling to post buckling deformation which progressively involves damage initiation of the composites (Jensen, et al. 2006).

Figure 6.8 presents a typical compressive stress-strain curve for untreated fibres. The curve indicates that the response was linear (pre-buckling) up to strength value of 30 MPa and strain value of 0.007. Following this stage, the composites began to yield. As strain increased further, the curve deviated from this linear proportionality and a geometrical nonlinear response (post-buckling) increased to a stress of around 65 MPa. Finally the failure stress point was reached. In the post-buckling path, the tangent modulus diverged in several points with different stages of modulus values. Varying recordings of modulus in the post-buckling path were due to the fact that, as the compressive loading increased, matrix cracks initiated and propagated along the interfaces (Jensen, et al. 2006). Crack propagation gradually reduced the load carrying capacity of the composite, thereby lowering the modulus at several points on the stress-strain curve. In Figure 6.8, α was the initial tangent modulus in the pre-buckling state and α_1, α_2 and α_3 were the tangent modulus in the post-buckling state.

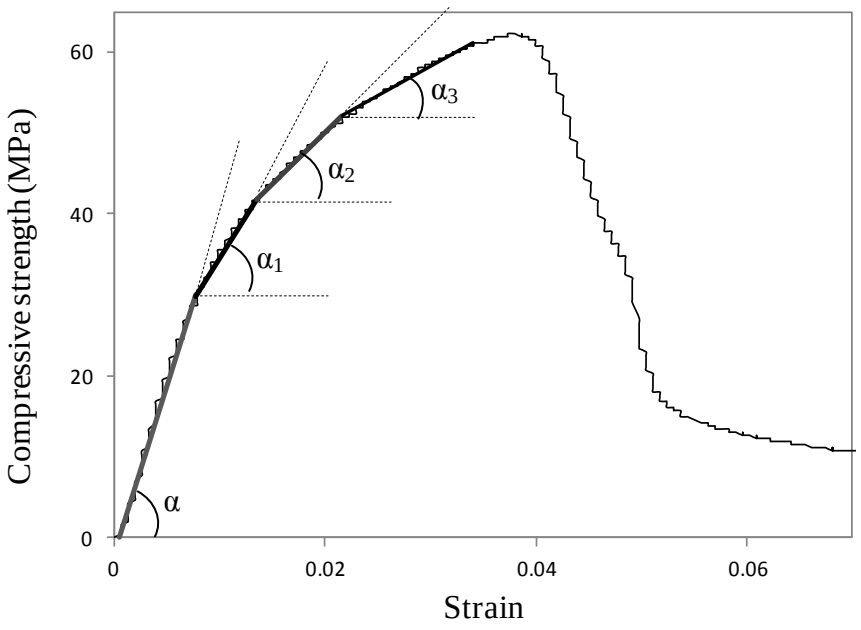

Figure 6.8: Typical compressive stress strain curve of the fibre composite

Fibre alkalisation on composites

Figure 6.9 shows typical compressive stress-strain curves of alkalised fibre composites, and their properties are summarised in Table 6.2. The changes in compressive strength, modulus and failure strain of the composites are presented in Figure 6.10. From Figure 6.10(a) it can be observed that, alkali treatments on untreated fibres increased their associated composite strength from 69 MPa to 75 MPa.

Table 6.2: Compressive properties of composites with different fibre treatments

Fibre treatments	Alkalisation						Alkalisation + Acetylation						Alkalisation + Silanisation					
	Strength (MPa)	Stages of modulus (GPa)				Strain at break (%)	Strength (MPa)	Stages of modulus (GPa)				Strain at break (%)	Strength (MPa)	Stages of modulus (GPa)				Strain at break (%)
% NaOH		α	α_1	α_2	α_3			α	α_1	α_2	α_3			α	α_1	α_2	α_3	
0	69.11 ±3.60	3.19 ±1.10	1.87 ±0.53	1.11 ±0.15	0.76 ±0.21	5.70 ±1.70	85.20 ±3.86	3.09 ±0.35	2.07 ±0.55	1.20 ±0.28	0.84 ±0.06	5.10 ±1.50	56.96 ±5.06	4.00 ±0.02	2.07 ±0.11	1.14 ±0.02	0.66 ±0.08	4.80 ±1.10
4	72.60 ±9.49	3.19 ±0.14	1.76 ±0.06	1.08 ±0.28	0.65 ±0.08	6.00 ±2.20	79.38 ±4.54	4.02 ±0.43	2.23 ±0.27	1.70 ±0.18	0.81 ±0.01	6.30 ±0.70	76.34 ±3.09	3.90 ±0.94	2.06 ±0.45	1.07 ±0.11	0.65 ±0.02	6.20 ±1.90
6	74.70 ±8.10	3.20 ±0.09	2.00 ±0.13	1.18 ±0.07	0.63 ±0.19	4.40 ±0.60	90.53 ±8.78	4.72 ±0.34	2.79 ±0.09	1.55 ±0.10	0.87 ±0.18	6.70 ±1.80	68.24 ±6.40	3.98 ±0.16	2.13 ±0.04	1.18 ±0.07	0.69 ±0.02	5.20 ±1.60
8	75.14 ±1.60	2.97 ±0.32	1.59 ±0.01	1.05 ±0.07	0.63 ±0.01	5.50 ±0.90	85.61 ±4.55	4.66 ±0.36	2.48 ±0.28	1.41 ±0.21	0.71 ±0.05	7.00 ±1.00	68.42 ±1.95	4.04 ±0.49	2.20 ±0.30	1.18 ±0.18	0.56 ±0.11	4.80 ±0.80
10	74.63 ±4.86	3.24 ±0.18	1.88 ±0.02	1.05 ±0.08	0.62 ±0.02	6.20 ±0.70	84.85 ±6.06	3.96 ±0.44	1.91 ±0.34	1.10 ±0.33	0.62 ±0.09	7.50 ±0.50	72.57 ±1.702	4.48 ±0.27	2.22 ±0.16	1.11 ±0.05	0.60 ±0.05	6.10 ±1.10

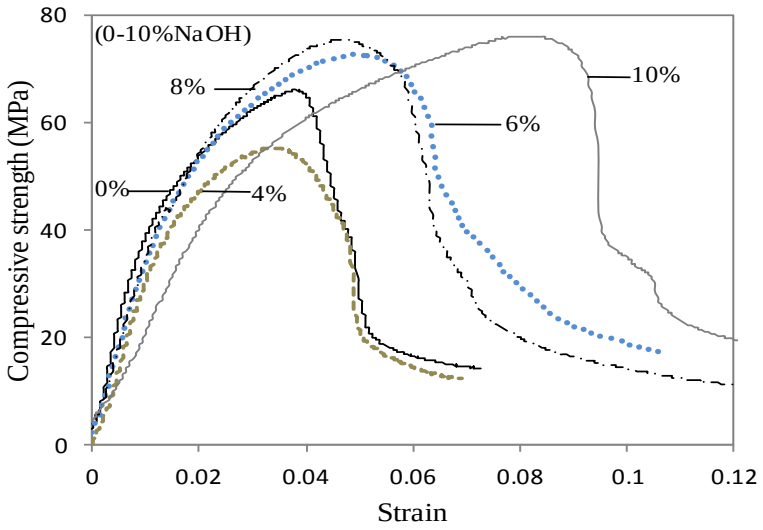

Figure 6.9: Typical compressive stress-strain curves for alkalised fibre composites

(a)

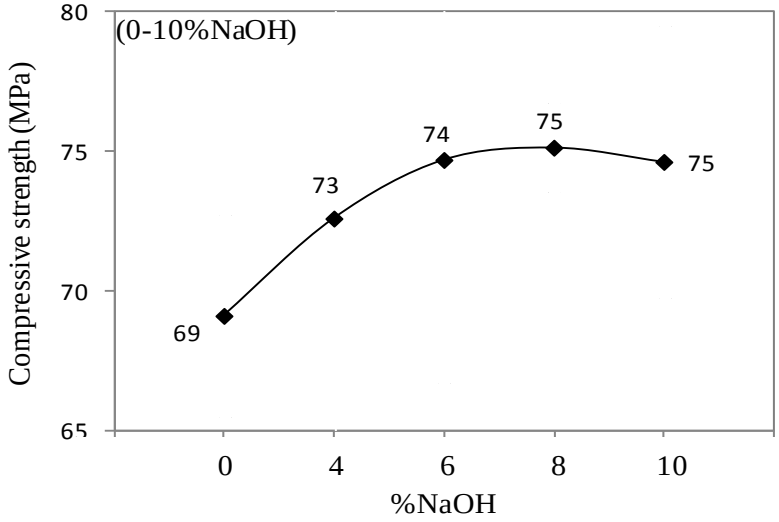

(b)

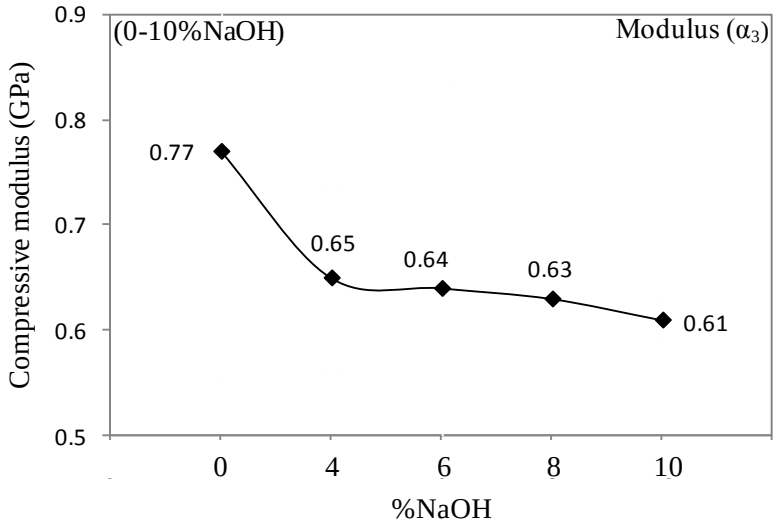

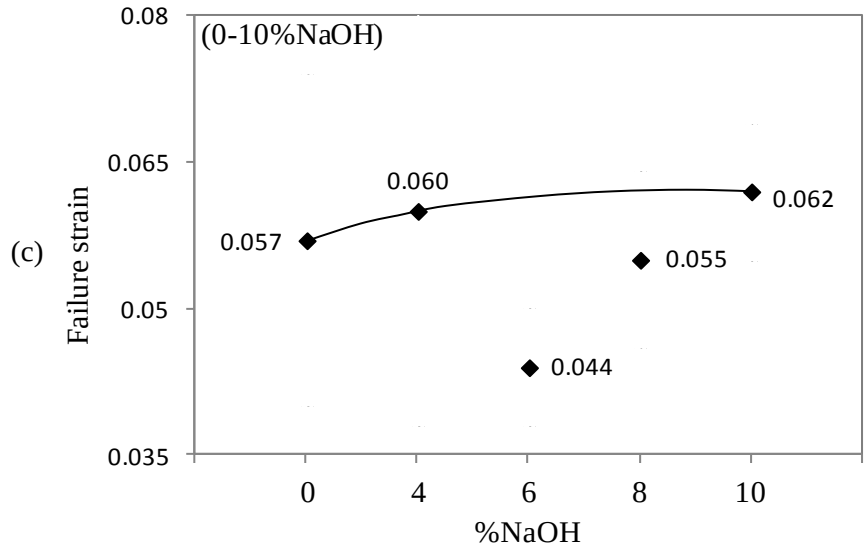

Figure 6.10: Compressive properties of alkalised fibre composites (a) strength (b) modulus (c) failure strain

Enhanced composite strengths were exhibited as a result of the removal of fibre surface coverings (hemicellulose and lignin) by NaOH treatments. The removal of the fibre surface coverings facilitated strong interfacial bonding with matrix materials. Strong interfaces prevented fibre buckling, which ultimately delayed the formation of matrix cracks. Greater stress transfer from matrix to fibres took place and thus composite strengths increased.

Although alkalised fibre composites showed increased strengths, the removal of fibre surface coverings created weaknesses within cellulose microfibrils. This has the effect of weakening fibres. During compression, weak cellulose microfibrils tended to buckle within the fibre. This microbuckling generated microstrains on fibres which ultimately produced extra strains at the fibre-matrix interface. The extra strain initiated microcracks at the bonded interface which gradually reduced the composites' load carrying capacity. As a result, the composite failed under large

deformations. Figure 6.10c highlights gradual increase in failure strains at higher concentrations of NaOH treatments (6-10%).

From Figure 6.10b it can be seen that the post-buckling moduli (α_3) gradually decreased as NaOH concentration increased. This clearly highlights the fact that fibre weaknesses were caused by alkali treatments. As discussed before, at α_3, progressive matrix cracking and fibre buckling produced large strains on neighbouring fibres. At this stage, weak fibres could not take further strains developed from buckling and matrix cracking. As a result, fibres failed at lower loads and the composites exhibited lower α_3 values.

Fibre acetylation on composites

Figure 6.11 shows a typical compressive stress-strain curve for NaOH pre-treated acetylated fibre composites, and their properties are summarised in Table 6.2. The changes in strength, modulus and failure strain of the acetylated composites are presented in Figure 6.12. Figures 6.12a and 6.12d show that acetyl treatments exhibit around 23% higher strength but 10% lower failure strain compared to untreated samples. These results indicated that, the acetyl groups were able to react with the hydroxyl groups that attached to the cellulose and developed strong bonding with the matrix. During composite deformation, strong interfaces prevented fibre buckling and provided higher frictional resistance against compression loading. Due to this, the applied compressive load rapidly increased and reached its peak at relatively small elongations. This resulted in higher strengths but lower failure strains of the treated composites.

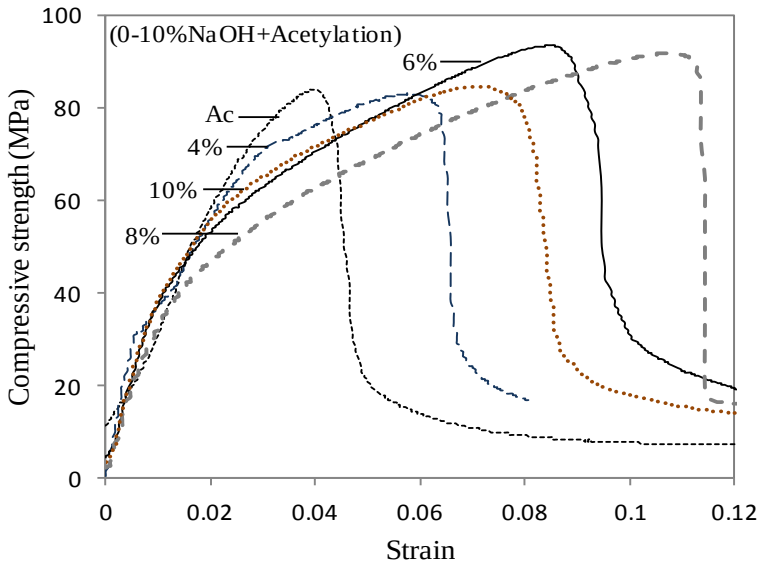

Figure 6.11: Typical compressive stress-strain curves of acetylated fibre composites

(a)

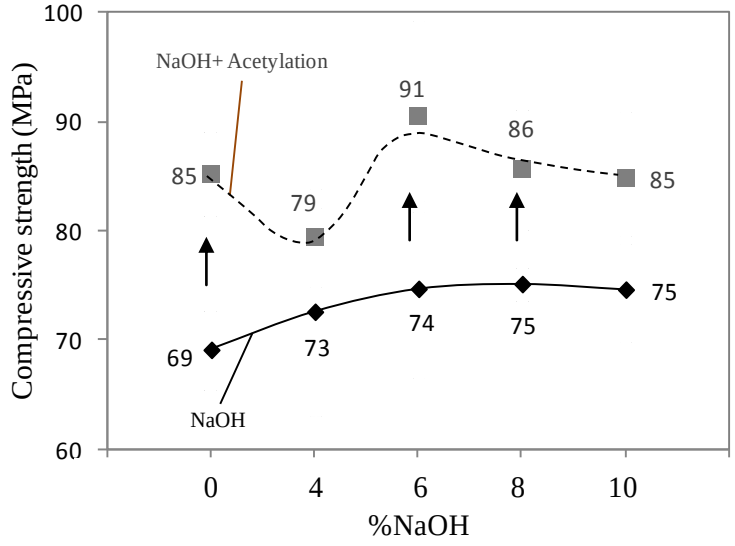

(b)

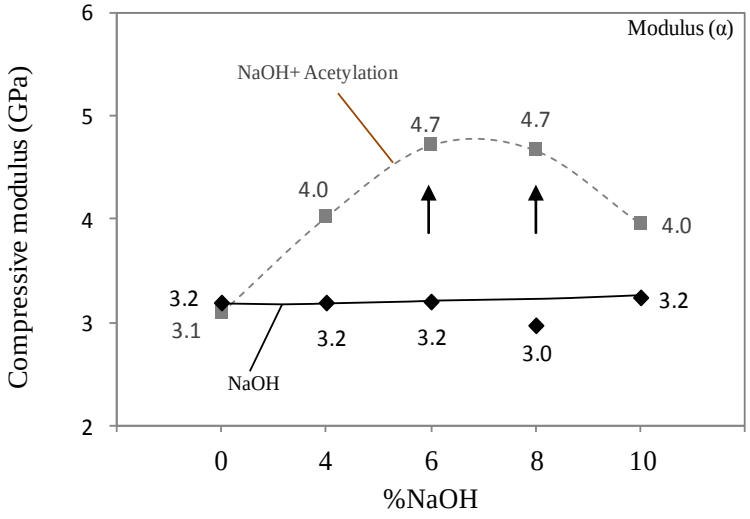

(c)

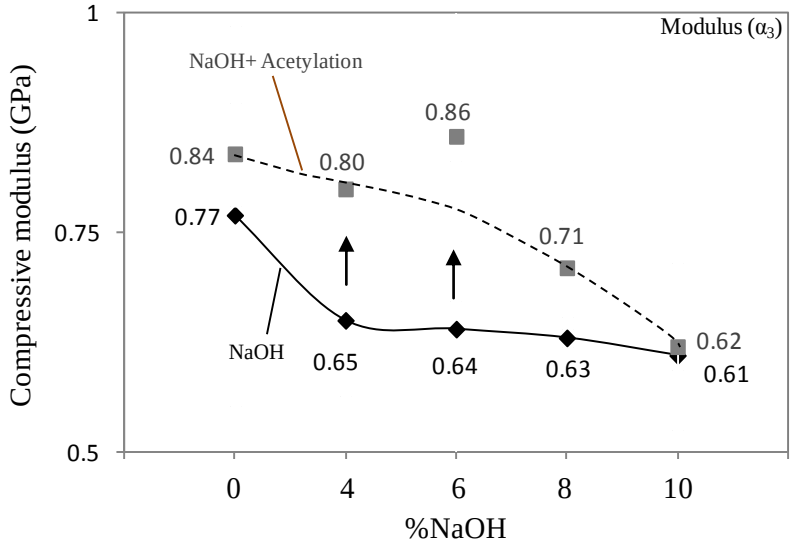

(d)

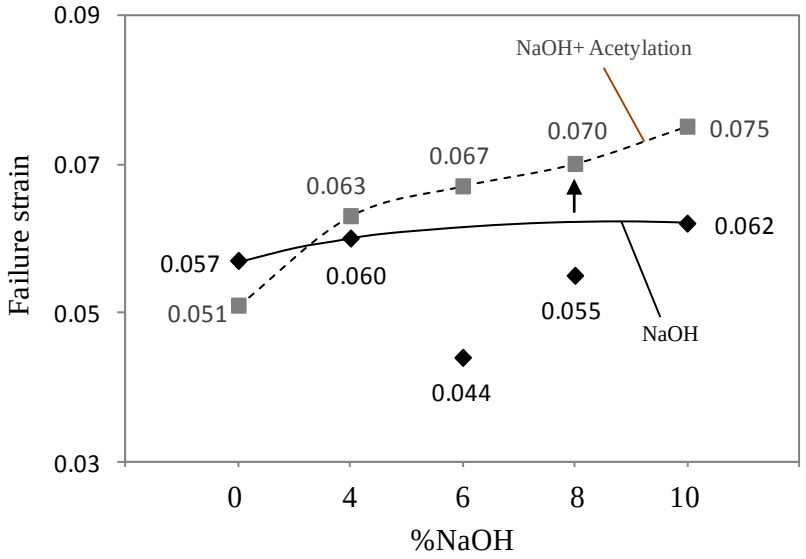

Figure 6.12: Compressive properties of alkali pre-treated acetylated fibre composites (a) strength (b) α (c) α_1 (d) failure strain

As can be observed from Figures 6.12b and 6.12c the moduli in post buckling states were higher for acetylated composites compared to untreated samples. Higher moduli indicated strong fibre-matrix bonding that had taken place at the interface for the treated fibre composites. As a result, fibre buckling was restricted thus minimising the chances of matrix crack initiation.

Similarly, acetylation on (4-10%) NaOH treated fibre composites exhibited higher strengths, moduli (α, α_1, α_2 and α_3) and breaking strains compared to the (4-10%) NaOH treated samples. These results confirm that strong interface bonding was achieved due to the removal of fibre surface coverings (hemicellulose and lignin) in two consecutive treatment processes. During compression loading fibres did not have sufficient space at their surrounding interfaces to develop fibre buckling which reduced the chances of matrix cracking. As a result, greater load transfers throughout the composites could be achieved and this justified higher compression properties of the composites.

Fibre silanisation on composites

Figure 6.13 illustrates the typical compressive stress-strain curves for NaOH pre-treated silanised fibre composites, and their properties are summarised in Table 6.2. The changes in strength of the silanised composites are presented in Figure 6.14. Figure 6.14 shows that silane treatments exhibit around 17% lower compressive strength compared to untreated samples. Cellulose surfaces in the untreated samples were covered by hemicellulose and lignin coverings. Silane molecules were unable to penetrate the fibre surfaces to react with hydroxyl groups that were attached with the cellulose. Rather, silane formed chemical linkages with the hydroxyl groups from the surface coverings (hemicellulose-lignin). Due to this, the silane did not facilitate strong couplings with fibres. Instead, it acted as an additional chemical layer on the fibre surfaces. During compression loading, the chemical layers also generated buckling strain on the fibres and their surrounding interfaces, and thus contributed to the formation of matrix cracking. Fibre buckling and matrix cracking reduced the

composites' load carrying capacities and thus exhibited lower compression properties.

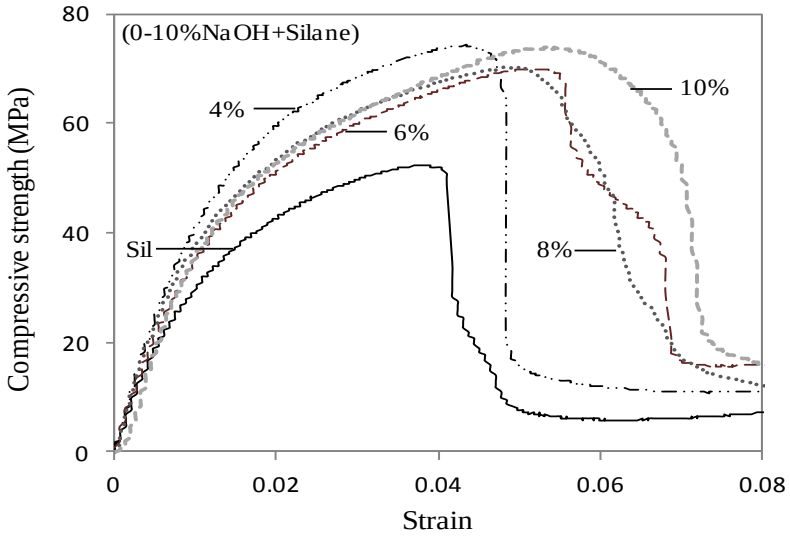

Figure 6.13: Typical compressive stress-strain curves of silanised fibre composites

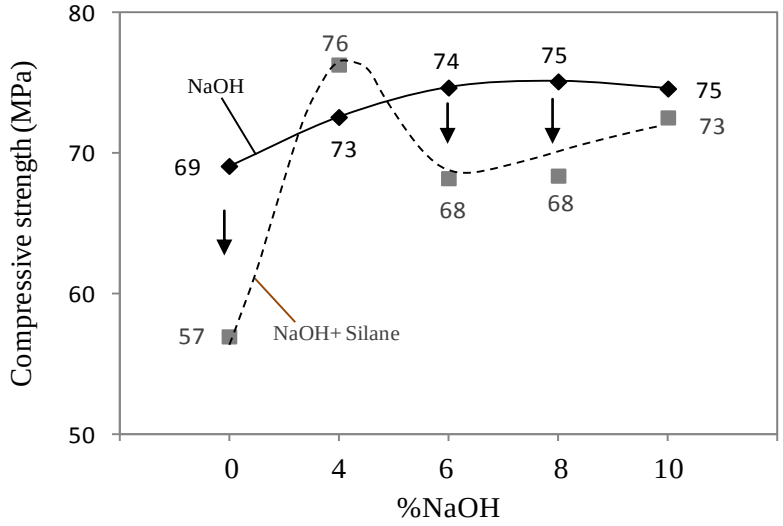

Figure 6.14: Compressive strength of alkali pre-treated silanised fibre composites

It can be seen from Figure 6.14 that, 4% NaOH pre-treated silanised samples exhibit higher compressive strengths compared to the original 4% NaOH treated samples. This again proved that the initial 4% NaOH concentration was not strong enough to

remove covering materials from the fibre surface effectively; rather it exposed fibre hydroxyl groups. Silane molecules then reacted with these hydroxyl groups and formed silanols. Silanols, in turn, formed strong couplings between fibre surfaces and the matrix. These chemical couplings promoted strong bonding at the interface. Strong interfaces enhanced the composites' load carrying capacities and produced higher compressive properties.

On the other hand, higher concentrations (6-10%) of NaOH treatments removed hemicellulose and lignin coverings and their associated hydroxyl groups from the fibres. Further silane treatments did not leave sufficient hydroxyl groups to form silanols. As a result, chemical couplings at the interface became less able in carrying compressive loads and thus lowered composite properties were exhibited.

Among all reinforcing fibre treatments, acetylated composites showed the best results in terms of strength, failure strain and modulus. Alkali treatments also exhibited similar composite properties. Higher composite properties indicated that treatments were effective in removing fibre surface coverings to provide strong interface bonding. Due to the presence of fibre surface coverings on untreated fibres, silane molecules were not able to form effective bonding with the fibre surfaces. As a consequence, weak bonding between the fibres and matrix took place and, silane treated composites showed weaker properties compared to the alkalised and acetylated samples.

Composites failure surface analysis

Figure 6.15a shows a flat wise view of a typical composite failure surface. The image indicates that the reinforced fibres were banded on a composite surface plane at an angle to the loading direction, and the fibres' bends were spread over the composite surface. This section of bent fibres is known as a kink band. Kink bands develop due to fibres buckling (Azzam 2007; Jensen, et al. 2006). This band forms in the post buckling state when the composite fail gradually under large deformations (ductile failure) (Azzam 2007; Cho, Chen & Daniel 2007).

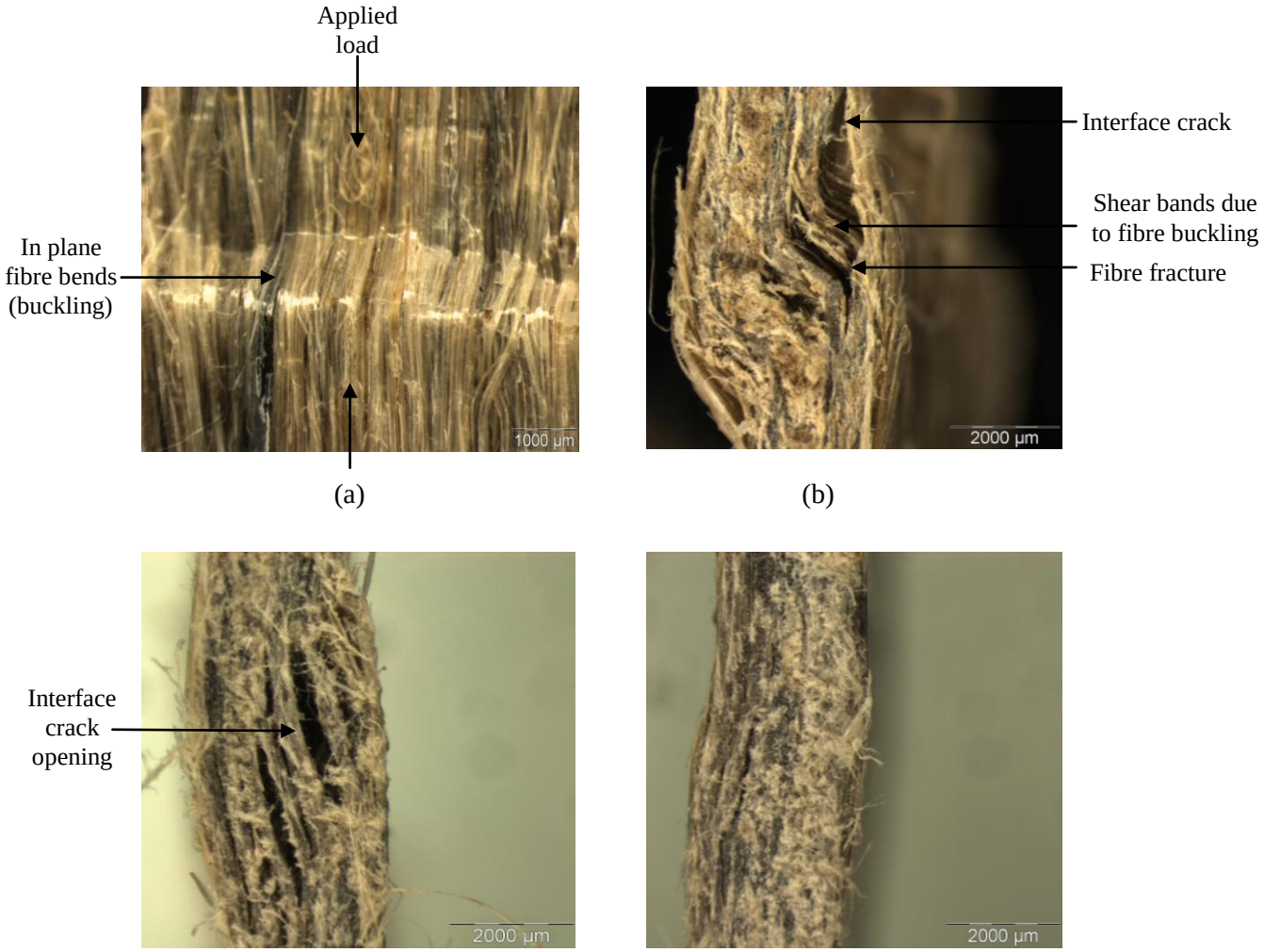

Figure 6.15: Microscopic images of failure surface for (a) flat-wise view (b) silanised (c) alkalised (d) acetylated composites

Figure 6.15b illustrates the failure surface of silane treated composites. It shows shear bands surrounded by the interface which has developed cracks. This indicated that weak interface bonding was prevalent facilitating the development of fibre buckling more easily in the matrix. Additionally, shear bands formed due to shear displacement of the buckled fibres. Progressive fibre buckling initiated interface cracking and generated shear bands on failure surfaces. Further observations of failure samples showed fractured fibres. This was again due to poor interface bonding which facilitated maximum fibre buckling. As a result, fibres reached a critical strength level sufficient to promote fibre fracturing.

On the other hand, Figure 6.15c shows multiple interface cracks on the alkalised composites. Compression properties decreased rapidly as the crack sizes increased. Similar failure modes were also observed for acetylated composites (Figure 6.15d). From Figures 6.15c and 6.15d it can be observed that the number and width of the crack openings for alkalised composites was higher compared to the acetylated fibre composites. This indicated that acetylated fibres formed stronger bonds with the matrix and had higher compression properties. Additionally, there was no evidence of fibres fracturing on the failure surface of alkalised and acetylated composites. This demonstrated that fibre buckling along the interface was insufficient to cause the fibres to fail. This again proved strong interface bonding resulted through the treatment of fibres.

6.2.3 Shear properties of composites

Iosipescu shear specimens were employed in experimentation. They had v-notches at the top and bottom edges, which reduced the cross-sectional area at the specimen centreline (Chapter 3, Section 3.6.3). The reduced cross-sectional area between the notches allowed shear stresses to be concentrated near the centre region (Bradley, et al. 2007).

During shear tests, specimens were mounted on both sides of the test fixture. One side of the fixture was moved vertically while the other side remained stationary. This action produced force couples on the specimen. The force couples generated two counteracting moments at the specimen's mid-sections. The induced moments exactly cancelled at the specimen mid-length, thus producing a pure shear loading state (Odegard & Kumosa 2000; Zhou, Green & Morrison 1995). Additionally, vertical displacement imposed compressive loads on the specimen's mid-sections. This action tended to cause fibre bending of the specimen. Consequently, the specimen also experienced tensile deformation. Such deformations also produced transverse normal stresses and transverse strain at the mid-section (Totry, et al. 2009). Tension and compression together, produced shear deformation at the specimen just below the V-notches (Mattoni & Zok 2005; Totry, Gonzalez & Lorca 2009). As a result, the stress fields on both sides of the notch-root axis experienced shear/transverse compression and shear/transverse tension simultaneously.

Tensile deformation along the fibres led to fibre fracture while compression in the same direction induced failure through localised fibre bending. Tensile deformation resulted in matrix cracking, interfacial debonding, fibre sliding, fibre fracture and

fibre pull-out (Pierron & Vautrin 1998; Zhou, Green & Morrison 1995). These outcomes led to the formation and propagation of microscopic cracks. However, transverse compression or shear deformation triggered fractures through the formation of matrix shear bands and delamination.

A typical shear stress-extension curve of a unidirectional fibre composite is plotted in Figure 6.16. The behaviour was initially linear followed by a non-linear transition when the extension was in the range of 1 mm to 4 mm. The extension (deformation) appeared with a large displacement that indicated a ductile failure process. In the large deformation zone, the fibres remained elastic and accommodated the large plastic deformation of the matrix caused by specimen bending. This led to continuous shear deformation until extensive fibre bending took place. At this stage, interface cracking initiated at the matrix and fibres held the failed matrix in position and continued to transfer shear loads. As the stress increased, additional shear bands formed due to more and more fibres bending with corresponding large displacements that led to fibre failure.

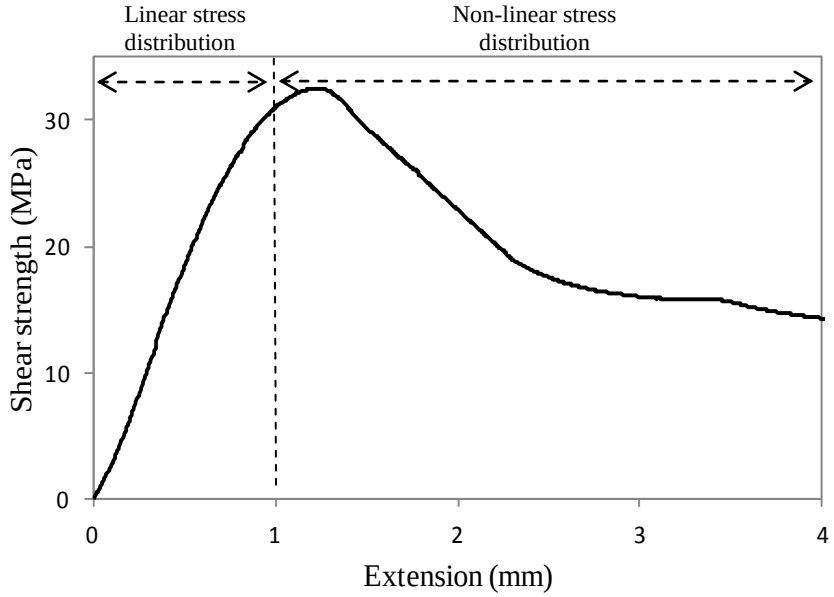

Figure 6.16: Typical shear stress- extension curve of fibre composites

Figure 6.17 (Odegard & Kumosa 2000) and 6.18 show different shear failure modes of the tested specimens. Axial shear cracking was observed at the mid-section of the specimen between notches. These axial cracks formed due to shear/transverse tension and shear/transverse compression of the specimen. Shear/transverse compression caused short cracks and shear/transverse tension caused long cracks along the fibre axis. Axial cracks also produced notch root splitting. Notch root splitting initiated at the root of the v-notch section and propagated along the fibre axis. The direction of the notch root axial split is dependent on the fibre directions. The splitting was predominantly caused by the large compressive stresses that were concentrated near the notch root.

Failure modes

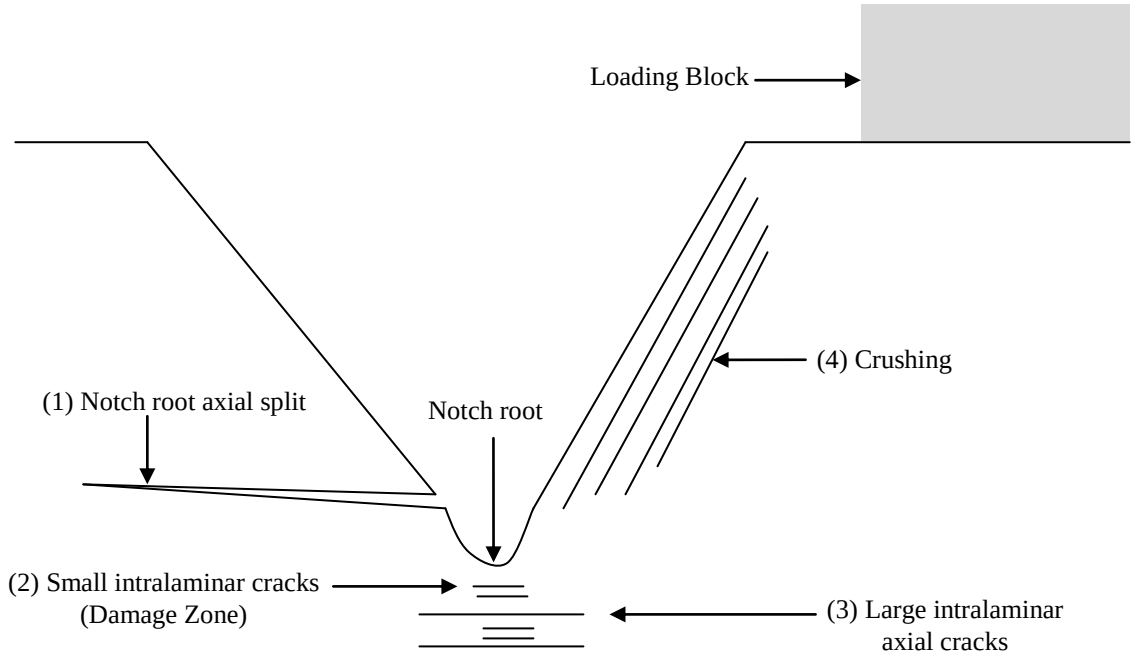

Figure 6.17: Typical shear failure modes of the composites

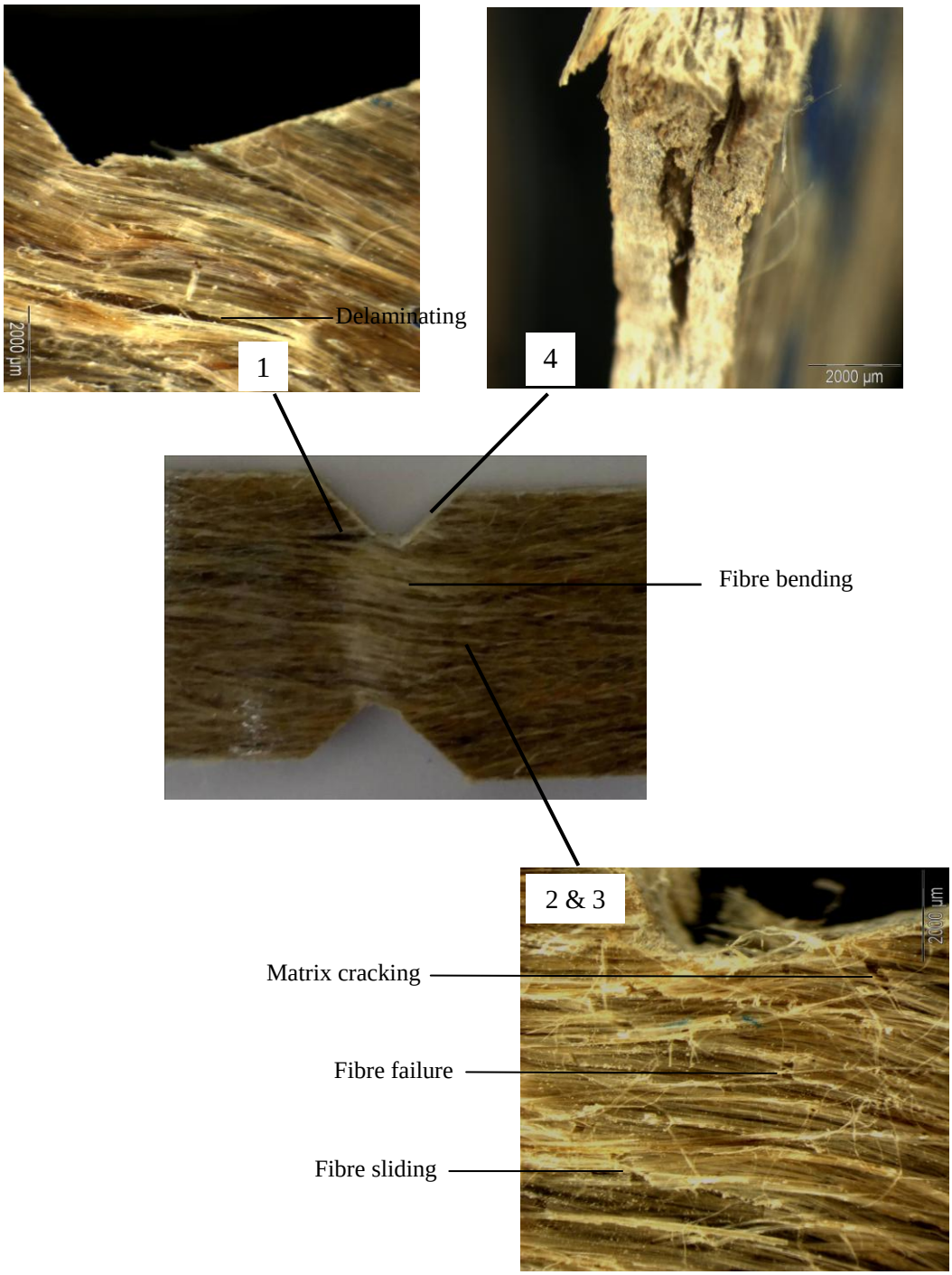

Figure 6.18: Shear failure modes of composites

A microscopy (OM) inspection of the specimens' mid-section showed fibre bending, matrix cracking, debonding, fibre sliding and fibre fracture. Large shear displacements at the specimen mid-section caused fibres to bend and led to plastic

deformation of the matrix. Plastic deformation initiated matrix cracking, interface debonding and fibre sliding. Fibre sliding was initiated due to weak interface bonding, while fibre fracture occurred due to fibre bending.

Table 6.3: Shear properties of composites with different fibre treatments

Fibre treatments	Alkalisation		Alkalisation + Acetylation		Alkalisation + Silanisation	
%NaOH	Strength (MPa)	Extension at break (mm)	Strength (MPa)	Extension at break (mm)	Strength (MPa)	Extension at break (mm)
0	25.48 ±0.39	1.34 ±0.13	26.83 ±3.00	1.42 ±0.18	28.41 ±4.63	1.15 ±0.15
4	14.05 ±1.55	0.65 ±0.16	28.73 ±3.99	1.34 ±0.19	26.28 ±1.83	1.47 ±0.11
6	32.55 ±1.62	1.22 ±0.01	29.65 ±5.67	1.20 ±0.08	27.38 ±3.69	1.49 ±0.15
8	34.45 ±3.98	1.47 ±0.14	31.92 ±1.75	1.31 ±0.14	21.11 ±2.05	1.18 ±0.25
10	36.80 ±2.24	1.55 ±0.11	27.09 ±5.06	1.39 ±0.07	24.29 ±3.28	1.52 ±0.18

Fibre alkalisation on composites

Figure 6.19 illustrates the typical shear stress-extension curves for alkalised fibre composites, and their properties are summarised in Table 6.3. The changes in the shear strength and extension of the alkalised composites are presented in Figure 6.20. Figures 6.20a and 6.20b show that, 4% NaOH treatments on fibres reduces their associated composite's strength and extension at break from 25 MPa to 14 MPa and from 1.3 mm to 0.6 mm respectively compared to the untreated samples. These results indicated that strong interface bonding was compromised due to ineffective removal of fibre surface coverings from 4% NaOH treated fibres. During shear loading, weak interfaces allowed for fibre bending inside the matrix (due to compression) and consequently fibre sliding from the matrix (due to tension). Thus, matrix cracking propagated throughout the sample which reduced the composite's load carrying capacity. As a result, treated composites failed under lower strength and lower extension at break than untreated samples.

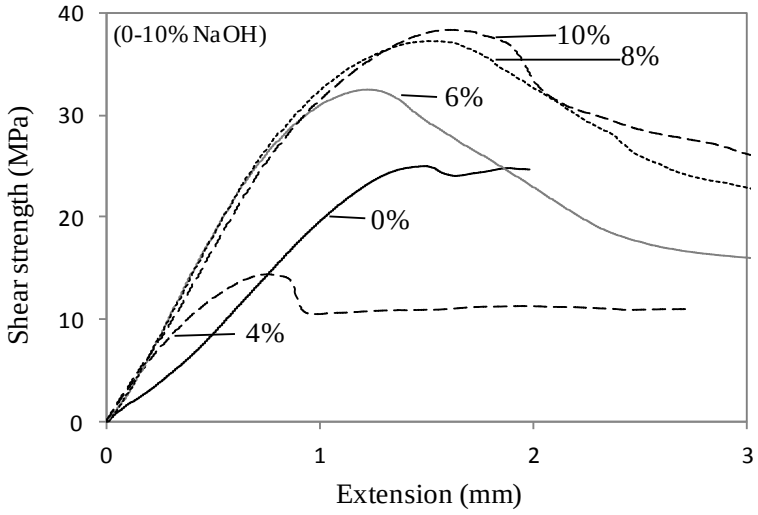

Figure 6.19: Typical shear stress-extension curves of alkalised fibre composites

(a)

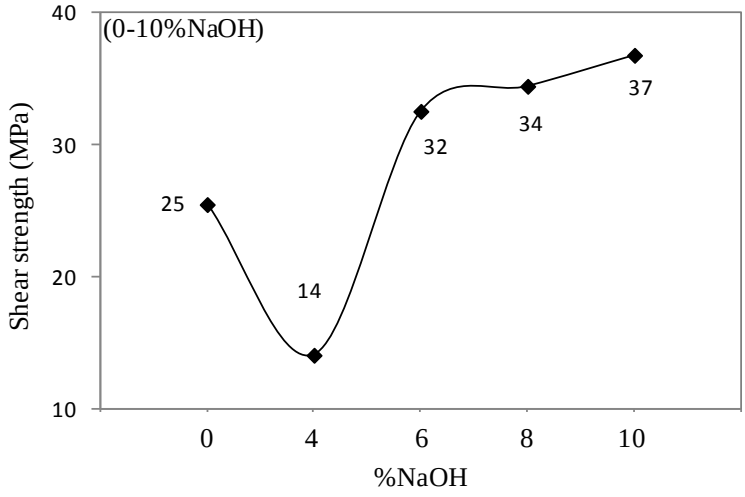

(b)

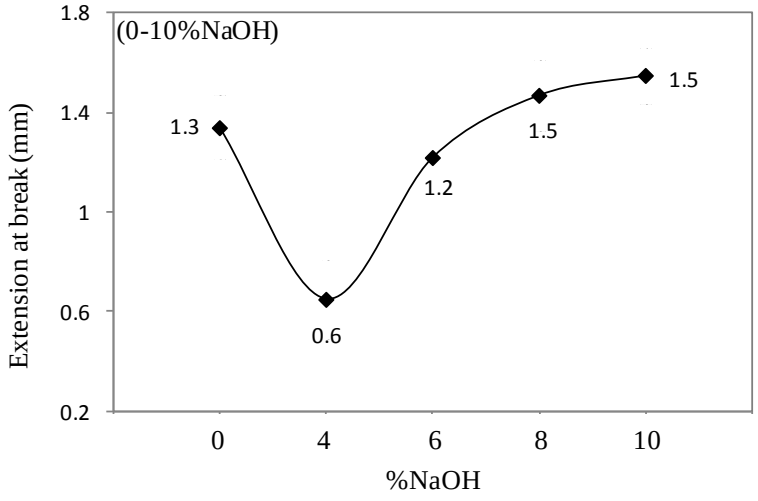

Figure 6.20: Shear properties of alkalised fibre composites (a) strength (b) extension at break

On the other hand, as treatment concentrations increased from 4% to 6% NaOH, the composite strength (from 14 MPa to 32 MPa) and extension at break (from 0.6 mm to 1.2 mm) greatly increased. At higher concentrations (8-10% NaOH), strength and extension at break stabilised at around 35 MPa and 1.5 mm. These results indicated that, at higher (6-10%) NaOH concentrations, hemicellulose and lignin coverings were removed from the cellulose surface and allowed for strong bonding with the matrix. Strong interface bonding reduced fibre bending and fibre sliding within the matrix during shear deformations. As a result, the load transfer capacity at the interface increased and composites exhibited higher shear properties.

Fibre acetylation on composites

Figure 6.21 shows the typical shear stress-extension curve for NaOH pre-treated acetylated fibre composites, and their properties are summarised in Table 6.3. The changes in strength and extension at break of the acetylated composites are presented in Figure 6.22. From Figure 6.22 it can be observed that acetyl treatments on 4% NaOH pre-treated samples increased more than double the strength and extension at break when compared to 4% NaOH treated samples. These results indicated that the 4% NaOH pre-treatment exposed fibre hydroxyl groups. Further acetylation esterified these hydroxyl groups within the pre-treated fibres and promoted strong bonding between fibres and matrix. This activity facilitated strong interface bonding thus justifying the higher shear strengths and extensions at break that were achieved.

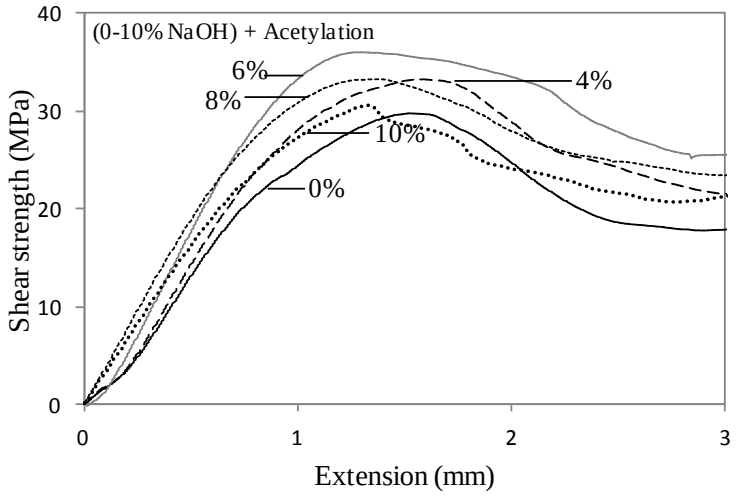

Figure 6.21: Typical shear stress-extension curves of acetylated fibre composites

(a)

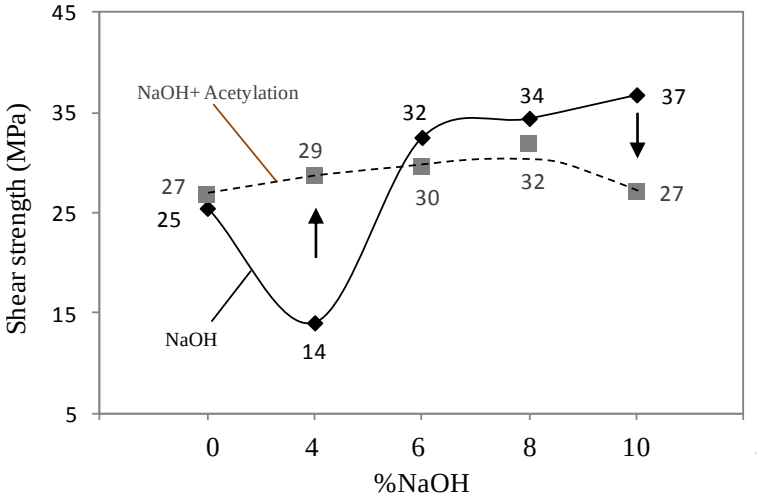

(b)

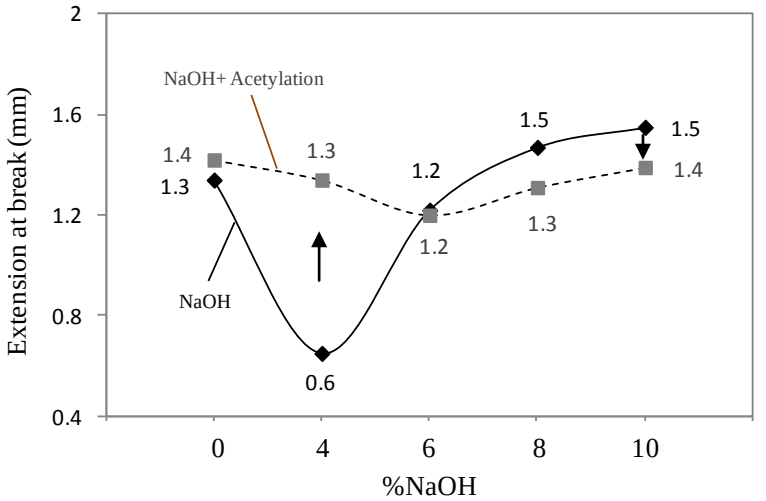

Figure 6.22: Shear properties of alkali pre-treated acetylated fibre composites (a) strength (b) extension at break

There was an optimum concentration level which allowed for stronger composite properties to be achieved. Beyond this limit, composite properties were compromised. Specifically, at higher concentrations (6-10%) of NaOH pre-treatment and further acetyl treatments on the fibres, excess removal of hemicellulose and lignin constituents took place. This caused fibre weaknesses in carrying shear loads. As can be seen in Figures 6.22a and 6.22b, the dual treated samples exhibited lowered shear strengths and extensions at break compared to the 6-10% NaOH treated samples.

Fibre silanisation on composites

Figure 6.24 presents a typical shear stress-extension curve for NaOH pre-treated silanised fibre composites, and their properties are summarised in Table 6.3. The changes in strength and extension at break of the silanised composites are presented in Figure 6.24. From Figure 6.24a it can be observed that silane treatments on alkali (0-4% NaOH) pre-treated fibres initially increased the composite's strength then significantly decreased their strength at higher pre-treatment concentrations (6-10% NaOH) compared to NaOH treated samples. When 4% NaOH treated fibre was then treated with silane, the hydroxyl groups reacted with silane to form silanols. Silanols produced strong couplings at the fibre matrix interface. During shear loading, strong interfaces reduced fibre bending and fibre sliding in the matrix and thus composites exhibited higher stress transfer capacities. As a result, silane treatments on 4% NaOH pre-treated composites showed over 85% higher shear strength compared to 4% NaOH treated samples.

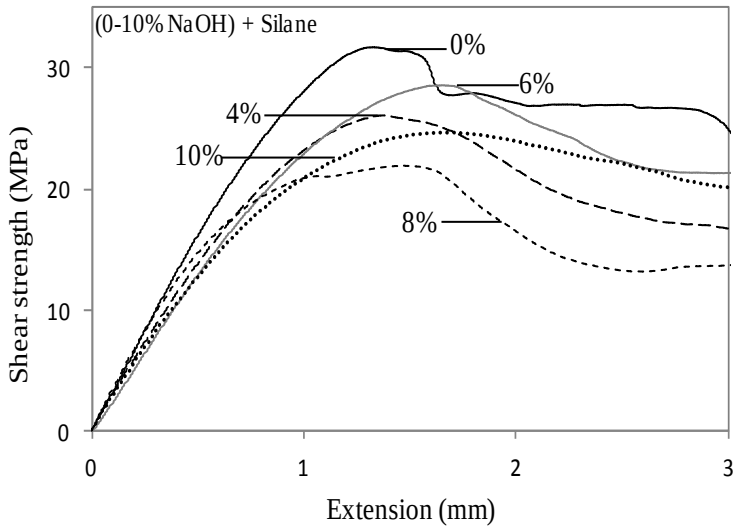

Figure 6.24: Typical shear stress-extension curves of silanised fibre composites

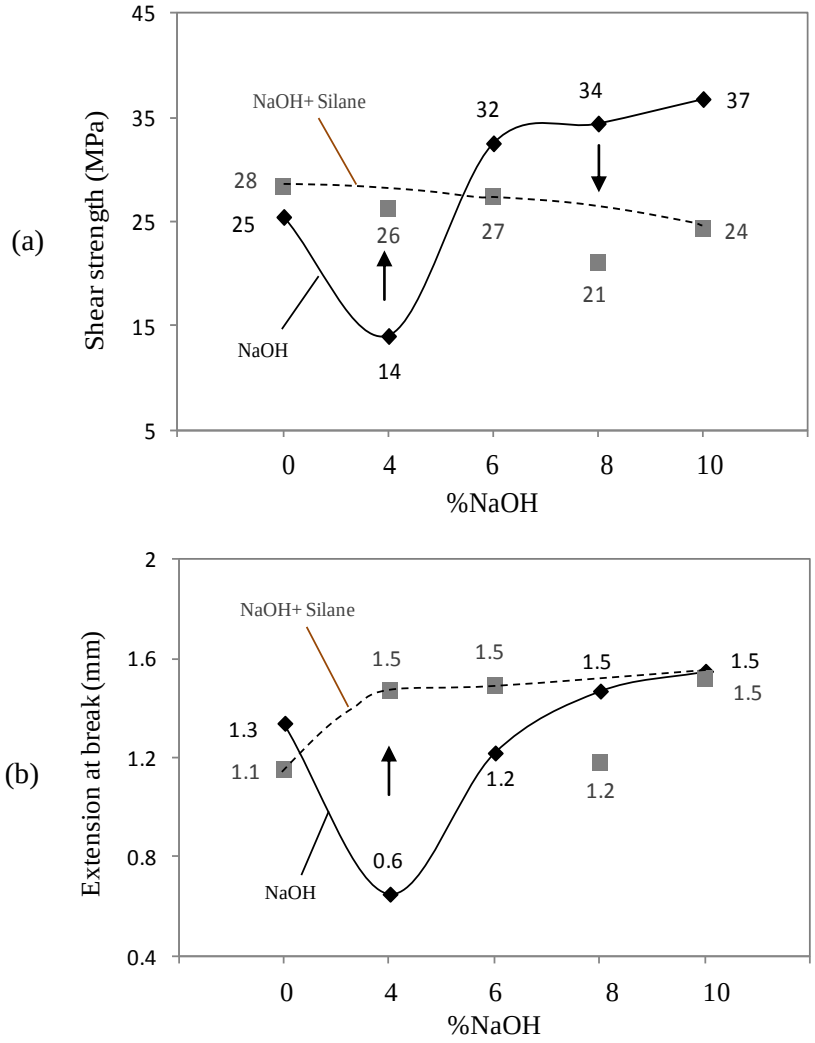

Figure 6.24: Shear properties of alkali pre-treated silanised fibre composites (a) strength (b) extension at break

At higher (6-10%) NaOH pre-treatment conditions, hydroxyl groups attached with hemicellulose and lignin were removed from the fibres. Silane treatments on the pre-treated fibres were ineffective as insufficient hydroxyl groups were left to form silanols, thus reducing coupling efficiency at their interfaces. Due to this, weak interface bonding was prevalent and composites failed at lower shear loads.

From Figure 6.24b it can be observed that 4-6% NaOH pre-treated silanised samples exhibits higher extension at break compared to the NaOH treated samples. Silane couplings at the interface experienced shear deformation during fibre bending. Further fibre bending caused a gradual breakdown of couplings and allowed the fibres to slide from their surrounding matrix. At this stage, silane coupling contributed additional shear resistance during composite deformation and exhibited higher extension at break. However, at higher (8-10%) NaOH pre-treatment concentrations, fibres became weak in resisting progressive fibre bending and thus failed at lower extensions compared to the NaOH treated samples.

Among all the above mentioned treatments, higher concentrations of NaOH (6-10%) exhibited higher shear strengths and deformations compared to untreated fibres. These results proved that higher NaOH concentrations effectively removed hemicellulose and lignin coverings from the cellulose surfaces in the fibres. Cellulose microfibrils then reacted with the matrix and provided strong interface bonding thus improving composite shear properties. On the other hand, acetyl treatments on the alkali pre-treated fibres showed improvements in the composite's shear strength and extension up to 4% NaOH pre-treatment conditions. At higher pre-treatment concentrations (6-10% NaOH) composite properties decreased. As

acetylation esterified hydroxyl groups and also removed the surface coverings from the 4% NaOH treated fibres, matrices formed strong bonding with cellulose microfibrils. During shear loading, strong interface bonding provided higher resistance against fibre bending and thus improved composite strength and extension. However, at higher NaOH pre-treatment concentrations, fibres had less available hydroxyl groups on the fibres. Further acetylation could not effectively esterify the hydroxyl groups. Due to this, weak interface bonding took place and composites exhibited lower shear properties. Similar observations were also made for alkali pre-treated silanised fibre composites. In this case, silane molecules could effectively form couplings with the 4% NaOH pre-treated fibres and composites exhibited higher shear properties. At higher (6-10%) NaOH pre-treatment concentrations, silanols could not form due to a lack of available hydroxyl groups on the pre-treated fibres. As a result, weak interface bonding took place and composites exhibited lower shear properties.

6.2.4 Flexural properties of composites

Flexural properties of composites were measured through conventional three-point bending tests. Flexural load was applied perpendicularly to the fibre direction. Initially, the loading nose came in contact with the upper surface of the specimen. Load was transferred from the elastic matrix to the fibres. Under incremental loading the fibres started to bend, and strained into the matrix. Bent fibres generated further strains to neighbouring fibres and caused them to bend also (Huang 2004). This led to fibre-matrix interface instability and generated disproportionately high stresses on the matrix. As a result, the matrix shifted from elastic to plastic deformation and initiated damage of the composites.

During flexural testing, the top and bottom faces of the specimen mid-section experienced compressive and tensile stresses. Compressive stresses produced large longitudinal tensile stresses on the lower surfaces of the specimen. The combination of vertical compressive stress and longitudinal tensile stress produced shear stresses (Jeng & Chen 2000; Lu, Kao & Su 1998). Figure 6.25 presents a schematic diagram which outlining the flexural load distribution on composites.

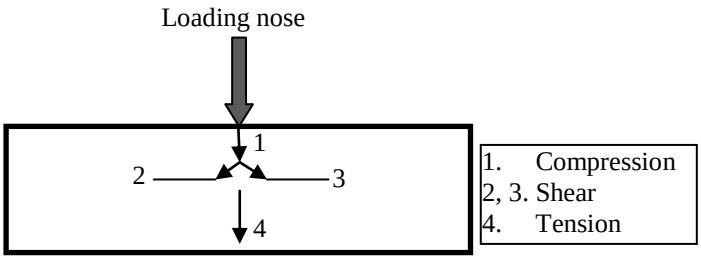

Figure 6.25: Schematic diagram of flexural load distribution on the composite

Figure 6.26 shows typical flexural failure modes of the tested samples. From this figure it can be observed that considerable damage appeared on the compression side of the specimen. An upper shear crack is visible just below the compressive crack. The compression cracks propagate downward causing the expansion of the upper shear cracks. Moreover, the compression and upper shear cracks produced the tension crack at the specimen's bottom layer. A shear crack is also visible at the bottom face of the specimen just above the tension crack. Tensile failure of the outermost fibres on the tension side is observed.

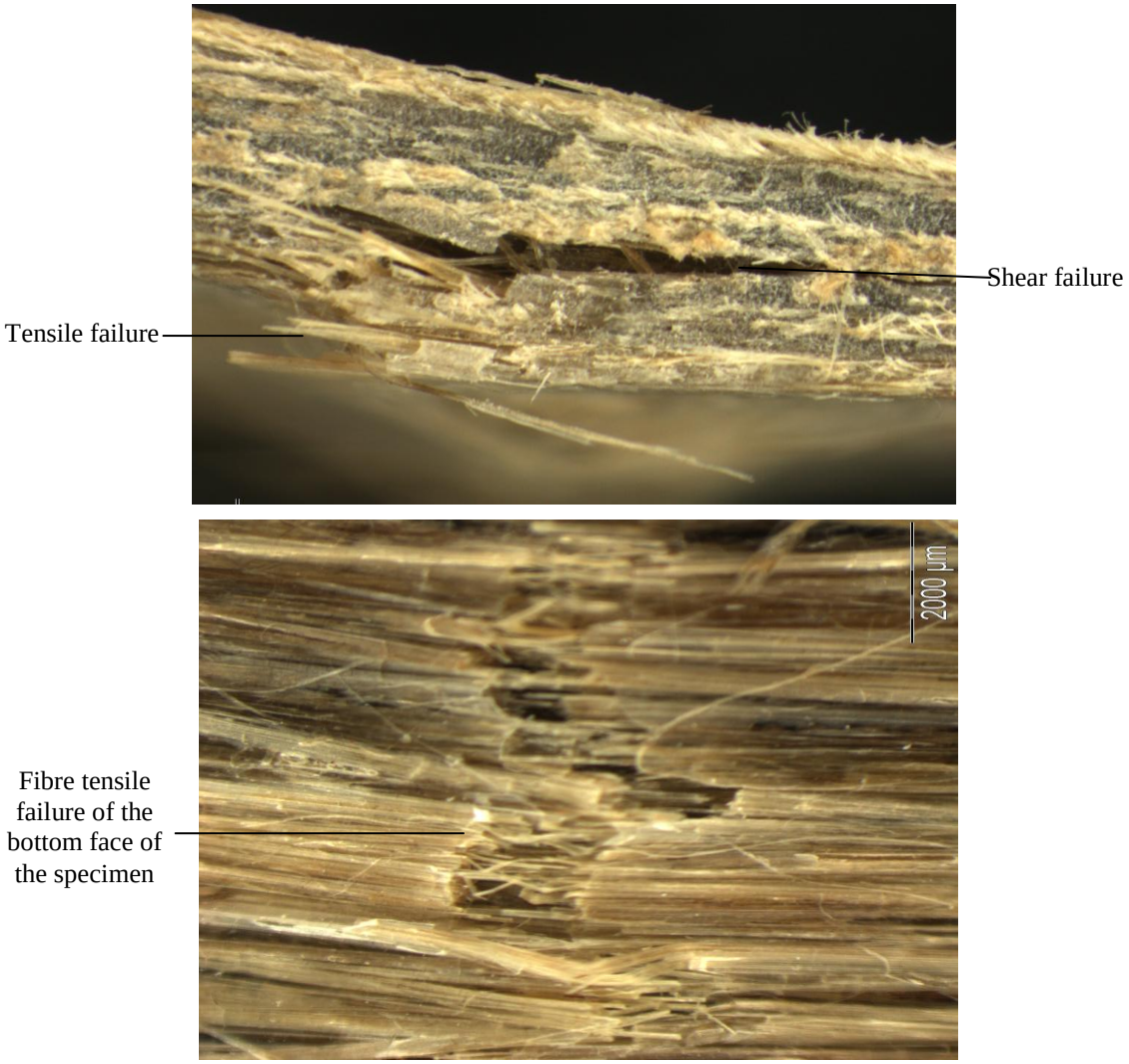

Figure 6.26: Typical flexural failure modes of tested samples

Figure 6.27 presents a typical flexural stress-strain curve for untreated fibre composites. The curve shows that the material response was linear (elastic-linear) up to the strength of around 80 MPa and strain of 0.0095 where both fibre and matrix behaved linearly. The linear elastic response was marked by α. Afterwards, the curve deviated from this linear proportionality and a geometric nonlinear response went up to a stress of about 190 MPa and the failure stress point was reached. At this stage,

the curve diverged in several points with different stages of modulus (α_1, α_2, α_3) values. The shape of the stress-strain curves indicated ductile failure. This type of failure showed that crack initiation took place at approximately regular intervals. Due to this, modulus values diverged at several points on the curve.

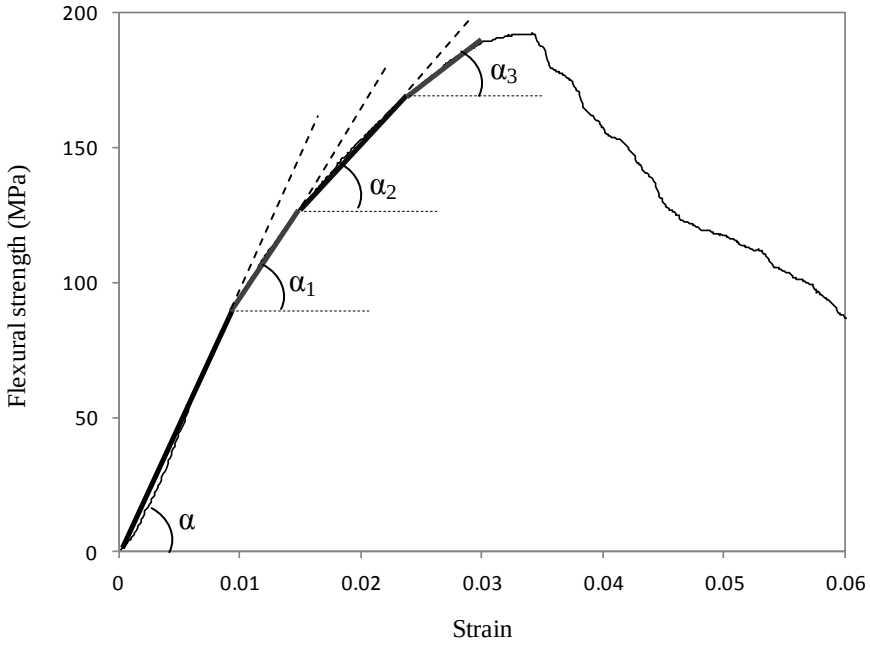

Figure 6.27: Typical flexural stress-strain curve of the fibre composite

Fibre alkalisation on composites

Figure 6.28 is a typical flexural stress-strain curve for alkalised fibre composites, and their properties are summarised in Table 6.4. The changes in flexural strength, modulus and failure strain of the alkalised composites are presented in Figure 6.29. From Figure 6.29 it was observed that lower concentrations (4%) of NaOH treatments on the fibres reduced composite flexural properties (strengths, modulus (α) and failure strain) compared to untreated samples. As treatment concentrations increased (6-10% NaOH), flexural properties also increased in comparison to 4% NaOH treated samples.

Table 6.4: Flexural properties of composites with different fibre treatments

Fibre treatments	Alkalisation						Alkalisation + Acetylation						Alkalisation + Silanisation					
	Strength (MPa)	Stages of modulus (GPa)				Strain at break (%)	Strength (MPa)	Stages of modulus (GPa)				Strain at break (%)	Strength (MPa)	Stages of modulus (GPa)				Strain at break (%)
% NaOH		α	α_1	α_2	α_3			α	α_1	α_2	α_3			α	α_1	α_2	α_3	
0	190.87 ±1.92	12.56 ±1.75	7.72 ±0.33	5.33 ±0.27	3.75 ±0.41	3.56 ±0.16	254.78 ±16.35	18.64 ±2.05	12.59 ±1.28	8.15 ±0.55	5.81 ±0.35	3.19 ±0.10	182.08 ±10.15	10.88 ±0.94	8.28 ±0.73	5.90 ±0.47	4.36 ±0.26	2.84 ±0.06
4	174.97 ±17.27	11.83 ±1.68	7.75 ±0.65	5.27 ±0.52	3.89 ±0.24	3.26 ±0.17	197.63 ±3.59	13.80 ±0.57	9.25 ±0.66	5.86 ±0.22	4.04 ±0.23	2.97 ±0.01	185.59 ±2.67	11.26 ±0.54	7.27 ±1.24	5.16 ±0.43	2.92 ±0.28	3.21 ±0.18
6	213.10 ±11.64	14.34 ±0.91	9.68 ±0.73	6.79 ±0.68	5.04 ±0.25	2.92 ±0.01	213.37 ±8.82	15.04 ±1.52	9.85 ±0.64	6.58 ±0.33	4.79 ±0.60	2.87 ±0.01	176.62 ±8.08	13.63 ±1.28	7.63 ±0.51	5.51 ±1.02	3.67 ±0.37	3.14 ±0.04
8	221.71 ±14.28	14.64 ±0.50	8.40 ±0.09	4.97 ±0.37	3.16 ±0.23	3.35 ±0.01	209.37 ±6.48	15.27 ±0.57	10.25 ±1.00	6.67 ±0.32	4.75 ±0.39	3.14 ±0.15	132.94 ±2.87	8.57 ±0.49	4.79 ±0.45	3.43 ±0.11	2.11 ±0.16	3.99 ±0.51
10	218.75 ±6.37	10.83 ±0.77	6.53 ±0.24	4.09 ±0.21	2.76 ±0.28	4.32 ±0.01	188.99 ±19.95	11.47 ±1.16	7.03 ±0.58	4.90 ±0.38	3.72 ±0.29	3.67 ±0.12	155.30 ±6.01	10.78 ±0.68	5.59 ±0.33	3.68 ±0.25	2.43 ±0.28	4.23 ±0.08

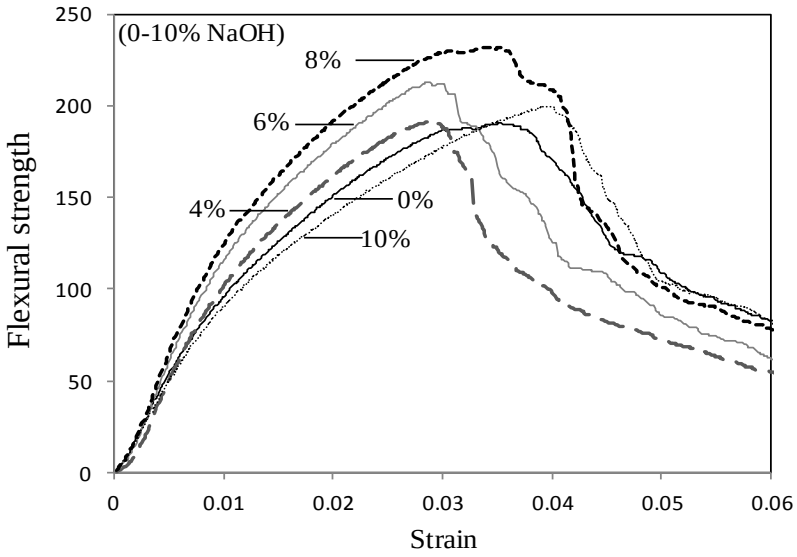

Figure 6.28: Typical flexural stress-strain curves of alkalised fibre composites

(a)

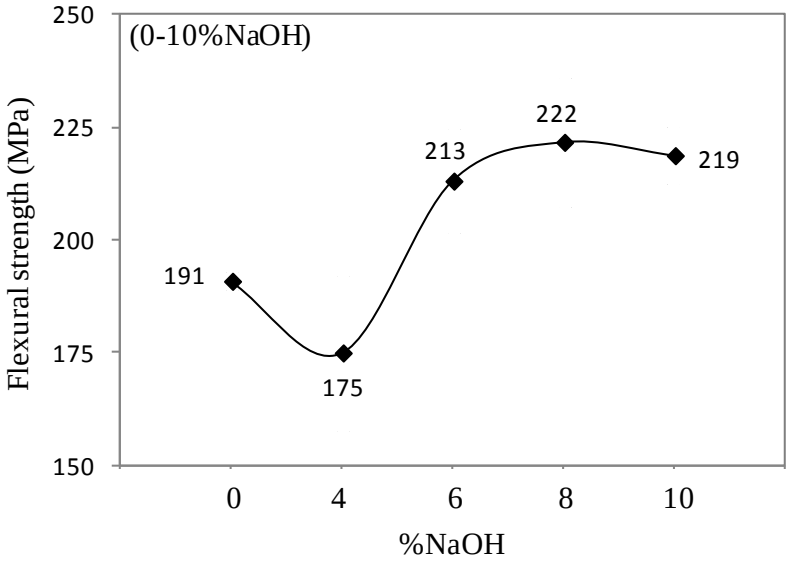

(b)

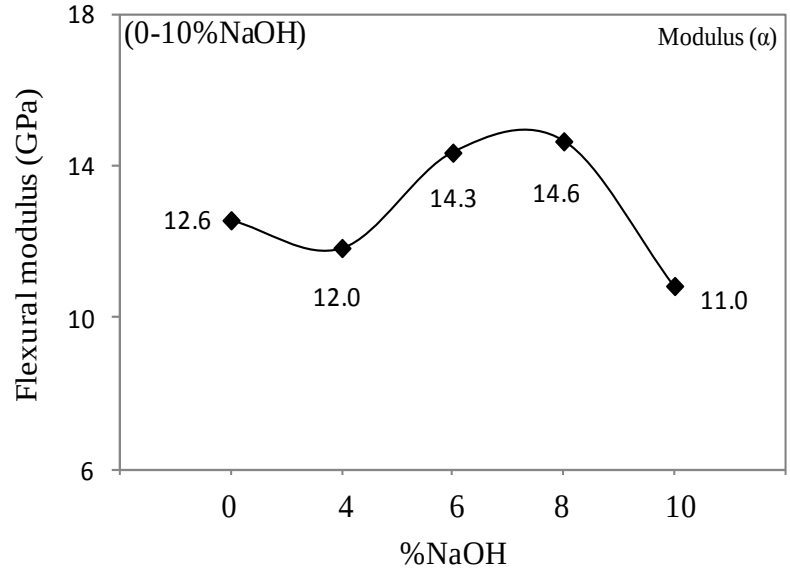

(c)

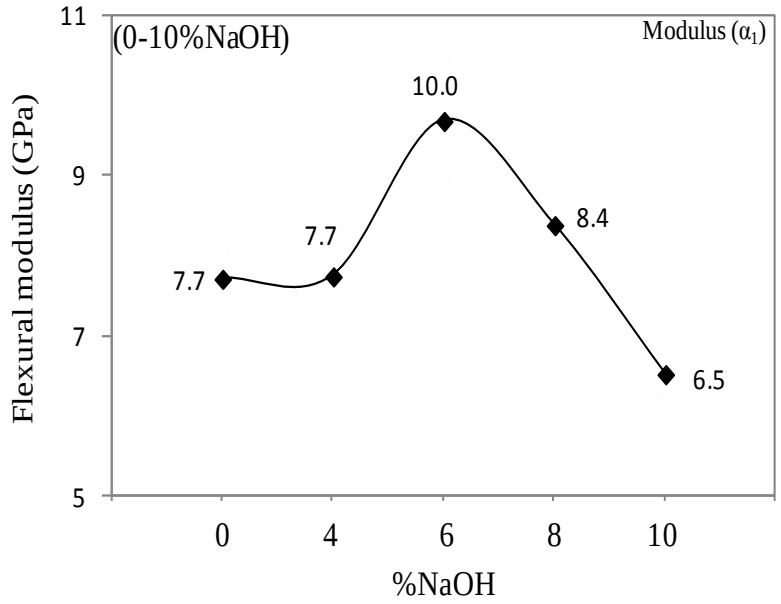

(d)

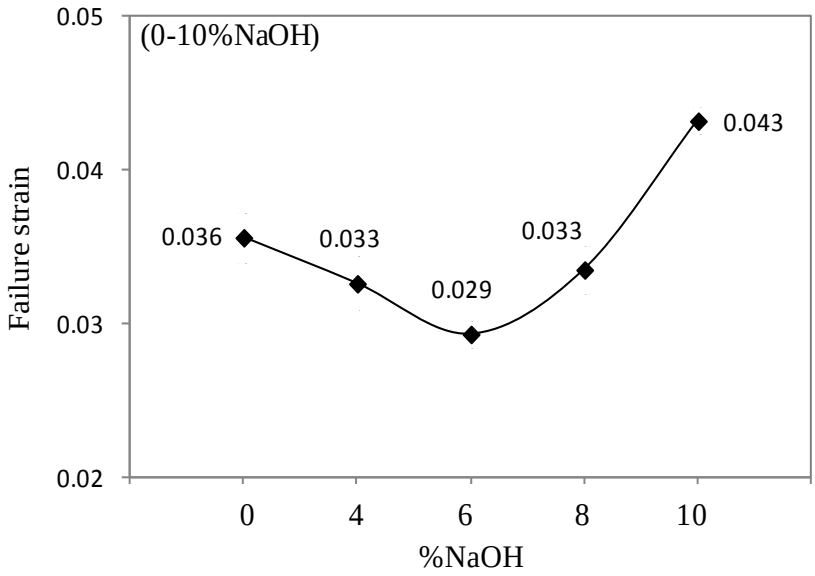

Figure 6.29: Flexural properties of alkalised fibre composites (a) strength (b) α (c) α1 (d) failure strain

As discussed in previous sections, lower treatment concentrations (4% NaOH) produced weak interface bonding between the fibres and matrix. Weak bonding reduced the matrix support to the fibres which ultimately lowered frictional resistance at their interface. During flexural loading, compressive cracking was initiated at weak interfaces due to fibres bending in the matrix. Compressive cracks generated further strains on neighbouring interfaces. The bottom surface of the

specimens experienced relatively higher tensile stresses due to the contribution of progressive compressive cracks. The higher tensile stresses and the progressive compressive cracks collectively caused tensile failure of the fibre and thus failure of overall composites. As a result, weak interface bonding reduced the composite's ultimate load carrying capacities and consequently reduced its strength, strain and modulus values.

However, at higher treatments concentrations (6-10% NaOH), composite strengths increased from around 175 MPa to 220 MPa compared to 4% NaOH treated samples. The enhanced composite properties were primarily governed by the higher degree of interface bonding which facilitated greater load transfer action of the samples. This was possibly due to the fact that higher NaOH concentrations effectively removed the hemicellulose and lignin coverings from the fibre surface. As a result, more accessible cellulose surfaces were exposed for matrix adhesion and thus produced strong interface bonding.

Beyond optimum concentration levels, fibres began losing their strength. During composite deformations, weak fibres gradually deformed at the strong fibre-matrix interfaces. From Figure 6.29d it can be seen that higher concentrations (6-10%) of NaOH treatments increase the composites failure strain. This was indicative of weak fibre deformation at their strong interface. Thus, the materials were able to sustain large deflections before the break. Similar observations were made from Figures 6.29b and 6.29c where the moduli (α, α_1) also decreased at higher treatment concentrations (6-10% NaOH). At α and α_1, interface cracks developed and propagated throughout the matrix. Weak fibres gradually lost their load carrying

capacities to bridge the matrix cracks and failed under large deformations, thus reducing composite moduli.

Fibre acetylation on composites

Figure 6.30 is a typical flexural stress-strain curve of NaOH pre-treated acetylated fibre composites, and their properties are summarised in Table 6.4. The changes in strength modulus and failure strain of the acetylated composites are presented in Figure 6.31. From Figure 6.31 it is observed that acetyl treatments on untreated fibres (0% NaOH) increase composites' strength from 191 MPa to 255 MPa which is an increase of 30%. Similarly, composites' moduli also increase (α=48%, α_1=63%, α_2=53%, α_3=55%) but the failure strain is decreased when compared to untreated samples (Table 6.4). These results indicated that acetylation removed the hemicellulose and lignin coverings and also esterified hydroxyl groups present within the fibre. Consequently, interface adhesion increased, allowing the composites to carry greater flexural loads at relatively small elongations. As a result, the flexural properties of the acetylated composites increased.

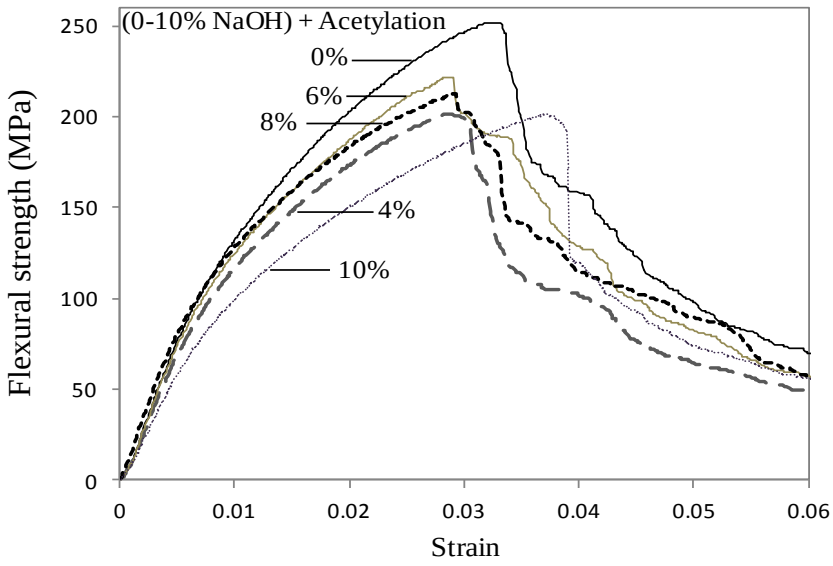

Figure 6.30: Typical flexural stress-strain curves of acetylated fibre composites

(a)

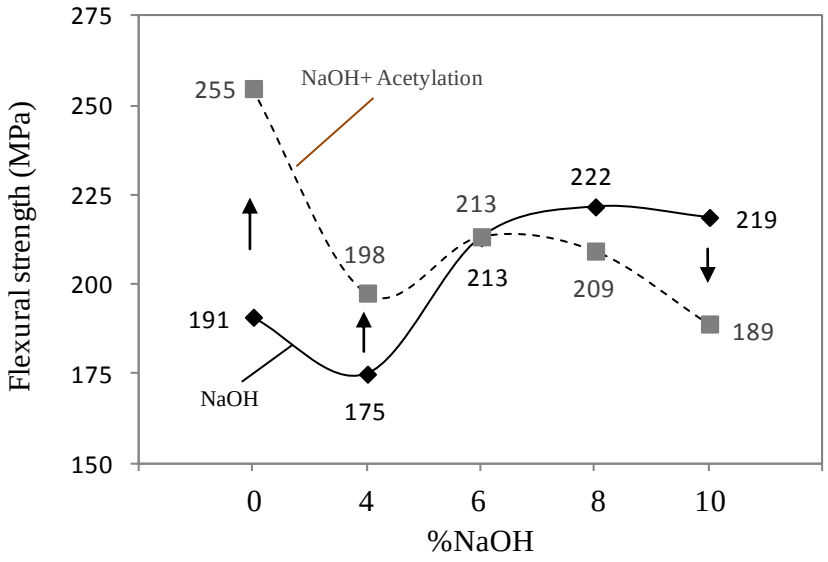
Flexural strength (MPa)
275
250
225
200
175
150
NaOH+ Acetylation
255
198
213
209
189
222
213
219
191
NaOH
175
0
4
6
8
10
%NaOH

(b)

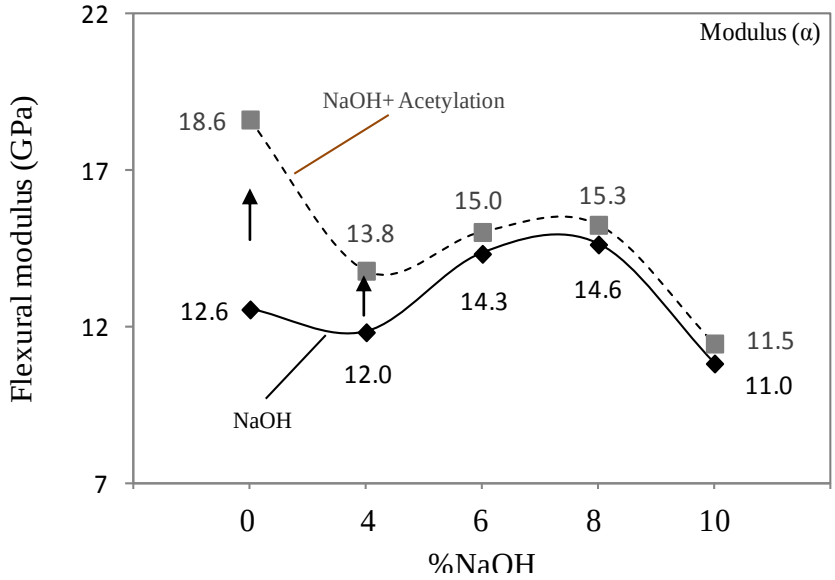
Flexural modulus (GPa)
Modulus (α)
22
17
12
7
NaOH+ Acetylation
18.6
13.8
15.0
15.3
11.5
12.6
12.0
14.3
14.6
11.0
NaOH
0
4
6
8
10
%NaOH

(c)

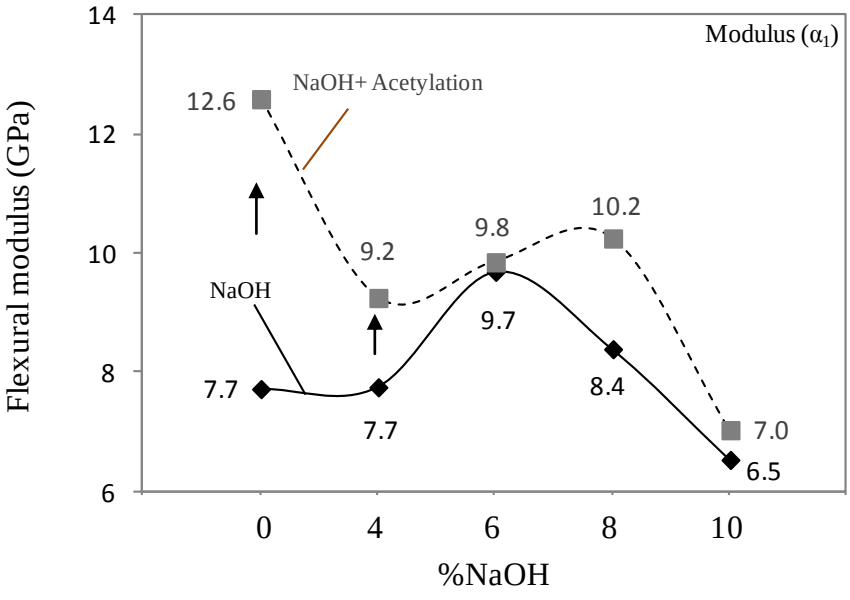
Flexural modulus (GPa)
Modulus (α1)
14
12
10
8
6
NaOH+ Acetylation
12.6
9.2
9.8
10.2
7.0
NaOH
7.7
7.7
9.7
8.4
6.5
0
4
6
8
10
%NaOH

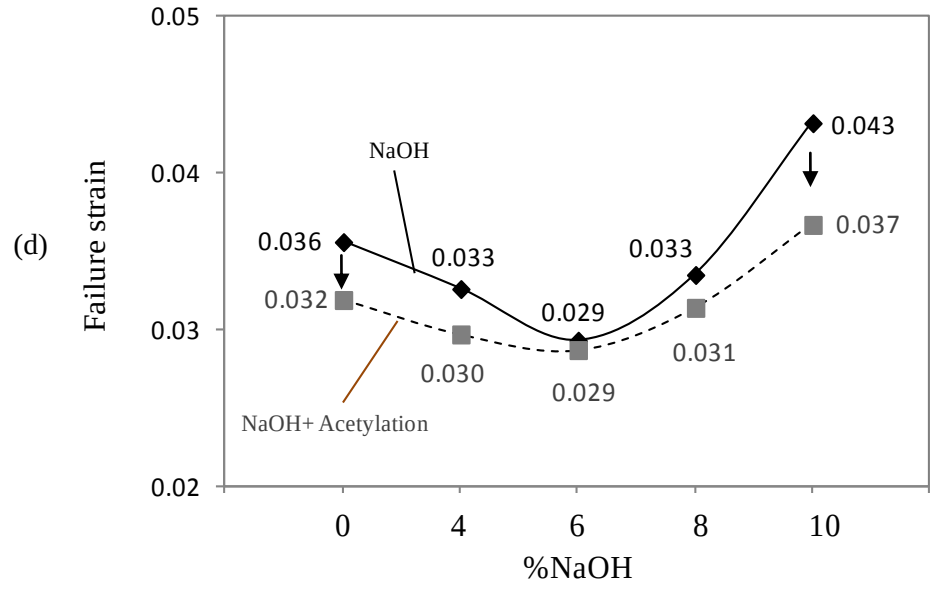

Figure 6.31: Flexural properties of alkali pre-treated acetylated fibre composites
(a) strength (b) α (c) α_1 (d) failure strain

Acetyl treatments on the 4% NaOH pre-treated sample also improved composites' strength and moduli compared to the 4% NaOH treated samples. The hydroxyl groups presented on the pre-treated fibre were esterified during acetyl treatments. Also, the hemicellulose and lignin constituents were removed through acetylation. Due to this, cellulose surfaces were more accessible for matrix adhesion which promoted strong fibre-matrix interface bonding. As a result, the application of two consecutive treatments on the fibres improved the composites' properties.

However, at higher (6-10%) NaOH pre-treatment concentrations, further acetylation caused greater removal of fibre surface coverings thus enhancing interface bonding. Fibres became weaker in strength due to the removal of hemicellulose and lignin covering materials. During flexural loading, weak fibres transferred compressive loads effectively through strong interfaces but suddenly failed under tensile loading. These observations can be further supported by the tensile (Section 6.2.1, Figure 6.5)

and compressive properties (Section 6.2.2, Figure 6.12) of the acetylated composites. Thus, 6-10% NaOH pre-treated acetylated samples exhibited lower flexural strength but higher modulus compared to the NaOH treated samples.

Fibre silanisation on composites

Figure 6.32 is a typical flexural stress-strain curve for silanised fibre composites, and their properties are summarised in Table 6.4. The changes in flexural strength and modulus of the silanised composites are presented in Figure 6.32. From Figure 6.32 it is observed that silane treatments on the untreated fibres reduced the composite's flexural strengths and moduli. These results indicated that silane molecules were unable to penetrate the untreated fibre surfaces due to the presence of surface coverings. As a result, weak interface bonding took place and the composites failed with lower flexural properties compared to the untreated sample.

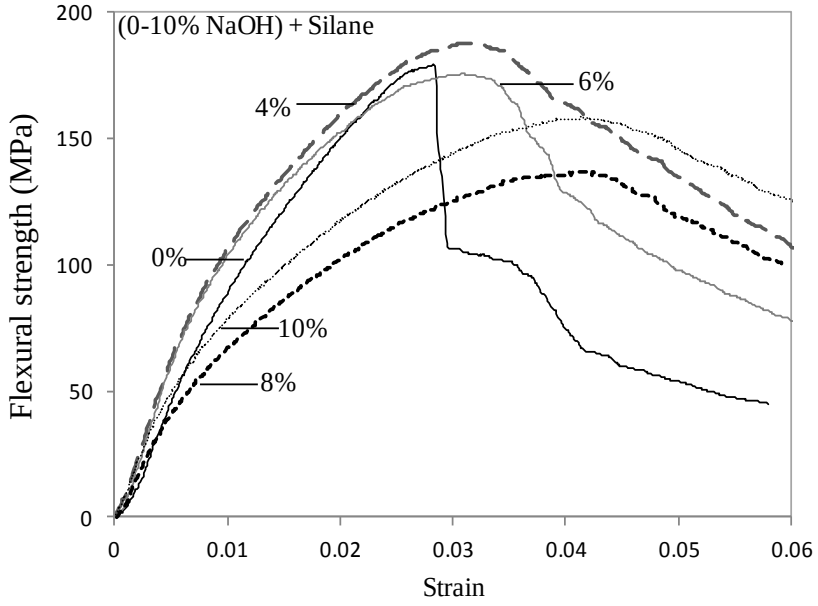

Figure 6.32: Typical flexural stress-strain curves of silanised fibre composites

(a)

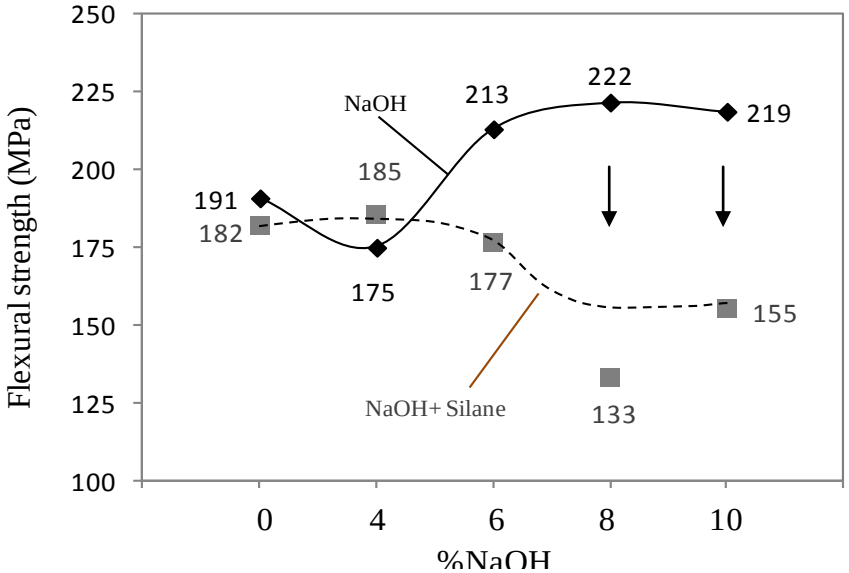

(b)

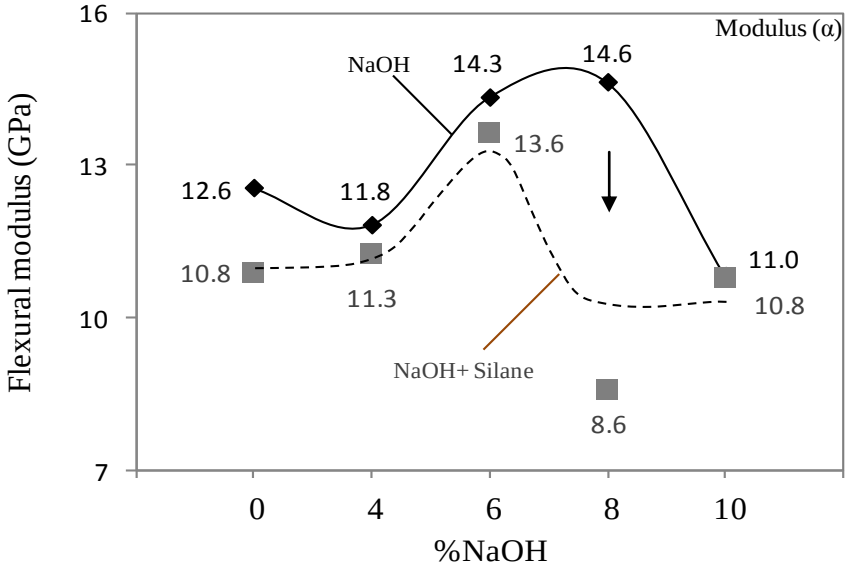

(c)

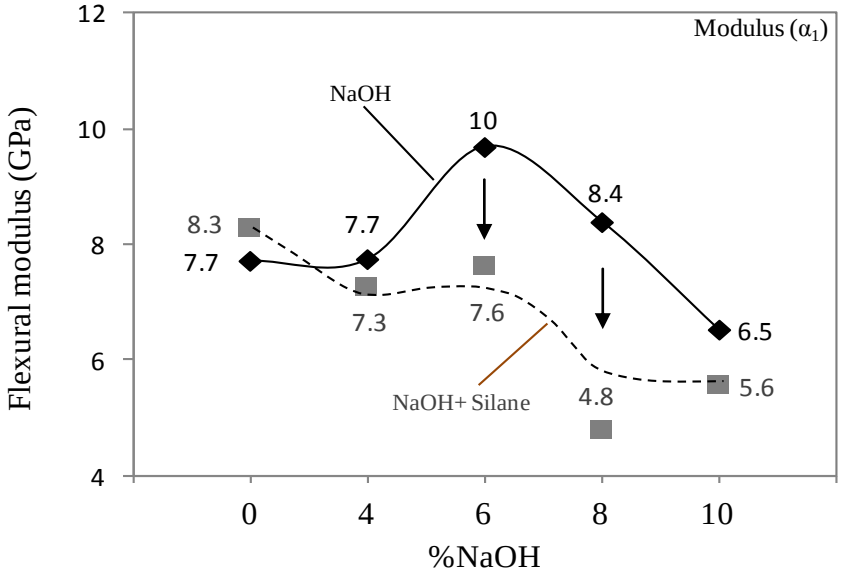

Figure 6.33: Flexural properties of alkali pre-treated silanised fibre composites (a) strength (b) α (c) α_1

However, silane treatments on the 4% NaOH pre-treated samples exhibited higher strength compared to the 4% NaOH treated samples. This again proved that silane molecules formed strong couplings with the pre-treated fibres in the presence of fibre hydroxyl groups. This provided strong bonding between the fibres and matrix, and the composites were able to transfer greater flexural loadings compared to the 4% NaOH treated samples (Figure 6.33a).

As pre-treatment concentrations (6-10% NaOH) increased, fibres lost their hydroxyl groups and silane molecules could not achieve sufficient reaction sites to form strong couplings with the fibres. This created weaknesses at the fibre-matrix interface. As a result, silanisation on the pre-treated fibres exhibited lower strengths and moduli compared to the 6-10% NaOH treated samples (Figure 6.33).

From the above analysis, it can be stated that higher concentrations (6-10%) of NaOH treatments on untreated fibres improved composite flexural properties. Fibre surface coverings were removed at higher treatment concentrations, which facilitated stronger bonding with the matrix and thus exhibited higher properties. However, acetyl treatments effectively removed fibre surface coverings and also esterified hydroxyl groups from the (0-4%) NaOH pre-treated fibres. Stronger interface bonding was achieved and composites exhibited higher flexural properties. Therefore, higher (6-10%) NaOH concentrations weakened fibres and further acetylation caused more losses of fibre strength. Consequently, at higher pre-treatment conditions, acetylated samples exhibited lower strengths. Similarly, silane treatments on the alkali pre-treated fibre composites initially showed higher strengths, but at higher pre-treatments conditions the samples exhibited lower

properties compared to the NaOH treated samples. This was due to the reduced amounts of hydroxyl groups being present on the pre-treated fibres forming strong silane couplings with the fibre. As a result, weak interface bonding took place and composites exhibited lower flexural properties.

6.2.5 Impact properties of composites

Impact testing utilises a sudden application of force to a part of a structure that produces gross damage in the structure. The damage absorbed by the material reflected the impact energy absorption capacity of the structure (Delfosse & Poursartip 1997).

During impact, the specimen generally experiences localised bending in which the upper face experiences compression whilst the lower face experiences tension (Hamada, Ramakrishna & Satoh 1995). Compressive stress at the upper face produces high progressive tensile stresses on the lower face. As the impact process progresses, the laminate continue to become strained under tension, until matrix cracking takes place. At this point, fibres are used to carry load to bridge the matrix crack. These cracks are extended to the neighbouring fibre and the fibre-matrix interfaces. Further matrix cracking produced stress concentrations on the bridging fibre (Shyr & Pan 2003; Singleton, et al. 2003). As a result, fibres undergo heavy tensile deformation and tend to slide or become pulled-out from the surrounding matrix. There is a substantial frictional resistance to sliding taking place because of the interface bonding (Reid & Zhou 2000). A higher frictional resistance from the interface delays the initiation of fibre sliding and thus improve the overall impact

resistance properties. Conversely, weak bonding allows the fibre to be pulled-out easily from the matrix and thus reduces the composites impact resistance capacity.

The impacted composite specimen can produce different damage modes simultaneously. The damage mode can be categorised as through matrix cracking, fibre matrix debonding, fibre pull-out from the surrounding matrix and fibre failure (Delfosse & Poursartip 1997; Hamada, Ramakrishna & Satoh 1995). Following matrix cracking, the fibre failures occur. The matrix cracking and fibre failure are an important source of impact energy absorption in composites.

A schematic diagram of the impact damage process was presented in Figure 6.34 (David-West, Nash & Banks 2008; Henkhaus 2003). At first, the projectile comes into contact with the specimen with an impact velocity. The projectile then starts to penetrate into the specimen and the surrounding matrix undergoes a compression-shear mode of damage, whereby the lower face of the specimen experiences a tension-shear mode of damage. During the entire impact process, as the projectile penetrates through the sample, frictional resistance from the interface develops. The amount of frictional resistance from the specimen is known as the energy absorption capacity of the sample (Belingardi, Cavatorta & Salvatore 2008).

The relationships between impact load, damage initiation and energy absorption were used to characterise the impact performance of the composites. Key impact parameters such as peak load, energy at peak load, deflection at peak load and absorbed energy data were recorded from the test. An analysis of force/time and force/ displacement curves allowed for the calculation of impact energy.

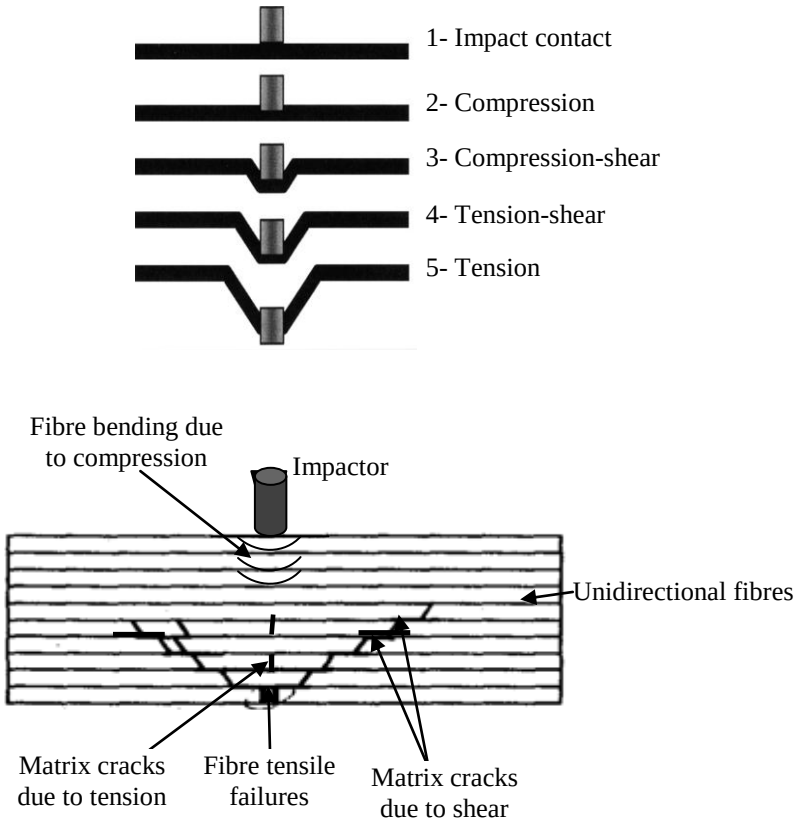

Figure 6.34: Schematic diagram of impact damage processes

Figure 6.35 shows typical impact force-deflection and energy-deflection curves of fibre composites. From Figure 6.35, the impact force at the contact stages between the projectile and specimen increased sharply to a maximum value, and then gradually decreased. The curve was linear up to the maximum force of around 315 N where the deformation recorded was about 12 mm. No damages were developed in the specimen at this stage. At the maximum force, a crack in the matrix was initiated and then cracks were propagated along the interfaces. The interface crack initiated debonding and delamination of the composites. From the maximum load, a rapid load drop of 210 N was observed which was accompanied by the formation of large cracking randomly orientated throughout the specimen. After the initial load drop, the curve was serrated. The load fluctuations were caused by various micro-fracture

processes in the specimen. At this stage, the magnitude of load fluctuations depended on the quality of interface bonding. The microcrack formation continues up to the specimen deformation of about 32 mm. Afterwards, progressive interface cracks spread away from the impact point and new debondings were created in neighbouring interfaces. As a result, load drops continued and reached at around 150 N with a deformation of about 33 mm. The load bearing capacity of the sample diminished as the impact forces decreased down zero, where the deformation was recorded as around 50 mm. At this stage, fibres were fractured in tension and final failure of the specimens took place.

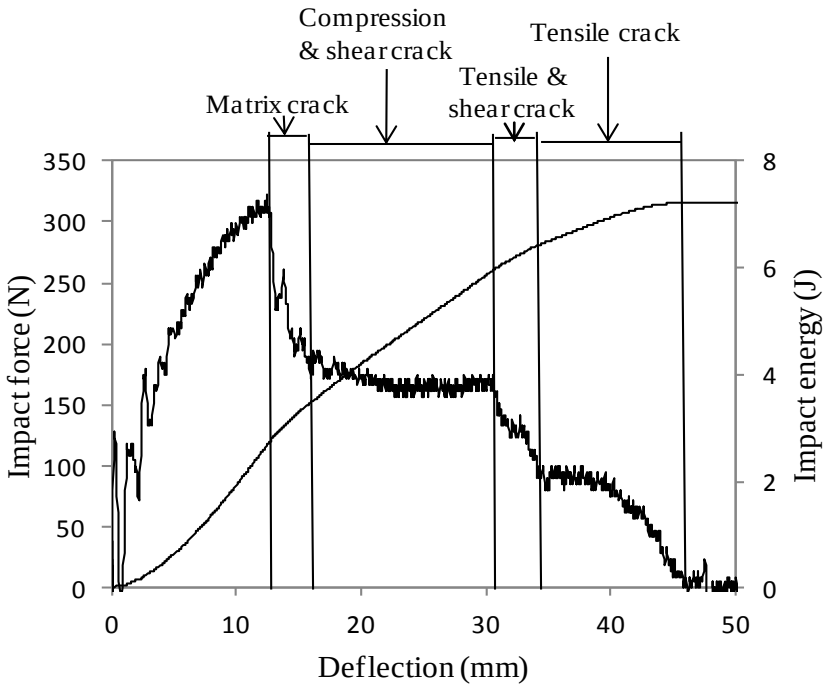

Figure 6.35: Typical impact force-deflection and energy-deflection curves of fibre composites

From Figure 6.36, using the total area under the force–time curve, it is possible to deduce the total energy require to initiate and propagate the specimen damage (Belingardi, Cavatorta & Salvatore 2008). The damage is initiated on the composites at a maximum impact energy (E_{Max}), corresponding to the maximum impact force.

Once the impact energy is high enough, the composite failures eventually take place. At this stage, the entire impact energies is absorbed (E_a) by the specimen. If the specimen does not completely fail, the projectile bounces back from the specimen. The energy created when the projectile bounces back is known as rebounded energy (E_r). When the specimen fails, the projectile is not rebound. Once the rebound energy became zero, all of the impactor energy is absorbed by the specimen and complete failure of the specimen occurs (Belingardi, Cavatorta & Salvatore 2008). From this discussion it can be stated that, the initial impacts create rebound cases, the later impacts increase the absorbed energy, thus decreasing the rebound energy. Here, the absorbed energy (E_a) was calculated by subtracting the rebound energy (E_r) from the maximum impact energy (E_{Max}). Additionally, the damage degree (DD) was calculated from the ratio of absorbed energy (E_a) to impact energy (E_{Max}) (Belingardi, Cavatorta & Salvatore 2008). Table 6.9 outlines the impact properties of the composites under different treatment conditions.

$$E_{Max} = E_a + E_r \quad (6.1)$$

$$DD = E_a / E_{Max} \quad (6.2)$$

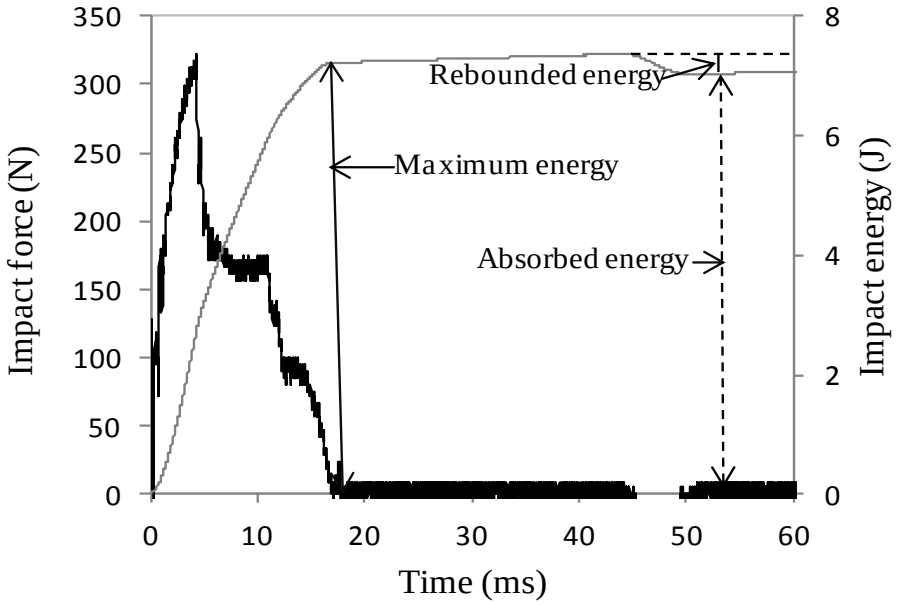

Figure 6.36: Typical impact force-time and energy-time curves of fibre composites

Table 6.5: Impact properties of composites with different fibre treatments

Fibre treatments	Alkalisation				Alkalisation + Silanisation				Alkalisation + Acetylation			
	Energy (J)				Energy (J)				Energy (J)			
% NaOH	E_{Max}	E_a	E_r	DD	E_{Max}	E_a	E_r	DD	E_{Max}	E_a	E_r	DD
0	7.60	7.25	0.34	0.95	6.76	6.37	0.38	0.94	5.92	5.56	0.36	0.93
	±0.22	±0.22	±0.01	±0.01	±0.42	±0.43	±0.05	±0.01	±0.73	±0.74	±0.02	±0.01
4	5.33	4.76	0.57	0.89	6.69	6.33	0.36	0.94	3.87	3.43	0.44	0.88
	±0.53	±0.46	±0.15	±0.02	±0.89	±0.92	±0.04	±0.01	±0.38	±0.38	±0.01	±0.01
6	5.86	5.33	0.52	0.90	6.90	6.51	0.39	0.94	6.93	6.63	0.30	0.95
	±0.69	±0.69	±0.08	±0.01	±0.11	±0.10	±0.08	±0.01	±1.43	±1.43	±0.06	±0.02
8	4.69	4.11	0.58	0.87	6.86	6.51	0.34	0.95	5.94	5.53	0.40	0.93
	±0.43	±0.36	±0.09	±0.01	±0.33	±0.33	±0.004	±0.001	±0.27	±0.27	±0.007	±0.01
10	5.53	5.00	0.52	0.90	7.25	6.91	0.34	0.95	5.17	4.74	0.43	0.92
	±0.69	±0.82	±0.13	±0.03	±0.43	±0.44	±0.01	±0.01	±0.49	±0.49	±0.09	±0.01

Fibre alkalisation on composites

Figure 6.37 shows the typical impact force-time and energy-time curves of alkalised fibre composites, and their properties are summarised in Table 6.5. The changes in E_a, E_r and DD of the alkalised composites are presented in Figure 6.38.

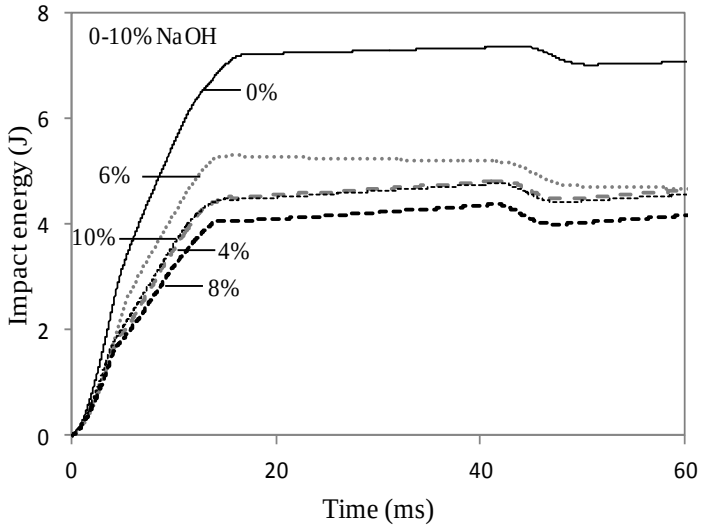

Figure 6.37: Typical impact energy-time curves of alkalised fibre composites

(a)

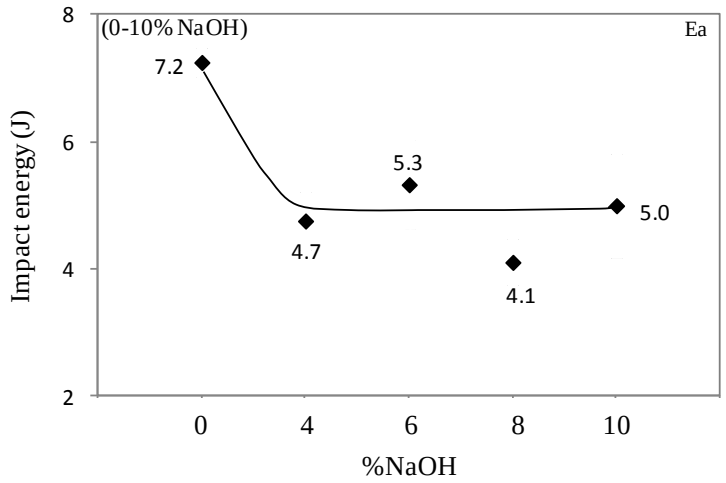

(b)

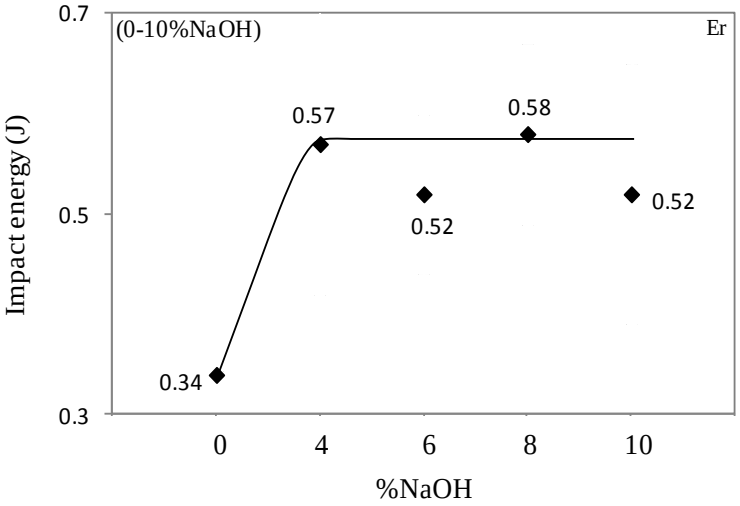

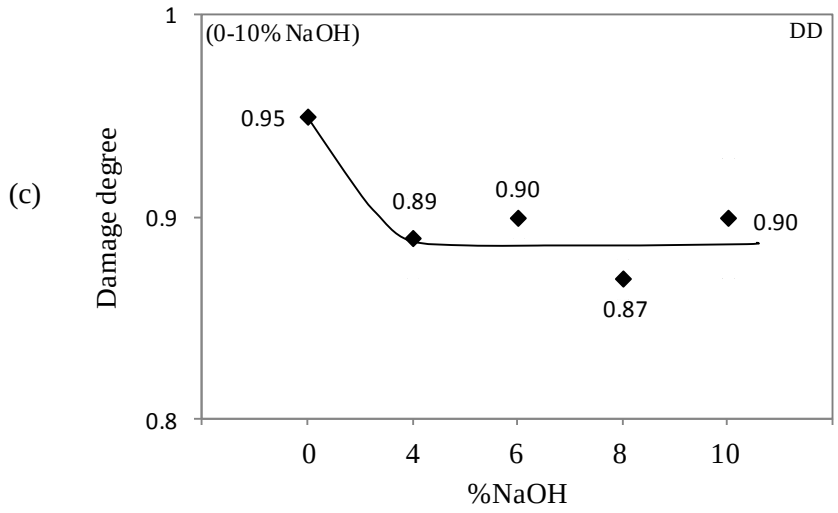

Figure 6.38: Impact properties of alkalised fibre composites (a) E_a (b) E_r (c) DD

During impact, the specimen simultaneously experienced compressive, shear and tensile loadings. Strong interface bonding between the fibre and matrix provided greater resistance during compression and shear. Conversely, strong fibre strength contributed to higher tensile properties.

From the previous sections, it was observed that alkali treatments removed fibre surface coverings and facilitated strong fibre-matrix interface bonding. Strong bonding provided higher compressive and shear strengths of the composites. However, due to the fibre weakness caused by the treatments, tensile properties of the composites were decreased.

From Figure 6.38 it can be seen that alkali treated fibre composites exhibited lower E_a and DD but higher E_r values compared to the untreated samples. The lower E_a indicates that, treated samples absorb less impact energy due to the strong interface bonding (Bledzki, et al. 2008). During impact, strong interface bonding generated higher resistances of fibre bending (during compression) and fibre sliding (during

shear) from their surrounding matrix. Due to this, the overall impact resistance properties of the treated composites increased and exhibited lower absorbed energies (Figure 6.38a).

Likewise, the higher E_r values for treated composites indicated that strong interfaces prevented the impactor from penetrating the samples and thus more rebounded cases were observed and recorded (Figure 6.38b). Similarly, the lower DD values indicated that the extent of impact damage was less on treated specimens (Figure 6.38c). These results again proved that the treated fibres provided strong interface bonding which were capable of resisting impact damages on the specimens.

Fibre acetylation on composites

Figure 6.39 illustrates the typical impact force-time and energy-time curves of NaOH pre-treated acetylated fibre composites, and their properties are summarised in Table 6.5. The changes in E_a, E_r and DD of the acetylated composites are presented in Figure 6.40.

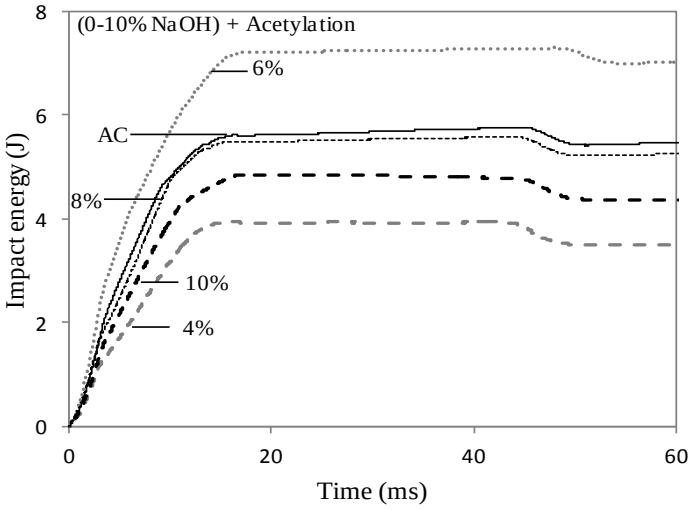

Figure 6.39: Typical impact energy-time curves of acetylated fibre composites

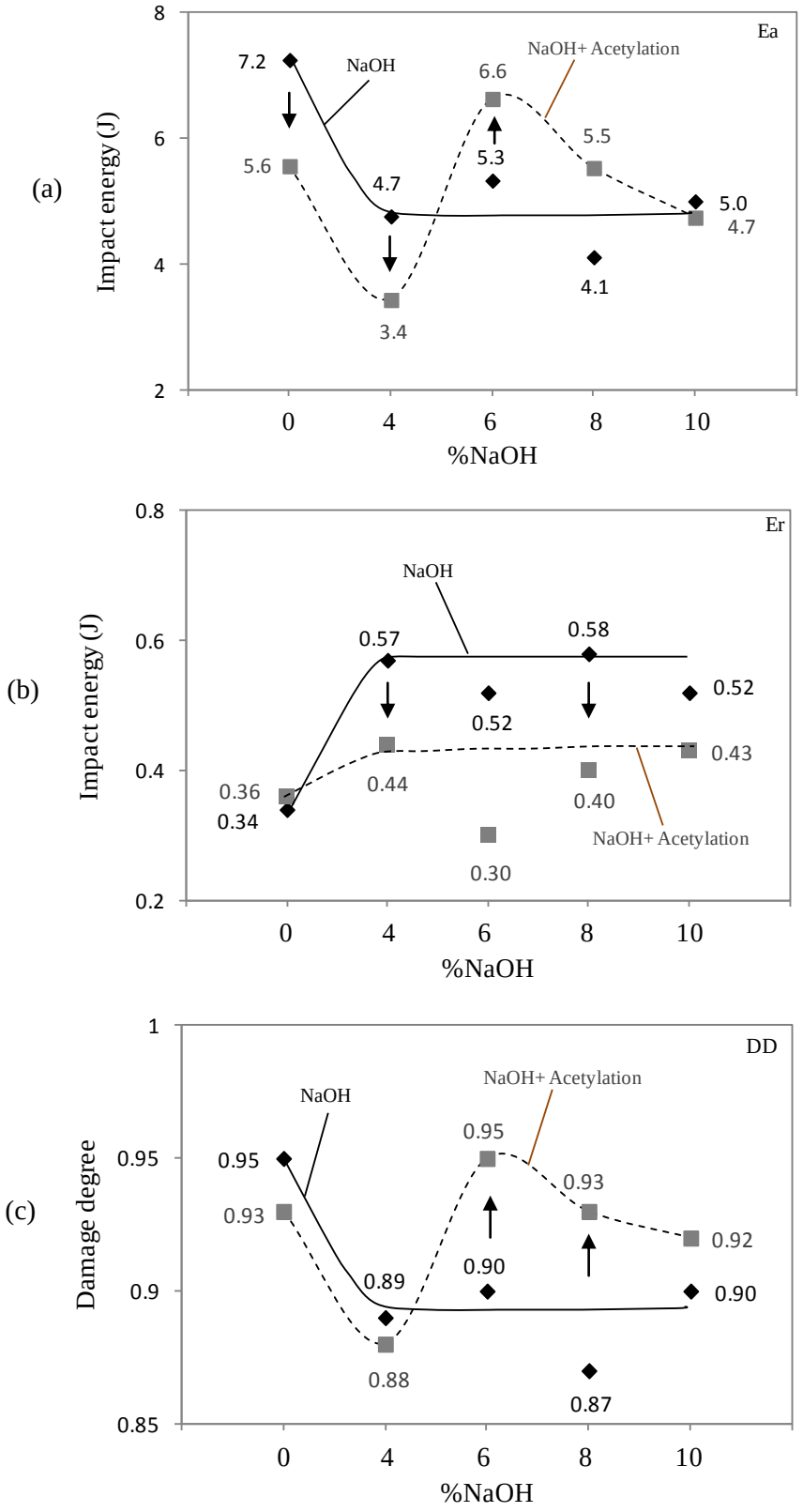

Figure 6.40: Impact properties of alkali pre-treated acetylated fibre composites (a) E_a (b) E_r (c) DD

From Figure 6.40 it can be observed that acetyl treatments on the (0-4%) NaOH treated fibres initially lower the composites' E_a and DD values compared to the NaOH treated samples. These results indicated that acetyl treatments on the (0-4%) NaOH treated fibres efficiently esterified the existed hydroxyl groups from the fibres and developed strong interface bonding with the matrix. The strong interface prevented the initiation of fibre bending (compression) and fibre sliding (shear) into the matrix. Consequently, the impact resistance properties of the composites increased. As a result, in the two consecutive treatment conditions, composites absorbed lower impact energy (E_a) and thus reduced the extent of damage (DD) compared to the NaOH treated samples.

On the other hand, at higher pre-treatment concentrations (6-10%) fibres were losing their strength. Further acetylation created more fibre weakness. During impact, weak fibres could not sustain the large tensile deformations (which exerted from the progressive compressive and shear deformations of neighbouring fibres) and thus easily failed at lower loads. As a result, the impactor could easily penetrate through the samples and lower rebounded values (E_r) were recorded compared to the NaOH treated samples (Figure 6.40b).

Fibre silanisation on composites

Figure 6.41 presents the typical impact force-time and energy-time curves of NaOH pre-treated silanised fibre composites, and their properties are summarised in Table 6.5. The changes in E_a, E_r and DD of the silanised composites are presented in Figure 6.42. From Figure 6.42 it can be observed that silane treatments on the alkali pre-treated fibres increased the composites E_a and DD values and decreased the E_r values

compared to the NaOH treated samples. These results clearly indicate that silane treatments on the alkali pre-treated fibres reduced the impact resistance properties of the composites. This may be due to the fact that, NaOH pre-treated fibres had less hydroxyl groups on their surface. Further, silane treatments could not get a sufficient amount of hydroxyl groups required to form silanols. Due to this, silanols could not develop strong interface bonding between the fibres and matrix.

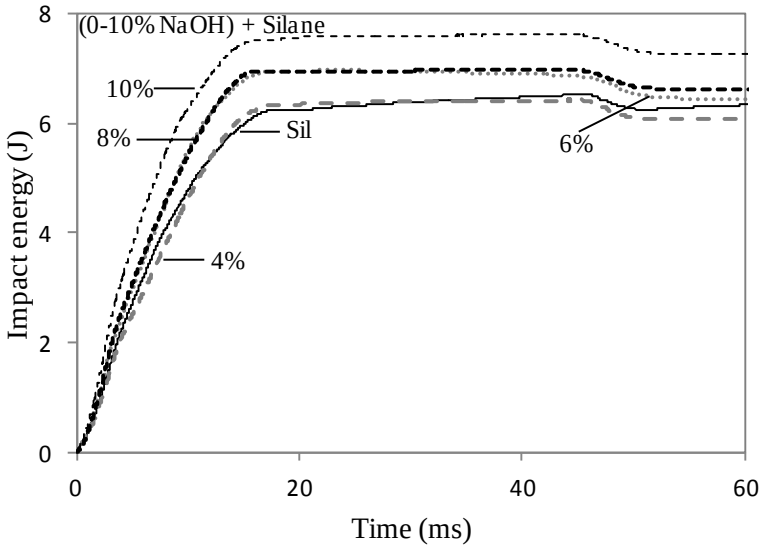

Figure 6.41: Typical impact energy-time curves of silanised fibre composites

(a)

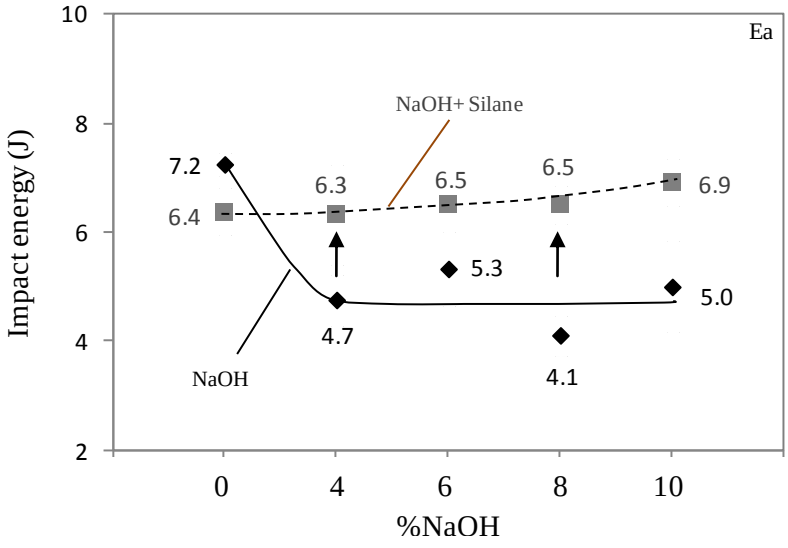

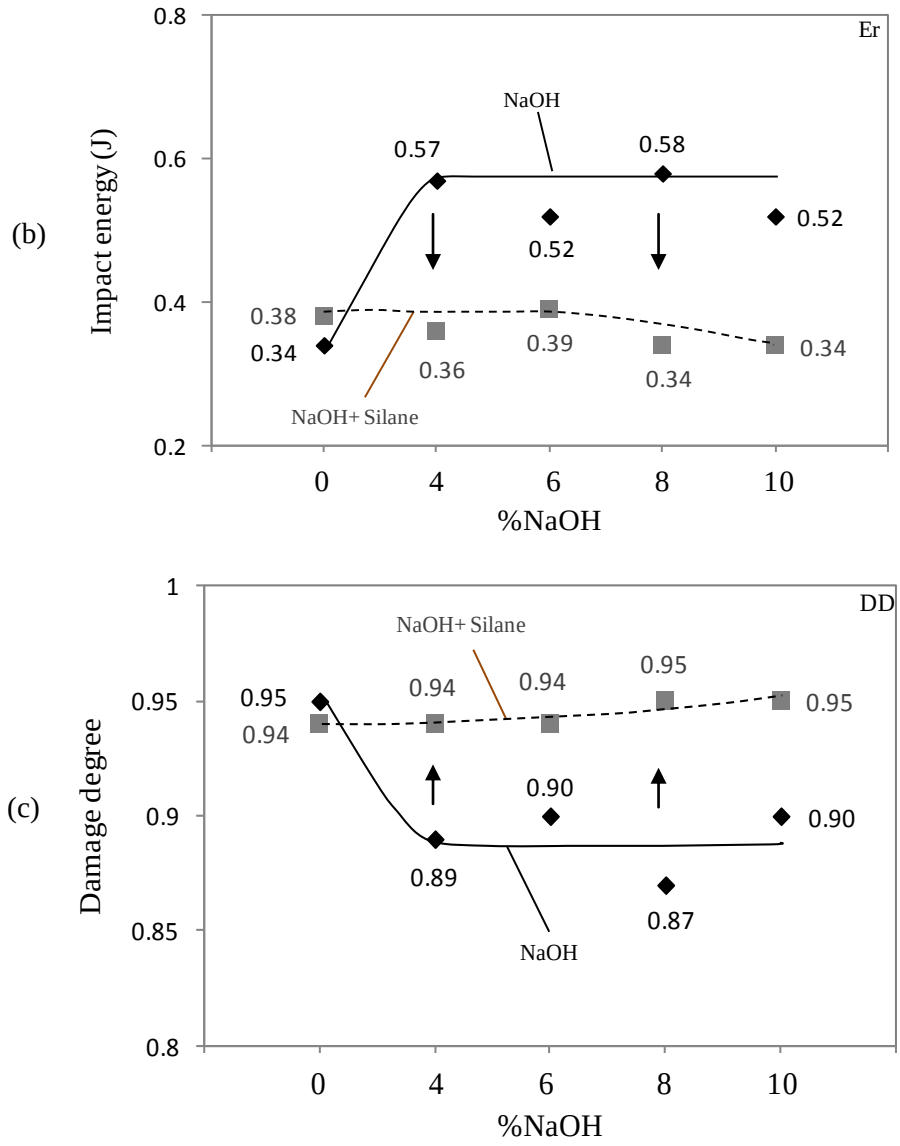

Figure 6.42: Impact properties of alkali pre-treated silanised fibre composites (a) E_a (b) E_r (c) DD

During impact loading, weak interfaces allowed fibre bending and fibres sliding into matrix. Additionally, silane couplings (chemical layer) at the interface also split by impact which imposed additional strains on the matrix. For this, matrix cracking was initiated, which progressively applied higher tensile stresses to the fibres at the bottom face of the specimen and composites eventually failed. Due to this, the impactor could easily penetrate through the samples and produce higher degrees of damage (Figures 6.42b and 6.42c). As a result, composites absorbed large impact

energies (Figure 6.42a) thus reducing the impact resistance properties compared to the NaOH treated samples.

Similar observations were also made for the NaOH pre-treated silanised composites during compressive (Section 6.2.2, Figure 6.14a), shear (Section 6.2.3, Figure 6.24a) and flexure (Section 6.2.4, Figure 6.33a) property analysis. In all these cases, alkali pre-treated silanised composites exhibited lower strengths compared to the NaOH treated samples. These results indicate that the bonding strengths decreased during two treatments conditions and thus reduced the impact properties of the composites.

From the above analysis, it can be stated that alkali treatments on the untreated fibres effectively removed the fibre coverings and thus developed strong interface bonding to resist impact damages of the composites. As a result, the impact resistance properties of the composites were increased, reducing damage propagations. On the other hand, acetyl treatments on the higher concentrations of NaOH pre-treated fibres reduced the fibres' ability to support impact loadings. Due to this, in two treatment conditions, composites exhibited lower impact properties compared to the NaOH treated samples. Similar impact properties were also recorded for alkali pre-treated silanised composites. As alkali pre-treatment removed the hydroxyl groups from the fibre, further silane treatment could not develop silanols to develop strong interface bonding. As a result, composites failed under lower impact resistance compared to the NaOH treated samples.

6.3 Summary

In this study, the effects on the mechanical properties of hemp fibres composites treated by different concentrations of alkali solution (NaOH) and followed by acetyl and silane treatments were analysed. Tension, compression, shear, flexural and impact tests were conducted to categorise their properties. In the experiments, it was found that NaOH could remove the hemicellulose and lignin attached on the surface of the fibres. These components may affect the interfacial bonding strength between the fibre and surrounding matrix.

4-10% NaOH treatments on fibres showed two distinguishable mechanical property features of the composites. 4% NaOH treated composites exhibited lower mechanical properties whereas 6-10% NaOH treatment cases produced higher properties when compared to the untreated fibre composites. The removal of hemicellulose and lignin coverings from the fibre as a result of 4% NaOH treatment was insufficient to promote effective bonding with the matrix. This treatment facilitated hydroxyl groups to react with atmospheric moisture. The existence of moisture at the interface lessened the load carrying capacity of the composites.

6-10% NaOH treated fibres effectively removed hemicellulose and lignin coverings as well as the hydroxyl groups from the fibre. This reaction provided ample accessibility for the matrix to react with the fibre cellulose. Thus, stronger interface boding was achieved, and composites exhibited greater mechanical properties.

These findings were further confirmed as was seen through the mechanical properties achieved in acetyl and silane treated composites. Both treatments facilitated strong

linkages with cellulose within the fibres, in the presence of hydroxyl groups. In both cases, 4% NaOH pre-treated acetylated and silanised composites exhibited greater mechanical properties. This was due to the effective esterification that took place. Silanol formation was also apparent and further produced strong interface bonding. The opposite results were achieved for higher concentrations of NaOH pre-treated cases.

Based on the above discussion, it can be stated that chemical treatments on hemp fibre enhances mechanical properties of their associated composites. Such improvements were achieved due to an absence of hemicellulose and lignin coverings at the fibre-matrix interface.

Chapter 7: Chemical Treatments on Hemp Fibre Sandwich Structures

7.1 Introduction

The mechanical properties of fibre reinforced composites do not only depend on fibre properties, but also on the fibre length and orientation in the polymer matrix. Long unidirectional fibres can uniformly distribute applied load throughout the composite structure, while in the case of short and random fibres the load distribution is discontinued. Additionally, random fibre orientation frequently changes load distribution paths and multidirectional stresses are imposed within a single plane. As a result, randomly oriented short fibre composites involve complex load distributions and their composite properties are relatively lower than that of long unidirectional fibre composites.

In this chapter, the effect of fibre chemical treatments on sandwich structures, particularly mechanical property analyses are outlined. Sandwich structures were used in order to model a complex load distribution between fibre and matrix. A concept of sandwich laminate was utilised in which short randomly oriented hemp fibre composites were used as a core, and long continuous hemp woven fabrics (longitudinal and transverse fibre directions are 0° & 90°) were used as skins. The skins were adhesively bonded onto the core to enable continuous load transfer throughout the sandwich structure. This method allowed for the determination of the effects of treatments on interface bonding strength in a complex distribution load scenario.

The sandwich structures were tested in various loading conditions and their flexural, shear and compressive behaviours were determined under different fibre treatment conditions. The failure modes of the tested samples such as core failure, skin delamination, fibre fracture and fibre-matrix debonding were also examined.

7.2 Result and discussion

7.2.1 Flexural properties of sandwich structures

The effect of chemical treatments on interface bonding between the fibre and matrix is reflected in the flexural properties of the structure. In flexural testing normal loads were applied to specimens. The skin located at the top and bottom planes carried compression and tension respectively, while the core experienced shear. The most common failure modes of sandwich structures under flexural loading are skin compressive/tensile failure, skin delamination, core shear failure and core tensile/compressive failure.

Fibre alkalisation on sandwich structures

Alkali treatments were applied to both short hemp fibres for the core and hemp woven fabrics for the skin.

Figure 7.1 shows the typical flexural stress-strain curves of alkalised sandwich structures, and Table 7.1 provides the summary of their results. The stress-strain curves of the alkalised samples (Figure 7.1) shows linear behaviour until the failure at the maximum stress. At the maximum stress, load dropped due to the tensile failure of the specimen. From Figure 7.2a, 4% NaOH treatments on the 0% NaOH (untreated) fibre reduced composite strength from 47 to 42 MPa, while at higher

treatment concentrations (6-10% NaOH) the strength increased and stabilised at about 60 MPa. Treatments also showed around 26% increase in modulus and 11% increase in failure strain compared to the 4% NaOH treated samples (Figures 7.2b and 7.2c). Higher composite properties indicated that strong bonding was provided through alkalisation of the fibres. Strong interface bonding was achieved due to a lack of hemicellulose and lignin constituents within 6-10% NaOH treated fibres.

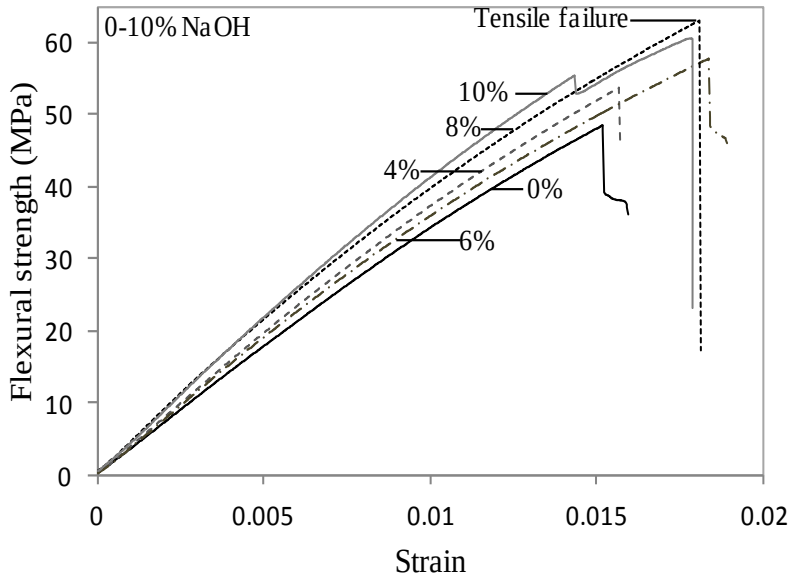

Figure 7.1: Typical flexural stress-strain curves of alkalised sandwich structures

Table 7.1: Flexural properties of the sandwich structures with different fibre treatments

Fibre treatments	Alkalisation			Alkalisation + Acetylation			Alkalisation + Silanisation		
%NaOH	Strength (MPa)	Modulus (GPa)	Failure strain (%)	Strength (MPa)	Modulus (GPa)	Failure strain (%)	Strength (MPa)	Modulus (GPa)	Failure strain (%)
0	47.50 ±1.38	3.44 ±0.21	1.60 ±0.29	44.47 ±2.27	3.74 ±0.25	1.48 ±0.16	49.65 ±3.50	3.14 ±0.45	2.12 ±0.29
4	42.23 ±7.79	3.55 ±0.40	1.59 ±0.26	48.15 ±5.80	3.58 ±0.21	1.51 ±0.23	42.64 ±1.61	3.69 ±0.29	1.41 ±0.11
6	56.84 ±3.45	3.63 ±0.11	1.87 ±0.07	53.00 ±2.46	3.41 ±0.09	1.83 ±0.17	46.69 ±3.26	4.00 ±0.13	1.35 ±0.12
8	59.20 ±3.80	4.47 ±0.14	1.69 ±0.25	54.68 ±1.33	3.93 ±0.10	1.82 ±0.14	52.66 ±4.67	3.40 ±0.54	1.58 ±0.13
10	59.00 ±1.44	4.46 ±0.08	1.76 ±0.01	51.44 ±4.98	3.60 ±0.30	1.71 ±0.09	53.40 ±5.96	3.74 ±0.21	2.16 ±0.23

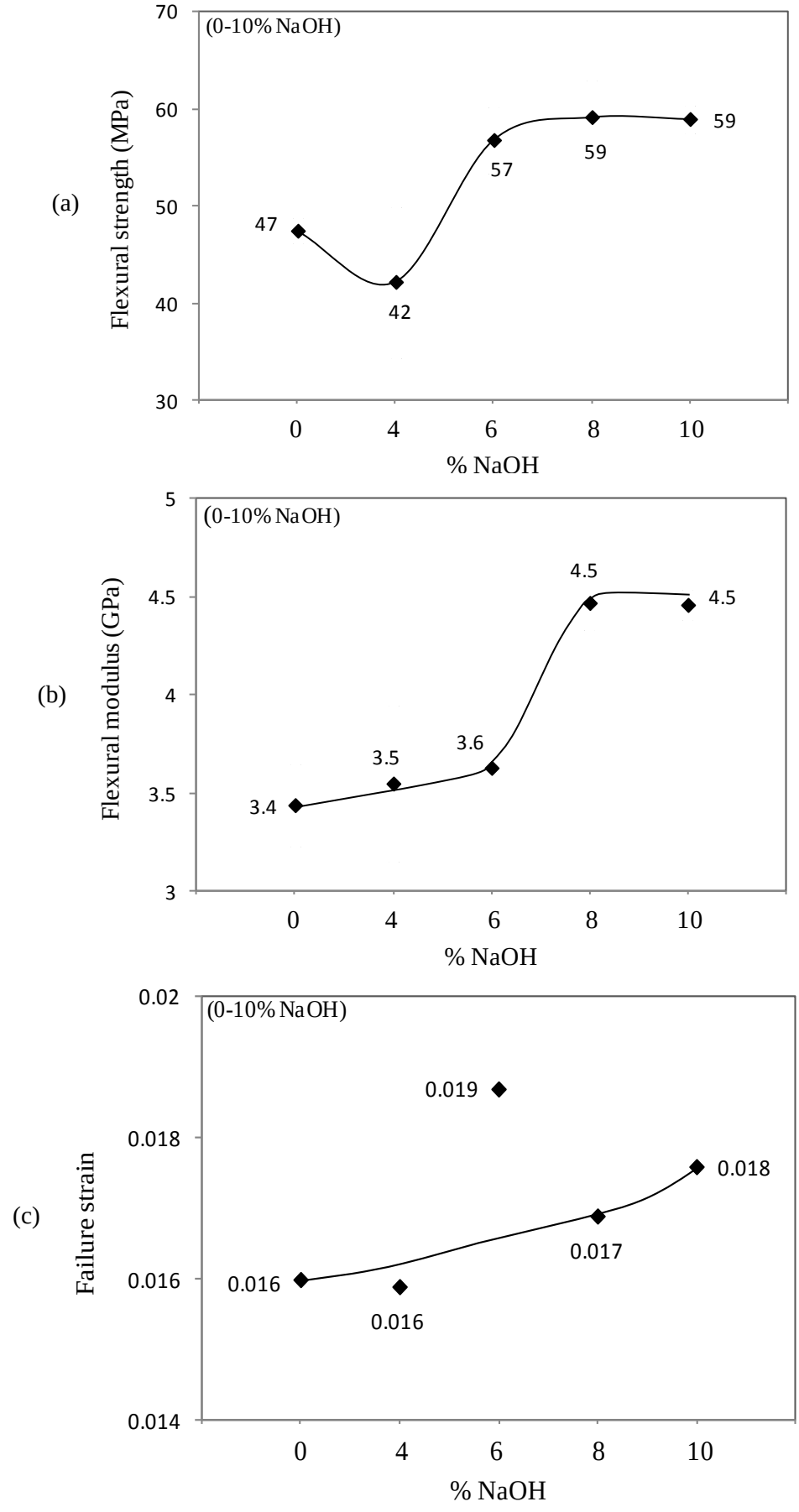

Figure 7.2: Flexural properties of alkalised sandwich structures (a) strength (b) modulus (c) failure strain

Fracture behaviours of the untreated and treated samples are presented in Figure 7.3. Tensile and shear failures of the core, tensile failures of the skin, and delamination of skin from the core took place. Figure 7.3a indicates that the tensile failure of the skin and core took place for untreated samples. For 4% NaOH treated samples, an upper skin delamination was seen (Figure 7.3b). However, for 6-10% NaOH treatment cases, core shear failure was observed (Figure 7.3c). Upper skin delamination indicated that weak bonding had taken place due to the presence of hemicellulose and lignin which were not completely removed from the fibre during 4% NaOH treatment cases. Thus, composites exhibited lower load carrying capacities. Core shear failure indicated that strong bonding had taken place in the 6-10% NaOH treatment cases.

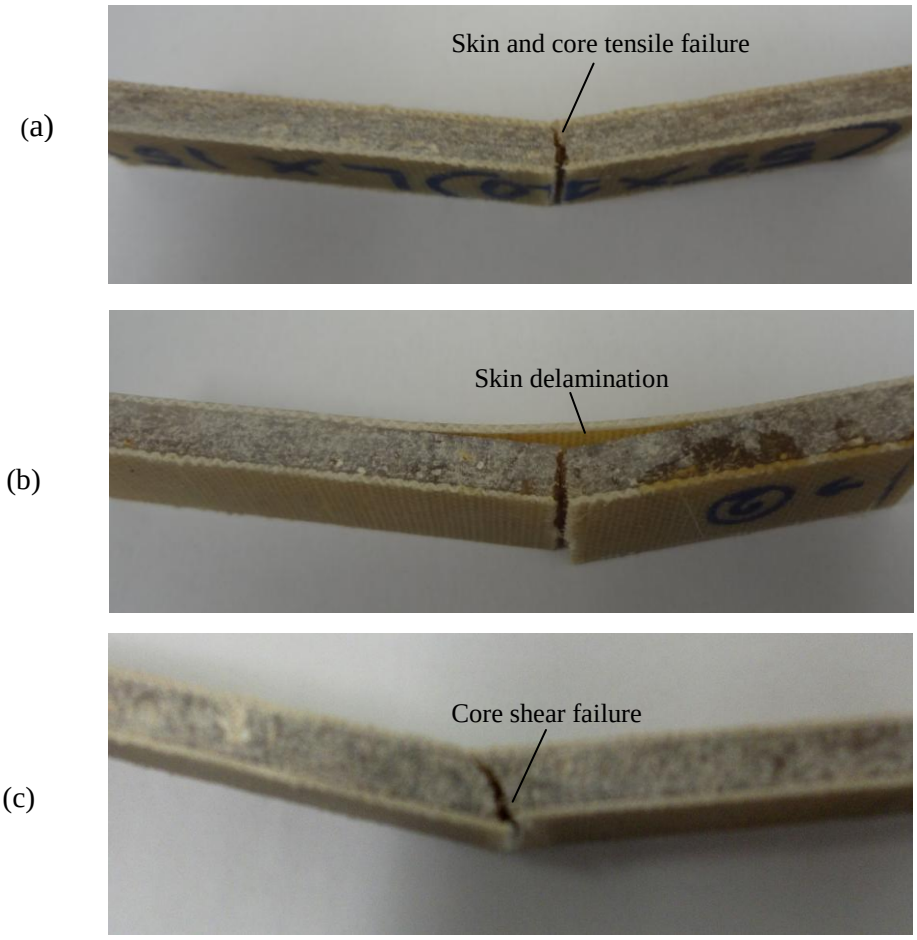

Figure 7.3: Flexural failure modes of (a) untreated (0% NaOH) (b) 4% NaOH (c) 6-10% NaOH treated samples

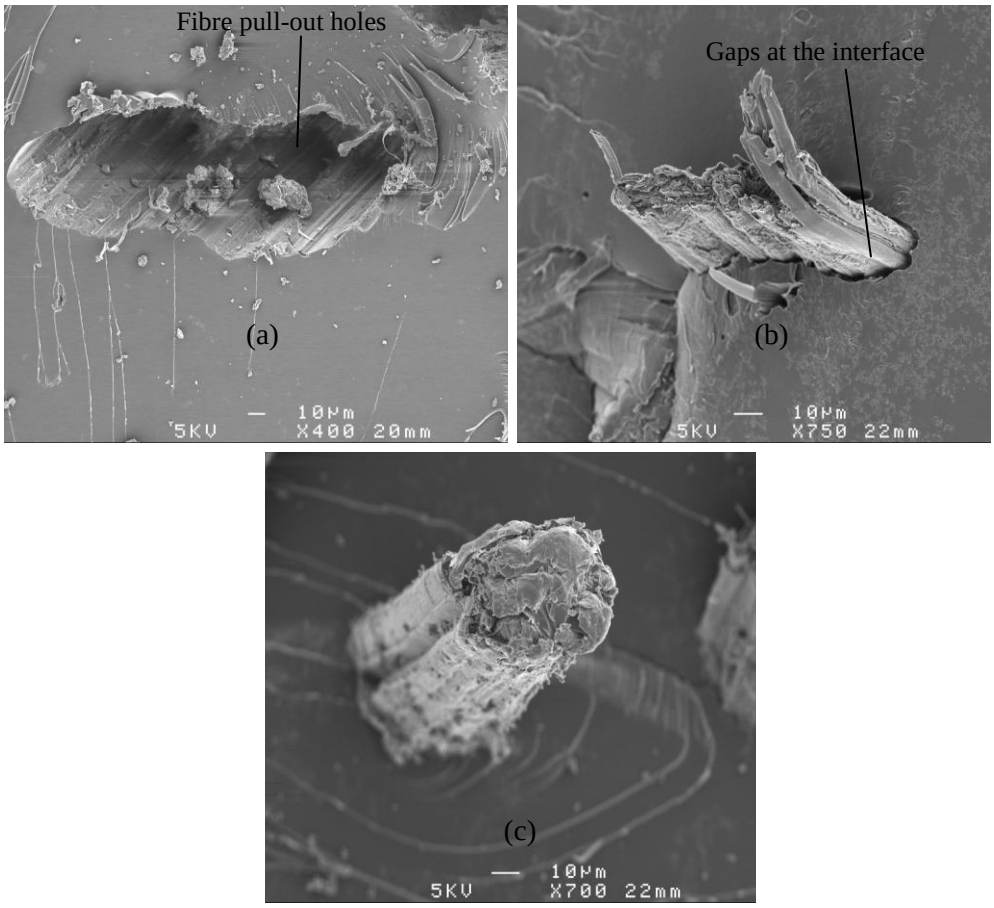

Figure 7.4: Micrographs of flexural failure surface of (a, b) untreated (c) NaOH treated samples

Figure 7.4 shows micrographs of flexural failure surfaces of untreated and alkalised composites (core). It was observed that some holes appeared on the fracture surfaces of the untreated samples and some gaps were present between the fibres and the matrix interfaces. Under the loading condition, fibres were pulled out from the matrix and so low strengths were exhibited. This was presumably due to the presence of hemicellulose and lignin coverings on the fibres surface which hindered the cellulose surfaces' reaction with the matrix. Due to this, weak interface bonding between fibre and matrix took place and the composites suffered with stress being transferred from the matrix to the fibres. This observation was a further indication of

the low strength and modulus values that were achieved under mechanical testing of the untreated samples.

On the other hand, alkali treated fibre composites (core) showed different fracture surfaces from the untreated samples. There were less fibre pull-out holes, and the gap between fibre and matrix was also unnoticeable. This indicated that alkali treatments improved fibre-matrix adhesion. These observations were compatible with the higher mechanical properties of the composites.

Fibre acetylation on sandwich structures

In Figure 7.5, the typical stress-strain curves of alkali pre-treated acetylated sandwich structures show linear elastic behaviour until failure. At the maximum stress, the samples failed in tension. The failure specimens also showed the tensile failure of the lower skin and core (Figure 7.6).

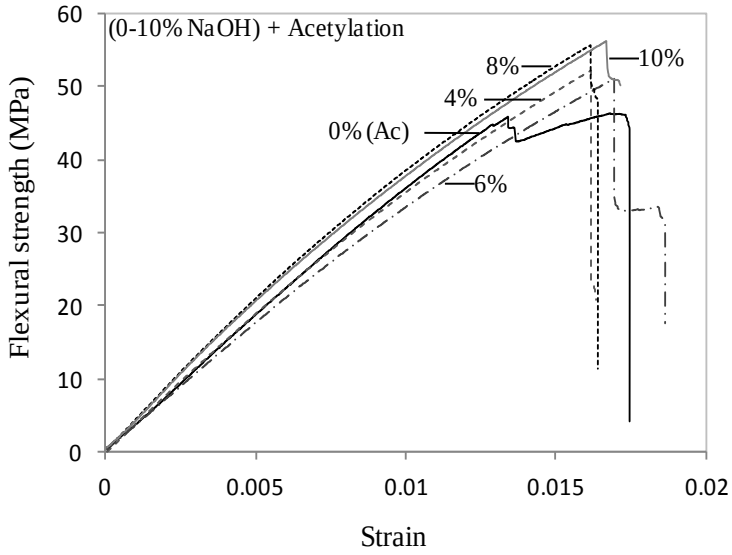

Figure 7.5: Typical flexural stress-strain curves of acetylated sandwich structures

Figure 7.6: Flexural failure modes of acetylated sample

Table 7.1 shows that acetylation on 0% NaOH samples exhibited around 9% higher modulus compared to the untreated samples. This result indicated that acetylation made the composites stiffer. This was due to the removal of weak boundary layers (hemicellulose and lignin) from the untreated fibre surfaces which facilitated strong interface bonding.

From Figure 7.7, it can be observed that acetylation on 4% NaOH pre-treated samples exhibited over 14% higher strength compared to the 4% NaOH treated sample. This result indicates that, acetyl groups could have effectively esterified the hydroxyl groups existing within the pre-treated fibres and facilitated strong fibre-matrix interface bonding.

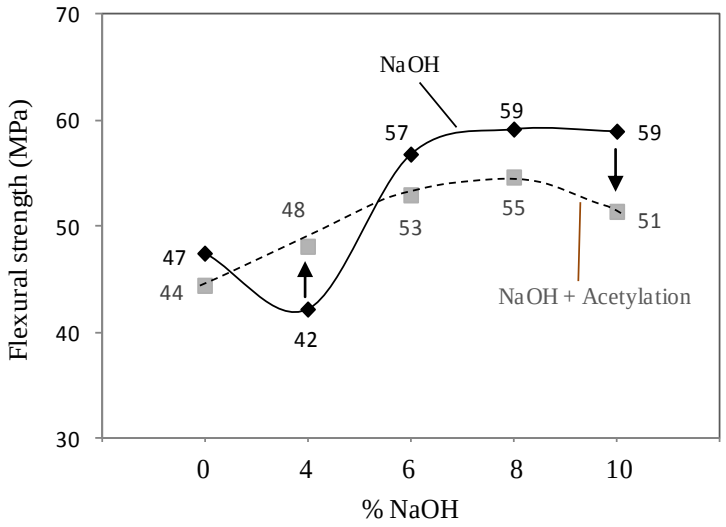

Figure 7.7: Flexural properties of alkali pre-treated acetylated sandwich structures

At higher pre-treatment concentrations (6-10% NaOH), the hydroxyl groups were removed from the fibres. Further acetylation had less hydroxyl groups within the fibre to make effective esterification of fibre. Also, in two treatments fibres strength weakened due to the excessive removal of hemicellulose and lignin constituents from the fibre. Consequently, the load carrying capacity of the composites was reduced which resulted lower in strengths when compared to the original 6-10% NaOH treated samples.

Fibre silanisation on sandwich structures

In Figure 7.8, typical stress-strain curves of silanised samples show linear elastic behaviour up to the maximum stress. After reaching the peak strength, multiple stages of strength drops were observed with progressive strain. After the load drop, the specimen continued to sustain the load as only the sandwich skins were still carrying the load. The strength drops indicated that gradual failures had taken place in the samples. At peak strength, cores failed in tension and upper skins delaminated. This was followed by tensile failure of the bottom skins (Figure 7.9). Stages of failure of the treated samples indicated good interface bonding had taken place between the fibre and matrix. However, the gradual load drops reduced the composites' overall strength compared to the NaOH treated samples (Figure 7.10).

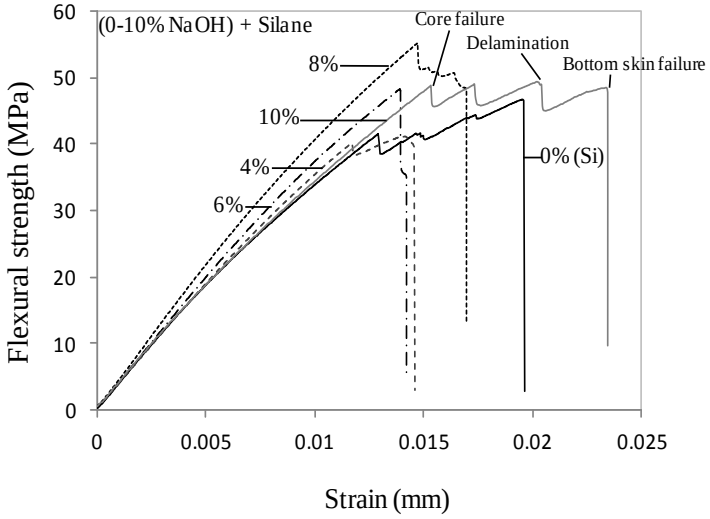

Figure 7.8: Typical flexural stress-strain curves of silanised sandwich structures

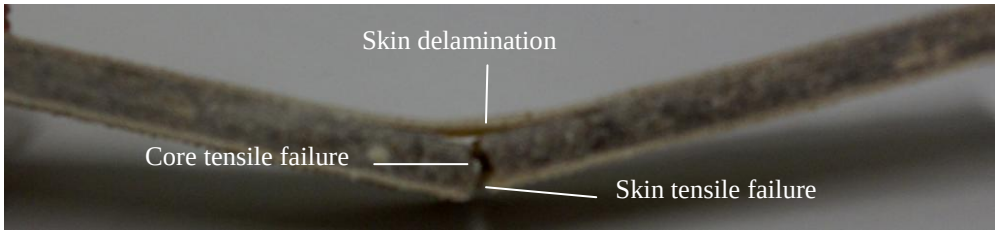

Figure 7.9: Flexural failure modes of silanised sample

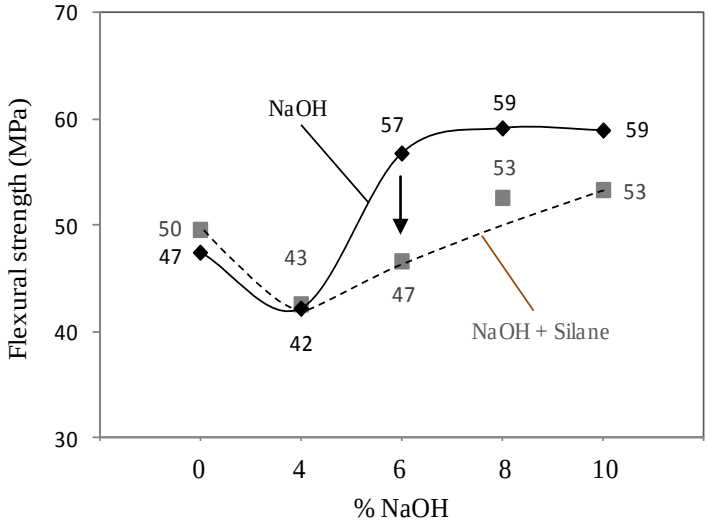

Figure 7.10: Flexural properties of alkali pre-treated silanised sandwich structures

7.2.2 Shear properties of sandwich structures

The most common test method to determine the shear properties of sandwich structures is the four-point bending test. The test method outlined is in Chapter 3, Section 3.6.4. The experimental results of the four-point bending test are discussed in relation to stress-strain curve and the failure mode of the structures.

Fibre alkalisation on sandwich structures

The typical stress-strain curves of alkalised specimens show a strength drop taking place before reaching peak strength (Figure 7.11). This strength drop indicates crack initiation at the specimen core. Then the specimen continued to carry load until the core failed in tension. Afterwards, a significant load drop was observed due to the tensile failure of the bottom skin of the specimens.

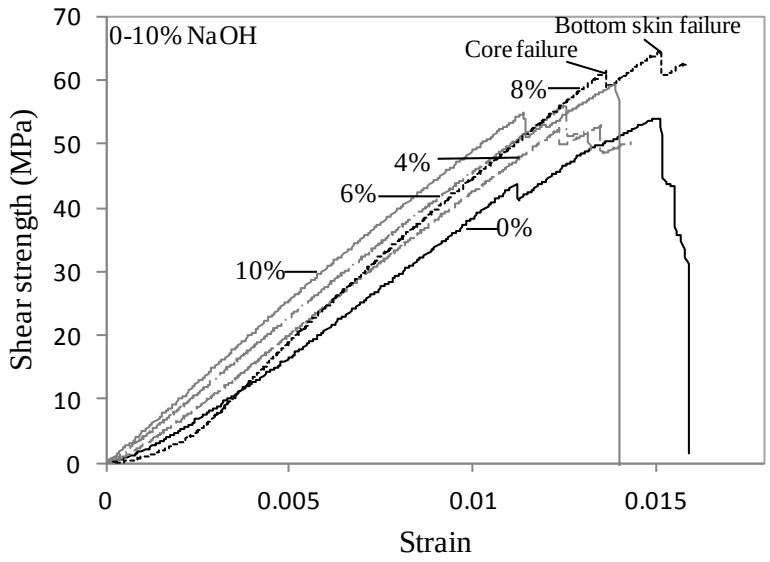

Figure 7.11: Typical shear stress-strain curves of alkalised sandwich structures

Table 7.2: Shear properties of the sandwich structure with different fibre treatments

Fibre treatments	Alkalisation			Alkalisation + Acetylation			Alkalisation + Silanisation		
%NaOH	Strength (MPa)	Modulus (GPa)	Failure strain (%)	Strength (MPa)	Modulus (GPa)	Failure strain (%)	Strength (MPa)	Modulus (GPa)	Failure strain (%)
0	56.59 ±2.81	4.52 ±0.30	1.51 ±0.11	44.78 ±2.51	3.88 ±0.34	1.60 ±0.12	57.27 ±3.28	3.77 ±0.18	1.96 ±0.16
4	52.11 ±2.47	4.30 ±0.07	1.34 ±0.05	43.85 ±2.60	3.69 ±0.18	1.42 ±0.04	42.94 ±3.21	3.62 ±0.24	1.61 ±0.22
6	55.87 ±3.33	4.56 ±0.03	1.37 ±0.11	46.86 ±2.33	3.93 ±0.23	1.32 ±0.02	48.56 ±2.93	3.77 ±0.21	1.55 ±0.13
8	64.58 ±0.77	5.10 ±0.21	1.67 ±0.13	59.67 ±3.10	4.17 ±0.06	1.64 ±0.10	47.31 ±5.09	3.75 ±0.31	1.68 ±0.31
10	68.61 ±5.90	4.94 ±0.17	1.91 ±0.16	53.50 ±4.64	3.97 ±0.19	1.47 ±0.14	52.72 ±4.56	3.67 ±0.40	1.92 ±0.42

In Figure 7.12, it can be observed that initial 4% NaOH treatments on the fibres reduced the composites' shear strengths and moduli compared to the 0% NaOH (untreated) samples. However, at higher treatment concentrations (6-10%NaOH) the strength and modulus increased by 21% and 11% respectively compared to the untreated samples. These results indicated that higher NaOH concentrations excited the cellulose surface by removing weak boundary layers (hemicellulose-lignin) from the fibre surfaces. Due to this, strong bonding at the interface was achieved and composites' exhibited stronger mechanical properties.

(a)

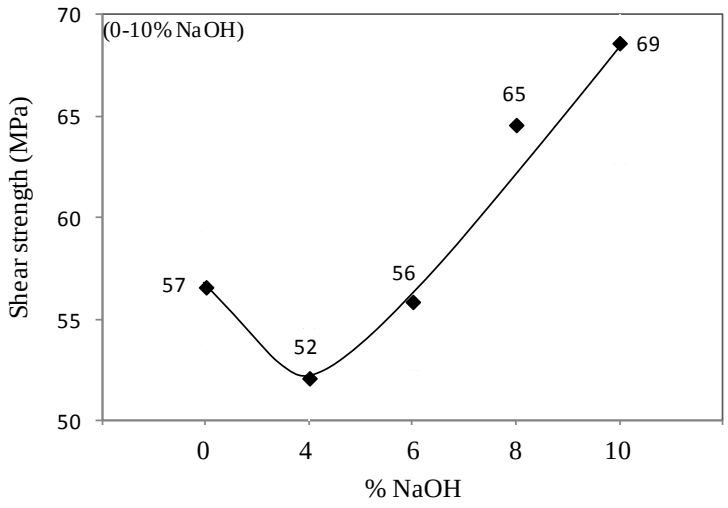

(b)

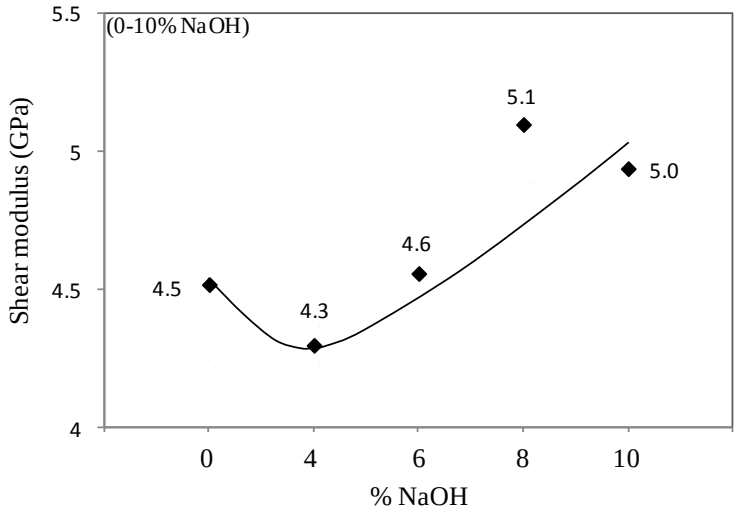

Figure 7.12: Shear properties of alkalised sandwich structures (a) strength (b) modulus

From Figure 7.13, it can be seen that 4% NaOH treated samples exhibited tensile failure of the core followed by debonding between the bottom skin and the core at the end of the specimen. For 6-10% NaOH treated samples, core failure in shear and tension and bottom skin failure in tension was observed. In this case, the delamination between the skins and cores was not observed proving that strong interface bonding was achieved at higher concentrations of NaOH treatments.

(a)

(b)

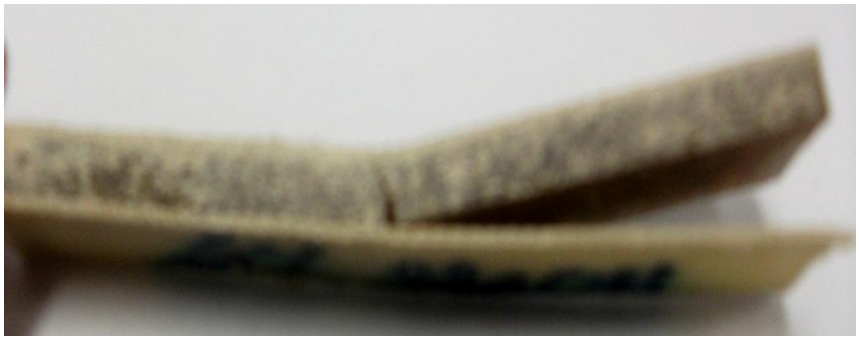

(c)

Figure 7.13: Shear failure modes of (a) 0% NaOH (b) 4% NaOH (c) 6-10% NaOH treated samples

Fibre acetylation on sandwich structures

Acetylated composites showed the tensile failures of the cores and bottom skins and delamination of upper skins from the core (Figure 7.14). Delamination reduced the composites' load carrying capacities as there was no stress transfer between the skins and cores. The stress and modulus associated with alkali pre-treated acetylated samples also exhibited lower values compared to the NaOH treated samples (Table 7.2).

Figure 7.14: Shear failure modes of acetylated sample

Fibre silanisation on sandwich structures

The typical stress-strain curves (Figure 7.15) of silanised samples exhibited several stages of strength drops before the peak strength. Accordingly, Figure 7.16 shows that the failure strain of alkali pre-treated silanised samples were higher compared to

the NaOH treated samples. Stronger properties resulted because silane coupling layers on the fibre surfaces were gradually broken down during loading. This provided shear resistance at the interface. Shear resistance allowed the longer deformation of the composites and thus enhanced the failure strain properties.

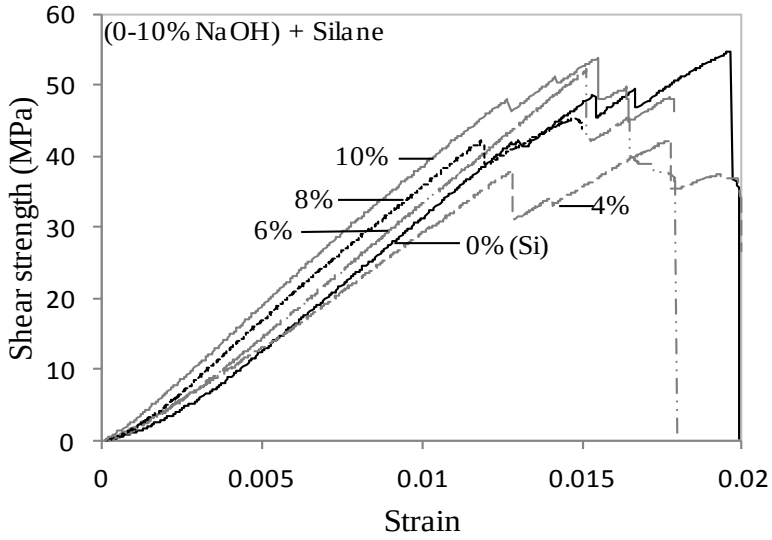

Figure 7.15: Typical shear stress-strain curves of silanised sandwich structures

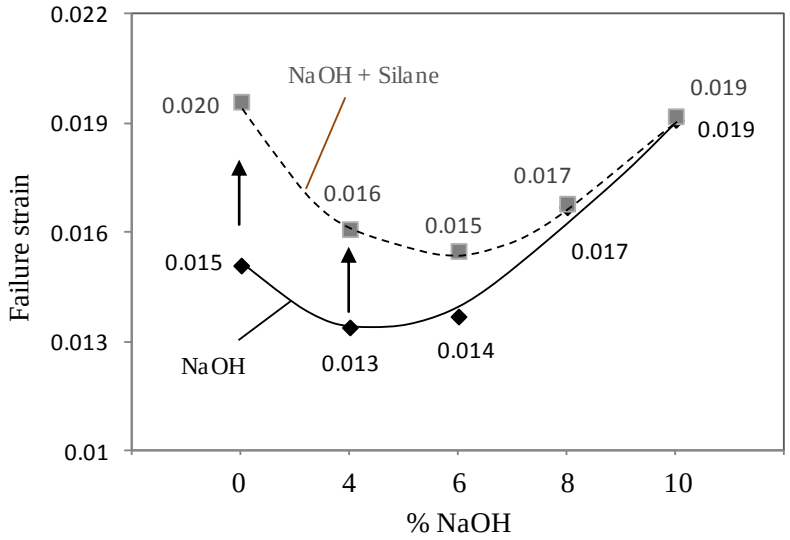

Figure 7.16: Shear properties of alkali pre-treated silanised sandwich structures

7.2.3 Compressive properties of sandwich structures

The compressive properties of sandwich structures can be measured through edgewise compression testing. The test methods are outlined in Chapter 3, Section 3.6.2. During compression testing, the applied load is mainly carried by the skins of the sandwich, whereas the core stabilises the structure and prohibits premature buckling of the skin. The compressive response (in-plane direction) of the sandwich structures depends on the degree of interface bonding strength. To analyse the compressive properties of the sandwich composites, stress-strain responses and failure mechanisms of the samples were investigated.

Fibre alkalisation on sandwich structures

Figure 7.17 shows the typical stress-strain behaviour of alkalised fibre composites, and Table 7.3 summarises their results. From Figure 7.18, it can be observed that NaOH treatments on the fibres improved composite strength and modulus compared to untreated samples. According to higher treatment concentrations (4-10% NaOH), the strength and modulus of the composites registered increases of around 23% and 16% respectively compared to the untreated samples. These results indicated that treatments contributed to strong interface bonding by removing weak boundary layers from the fibre surfaces.

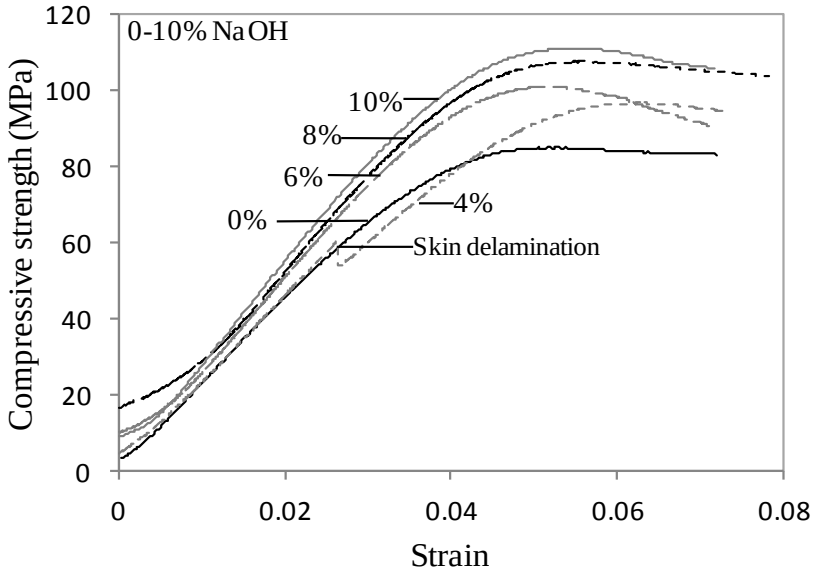

Figure 7.17: Typical compressive stress-strain curves of alkalised sandwich structures

Table 7.3: Compressive properties of the sandwich structure with different fibre treatments

Fibre treatments	Alkalisation		Alkalisation + Acetylation		Alkalisation + Silanisation	
%NaOH	Strength (MPa)	Modulus (GPa)	Strength (MPa)	Modulus (GPa)	Strength (MPa)	Modulus (GPa)
0	89.95 ±10.65	2.28 ±0.17	90.16 ±6.59	2.60 ±0.12	90.46 ±6.99	2.52 ±0.18
4	98.49 ±1.74	2.33 ±0.14	96.59 ±3.78	2.67 ±0.06	88.53 ±3.77	2.35 ±0.17
6	101.60 ±9.44	2.60 ±0.11	97.97 ±1.92	2.62 ±0.05	97.71 ±5.52	2.57 ±0.06
8	107.64 ±2.40	2.43 ±0.15	85.76 ±3.47	2.39 ±0.17	93.71 ±4.30	2.58 ±0.19
10	111.04 ±3.86	2.65 ±0.06	95.59 ±2.44	2.65 ±0.04	82.16 ±1.80	2.29 ±0.11

(a)

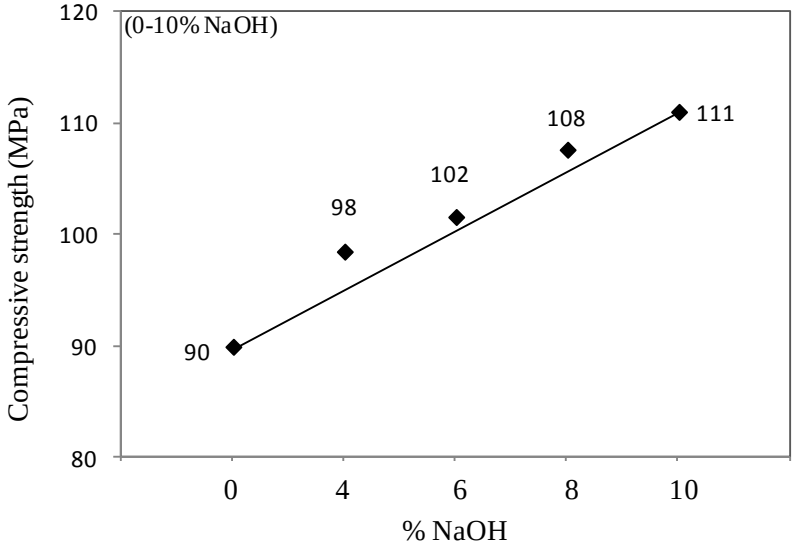

(b)

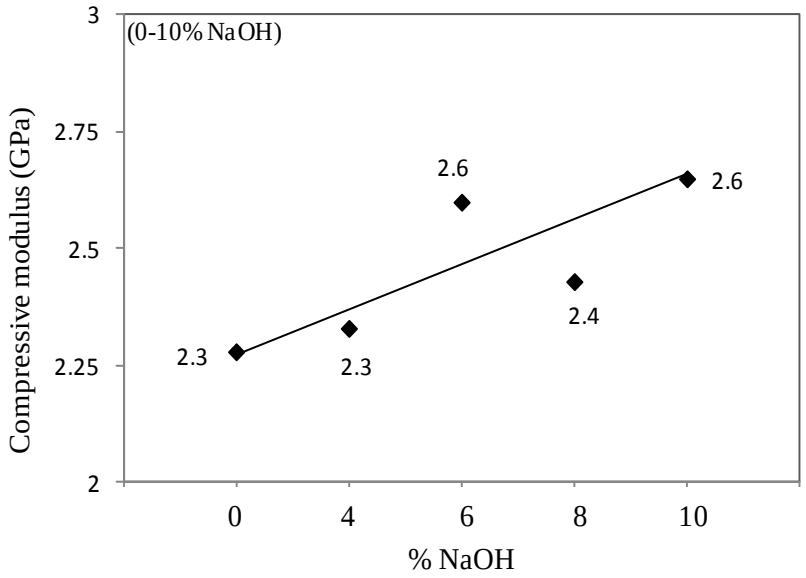

Figure 7.18: Compressive properties of alkalised sandwich structures (a) strength (b) modulus

From Figure 7.19, it can be seen that core crushing in untreated samples was evident which indicated poor interface bonding. Skin delamination was observed for 4% NaOH treated samples while shear crimping with no skin delamination was evident for 6-10% NaOH treated samples. In addition, from stress-strain curves (Figure 7.17), a strength drop was observed at 0.026 strain for 4% NaOH treated samples. This indicated skin delaminations of the core. Conversely, for other samples, such strength drops were not appeared. These results again prove that higher (6-10%) NaOH concentrations contributed to the strong interface bonding and thus the composite exhibited higher compression properties.

(a) (b) (c)

Figure 7.19: Compression failure mode of (a) 0% NaOH (b) 4% NaOH (c) 6-10% NaOH treated samples

Fibre acetylation on sandwich structures

From the stress-strain curves in Figure 7.20 it can be observed that, at peak stress, a small load drop has taken place due to the skin delamination from the core. Afterwards, the core is carrying the compressive load and the curves exhibits ductile deformations. Figure 7.21 also shows the skin delaminations followed by the core shear crimping.

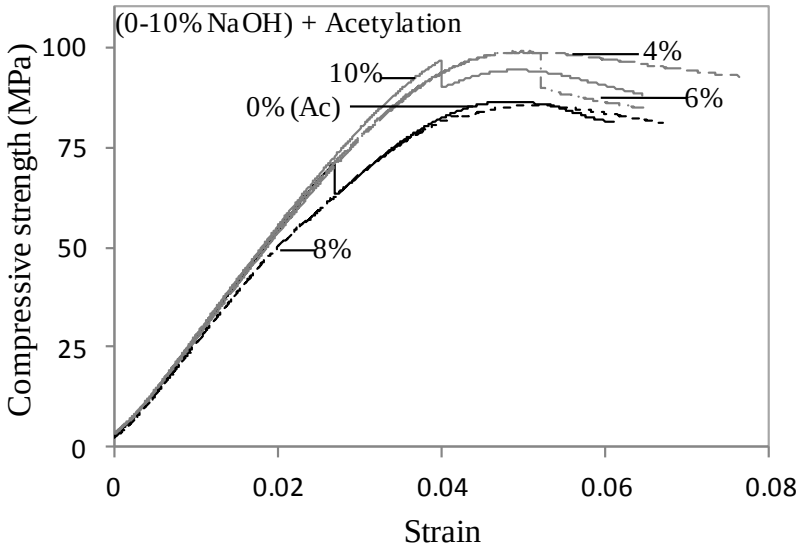

Figure 7.20: Typical compressive stress-strain curves of acetylated sandwich structures

Figure 7.21: Compressive failure mode of acetylated sample

From Figure 7.22, it can be seen that acetyl treatments on the 0-4% NaOH treated fibres increases composite modulus around 14%. However, acetylation on higher

concentrations of (6-10%) NaOH treated fibres does not improve modulus values. These results indicated that strong interface bonding was taking place due to effective estrification of fibre hydroxyl groups as well as the removal of hemicellulose and lignin coverings from the (0-4% NaOH) pre-treated fibre surfaces during acetylation. As a result, the strong interface could transfer greater compression load and thus treated samples exhibited higher composite properties. However, due to the fibre weakness induced by the two treatments (at higher concentrations of NaOH and acetylation), composites deform under lower compressive loads. As a result, at higher pre-treatment concentrations, acetylated composites had lower modulus than the NaOH treated samples.

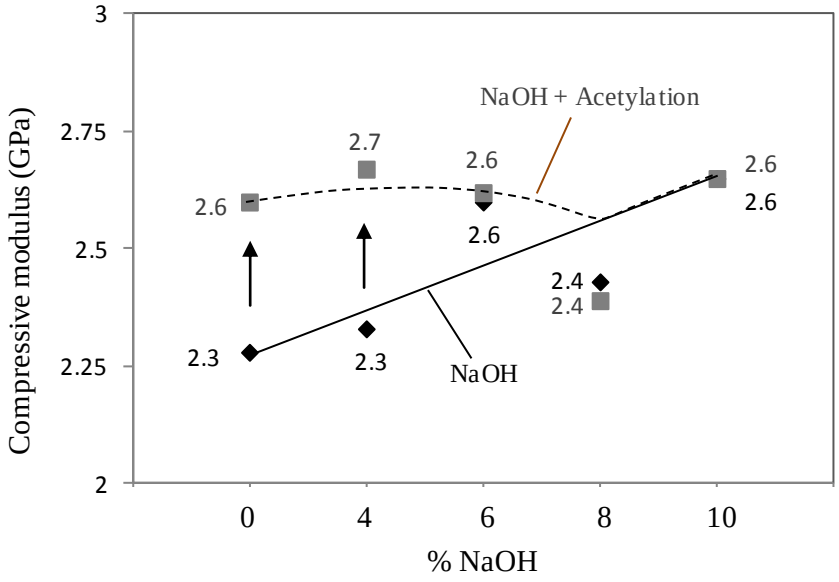

Figure 7.22: Compressive properties of alkali pre-treated acetylated sandwich structures

Fibre silanisation on sandwich structures

Similar to acetylated samples, the stress-strain curves of alkali pre-treated silanised samples also showed load drops at the peak strength (Figure 7.23) and the skin delamination from the core (Figure 7.24).

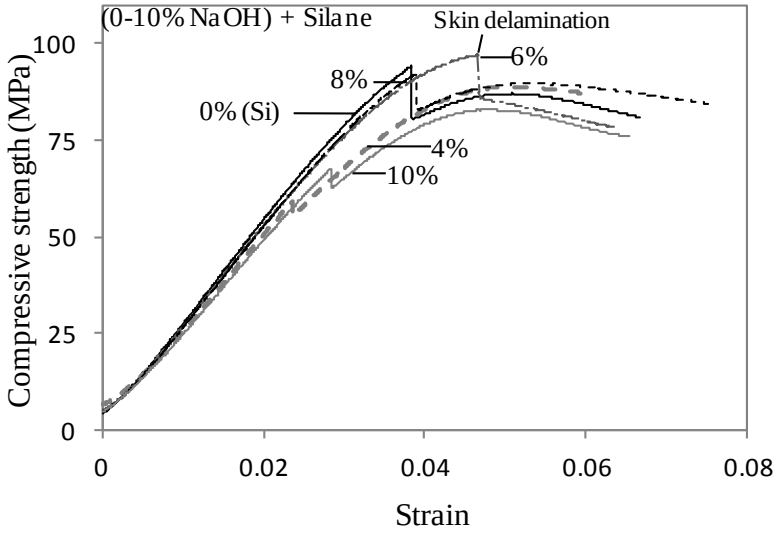

Figure 7.23: Typical compressive stress-strain curves of silanised sandwich structures

Figure 7.24: Compressive failure mode of silanised sample

From Figure 7.25, it can be observed that silane treatments on the alkalised fibres reduced composite strengths compared to the NaOH treated samples. This may be due to the fact that silane couplings formed an additional chemical layer onto the fibre surface. During compression loading, fibre buckling generated strains onto the neighbouring fibres. At this stage, the chemical layers on the fibres produced extra strains onto the neighbouring fibres. This additional strain disproportionately induced higher stresses among the buckled fibre interfaces and thus failure of the composites

was initiated. Due to this, silanised composites deformed under lower compressive loads compared to the NaOH treated samples.

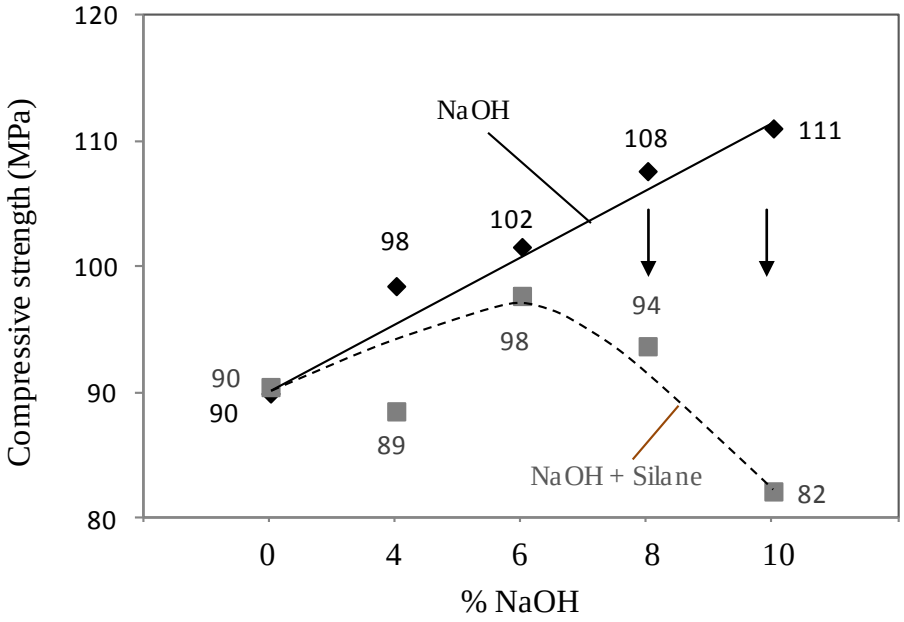

Figure 7.25: Compressive properties of alkali pre-treated silanised sandwich structures

It can be noted that, silane treatment on the 10% NaOH treated fibres suffered maximum strength losses (26%) compared to the NaOH treated samples (Figure 7.25). This may be due to the fact that 10% NaOH pre-treated fibre lost their structural strength in carrying extra bucking strains generated from the silane chemical layers. As a result, silane treatments on the 10% NaOH treated fibres exhibited lower composite strengths.

7.3 Summary

In this study it was observed that the mechanical properties of hemp fibre sandwich structures were highly influenced by their interface bonding strength. Chemically treated fibre samples showed improved fibre matrix adhesion properties when compared to the untreated samples. According to the results, higher concentrations of NaOH treated samples exhibited stronger mechanical properties when compared to

other treated (acetyl and silane treatments) samples. This may have been due to the effective removal of hemicellulose and lignin constituents from the fibres which contributed to stronger fibre-matrix interface bonding. Different failure modes of the tested samples were observed. Skin delamination from the core reduced the overall composite properties. This failure event was less observed at higher concentrations of NaOH treated samples. This was further evidence that the removal of hemicellulose and lignin constituents from the fibres after treatment provided stronger interface adhesion properties.

Chapter 8: Conclusion and Proposals for Future Work

From this study, a greater understanding of the effects of chemical treatments on natural fibres and their composite properties were achieved.

Effects of chemical treatments on fibre

Hemp fibre properties were found to be highly influenced by changes in the amounts of cellulose, hemicellulose and lignin constituents within the fibre. Alkali (0-10% NaOH), acetyl and silane treatments on fibres reacted with constituent contents by varying their amounts. Chemical analysis revealed that, 4-10% NaOH solution reduced hemicellulose and lignin amounts compared to untreated fibres. Further acetyl treatments on alkalised fibres created more losses of lignin constituents. Conversely, silane treatments formed couplings with fibre constituents, thereby forming a chemical layer on the fibre. This effect increased the overall weight percentages of fibre constituents.

An analysis of fibre surface morphology revealed that cellulose provided the main structural basis for the fibre and had the cleanest surface appearances, whilst hemicellulose and lignin had black in colour and gummy in appearances and adhered onto the cellulose surface. The prevalence of fibre constituents was observed on the untreated fibre surfaces. Alkalised and acetylated fibre surfaces exhibited clean distinctive microfibril separation. Alternatively, silanised fibre surfaces exhibited a visible chemical layer.

FTIR analysis proved that hemicellulose and lignin functional groups were not present on the alkalised and acetylated fibres. TGA and DSC analyses revealed that moisture absorption by the fibre was primarily caused due to the presence of hemicelluloses. Hemicelluloses also exhibited lower thermal stability compared to cellulose and lignin constituents. Cellulose showed higher decomposition temperatures compared to lignin, and lignin decomposed over a broad temperature range. Treated fibres showed higher thermal decomposition temperatures compared to the untreated fibres.

Tensile tests on hemp fibres revealed higher strength when fibre cross-sections were considered as diameter instead of fibre width along their lengths. Tensile properties of hemp fibres were reduced by the action of (4-10%) NaOH treatments. Cellulose microfibrils became weaker in tension due to the removal of their binder materials (hemicellulose and lignin) as a result of treatment. Acetyl treatments on the alkalised fibres lessened their strength values. However, silane couplings provided support to the cellulose microfibrils against tensile deformation and thus silanised samples exhibited higher failure strain properties.

Effects of chemical treatments on composites

Chemical treatments lowered fibre strength but the removal of hemicellulose and lignin coverings allowed for the direct bonding between cellulose microfibrils and the polyester matrix. The treatment effects on interface bonding in long unidirectional hemp fibre polyester composites were characterised by performing property analysis through tensile, compression, shear, flexural and impact tests.

Mechanical testing revealed that interface bonding between NaOH treated fibres and the polyester matrix increased due to an absence of hemicelluloses and lignin coverings on cellulose surfaces. This caused the absence of the majority of fibre hydroxyl groups (-OH). In the case of 4% NaOH concentrations, hemicellulose and lignin coverings were present on the cellulose surface and their orientations allowed hydroxyl groups to absorb atmospheric moisture. The presence of moisture at the interface resulted in a very weak load transfer capacity of fibres and thus their composites had poor properties compared to the untreated samples. However, this tendency was not observed for samples under higher concentrations (6 – 10%) of NaOH treatment. Stronger interfacial bonding strength promoted better stress transfer between fibres and matrix, and thus, higher mechanical strength was exhibited. As hemicellulose and lignin coverings were removed under a higher concentration of NaOH treatment, the strength of the fibres was lower as compared with an untreated fibre case.

For acetyl treatments on NaOH (up to 4%) treated fibre, the mechanical properties of composites increased. This was due to the fact that acetylation effectively esterifed OH groups on the NaOH treated fibre's surface. However, by applying higher concentration acetyl treatment, properties of the fibre were weakened.

Silane treatments on NaOH (up to 4%) treated fibre achieved similar mechanical results to acetyl treatment. The mechanical strengths of composites increased due to a successful formation of silanols on the fibre's surface. These silanols promoted strong couplings between the fibre surfaces and matrix. However, the results were reversed for fibres treated with over 6% concentration of NaOH pre-treatment.

Similar mechanical properties were observed for sandwich structures. Different failure modes of the tested samples revealed that core failure and skin delamination from the core reduced the overall composite properties. These failure events were unnoticeable at higher concentrations of NaOH treated samples. The microstructure of the composites failure surface also showed improved fibre-matrix interfacial bonding for the treated composites. These micrographs confirmed the results achieved by composite mechanical properties.

Based on the discussions above, it can be concluded that chemical treatments on hemp fibres can enhance the mechanical strength of its composites. Improvements are governed by the removal of hemicellulose and lignin from the fibre, which provides a platform for better chemical reactions between fibres and matrix. However, due to the removal of these two components, the fibre itself, becomes relatively weak and cannot withstand higher loads when compared with untreated cases.

Proposals for future work

The following aspects need to be further studied in more detail to further improve the properties of hemp fibres and their roles as reinforcements in polyester composites. Some recommendations for future work have been proposed:

- Environmental degradation behaviours of hemp fibre polyester composites need to be studied through outdoor weathering tests in order to analyse the properties of such structures. The effect of environment factors on interface bonding strength need to be understood through mechanical property analysis. Such environmental factors include moisture resistance, UV index and

sunlight. The thermal and mechanical properties of fibre composites need to be investigated after they have been periodically exposed to natural weathering. The treatment effects on fibre matrix interface bonding on natural weathering condition also need to be analysed in order to gain greater understanding of natural fibre composite structures.

- In order to achieve a greater understanding of interface bonding strength in treated fibre composites, dynamic mechanical testing through fatigue and delamination analysis need to be conducted. Through dynamic loadings, treatment effects on interface bonding can be investigated in more detail. By conducting such dynamic mechanical testing, the fatigue life of fibre reinforced polymer composites can be observed. This process would ultimately reveal further mechanical properties of nature fibre composites.

- Theoretical modelling of hemp fibre polyester composites need to be established using the results observed from this study. The model will help in the analysis of treatment effects on fibre matrix interface bonding and composite failure mode analysis. Moreover, this modelling process would be beneficial in analysing parameters which can be used to improve and optimise fibre properties and their associated roles as reinforcements in composite materials.

- Some systematic statistical analyses on the mechanical property results of fibre and their reinforced composites need to be carried out. These analyses will

provide the statically prove the mechanical property improvement of fibres and their reinforced composites under different treatment conditions.

References

Abdelmouleh, M, Boufi, S, Belgacem, M & Dufresne, A 2007, 'Short natural-fibre reinforced polyethylene and natural rubber composites: Effect of silane coupling agents and fibres loading', *Composites science and technology*, vol. 67, no. 7, pp. 1627-39.

Adekunle, K, Akesson, D & Skrifvars, M 2010, 'Biobased composites prepared by compression molding with a novel thermoset resin from soybean oil and a natural-fiber reinforcement', *Journal of Applied Polymer Science*, vol. 116, no. 3, pp. 1759-65.

Adusumalli, RB, Muller, U, Weber, H, Roeder, T, Sixta, H & Gindl, W 2006, 'Tensile testing of single regenerated cellulose fibres', Wiley Online Library, pp. 83-8.

Azzam, H 2007, 'Compressive properties of stretch-broken carbon fiber (SBCF)/polyamide 12 commingled unidirectional composites', *Journal of Engineering and Applied Science*, vol. 54, no. 4, p. 409.

Ball, R, McIntosh, A & Brindley, J 2004, 'Feedback processes in cellulose thermal decomposition: implications for fire-retarding strategies and treatments', *Combustion Theory and Modelling*, vol. 8, no. 2, pp. 281-91.

Beckermann, G 2007, 'Performance of hemp-fibre reinforced polypropylene composite materials', PhD thesis, The University of Waikato.

Beckermann, G & Pickering, KL 2008, 'Engineering and evaluation of hemp fibre reinforced polypropylene composites: Fibre treatment and matrix modification', *Composites Part A: Applied Science and Manufacturing*, vol. 39, no. 6, pp. 979-88.

Belingardi, G, Cavatorta, MP & Salvatore Paolino, D 2008, 'Repeated impact response of hand lay-up and vacuum infusion thick glass reinforced laminates', *International Journal of Impact Engineering*, vol. 35, no. 7, pp. 609-19.

Bjerre, AB, Schmidt, AS & Riso, F 1997, *Development of chemical and biological processes for production of bioethanol: Optimization of the wet oxidation process and characterization of products*, Riso National Laboratory.

Bledzki, A & Gassan, J 1999, 'Composites reinforced with cellulose based fibres', *Progress in polymer science*, vol. 24, no. 2, pp. 221-74.

Bledzki, A, Mamun, A, Lucka, M & Gutowsk, V 2008, 'The effects of acetylation on properties of flax fibre and its polypropylene composites', *eXPRESS Polymer Letters*, vol. 2, no. 6, pp. 413-22.

Bradley, L, Bowen, C, McEnaney, B & Johnson, D 2007, 'Shear properties of a carbon/carbon composite with non-woven felt and continuous fibre reinforcement layers', *Carbon*, vol. 45, no. 11, pp. 2178-87.

Brebu, M & Vasile, C 2010, 'Thermal degradation of lignin—A review', *Cellulose Chemistry & Technology*, vol. 44, no. 9, p. 353.

Chattopadhyay, H & Sarkar, P 1945, 'A new method for the estimation of cellulose', Dacca University.

Cho, J, Chen, J & Daniel, I 2007, 'Mechanical enhancement of carbon fiber/epoxy composites by graphite nanoplatelet reinforcement', *Scripta Materialia*, vol. 56, no. 8, pp. 685-8.

Cicala, G & Lo Faro, C 2012, 'Material Selection: Polymeric Composites Matrix', in *Wiley Encyclopedia of Composites*, John Wiley & Sons, Inc.

Corrales, F, Vilaseca, F, Llop, M, Gironcs, J, Mendez, J & Mutjc, P 2007, 'Chemical modification of jute fibers for the production of green-composites', *Journal of hazardous materials*, vol. 144, no. 3, pp. 730-5.

Dash, BN, Rana, AK, Mishra, SC, Mishra, HK, Nayak, S & Tripathy, S 2000, 'Novel low-cost jute–polyester composite. II. SEM observation of the fractured surfaces', *Polymer-Plastics Technology and Engineering*, vol. 39, no. 2, pp. 333-50, viewed 2012/06/27.

David-West, O, Nash, D & Banks, W 2008, 'An experimental study of damage accumulation in balanced CFRP laminates due to repeated impact', *Composite Structures*, vol. 83, no. 3, pp. 247-58.

Delaet, M, Lataillade, J & Wolff, C 1994, 'Intralaminar shear loading effects on the damage process of multiply composites at impact rates', *Journal de Physique*, vol. 4, no. 4, pp. 213-8.

Delfosse, D & Poursartip, A 1997, 'Energy-based approach to impact damage in CFRP laminates', *Composites Part A: Applied Science and Manufacturing*, vol. 28, no. 7, pp. 647-55.

Devi, LU, Bhagawan, S & Thomas, S 1997, 'Mechanical properties of pineapple leaf fiber-reinforced polyester composites', *Journal of Applied Polymer Science*, vol. 64, no. 9, pp. 1739-48.

Dhakal, H, Zhang, Z & Richardson, M 2007, 'Effect of water absorption on the mechanical properties of hemp fibre reinforced unsaturated polyester composites', *Composites science and technology*, vol. 67, no. 7, pp. 1674-83.

Doan, TTL, Gao, SL & Mader, E 2006, 'Jute/polypropylene composites I. Effect of matrix modification', *Composites science and technology*, vol. 66, no. 7, pp. 952-63.

Eichhorn, S & Young, R 2004, 'Composite micromechanics of hemp fibres and epoxy resin microdroplets', *Composites science and technology*, vol. 64, no. 5, pp. 767-72.

Esfandiari, A 2007, 'Mechanical Properties of PP/Jute and Glass Fibers Composites: The Statistical Investigation', *Journal of Applied Sciences*, vol. 7, no. 24, pp. 3943-50.

Fakirov, S & Bhattacharyya, D 2007, *Handbook of engineering biopolymers: homopolymers, blends and composites*, Hanser Gardner Pubns.

Fan, M 2010, 'Characterization and performance of elementary hemp fibres: factors influencing tensile strength', *BioResources*, vol. 5, no. 4, pp. 2307-22.

Feih, S, Thraner, A & Lilholt, H 2005, 'Tensile strength and fracture surface characterisation of sized and unsized glass fibers', *Journal of Materials Science*, vol. 40, no. 7, pp. 1615-23.

Fischer, G 2004, 'Characterization of Fiber-Reinforced Cement Composites by their Tensile Stress-Strain Behaviour and Quantification of Crack Formation', *proceedings of BEFIB*, pp. 20-2.

Fleck, N, Jelf, P & Curtis, P 1995, 'Compressive failure of laminated and woven composites', *Journal of composites technology & research*, vol. 17, no. 3, pp. 212-20.

Fleck, NA & Liu, D 2001, 'Microbuckle initiation from a patch of large amplitude fibre waviness in a composite under compression and bending', *European Journal of Mechanics – A/Solids*, vol. 20, no. 1, pp. 23-38.

George, J & Verpoest, JI 1999, 'Mechanical properties of flax fibre reinforced epoxy composites', *Die angewandte makromolekulare Chemie*, vol. 272, no. 1, pp. 41-5.

George, J, Sreekala, MS & Thomas, S 2001a, 'A review on interface modification and characterization of natural fiber reinforced plastic composites', *Polymer Engineering & Science*, vol. 41, no. 9, pp. 1471-85.

George, J, Sreekala, MS & Thomas, S 2001b, 'A review on interface modification and characterization of natural fiber reinforced plastic composites', *Polymer Engineering and Science*, vol. 41, no. 9, pp. 1471-85.

Goda, K, Sreekala, M, Gomes, A, Kaji, T & Ohgi, J 2006, 'Improvement of plant based natural fibers for toughening green composites—Effect of load application during mercerization of ramie fibers', *Composites Part A: Applied Science and Manufacturing*, vol. 37, no. 12, pp. 2213-20.

Gonzalez, C & Lorca, J 2007, 'Mechanical behaviour of unidirectional fiber-reinforced polymers under transverse compression: microscopic mechanisms and modeling', *Composites science and technology*, vol. 67, no. 13, pp. 2795-806.

Hamada, H, Ramakrishna, S & Satoh, H 1995, 'Crushing mechanism of carbon fibre/PEEK composite tubes', *Composites*, vol. 26, no. 11, pp. 749-55.

Han, CD & Lem, KW 1984, 'Chemorheology of thermosetting resins. IV. The chemorheology and curing kinetics of vinyl ester resin', *Journal of Applied Polymer Science*, vol. 29, no. 5, pp. 1879-902.

Hayes, BS & Gammon, LM 2010, *Optical Microscopy of Fiber-Reinforced Composites*, ASM International.

Henkhaus, K 2003, 'Overview of research on composite material impact behaviour', in 16th ASCE Engineering Mechanics Conference: *proceedings of the16th ASCE Engineering Mechanics Conference* Seattle, pp. 16-8.

Hu, W, Ton-That, MT, Perrin-Sarazin, F & Denault, J 2010, 'An improved method for single fiber tensile test of natural fibers', *Polymer Engineering & Science*, vol. 50, no. 4, pp. 819-25.

Huang, ZM 2004, 'Progressive flexural failure analysis of laminated composites with knitted fabric reinforcement', *Mechanics of materials*, vol. 36, no. 3, pp. 239-60.

Ilomaki, KM 2012, 'Adhesion Between Natural Fibers and Thermosets', Master thesis, Tampere University of Technology.

Jafari, M, Nikkhah, A, Sadeghi, A & Chamani, M 2007, 'The effect of Pleurotus spp. fungi on chemical composition and in vitro digestibility of rice straw', *Pakistan Journal of Biological Sciences*, vol. 10, no. 15, pp. 2460-4.

Jelf, P & Fleck, N 1992, 'Compression failure mechanisms in unidirectional composites', *Journal of composite materials*, vol. 26, no. 18, pp. 2706-26.

Jeng, CC & Chen, M 2000, 'Flexural failure mechanisms in injection-moulded carbon fibre/PEEK composites', *Composites science and technology*, vol. 60, no. 9, pp. 1863-72.

Jensen, FM, Falzon, B, Ankersen, J & Stang, H 2006, 'Structural testing and numerical simulation of a 34 m composite wind turbine blade', *Composite Structures*, vol. 76, no. 1-2, pp. 52-61.

John, MJ & Anandjiwala, RD 2008, 'Recent developments in chemical modification and characterization of natural fiber-reinforced composites', *Polymer Composites*, vol. 29, no. 2, pp. 187-207.

Joseph, K, Thomas, S & Pavithran, C 1996, 'Effect of chemical treatment on the tensile properties of short sisal fibre-reinforced polyethylene composites', *Polymer*, vol. 37, no. 23, pp. 5139-49.

Joseph, P, Mathew, G, Joseph, K, Groeninckx, G & Thomas, S 2003, 'Dynamic mechanical properties of short sisal fibre reinforced polypropylene composites', *Composites Part A: Applied Science and Manufacturing*, vol. 34, no. 3, pp. 275-90.

Joseph, P, Joseph, K, Thomas, S, Pillai, C, Prasad, V, Groeninckx, G & Sarkissova, M 2003, 'The thermal and crystallisation studies of short sisal fibre reinforced polypropylene composites', *Composites Part A: Applied Science and Manufacturing*, vol. 34, no. 3, pp. 253-66.

Kalaprasad, G, Francis, B, Thomas, S, Kumar, CR, Pavithran, C & Groeninckx, G 2004, 'Effect of fibre length and chemical modifications on the tensile properties of intimately mixed short sisal/glass hybrid fibre reinforced low density polyethylene composites', *Polymer international*, vol. 53, no. 11, pp. 1624-38.

Kalia, S, Kaith, B & Kaur, I 2009, 'Pretreatments of natural fibers and their application as reinforcing material in polymer composites—a review', *Polymer Engineering & Science*, vol. 49, no. 7, pp. 1253-72.

Kasuga, T, Ota, Y, Nogami, M & Abe, Y 2001, 'Preparation and mechanical properties of polylactic acid composites containing hydroxyapatite fibers', *Biomaterials*, vol. 22, no. 1, pp. 19-23.

Keener, T, Stuart, R & Brown, T 2004, 'Maleated coupling agents for natural fibre composites', *Composites Part A: Applied Science and Manufacturing*, vol. 35, no. 3, pp. 357-62.

Khalil, H, Ismail, H, Rozman, H & Ahmad, M 2001, 'The effect of acetylation on interfacial shear strength between plant fibres and various matrices', *European Polymer Journal*, vol. 37, no. 5, pp. 1037-45.

Kim, HJ & Eom, YG 2001, 'Thermogravimetric analysis of rice husk flour for a new raw material of lignocellulosic fiber thermoplastic polymer composites', *Journal of the Korean Wood Science and Technology*, vol. 20, no. 3, pp. 59-67.

Kitsutaka, Y & Takahashi, Y 2001, 'Fracture mechanics based bending failure analysis for fiber reinforced light-weight concrete panel considering crack dispersion effect', *Journal of Structural and Construction Engineering*, no. 541, pp. 37-42.

Ku, H, Wang, H, Pattarachaiyakoop, N & Trada, M 2011, 'A review on the tensile properties of natural fibre reinforced polymer composites', *Composites Part B: Engineering*.

Li, H, Burts, E, Bears, K, Ji, Q, Lesko, J, Dillard, D, Riffle, J & Puckett, P 2000, 'Network structure and properties of dimethacrylate-styrene matrix materials', *Journal of composite materials*, vol. 34, no. 18, pp. 1512-28.

Li, X, Tabil, L & Panigrahi, S 2007, 'Chemical Treatments of Natural Fiber for Use in Natural Fiber-Reinforced Composites: A Review', *Journal of Polymers and the Environment*, vol. 15, no. 1, pp. 25-33.

Li, X, Panigrahi, S & Tabil, L 2009, 'A study on flax fiber-reinforced polyethylene biocomposites', *Applied Engineering in Agriculture*, vol. 25, no. 4, pp. 525-31.

Li, X, Panigrahi, S, Tabil, L & Crerar, W 2004, 'Flax fiber-reinforced composites and the effect of chemical treatments on their properties', *Paper No. MB04-305. St Joseph, MI: American Society of Agricultural and Biological Engineers*.

Liu, Q, Zhong, Z, Wang, S & Luo, Z 2011, 'Interactions of biomass components during pyrolysis: A TG-FTIR study', *Journal of Analytical and Applied Pyrolysis*, vol. 90, no. 2, pp. 213-8.

Lojewska, J, Miskowiec, P, Lojewski, T & Proniewicz, LM 2005, 'Cellulose oxidative and hydrolytic degradation: In situ FTIR approach', *Polymer Degradation and Stability*, vol. 88, no. 3, pp. 512-20.

Lu, W, Kao, P & Su, A 1998, 'Flexural failure of unidirectional carbon/epoxy composites: Effects of interleaving and flexural rate', *Journal of Polymer Research*, vol. 5, no. 3, pp. 133-42.

Madsen, B 2004, 'Properties of plant fibre yarn polymer composites', PhD thesis, Technical University of Denmark, BYG-DTU.

Manalo, AC, Aravinthan, T & Karunasena, W 2010, 'Flexural behaviour of glue-laminated fibre composite sandwich beams', *Composite Structures*, vol. 92, no. 11, pp. 2703-11.

Manikandan, NK, Thomas, S & Groeninckx, G 2001, 'Thermal and dynamic mechanical analysis of polystyrene composites reinforced with short sisal fibres', *Composites science and technology*, vol. 61, no. 16, pp. 2519-29.

Mattoni, MA & Zok, FW 2005, 'Strength and Notch Sensitivity of Porous-Matrix Oxide Composites', *Journal of the American Ceramic Society*, vol. 88, no. 6, pp. 1504-13.

Menczel, JD, Judovits, L, Prime, RB, Bair, HE, Reading, M & Swier, S 2009, 'Differential scanning calorimetry (DSC)', *Thermal Analysis of Polymers*, pp. 7-239.

Mengeloglu, F & Karakus, K 2008, 'Thermal degradation, mechanical properties and morphology of wheat straw flour filled recycled thermoplastic composites', *Sensors*, vol. 8, no. 1, pp. 500-19.

Mishra, S, Mohanty, A, Drzal, LT, Misra, M, Parija, S, Nayak, S & Tripathy, S 2003, 'Studies on mechanical performance of biofibre/glass reinforced polyester hybrid composites', *Composites science and technology*, vol. 63, no. 10, pp. 1377-85.

Misra, S, Misra, M, Tripathy, S, Nayak, S & Mohanty, A 2002, 'The influence of chemical surface modification on the performance of sisal-polyester biocomposites', *Polymer Composites*, vol. 23, no. 2, pp. 164-70.

Mohanty, A, Misra, M & Hinrichsen, G 2000, 'Biofibres, biodegradable polymers and biocomposites: An overview', *Macromolecular Materials and Engineering*, vol. 276, no. 1, pp. 1-24.

Mohanty, A, Misra, M & Drzal, LT 2005, *Natural fibers, biopolymers, and biocomposites*, CRC Press Taylor & Francis Group 6000 Broken Sound Parkway NW.

Mohanty, S, Verma, S, Nayak, S & Tripathy, S 2004, 'Influence of fiber treatment on the performance of sisal–polypropylene composites', *Journal of Applied Polymer Science*, vol. 94, no. 3, pp. 1336-45.

Mohanty, S, Nayak, S, Verma, S & Tripathy, S 2004, 'Effect of MAPP as a Coupling Agent on the Performance of Jute–PP Composites', *Journal of reinforced plastics and composites*, vol. 23, no. 6, pp. 625-37.

MonteiroI, SN, RodriguezI, RJS, da CostaI, LL, Godinho, T, PortelaI, R & SantosII, NSS 2010, 'Thermal behaviour of buriti biofoam', *Revista Matéria*, vol. 15, no. 2, pp. 104-9.

Muzzy, JD & Kays, AO 1984, 'Thermoplastic vs. thermosetting structural composites', *Polymer Composites*, vol. 5, no. 3, pp. 169-72.

Mwaikambo, LY & Ansell, MP 1999, 'The effect of chemical treatment on the properties of hemp, sisal, jute and kapok fibres for composite reinforcement', *Die angewandte makromolekulare Chemie*, vol. 272, pp. 108-16.

Mwaikambo, LY & Ansell, MP 2002, 'Chemical modification of hemp, sisal, jute, and kapok fibers by alkalization', *Journal of Applied Polymer Science*, vol. 84, no. 12, pp. 2222-34.

Mwaikambo, LY, Tucker, N & Clark, AJ 2007, 'Mechanical Properties of Hemp-Fibre-Reinforced Euphorbia Composites', *Macromolecular Materials and Engineering*, vol. 292, no. 9, pp. 993-1000.

Odegard, G & Kumosa, M 2000, 'Determination of shear strength of unidirectional composite materials with the Iosipescu and 10° off-axis shear tests', *Composites science and technology*, vol. 60, no. 16, pp. 2917-43.

Ouajai, S & Shanks, R 2005, 'Composition, structure and thermal degradation of hemp cellulose after chemical treatments', *Polymer Degradation and Stability*, vol. 89, no. 2, pp. 327-35.

Park, JM, Quang, ST, Hwang, BS & DeVries, KL 2006, 'Interfacial evaluation of modified Jute and Hemp fibers/polypropylene (PP)-maleic anhydride polypropylene copolymers (PP-MAPP) composites using micromechanical technique and nondestructive acoustic emission', *Composites science and technology*, vol. 66, no. 15, pp. 2686-99.

Paul, S, Joseph, K, Mathew, G, Pothen, L & Thomas, S 2010, 'Influence of polarity parameters on the mechanical properties of composites from polypropylene fiber and short banana fiber', *Composites Part A: Applied Science and Manufacturing*, vol. 41, no. 10, pp. 1380-7.

Paul, S, Oommen, C, Joseph, K, Mathew, G & Thomas, S 2010, 'The role of interface modification on thermal degradation and crystallization behaviour of composites from commingled polypropylene fiber and banana fiber', *Polymer Composites*, vol. 31, no. 6, pp. 1113-23.

Peng, F, Ren, J-L, Xu, F, Bian, J, Peng, P & Sun, R-C 2009, 'Fractional Study of Alkali-Soluble Hemicelluloses Obtained by Graded Ethanol Precipitation from Sugar Cane Bagasse', *Journal of Agricultural and Food Chemistry*, vol. 58, no. 3, pp. 1768-76, viewed 2012/06/27.

Pickering, KL, Li, Y, Farrell, RL & Lay, M 2007, 'Interfacial Modification of Hemp Fiber Reinforced Composites Using Fungal and Alkali Treatment', *Journal of Biobased Materials and Bioenergy*, vol. 1, no. 1, pp. 109-17.

Pierron, F & Vautrin, A 1998, 'Measurement of the in-plane shear strengths of unidirectional composites with the Iosipescu test', *Composites science and technology*, vol. 57, no. 12, pp. 1653-60.

Placet, V 2009, 'Characterization of the thermo-mechanical behaviour of Hemp fibres intended for the manufacturing of high performance composites', *Composites Part A: Applied Science and Manufacturing*, vol. 40, no. 8, pp. 1111-8.

Prasad, S, Pavithran, C & Rohatgi, P 1983, 'Alkali treatment of coir fibres for coir-polyester composites', *Journal of Materials Science*, vol. 18, no. 5, pp. 1443-54.

Rahman, MM, Mallik, AK & Khan, MA 2007, 'Influences of various surface pretreatments on the mechanical and degradable properties of photografted oil palm fibers', *Journal of Applied Polymer Science*, vol. 105, no. 5, pp. 3077-86.

Randriamanantena, T, Razafindramisa, FL, Ramanantsizehena, G, Bernes, A & Lacabane, C 2009, 'Thermal behaviour of three woods of Madagascar by thermogravimetric analysis in inert atmosphere', *proceedings of theFourth high-energy physics international conference* Antananarivo, Madagascar, pp. 1-10.

Ranganathan, S & Mantena, PR 2003, 'Axial loading and buckling response characteristics of pultruded hybrid glass-graphite/epoxy composite beams', *Journal of reinforced plastics and composites*, vol. 22, no. 7, pp. 671-9.

Ray, D, Sarkar, B, Rana, A & Bose, N 2001, 'Effect of alkali treated jute fibres on composite properties', *Bulletin of Materials Science*, vol. 24, no. 2, pp. 129-35.

Reh, U, Kraepelin, G & Lamprecht, I 1986, 'Use of differential scanning calorimetry for structural analysis of fungally degraded wood', *Applied and environmental microbiology*, vol. 52, no. 5, pp. 1101-6.

Reid, SR & Zhou, G 2000, *Impact behaviour of fibre-reinforced composite materials and structures*, CRC Woodhead Publishing Limited, 80 High Street, Sawston, Cambridge, CB22 3HJ, UK.

Rout, J, Misra, M, Tripathy, S, Nayak, S & Mohanty, A 2001, 'The influence of fibre treatment on the performance of coir-polyester composites', *Composites science and technology*, vol. 61, no. 9, pp. 1303-10.

Rowell, RM & Young, RA 1997, *Paper and composites from agro-based resources*, CRC Press Inc. Taylor & Francis Group, United States.

Saheb, DN & Jog, J 1999, 'Natural fiber polymer composites: a review', *Advances in Polymer Technology*, vol. 18, no. 4, pp. 351-63.

Sapieha, S, Allard, P & Zang, Y 1990, 'Dicumyl peroxide-modified cellulose/LLDPE composites', *Journal of Applied Polymer Science*, vol. 41, no. 9-10, pp. 2039-48.

Seki, Y 2009, 'Innovative multifunctional siloxane treatment of jute fiber surface and its effect on the mechanical properties of jute/thermoset composites', *Materials Science and Engineering: A*, vol. 508, no. 1-2, pp. 247-52.

Sever, K, Sarikanat, M, Seki, Y, Erkan, G & Erdoğan, ÜH 2010, 'The Mechanical Properties of γ-Methacryloxypropyltrimethoxy silane-treated Jute/Polyester Composites', *Journal of composite materials*, vol. 44, no. 15, pp. 1913-24.

Sgriccia, N, Hawley, M & Misra, M 2008, 'Characterization of natural fiber surfaces and natural fiber composites', *Composites Part A: Applied Science and Manufacturing*, vol. 39, no. 10, pp. 1632-7.

Shyr, TW & Pan, YH 2003, 'Impact resistance and damage characteristics of composite laminates', *Composite Structures*, vol. 62, no. 2, pp. 193-203.

Singleton, A, Baillie, C, Beaumont, P & Peijs, T 2003, 'On the mechanical properties, deformation and fracture of a natural fibre/recycled polymer composite', *Composites Part B: Engineering*, vol. 34, no. 6, pp. 519-26.

Smith, BC 2009, *Fundamentals of Fourier transform infrared spectroscopy*, CRC Press Taylor & Francis Group, 6000 Broken Sound Parkway NW.

Sreekala, M, Kumaran, M, Joseph, S, Jacob, M & Thomas, S 2000, 'Oil palm fibre reinforced phenol formaldehyde composites: influence of fibre surface modifications on the mechanical performance', *Applied Composite Materials*, vol. 7, no. 5, pp. 295-329.

Stuart, B 2005, *Infrared Spectroscopy: Fundamentals and Applications*, John Wiley & Sons, Ltd, Chichester, England

Sun, XF, Sun, RC, Fowler, P & Baird, MS 2005, 'Extraction and characterization of original lignin and hemicelluloses from wheat straw', *Journal of Agricultural and Food Chemistry*, vol. 53, no. 4, pp. 860-70.

Taj, S, Munawar, MA & Khan, S 2007, 'Natural fiber-reinforced polymer composites', *proceedings of thePakistan academy of sciences* pp. 129-44.

Tajeddin, B, Abdul Rahman, R, Chuah, L, Ibrahim, NA & Yusof, YA 2009, 'Thermal properties of low density polyethylene-filled kenaf cellulose composites', *European Journal of Scientific Research*, vol. 32, no. 2, pp. 223-30.

Thakur, VK & Singha, AS 2010, 'Physico-chemical and mechanical characterization of natural fibre reinforced polymer composites', *Iranian Polymer Journal*, vol. 19, no. 1, pp. 3-16.

Torres, F & Cubillas, M 2005, 'Study of the interfacial properties of natural fibre reinforced polyethylene', *Polymer testing*, vol. 24, no. 6, pp. 694-8.

Totry, E, Gonzalez, C & Llorca, J 2009, 'Mechanical behaviour of composite materials in shear: experiments and simulations', *Anales de Mecánica de la Fractura*, vol. 26, no. 1, pp. 187-92.

Totry, E, González, C, LLorca, J & Molina-Aldareguía, J 2009, 'Mechanisms of shear deformation in fiber-reinforced polymers: experiments and simulations', *International journal of fracture*, vol. 158, no. 2, pp. 197-209.

Tserki, V, Zafeiropoulos, N, Simon, F & Panayiotou, C 2005, 'A study of the effect of acetylation and propionylation surface treatments on natural fibres', *Composites Part A: Applied Science and Manufacturing*, vol. 36, no. 8, pp. 1110-8.

Valadez-Gonzalez, A, Cervantes-Uc, J, Olayo, R & Herrera-Franco, P 1999, 'Chemical modification of henequen fibers with an organosilane coupling agent', *Composites Part B: Engineering*, vol. 30, no. 3, pp. 321-31.

Vallo, C, Kenny, JM, Vazquez, A & Cyras, VP 2004, 'Effect of chemical treatment on the mechanical properties of starch-based blends reinforced with sisal fibre', *Journal of composite materials*, vol. 38, no. 16, pp. 1387-99.

Van, DJO & Beukers, A 1999, 'The potential of a new rigid-rod polymer fibre (M5') in advanced composite structures', *Polymer*, vol. 40, no. 4, pp. 1035-44.

Walker, JCF 2006, *Primary wood processing: principles and practice*, vol. 2nd edition, Springer Verlag, Netherlands.

Wang, B, Panigrahi, S, Tabil, L & Crerar, W 2007, 'Pre-treatment of Flax Fibers for use in Rotationally Molded Biocomposites', *Journal of reinforced plastics and composites*, vol. 26, no. 5, pp. 447-63.

Wang, K, Jiang, JX, Xu, F, Sun, RC & Baird, MS 2010, 'Influence of steam pressure on the physicochemical properties of degraded hemicelluloses obtained from steam-exploded Lespedeza stalks', *BioResources*, vol. 5, no. 3, pp. 1717-32.

Yang, H, Yan, R, Chen, H, Lee, DH & Zheng, C 2007, 'Characteristics of hemicellulose, cellulose and lignin pyrolysis', *Fuel*, vol. 86, no. 12-13, pp. 1781-8.

Zadorecki, P & Flodin, P 1985, 'Surface modification of cellulose fibers. II. The effect of cellulose fiber treatment on the performance of cellulose–polyester composites', *Journal of Applied Polymer Science*, vol. 30, no. 10, pp. 3971-83.

Zakaria, S & Poh, LK 2002, 'Polystyrene-benzoylated EFB reinforced composites', *Polymer-Plastics Technology and Engineering*, vol. 41, no. 5, pp. 951-62.

Zhou, G, Green, E & Morrison, C 1995, 'In-plane and interlaminar shear properties of carbon/epoxy laminates', *Composites science and technology*, vol. 55, no. 2, pp. 187-93.